Reconstruction of Miocene vegetation based on the palynology of core material from Langebaanweg, South Africa

Name: Moteng Elizabeth Moseri

Student number: 1102729

ORCID Number: 0000-0001-8135-4342

Supervisor: Dr. Frank H. Neumann

Co-Supervisor: Prof. Marion K. Bamford

A dissertation submitted to the Faculty of Science, University of the Witwatersrand, in fulfilment of the requirements for the degree of Master of Science.

Evolutionary Studies Institute, University of the Witwatersrand, Johannesburg: Private Bag 3, Wits, 2050, Johannesburg, South Africa. 15 December 2021

DECLARATION

I declare that this dissertation is my own unaided work. It is being submitted for the Degree of Master in the University of the Witwatersrand, Johannesburg. It has not been submitted before for any degree or examination in any other university.

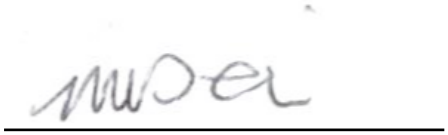

Moteng Elizabeth Moseri

Abstract

The Cape Floristic Region (CFR) houses a diverse range of plant species that are characteristic of a Mediterranean-type climate that was established in the Neogene. The Elandsfontyn Formation at Langebaanweg (LBW) reveals the evolutionary history of fynbos vegetation, the exact timing of which is still uncertain. Pollen, spores and dinoflagellate cysts recovered from Core BH2 preserving Elandsfontyn Formation deposits are identified to conduct a palaeoenvironmental reconstruction of the deposits at LBW. A standard palynological procedure was applied to process the sediments and produce 76 samples which were analysed with a light microscope. A total of 104 palynomorph taxa including pollen, spores and dinoflagellate cysts were recorded to determine the timing of evolution of the fynbos biome and statistically analysed to create clusters of palynomorph indicators, which may be linked to certain climatic parameters. The palynological and statistical results confirm the existence of a subtropical-tropical forest dominated by Podocarpaceae, palms, vines and ferns, providing evidence of wet conditions caused by summer rainfall. The possible existence of Araucariaceae – a typical Gondwana element currently extinct in Africa - is documented in this study but requires confirmation from SEM studies. Wetlands comprising Sparganiaceae, Restionaceae, Cyperaceae and Poaceae were common, pointing to a high water table. Mangrove tree pollen were rarely recorded, possibly implying that mangrove swamps might have been confined to the coastline. Patches of proto-fynbos probably provided an understorey component of the subtropical forests and co-fluctuated with the forest elements. A considerable marine influence was imposed on the terrestrial environment, inferred by three marine transgressions in the *Apteodinium spiridoides* zone (18.96–18.24 m) and a fourth and final event in the *Operculodinium centrocarpum* zone (16.865–13.4 m), which are probably linked to global late Oligocene sea level changes. Dinoflagellate cysts belonging to *Apteodinium spiridoides*, *Opeculodinium centrocarpum*, *Spiniferites mirabilis* were abundant and occurred with other marine indicators, such as benthic microforaminiferal test linings and algal cysts. Savanna woodlands with *Alchornea* (*Psilatricolporites quenua*), Combretaceae and *Brachystegia* (*Peregrinipollis nigericus*) gradually replaced the subtropical forests, possibly due to more arid conditions and enhanced seasonality. Similar assemblages with common extinct taxa were recorded at Saldanha Bay, Rondeberg, Noordhoek, and Knysna and show possible floristic links to sites in other Southern Hemisphere regions, including South America, Antarctica, Australia and New Zealand. A late Oligocene (early Chattian) to early Miocene (early Burdigalian) age is inferred for

Elandsfontyn Formation at LBW based on the presence of *Mutisiapollis viteauensis*, *Tubuliflodites antipodica*, *Apteodinium spiridoides*, *Chiropteridium lobospinosum* and *Cordosphaeridium minimum*.

Acknowledgements

I would like to sincerely thank my supervisors, Dr. Frank Neumann and Prof. Marion Bamford for entrusting me with this research project and their constant guidance, motivation and patience until its completion. They were always willing to edit my work, including posters, funding applications and presentations. Furthermore, they have instilled in me valuable scientific skills, encouraged me to step out of my comfort zone and be confident in myself.

This project would not have been possible without the funding support from the National Research Foundation (NRF), the Centre of Excellence in Palaeosciences (CoE) and the Palaeontological Scientific Trust (PAST). Through their financial support, I was able to pay for my tuition, accommodation and living expenses throughout my studies. I am grateful to the International Paleontological Society for awarding me the Sepkoski Grant, which enabled me to purchase a microscope to use for my research and to invest in my scientific career.

I am also grateful to the palynology laboratory technician, Prosper Bande for guiding me through the lab techniques, the entire palaeoecology team (Angela Effiom, Kevwe Eweto, Dr. Irene Esteban, Nikiwe Ndlovu and Bongekile Zwane) at the Evolutionary Studies Institute for helping me with any identification challenges, providing academic resources and uplifting my spirits when needed. Many thanks to Dr. Tea Jashashvili for taking time out of her busy schedule to assist me with the Principal Components Analysis method.

Lastly, I would like to thank my parents, siblings, nieces, nephews and friends for their endless love, support, patience, and kindness throughout my Masters. Their constant cheering was a great source of happiness which kept me going when I felt de-motivated.

CONTENTS

List of Figures

List of Plates:

List of Tables

List of Abbreviations

- LBW – Langebaanweg
- BUS – Benguela Upwelling System
- CFR – Cape Floristic Region
- MCO – Miocene Climatic Optimum
- MTC – Mediterranean-type climate
- PAAZ – Pollen Assemblage and Abundance Zone
- PCA – Principal Components Analysis
- PC – Principal Component
- SEM – Scanning Electron Microscopy

- WCNP – West Coast National Park

List of Appendices

Appendix A: Nomenclature and botanical affinity of the most important palynomorphs from Langebaanweg, including taxa in photo plates and discussed in the text

Appendix B: Percentages of the Langebaanweg palynomorphs to determine palynomorph fluctuations across Core BH2

Appendix C: Spreadsheet used for the PCA. 1 = Presence in sample and 0 = Absence in sample of selected taxa from eight ecological groups

Appendix D: Loading matrix of the first five principal components (Prin1–Prin5) for the PCA with ecological groups as variables) for the PCA. Only PC1 and PC2 were included in the study

Appendix E: Comprehensive pollen diagram of palynomorphs from Elandsfontyn Formation, Langebaanweg

CHAPTER 1: GENERAL INTRODUCTION

1.1 MIOCENE PALAEOECOLOGY OF SOUTHERN AFRICA

The Miocene, spanning from c. 23.03−5.33 Ma, is a time period characterised by climatic shifts and palaeogeographic changes that shaped today's world's ecosystems (Coetzee, 1983; Pound *et al*., 2012). These global changes include the uplift of mountain chains e.g., the European Alps, the establishment of modern ocean currents, further Arctic and Antarctic glaciations, increasing aridity within continents, decreasing CO_2 levels and a global cooling trend (Pound *et al*., 2012; Steinthorsdottir *et al*., 2021). Warm temperatures of the Miocene (7−8℃ warmer than today) caused by high concentrations of CO_2 culminated in the Miocene Climatic Optimum (MCO), which lasted from ~16.9–14.7 Ma (Henrot *et al*., 2010; Sciscio *et al*., 2013; Steinthorsdottir *et al*., 2021). The complex interactions of physical global changes were responsible for the reduction of the temperatures following the MCO (Henrot *et al*., 2010; Sciscio *et al*., 2013).

The Cape Floristic Region (CFR) occupies a ± 90 760 km^2 area with ≥ 9251 plant species, of which ca. 68 % are endemic (Manning and Goldblatt, 2012; Mucina and Rutherford, 2006). The diverse flora of this region is considered one of the six floral kingdoms of the world (Takhtajan, 1986). In addition, this region represents one of the five Mediterranean-type climate (MTC) ecosystems of the world that is assumed to have developed in the Neogene (Rundel, 2019). Within the Cape Floristic Region occurs the predominant sclerophyllous and largely treeless fynbos vegetation, dominated by Asteraceae, Ericaceae, Fabaceae, Iridaceae, Proteaceae and Restionaceae (Born *et al*., 2007; Manning and Goldblatt, 2012; Rundel, 2019; van Santen and Linder, 2020). The vast diversity and ecological heritage of this region enhances the importance of mapping the effects of climate change on its evolution.

This unique floral arrangement of the Cape region did not exist during early and middle Miocene, when a subtropical to tropical woodland vegetation – based on palynological analyses of the Elandsfontyn Formation - covered most of the low-lying areas and co-existing proto-fynbos vegetation was restricted to erosion-resistant sandstone mountains (Coetzee, 1980; Linder and Hardy, 2004; van Santen and Linder, 2020). A late Miocene age was suggested for the radiation of the fynbos flora, initiated by the change from a summer-wet to

summer-dry climate (Dupont *et al*., 2011; van Santen and Hardy, 2020). Dating of the deposits relied on a patchy fossil pollen record that cannot be easily interpreted in terms of climatic change (Coetzee and Rogers, 1982; Linder, 2003; van Santen and Linder, 2020). In addition, southern African sedimentary deposits that can document these dramatic changes and demonstrate how global climatic fluctuations have changed the regional vegetation are scarce along the southern and western coast (Neumann and Bamford, 2013; Sciscio *et al*., 2016). As of today, the cause and timing of this transition remains unclear.

The Langebaanweg (LBW) region in the Western Cape Province of South Africa provides a record of physical and climatic changes in the form of fossil diversity preserved in the West Coast National Park (WCNP) (Roberts *et al*., 2011; Sciscio *et al*., 2013). Core BH2, utilised in this study, was drilled at LBW 'E' Quarry capturing Miocene–Pliocene sediments representing the Elandsfontyn and Varswater formations of the Sandveld Group (Fig. 1) (Sciscio *et al*., 2013). The (Oligocene)–Miocene Elandsfontyn and Mio-Pliocene Varswater formations were deposited by the palaeo-Berg River, the predecessor of the modern-day Berg River in the southwestern Cape (Coetzee and Muller, 1984; Sciscio *et al*., 2013; Roberts *et al*., 2017). Evidence of fossil palynomorphs collected from the Elandsfontyn and Varswater formations are thus essential to reconstruct a Miocene environment and the early evolution of the fynbos biome for the LBW site.

Studies of the LBW and Saldanha Bay palaeoflora were conducted to understand fluctuations in climatic conditions and the reconstruction of palaeoenvironments (Roberts *et al*., 2013; 2017; Sciscio *et al*., 2013). Coetzee and Rogers (1982) studied pollen assemblages from core sections of clayey silt and silty clay belonging to the Elandsfontyn Formation at LBW. Two pollen zones are recognized in the study: pollen zone Sa and pollen zone Sb, each depicting dissimilar characteristics (Coetzee and Rogers, 1982). Pollen zone Sa is characterised by clayey silt and sub-tropical to tropical vegetation, including palms and dominant *Podocarpus* spp. (Coetzee and Rogers, 1982). Palm pollen is reduced significantly, whereas *Podocarpus* spp. declined by just 1% in the silty clay pollen zone Sb (Coetzee and Rogers, 1982). Palm pollen, Casuarinaceae – now restricted to Australia, Pacific islands and South-East Asia (Coetzee and Praglowski, 1984) –, Chloranthaceae, Sarcolaenaceae and Winteraceae (basal angiosperms), all elements of subtropical vegetation, are now extinct at the Cape;however, they were retrieved in the Elandsfontyn Formation, along with Poaceae, Restionaceae, Proteaceae, Sapotaceae and Myricaceae (Coetzee and Rogers, 1982; Coetzee and Muller,

1984; Neumann and Bamford, 2015; Roberts *et al*., 2017). These changes are attributed to the shift from a sub-tropical to a Mediterranean climate and the northward migration of the palaeo-Berg River (Coetzee and Rogers, 1982; Roberts *et al*., 2011; Roberts *et al*., 2017).

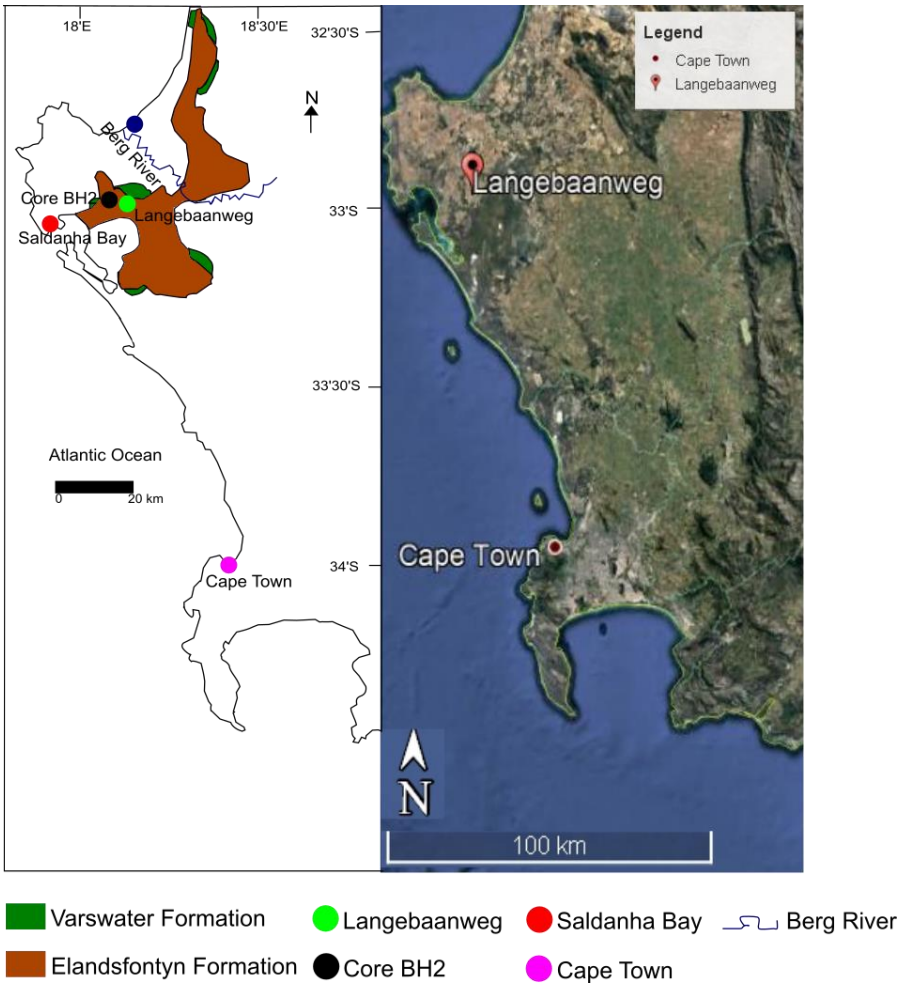

Figure 1. Locality map of the LBW region indicating the study area and location of Core BH2 (in relation to the geological extents of the Elandsfontyn Formation (brown), Sandveld Group; (adapted from Sciscio *et al*., 2013). Terrestrial map taken from Google Earth (2021).

Neumann in Sciscio *et al*. (2013) conducted a preliminary palynological study on core BH2 in which 49 samples were processed using a standard procedure. Each sample yielded approximately 250 pollen grains and other identified palynomorphs, including, spores, algae, acritarchs, microforaminiferal test linings and dinoflagellate cysts (Sciscio *et al*., 2013). However, the samples were not sieved, and many pollen grains were concealed by debris

(Sciscio *et al*., 2013). The pollen profile appeared discontinuous, and a pollen zonation was not achieved. Dinoflagellate cysts, which could, may be used to estimate an age of the deposits, were only superficially described, and provisionally assigned to a single genus (Sciscio *et al*., 2013). Fynbos elements such Ericaceae, Restionaceae, Proteaceae and Poaceae (evidenced by both pollen and a few phytoliths) are present throughout the core profile but co-fluctuate with the forest and subtropical plants (Sciscio *et al*., 2013). Coetzee and Rogers (1982) recorded similar palynomorphs - except for dinoflagellates - including Podocarpaceae, palms, Casuarinaceae, Oleaceae, Restionaceae, Sparganiaceae, Proteaceae, Asteraceae and Zygnemataceae in their LBW study.

Several sites in the vicinity of LBW, including Saldanha Bay (Roberts *et al*., 2017), Knysna (Carr *et al*., 2010), Rondeberg (Roberts *et al*., 2013) and Noordhoek (Sciscio *et al*., 2016), have also preserved Elandsfontyn Formation deposits which correspond with the environmental changes that depict the transition from a subtropical/tropical environment to a fynbos dominated environment. The meandering palaeo-Berg River is an important factor in the environmental fluctuations observed at Saldanha Bay (Coetzee, 1983; Roberts *et al*., 2017). This migration is assumed to have initiated a riparian tropical forest, followed by dominant palm vegetation and finally, a freshwater swamp associated with flooding at Saldanha Bay (Coetzee, 1983).). In a study conducted by Roberts *et al*. (2017), based on marine core material from Saldanha Bay, a late Oligocene–early Miocene age is inferred for sediments of the Elandsfontyn Formation that depict a diverse range of vegetation. The flora includes a *Podocarpus*-dominated subtropical forest with abundant palaeotropical *Lygodium* fern spores; a riparian/swamp forest with elements of Arecaceae (palms), Myricaceae and Sapotaceae; and a subtropical woodland-thicket – absent at other Neogene sites (LBW, Noordhoek and Rondeberg) – that is characterised by subtropical woodland elements including Euphorbiaceae, Caesalpiniaceae and Combretaceae (Roberts *et al*., 2017). The pollen fluctuations were inferred to be the result of a marine transgression, as opposed to climate change (Roberts *et al*., 2017).

Neogene pollen-bearing sediments including lignite seams that were previously exploited are also known from the southern Cape coast northeast of Knysna (Carr *et al*., 2010). The Makhulu Quarry is a location of interest for many palynological studies based on these lignite deposits. Several studies (Thiergart *et al*., 1963; Carr *et al*., 2010; Goble, 2015) indicate the presence of palms, *Podocarpus*-type, *Widdringtonia* (Cupressaceae), and Asteraceae. Palms

are extinct at the southern Cape, including the local region around the Makhulu Quarry (Carr *et al*., 2010). These fossil pollen types are associated with a palm-dominated, subtropical/tropical palaeoenvironment surrounded by trees, shrubs and grasses (Carr *et al*., 2010). Due to the similarities displayed by the palynomorphs found in the Knysna lignites and Elandsfontyn Formation, a provisional middle Miocene age was suggested for the lignites (Carr *et al*., 2010).

Rondeberg, situated 60 km north of Cape Town, hosts extensive Neogene clay deposits that were palynologically analysed. In a pilot study by Roberts *et al*. (2013), the results showed that spores and pollen of gymnosperms and angiosperms were well preserved, comprising abundant palms, *Podocarpus*-type, Rhamnaceae, Restionaceae and Ericaceae The presence of palm pollen is suggestive of a dominant subtropical/tropical climate (Roberts *et al*., 2013). The Rondeberg deposits are assumed to be slightly younger than the LBW and Noordhoek deposits, which were both deposited during lower sea levels (Sciscio, 2011).

The Elandsfontyn Formation at Noordhoek, south of LBW preserves palynomorphs similar to those found at LBW, such as *Arecipites*, *Casuarina*, *Podocarpidites* and Myrtaceae (Coetzee and Rogers, 1982; Sciscio *et al*., 2016). The deposits, with an early to middle Miocene age (Sciscio *et al*., 2016) depict the presence of forest (Podocarpaceae and Cupressaceae) and subtropical-tropical elements (palms, Euphorbiaceae, Combretaceae) with some proto-fynbos elements such as Proteaceae, Thymelaceae, Restionaceae, Rosaceae and Gramineae (Coetzee, 1983; Coetzee and Muller, 1984). Saldanha Bay and Noordhoek, both occurring along the Cape Peninsula, generally show alternating conifer-dominated forests and palm-dominated subtropical vegetation during the Miocene (Coetzee, 1981).

The similarity of fossil pollen assemblages in these areas suggests that the timing of transition might be consistent; however, more studies are required to achieve precise dating and to show that dinoflagellate cysts can be successfully used to constrain the age of the deposits at LBW and to correlate it to other sites.

1.2 Influence of the Benguela Upwelling System on climatic and vegetative fluctuations

Global pole-to-equator climatic gradients steepened, and glaciation of Antarctica occurred by the middle Miocene, resulting in the development of the Benguela Upwelling System (BUS)

at ca. 10 Ma associated with the cool Benguela Current along the South African Atlantic seaboard (Linder and Hardy, 2004; Roberts *et al*., 2011, Sciscio *et al*., 2013). The South Atlantic Anticyclone governs the modern climate, along with the Benguela Current (Fig. 2) and those climatic factors together with the occurrence of oligotrophic soils derived from the erosion of Cape sandstones are probably fundamental for the successful expansion of the fynbos flora during the Miocene (Coetzee and Rogers, 1982; Roberts *et al*., 2013; Roberts *et al*., 2017; van Santen and Linder, 2020). These factors may have facilitated a change from a palm-dominated subtropical vegetation to modern day fynbos and grasslands during the Neogene, however, the exact timing of this change needs to be further investigated (Henrot *et al*., 2010; Dupont *et al*., 2011; Roberts *et al*., 2011; Pound *et al*., 2012; Hoetzel *et al*., 2013; Sciscio *et al*., 2013, van Santen and Linder, 2020).

An enhancement in the quality of cold water, due to upwelling associated with the advancement of the BUS in the late Miocene (9-10 Ma), increased dinoflagellate occurrence along the southwestern coast of southern Africa (Dupont *et al*., 2011; Heinrich *et al*., 2011; Rommerskirchen *et al*., 2011). The BUS forms one of four major upwelling regions of the world that are characterised by distinctive dinoflagellate communities. Dinoflagellates are diverse marine and freshwater planktonic organisms that represent useful environmental and biostratigraphic indicators. They reflect enhanced productivity (nutrient availability) and specific sea surface conditions (temperature, salinity and ice cover) of associated surface waters as well as the regional climate (Marret and Zonneveld, 2003; Pitcher and Joyce, 2009; Heinrich *et al*., 2011). Nutrient enrichment in the BUS enhances phytoplankton blooms supporting pelagic fishes (Burger *et al*., 2020), however, these blooms can be harmful on account of their high biomass which induce anoxic conditions (Fawcett *et al*., 2007; Pitcher and Joyce, 2009; Pitcher and Louw, 2021).

The late Miocene to early Pliocene saw an increase in C_4, plants including grasses on the southwestern coast of Africa and globally, due to the global climatic changes occurring in the Miocene (Rossouw *et al*., 2009; Henrot *et al*., 2010; Hoetzel *et al*., 2013; Sciscio *et al*., 2013). This expansion of grasses led to the intensification of fire activity, providing combustible material preserved as charred particles (Hoetzel *et al*., 2013). It is assumed that around this time period, major fynbos elements were becoming more established and dominant (Sciscio *et al*., 2013). In a study by Hoetzel *et al*. (2013), the increasing occurrence of Poaceae was correlated with the formation of open grasslands from the late Miocene to the

early Pliocene. Mediterranean-type climate ecosystems are prone to regular fire activity occurring mostly in the warm dry summer months. The increasing aridification trend in the Miocene is associated with the onset of fire – a consequence of seasonal summer drought – in MTCs (Rundel *et al*., 2018). Recurrent fire activity enabled MTCs to develop persistence strategies that had a long-term effect on the creation of higher species diversity (Rebelo *et al*., 2006; Manning and Goldblatt, 2012; Rundel *et al*., 2018) that is observed in the CFR today.

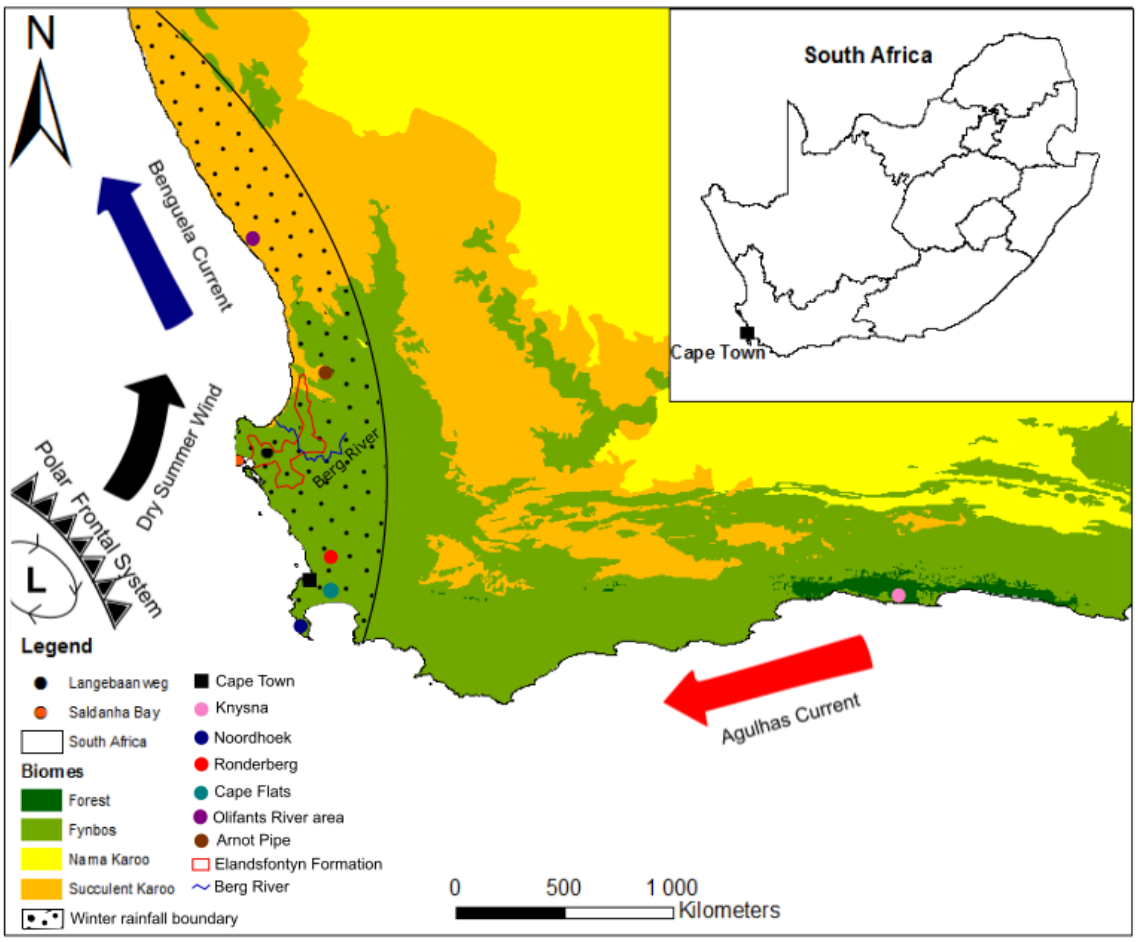

Figure 2. Neogene sites on the southwestern Cape, based on the position of the South Atlantic Anticyclone and the Benguela Upwelling System; (adapted from Roberts *et al*., 2013). The cold Benguela Current flows and coastal low pressure systems (L) induce dry wind over the interior of southwestern South Africa. The warm Agulhas Current transports warm water from the Indian Ocean to the south of the Cape. The Forest (dark green), Fynbos (light green), Nama Karoo (yellow) and Succulent Karoo (orange) biomes and the winter rainfall boundary (dotted area) are indicated on the map. The Elandsfontyn Formation, deposited by the paleo-Berg River, is shown by the red bounded area.

1.3 REGIONAL SETTING

1.3.1 Geographical and geological setting

The coastal town of LBW is situated ~120 north of Cape Town and c. 30 m above sea level (Eze and Meadows, 2013). It lies on a coastal platform of the southwestern coast with its landward and eastern side to the Great Escarpment (Sciscio *et al*., 2013). The escarpment was formed in the late Mesozoic and uplifted during the Pliocene (Roberts *et al*., 2011; 2017; Sciscio *et al*., 2013). The platform has been subjected to Oligocene and Miocene marine transgressions contributing to the sedimentation and marine productivity periodically along the southwestern coast area (Coetzee, 1983; Roberts *et al*., 2011; Sciscio *et al*., 2013).

The Neoproterozoic Cape Granite at LBW is overlain by Cenozoic sediments of the Sandveld Group (Roberts *et al*., 2011). The fluvial Elandsfontyn Formation is overlain by the marine Varswater Formation, which is overlain by calcified aeolianites of the Langebaan Formation and finally, sand sheets of the Springfontyn Formation (Roberts *et al*., 2011). Provisional biostratigraphic ages of middle Miocene, Mio-Pliocene, Pleistocene and Pleistocene/Holocene were assigned to the Elandsfontyn, Varswater, Langebaan and Springfontyn formations, respectively, at LBW (Sciscio *et al*., 2013). The Elandsfontyn Formation is approximately 60 km thick at LBW, having formed in depressions within the Neoproterozoic granites (Roberts and Brink, 2002; Roberts *et al*.,2011).

The LBW embayment was formed adjacent to the Saldanha Bay embayment and therefore both preserve sediments of the Sandveld Group deposited by the palaeo-Berg River which extended southwards to the coastline at Saldanha Bay and northwards from LBW (Roberts *et al*., 2011; 2017). Seismic studies at Saldanha Bay revealed that the Cape granites were incised by fluvial channels, forming these depressions up to 100 m thick during periods of sea level lowstands (Roberts *et al*., 2011; Roberts *et al*., 2017).

1.3.2 Modern vegetation

The LBW is currently home to a rich floral assemblage and was previously described as being comprised of three elements of the fynbos biome (Coetzee and Muller, 1984; Ruddiman *et al*., 1989; Roberts *et al*., 2011; Roberts *et al*., 2017) including restioid (Restionaceae graminoids), ericoid (fine-leaved, needle-like) and proteoid (Proteaceae) components (Coetzee, 1983; Coetzee and Muller, 1984; Sciscio *et al*., 2013). The fynbos

biome is subdivided into three vegetation categories, including the fynbos, renosterveld and strandveld types (Rebelo *et al*., 2006; Manning and Goldblatt, 2012).

The fynbos complex is characterised by evergreen, fire-prone shrubland in association with leaf spinescence and high sedge content, characterised predominantly by Restionaceae, Ericaceae and Proteaceae growing on nutrient-poor substrates (Rebelo *et al*., 2006). Additionally, wetland habitats often dominated by a single species (Restionaceae, Ericaceae, or Poaceae) are common in fynbos heathland (Rebelo *et al*., 2006). Renosterveld is typically without a high percentage of fynbos components such as Proteaceae, Ericaceae, less than 5-10% of Restionaceae and abundant grasses and geophytes occurring on clay-rich soils (Moll *et al*., 2984; Rebelo *et al*., 2006). Strandveld is comprised of low, sclerophyllous shrublands that typically grow close to the coast on a range of soft (beach sand) to hard substrates (granites, limestones, etc.) (Rebelo *et al*., 2006). Although restioid shrubs and succulents (in arid conditions) can occur in the strandveld thicket, proteoid and ericoid components are respectively absent and rare (Moll *et al*., 1984; Rebelo *et al*., 2006; Manning and Goldblatt, 2012). LBW is associated with the "FS 3 Saldanha Flats Strandveld" unit of the strandveld complex consisting of sclerophyllous shrubs, geophytes and herbs growing on sands adjacent to coastlines (Rebelo *et al*., 2006).

The fynbos biome occurs on the Cape Fold Belt and adjacent lowland valleys, along the Atlantic Ocean and the southern region of the Indian Ocean. To the north and northeast, close to the Cape Fold Belt, the Succulent Karoo biome occurs (Rebelo *et al*., 2006). The main biome is bounded to the north by the Olifants River Valley and the Bokkeveld Plateau with some patches extending further north to Namaqualand (Rebelo *et al*., 2006). In the east, the Albany Thicket Biome (Eastern Cape, South Africa) defines the transition zone (Rebelo *et al*., 2006).

1.4 RESEARCH QUESTIONS

The following questions are proposed to explain the transition of vegetation in the southwestern Cape of South Africa:

1. Does climate change, linked to the development of the Benguela Upwelling System, induce a transition in the vegetation?

2. Are local vegetation fluctuations linked to water table changes which are triggered by marine transgression cycles?

3. Will dinoflagellate cysts, described by Dupont *et al*. (2011) and Roberts *et al*. (2017), allow for a biostratigraphic correlation of the timing of the establishment of the fynbos flora?

1.5 Aims

This study intends to reconstruct the palaeoecological environment and local climatic conditions during the deposition of the Elandsfontyn Formation in the Neogene through the analysis of pollen, spores and dinoflagellate cysts. This can, potentially, provide biostratigraphic information that may contribute to understanding the timing and cause of the transition of Neogene subtropical/tropical vegetation to the fynbos flora at LBW. The preliminary results of Core BH2 from Sciscio *et al*. (2013) provide inadequate evidence for a biostratigraphic evaluation due to a low sample number (ca. 40 samples) with a limited level of pollen identification and the inadequate identification of dinoflagellate cysts. A correct identification of dinoflagellate cysts, which can be very useful index fossils due to their abundance, fast evolution, and wide distribution, is necessary to establish a biostratigraphy-based chronology. A study of the Elandsfontyn Formation sediments at Saldanha Bay has demonstrated the potential of dinoflagellate cyst analysis for an age estimate of the deposits (Roberts *et al*., 2017).

This study aims to give a more detailed description of the reprocessed sediments (thus an improved palaeo-vegetation record) containing the pollen types reviewed by Sciscio *et al*. (2013), including 36 additional samples allowing a higher sample resolution, by incorporating research developments in the understanding of Miocene palynoflora in the region as provided by, e.g., Roberts *et al*. (2017) and Grimsson *et al*. (2017). Palynomorphs are critical in reconstructing the palaeoecological environment at LBW and possibly, palaeogeographical conditions which were dominant during the deposition of the Elandsfontyn Formation. Fluctuations of palynomorphs can be related to influences by the regional climate, sea level changes and local environmental conditions.

1.6 Objectives

In order to achieve the aims of this study, the following objectives are suggested:

1. Document and identify the dominant palynomorph types (pollen, spores, algae, dinoflagellate cysts) from Core BH2 using light microscopy.

2. Allocate botanical affinities to the palynomorphs to enhance the palaeoecological information and improve the biostratigraphy of the Elandsfontyn Formation using dinoflagellate cyst analysis.

3. Analyse pollen composition trends and decipher the environmental and/or climatic conditions.

CHAPTER 2: MATERIALS AND METHODS

2.1 MATERIALS – SAMPLE COLLECTION

Core BH2 from the Elandsfontyn Formation was drilled at LBW and processed for the analysis of palynomorphs. The Elandsfontyn Formation consists of fine sands and silts, alternating with carbonaceous clays and peats which are more prominent at the top of the formation (Roberts *et al*., 2011; Sciscio *et al*., 2013). The peaty material of Core BH2 is denoted by the brown to black colouration (Sciscio *et al*., 2013). The core spans a depth of ca. 33.03 m below the surface. According to Sciscio *et al*. (2013), the Elandsfontyn Formation represents overbank fines deposited in an alluvial plain on a coastal platform. A total number of 76 samples provided for this study were processed and partly reprocessed at Forschungsstelle für Paläobotanik, Münster (University of Münster/Germany) in 2015/2016. The pollen preparation procedure (Fig. 3) involved the addition of HCl, 40 % HF, Schultze's solution, KOH and a heavy liquid separation using sodium polytungstate with a density of 2.0 to obtain pollen and charcoal residues (Roberts *et al*., 2017). The lab procedure was conducted as follows (Wood *et al*., 1996):

1) Crushing of the sample with a pestle and mortar. Crushing of the sample may lead to crumbling of the charcoal, thus creating a bias of the palynomorphs

2) Coarse sieving with 250 µm (mesh width) to remove organic material, e.g., twigs and large charcoal and retrieve the residue

3) Carbonate test with 30% HCl, rinsing with aqua dest (distilled water) and decanting. HCl was used to dissolve carbonates

4) 40% HF left overnight in PET cups. This was done to remove silicates

5) Rinsing with aqua dest and decanting until the solution was neutral, measured using pH paper

6) Schultze's solution (saturated solution of $KClO_3$ and enough HNO_3 to yield approximately 10% acid). Schultze's solution acts as an oxidation agent, destroying many plant fragments and making the pollen and spores paler

7) Dehumification using 5% KOH

8) Fine sieving with 6 µm (mesh width) to retrieve the residue

9) Heavy liquid separation with sodium polytungstate (2g/ml)

10) Fine sieving with 6 µm (mesh width) of < 2g/ml of the sample (supernatant) to acquire particles ≤ 250 µm and ≥ 6 µm

11) Centrifuging with distilled water at 2500 rotations/minute (rpm) and decanting

12) Transferral of sample into Eppendorf capsule and adding 2–3 triglycerol waters

13) Mounting of slides in glycerol jelly

The samples were stored for some time at the Forschungsstelle für Paläobotanik in Münster, Germany (Roberts *et al*., 2017) and eventually returned to the Evolutionary Studies Institute.

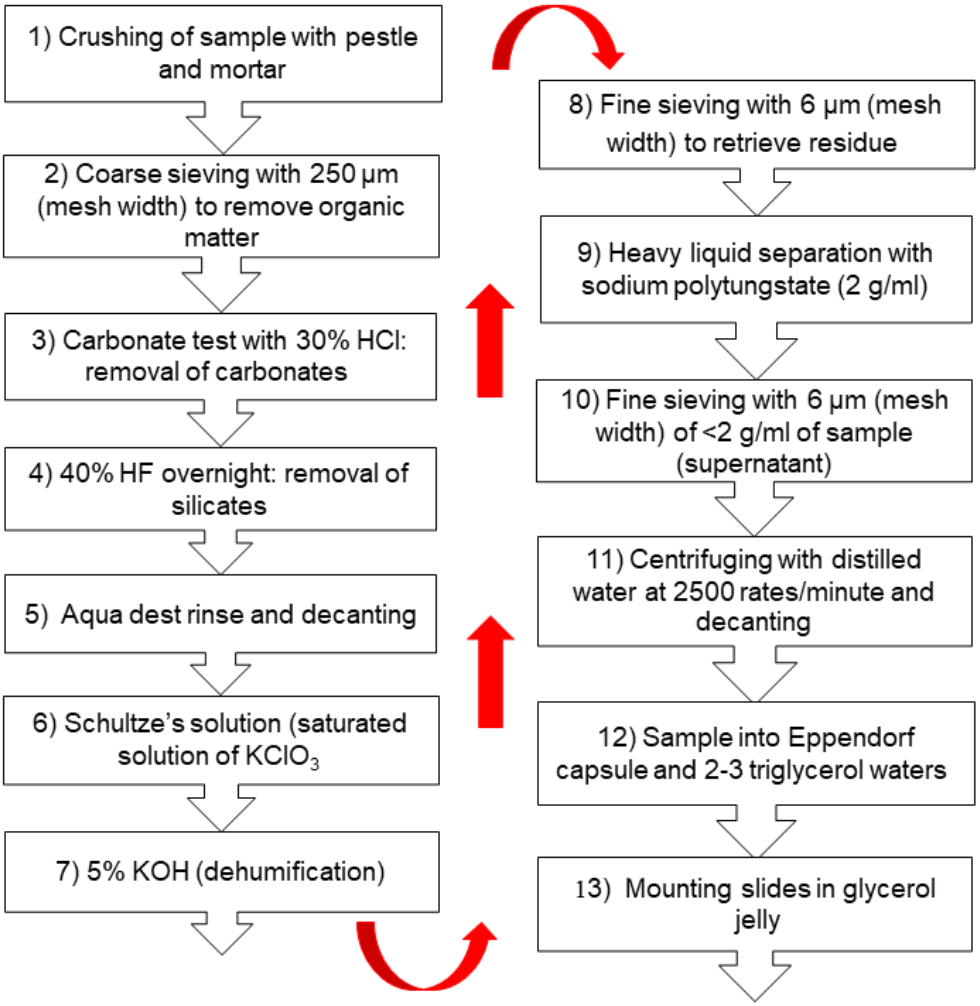

Figure 3. A summary of the pollen preparation procedure used for pollen and charcoal samples for the Elandsfontyn Formation sediments from LBW.

2.2 LIGHT MICROSCOPY

The palynomorphs (104 in total) were identified and counted per sample using a manual Olympus BX5 light microscope under ×400 and ×1000 magnification (using immersion oil) and photographed with Olympus Stream image analysis software at the Evolutionary Studies Institute, University of the Witwatersrand.

Palynomorphs were identified and the botanical affinity of fossil taxa was explored using the modern pollen reference collection at the Evolutionary Studies Institute (University of the Witwatersrand) and available literature for Miocene pollen and spores of the Western Cape palynoflora in order to provide more information regarding possible botanical affinities of certain fossil taxa (Coetzee and Rogers, 1982; Coetzee and Muller, 1984; Stuchlik *et al*., 2001; 2002; 2009; 2014; Sciscio *et al*., 2013; Roberts *et al*., 2013; 2017; Grimsson *et al*., 2017; 2018; 2019).

2.3 ANALYTICAL METHODS

2.3.1 Data documentation and statistical analysis

Following the identification of pollen grains, a percentage pollen diagram was created using TILIA 1.7.16, with terrestrial taxa considered as the pollen sums (with a maximum pollen sum of 1034). Palynomorphs were placed in ecological groups (gymnosperms; palms and other monocots; subtropical arboreal dicotyledons; thicket woodland; proto-fynbos; herbs and shrublets; aquatics and swamp plants; cryptogams; freshwater phytoplankton; marine-brackish phytoplankton; varia; fungi; microforaminiferal linings) and total sums were calculated for each group. Fungi and pollen varia were excluded from the total palynomorph sum due to the possibility that they (fungi) may have grown in the sediments after deposition and that their affinity (pollen varia) is uncertain. The total palynomorph sum was used to determine percentages of each taxon and all ecological groups at all levels. Palynomorph zonation (biostratigraphy) was conducted using CONISS (TILIA 1.7.16) to identify trends in the palynomorph composition. CONISS uses hierarchical cluster analysis to group similar palynomorphs into clusters. These clusters were then merged and used to delineate Palynomorph Abundance and Assemblage Zones (PAAZs) according to the most abundant palynomorph within a cluster. PAAZs are useful for the biostratigraphy (based on index fossils within a PAAZ) of and age correlation between geological deposits.

The Principal Components Analysis (PCA) method was used to explore the variance between palynomorph groups to understand the palaeoenvironmental changes at LBW. The JMP® Pro 16.0.0, 2021 SAS Institute Inc statistical software was used to run a PCA to emphasize variations of the study groups and to underline trends in the palynological data set. The obtained results can be used to interpret the relationship between palynomorph association and environmental changes at a given time point. According to Hammer and Harper (2006), PCA is a data dimensionality reducing method mostly used to depict the significant variance of a dataset corresponding to lower numbers of principal components capturing the most important information in a multidimensional coordinate system. For the PCA, 48 selected pollen and spore taxa) were transformed into a smaller number of principal components using presence (1) and absence (0) values instead of percentages for the taxa. This was done to eliminate the influence of the weight of selected taxa because of distributional differences related to taphonomy and corresponding natural plant distribution in the ecosystem. An Excel spreadsheet was created for the 48 selected taxa, where they were grouped according to similar habitats and implied climatic conditions. These groups consist of forest, subtropical, woodland thicket, proto-fynbos, herbs and shrublets, wetland and cryptogam species. Assigning the taxa into ecological groupings reduces and standardises the number of variables and improves the strength of any correlation trends. The percentages of the taxa at each depth level were changed to 0 or 1, according to whether they were absent or present in those depths. The spreadsheet was exported to JMP, where the analysis was run, and corresponding graphs were produced for the dataset. These graphs are interpreted in Chapter 3 (3.3) and Chapter 4 (4.1.2).

Taxa were selected based on their variation and consistent occurrence throughout the sequence, their dominance in particular depths and across the entire sequence, their importance as climatic indicators (e.g., *Peregrinipollis nigericus* and *Zonocostites ramonae*) and their reliable preservation throughout the core. Species such Podocarpaceae, Arecaceae, Oleaceae, Araliaceae, Vitaceae, Proteaceae, Asteraceae and Poaceae were also kept. Over-represented or dominant species, such as dinoflagellates, Sparganiaceae, Restionaceae and fungi were excluded to remove their distorting influence in depths 18.96–17.28 m. Algae and microforaminiferal linings were removed because they only occurred in very low percentages, and it is assumed that their influence on the palaeoenvironment was not

discernible. Depths 16.45–1.61 m are characterised by a low palynomorph content and as a result, were also excluded from the PCA. Pollen-derived patterns of change rely on comparison of the ratios of indicator pollen types over time. In order to find indicator species could signal climate parameters, such as temperature, moisture, etc., PCA was used to objectively isolate co-varying taxa in the given data set at a given data point (Hammer *et al*., 2001; Hammer and Harper, 2006). This is necessary to create the group of taxa describing the relationship between plant species and climate. The different patterns of these constellations of groups in each geological layer will also show how the climate changes can affect these constellations.

CHAPTER 3: RESULTS

3. 1 LANGEBAANWEG PALYNOFLORA

In this section, only the most abundant and ecologically important palynomorphs (pollen, spores, and dinoflagellate cysts) are described. Most of the botanical affinities were based on Stuchlik *et al*. (2001; 2002; 2009; 2014), but additional literature sources were used where required. Fossil palynomorphs are assigned names (existing nomenclature) alluding to a relation with an extant taxon based on similar morphological features. "Preceding description" refers to the morphological descriptions of the taxa based on existing or previous literature from any study across the globe where the taxa were found. "Morphological description" defines the observations and measurements made from this study. "Diagnosis" is based on morphological features which distinguish the taxon from other similar taxa. Photos of these palynomorphs can be found in Plate 1 and 2.

3.1.1 Cryptogams

3.1.1.1 Trilete spores

Genus: *Cyathidites* Couper 1953

Type: *Cyathidites australis* Couper 1953

Cyathidites australis Couper 1953 (Plate 2, Fig. H)

Preceding description: Trilete spores; well-defined laesurae comprising two-thirds of the spore radius; spores triangular, with rounded apices and concave sides; exine psilate; equatorial diameter 46–60 µm; exine 1 µm thick (Scholtz, 1985).

Morphological description: Trilete spores; concave, triangular amb with rounded apices; dimension 48–60 ×44–60 *µm*; exine 2 µm thick and 1–2 µm at the apices; surface psilate; laesurae straight, reaching about two-thirds of the spores' radius, with a length of 15–25µm.

Diagnosis: A concave triangular amb with rounded apices and laesurae measuring two-thirds of the spore radius (Scholtz, 1985; de Villiers and Cadman, 1997). Spores resemble those of *C. minor* but are rounder and have a thicker exine (Askin, 1990; de Villiers & Cadman, 1997).

Stratigraphic range: Jurassic–Cretaceous (Raine *et al*., 2011). Middle Jurassic Ohika Beds, New Zealand (Couper, 1953); Lower to Middle Jurassic sediments from Rajasthan, India (Srivastava, 1966); Upper Cretaceous Seymour Island, Antarctica (Askin, 1990); early Eocene sediments from Patagonia, Argentina (Barreda *et al*., 2020); Oligocene–Miocene of Tasmania, Australia (Tarran *et al*., 2017).

Botanical affinity: Cyatheaceae (Barreda *et al*., 2020). Couper (1953) compared this fossil taxon to the spore of the extant tree-fern *Thyrsopteris elegans*.

Geographic occurrence: Tree-ferns are distributed in the wet tropics and temperate regions of the Southern Hemisphere (Lehnert, 2009).

Distribution of fossil taxon in southern Africa: *Cyathidites* from Cretaceous sediments, the offshore Orange Basin (Sandersen *et al*., 2011; Adekola *et al*., 2014); Upper Cretaceous–middle Palaeocene sediments from Arnot Pipe (Scholtz, 1985); Tertiary sediments from Knysna (Thiergart *et al*., 1963) and Koingnass, Namaqualand (de Villiers and Cadman, 2001); late Oligocene–early Miocene, Saldanha Bay (Roberts *et al*., 2017).

Genus: *Leiotriletes* (Naumowa 1937) Potonié & Kemp 1954

Type: *Leiotriletes sphaerotriangulus* (Loose 1932) Potonié & Kemp 1954

Leiotriletes maximus (Pflug in Thomson and Pflug 1953) Krutzsch 1959 (Plate 2, Fig. K)

Preceding description: Trilete spores; triangular amb with convex sides and rounded apices; two-layered exine that is ~2 µm thick and 3.5 µm thick at apices; surface psilate to slightly punctate; laesurae straight, bifurcating at the end and reaching two-thirds of the spore radius; labrum surrounding laesurae not well-defined; dimension 75–81 µm (Stuchlik *et al*., 2001).

Morphological description: Trilete spores with a triangular to subtriangular amb consisting of convex sides; polar axis 85–114 µm and equatorial diameter 73–110 µm; exine divided into two layers, 2–5 µm thick at the sides and 2–6 µm at the apices; surface psilate; laesurae 35–55 µm, reaching 2/3 of the spore radius.

Diagnosis: Specimens from this study are ca. 20% larger than those described by Stuchlik *et al*. (2001). Additionally, they are distinguished from *L. maxoides* by the larger size and the distinctiveness of the labrum (Stuchlik *et al*., 2001).

Stratigraphic range: Oligocene–middle Miocene (Stuchlik *et al*., 2001). lower Oligocene, Kap Brewster, East Greenland (Birkenmajer *et al*., 2010); Miocene of Central Poland (Stuchlik *et al*., 2001; Worobiec *et al*., 2009); early Miocene of the Aspiras Basin, north-west Anatolia, Turkey (Durak *et al*., 2020).

Botanical affinity: Lygodiaceae (Stuchlik *et al*., 2001). *Leoitriletes maximus* spores resemble those of the extant *Lygodium* (Stuchlik *et al*., 2001).

Geographic occurrence of extant taxa: *Lygodium* spores are found in tropical and subtropical regions in the northern (America and Asia) and southern (Africa and Australia) hemispheres (Stuchlik *et al*., 2001).

Distribution of fossil taxon in southern Africa: Rare; late Oligocene–early Miocene, Saldanha Bay (Roberts *et al*., 2017).

Leiotriletes maxoides Krutzsch 1952 (Plate 2, Fig. L)

Preceding description: Trilete spores; triangular to sub-triangular amb with rounded apices; exine 1.5 µm thick, thicker at apices; surface psilate; bifurcating laesurae, reaching two-thirds of the spore radius and surrounded by a distinct labrum; dimension 56–80 µm (Stuchlik *et al*., 2001).

Morphological description: Trilete spores; triangular amb with rounded convex sides; polar axis 56–75 µm and equatorial diameter 51–70 µm; exine 1.5–2 µm thick and 2–3 µm thick at apices; psilate surface; laesurae 21–35 µm long, reaching two-thirds of the spore radius and divided into two at the ends.

Diagnosis: Distinguished by its distinct labrum and size (Stuchlik *et al*., 2001). In this study, *L. maxoides* is two-thirds smaller than *L. maximus* but sizes may overlap in some specimens (own observation).

Stratigraphic range: middle Eocene–middle Miocene (Stuchlik *et al*., 2001). upper Eocene Bohemia, Czech Republic (Knobloch and Konzalová, 1998); lower Oligocene–middle Miocene, Central Poland and lower–middle Miocene, southwestern Poland (Stuchlik *et al*., 2001); early Miocene Aspiras Basin, north-west Anatolia, Turkey (Durak *et al*., 2020); Miocene Agbada Formation, Niger Delta, Nigeria (Bankole *et al*., 2014).

Botanical affinity: Lygodiaceae (Stuchlik *et al*., 2001). Compared to the modern taxa of *Lygodium* (Stuchlik *et al*., 2001).

Geographic occurrence of extant taxa: *Lygodium* spores occur in tropical and subtropical regions in the northern (America and Asia) and southern (Africa and Australia) hemispheres (Stuchlik *et al*., 2001).

Distribution of fossil taxon in southern Africa: Rare; late Oligocene–early Miocene, Saldanha Bay (Roberts *et al*., 2017).

Leiotriletes wolffii Krutzsch 1962 (Plate 2, Fig. M)

Preceding description: Trilete spores often oriented equatorially; triangular amb formed by rounded apices and concave sides; exine 1–1.5 μm and thicker at apices; psilate surface; Laesurae surrounded by unclear thickening, nearly reach the equator; dimension 30–40 μm (Stuchlik *et al*., 2001).

Morphological description: Trilete spores; slightly concave triangular amb; polar axis 35–40 × 42–49 μm; two-layered exine 2 μm thick at both the sides and apices; inner and outer layers of exine both 1 μm; surface of spore psilate; laesurae 10–18 μm long, almost reaching the equator and often surrounded by a labrum.

Diagnosis: Dimensions of the specimens from this study can be differentiated from *L. maximus* and *L. maxoides* by the smaller size (ca. 15% smaller) and slightly concave sides (Stuchlik *et al*., 2001).

Stratigraphic range: upper Eocene–Pliocene (Stuchlik *et al*., 2001). middle–late Eocene Başçeşme Formation, western Anatolia, Turkey (Akkiraz *et al*., 2006); lower Oligocene, Kap Brewster, East Greenland (Birkenmajer *et al*., 2010); lower–middle Miocene, Poland (Stuchlik *et al*., 2001); early late Pliocene from the Red Crag Formation, eastern England (Head, 1998).

Botanical affinity: Lygodiaceae (Stuchlik *et al*., 2001). Spores are similar to those of *Lygodium* (Stuchlik *et al*., 2001).

Geographic occurrence of extant taxa: *Lygodium* spores are distributed in tropical and subtropical regions in the northern (America and Asia) and southern (Africa and Australia) hemispheres (Stuchlik *et al*., 2001).

Distribution of fossil taxon in southern Africa: late Oligocene–early Miocene, Saldanha Bay (Roberts *et al*., 2017).

Genus: *Gleicheniidites* Ross 1949 emend. Skarby 1964

Type: *Gleicheniidites senonicus* Ross 1949 emend. Skarby 1964

Gleicheniidites sp. de Villiers and Cadman 1997 (Plate 2, Fig. I)

Preceding description: Trilete spores; triangular amb with concave sides and rounded apices; exine (exospore) 1–2 µm thick but much thickened in interradial regions; surface psilate; dimension 19–35 µm (de Villiers and Cadman, 1997).

Morphological description: Trilete spores with polar axis 41–51 µm and equatorial diameter of 45–53 µm; triangular amb consisting of concave sides and slightly rounded apices; 4–8 µm thick at interradial areas - forming exine folds on the distal face - and 3–4 µm at the apices; surface psilate; laesura arms straight and reach the apices, with a length of 19–34 µm.

Diagnosis: Distal folds and thickened interradial areas distinguish the genus *Gleicheniidites* from other genera in the same family (Bolchovitina, 1966).

Stratigraphic range: *Gleicheniidites*, Jurassic-Oligocene (Bolchovitina, 1966). *Gleicheniidite*s sp. discovered at the Permian–Triassic boundary in South China (Peng *et al*., 2006); *Gleicheniidites* noted from Upper Jurassic, southern England and *Gleicheniidites senonicus* and *Gleicheniidites minor* described from Lower Cretaceous, Germany (Dörhöfer and Norris, 1977); *Gleicheniidites senonicus* from early–middle Eocene, Nevada, United States of America (Wingate, 1983); Oligocene–early Miocene in northwest Australia (Macphail and Hill, 2018).

Botanical affinity: Gleicheniaceae (Raine *et al*., 2011). Modern analogues of the genus *Gleicheniidites* include *Calymella alpina* (R. Brown) Presl, *D. dicarpa* (R. Brown) Presl and *Gleicheniastrum circinnatum* (Swartz) Nakai (Bolchovitina, 1966).

Geographic occurrence of extant taxa: Gleicheniaceae is distributed worldwide in tropical and subtropical regions (Zhenghao and Deng, 2017).

Distribution of fossil taxon in southern Africa: *Gleicheniidites* described from Cretaceous Orange Basin (Adekola *et al*., 2014); Tertiary sediments, Namaqualand (de Villiers and Cadman, 1997); Late Oligocene–Early Miocene, Saldanha Bay (Roberts *et al*., 2017).

3.1.1.2 Monolete spores

Genus: *Laevigatosporites* Ibrahim 1933

Type: *Laevigatosporites vulgaris* Ibrahim 1933

Laevigatosporites haardti (Potonié & Venitz 1934) Thomson & Pflug 1953 (Plate 2, Fig. J)

Preceding description: Monolete spores; bean-shaped in equatorial view; ellipsoidal amb; exine 1.5–2 µm thick; surface psilate; laesurae ~25 µm long; dimensions: equatorial diameter 31–45 µm and polar axis 21–26 µm (Stuchlik *et al*., 2001).

Morphological description: Bean-shaped, monolete spores; polar axis 41–57 µm and equatorial diameter of 28–39 µm; exine 1–2 µm thick; surface psilate; laesurae 28 µm long.

Diagnosis: Dimensions ca. 10% smaller than those described by Stuchlik *et al*. (2001). Spores are characteristically bean-shaped, psilate and lack perisporium (Stuchlik *et al*., 2001),

Stratigraphic range: Lower Cretaceous–Neogene (Stuchlik *et al*., 2001). Upper Campanian, Cretaceous, Sakhalin, Russia (Takahashi, 1997); Miocene, Niger Delta, Nigeria (Bankole *et al*., 2014); Palaeocene volcaniclastic sequence, North Sea (Jolley and Morton, 1992); Eocene of Czech Republic and Germany (Knobloch and Konzalová, 1998); lower Oligocene, East Greenland (Birkenmajer *et al*., 2010); Miocene, Niger Delta, Nigeria (Bankole *et al*., 2014); abundant in the Neogene of Poland (Stuchlik *et al*., 2001).

Botanical affinity: There are several families to which *Laevigatosporites* is related to, including, Aspleniaceae, Blechnaceae, Davalliaceae, Dryopteridaceae, Elaphoglossaceae, Hypolepidaceae, Lindsaeaceae, Lomariopsidaceae, Oleandraceae, Polypodiaceae, Pteridaceae, Thelypteridaceae and Vittariaceae (Stuchlik *et al*., 2001).

Geographic occurrence of extant taxa: These families occur in tropical to temperate regions on both hemispheres (Stuchlik *et al*., 2001).

Distribution of fossil taxon in southern Africa: *Laevigatosporites* sp. from Cretaceous sediments, Orange Basin (Adekola *et al*., 2014); de Villiers and Cadman (1997) described *Laevigatosporites* sp. from Tertiary sediments, Namaqualand; late Oligocene–early Miocene sediments, Saldanha Bay (Roberts *et al*., 2017); *Laevigatisporites* from late Cenozoic sediments, Noordhoek (Coetzee, 1978).

3.1.2 Gymnosperms

3.1.2.1 Inaperturate pollen

Genus: *Araucariacites* Cookson ex Couper 1953

Type: *Granulatisporites (Araucariacites) australis* Cookson 1947

cf. *Araucariacites australis* Cookson ex Couper 1953 (Plate 1, Fig. D)

Preceding description: Inaperturate; large pollen grains; flattened and crumpled; granulate exine, 0.5 µm thick; dimension: 50–60 µm (Scholtz, 1985).

Morphological description: Inaperturate; large, circular grains 67–85 µm; exine 1–2 µm thick; granulate surface.

Diagnosis: Specimens described from this study are ca. 5% larger than those described by Scholtz (1985). cf. *Araucariacites australis* is characteristically large, inaperturate and in most cases, crumpled (Scholtz, 1985). SEM studies on the fossil specimen and modern Araucariaceae pollen will be necessary to verify the identification of this taxon as it was only identified applying light microscopy.

Stratigraphic range: Triassic–Neogene (Raine *et al*., 2011). Upper Jurassic–Lower Cretaceous, South India (Jha *et al*., 2017); Late Triassic, Svalbard (Paterson and Mangerud, 2015); Upper Cretaceous–Palaeocene, Seymour Island, Antarctica (Askin, 1990); late Eocene–Oligocene, Waikato Basin, New Zealand (Pocknall, 1991); early late Oligocene, southern South America (Barreda *et al*., 2009); Araucariaceae from upper Miocene–lower Pliocene, southeastern Australia (Macphail, 1999); Tertiary, Kerguelen Archipelago (Cookson, 1947).

Botanical affinity: Araucariaceae (Scholtz, 1985). Associated with the recent genus *Araucaria* (Scholtz, 1985).

Geographic occurrence of extant taxa: *Araucaria* occurs in temperate and tropical regions along the edges of the Pacific and particularly dominant in forests of the Southern Hemisphere (Dettmann and Jarzen, 1990), however, it was formerly widespread in both hemispheres in the Mesozoic (Dettmann and Jarzen, 1990; Dettmann and Clifford, 2005).

Distribution of fossil taxon in southern Africa: Lower Cretaceous sediments from the east coast of southern Africa (Scott, 1976; McLachlan and Pieterse, 1978); Cretaceous sediments in the interior (Scholtz and Deacon, 1982); Lower Cretaceous sediments at Arnot Pipe (Scholtz, 1985); Cretaceous sediments, Orange Basin (Adekola *et al*., 2014); *Araucariacites* sp. from Eocene sediments, Namibian coast (Scott *et al*., 2006); Tertiary sediments, Namaqualand (de Villiers and Cadman, 1997); late Oligocene–early Miocene, Saldanha Bay (Roberts *et al*., 2017).

3.1.2.2 Bisaccate pollen

Genus: *Podocarpidites* Couper 1953

Type: *Podocarpidites ellipticus* Cookson 1947 ex Couper 1953

Podocarpidites ellipticus Cookson 1947 ex Couper 1953 (Plate 1, Fig. B)

Preceding description: Bisaccate or (rarely) trisaccate; circular to ellipsoidal corpus; exine thick at proximal face, forming verrucae; sacci semi-circular and larger than corpus; surface on sacci alveolate and alveolar layer 3.5–4.0 µm thick; torn muri on alveolar layer; alveolae elongate at attachment area, where axis of attachment shorter than breadth of corpus; verrucae 1.5–2.0 µm under SEM, covered by microgranules (0.2–0.5 µm); sacci surface smooth (Stuchlik *et al*., 2002).

Morphological description: Pollen grains bisaccate; overall width 44–70 µm. Corpus elliptical; corpus width 29–40 µm and length of 38–49 µm in polar view; corpus biconvex in equatorial view, with depth 19–23 µm; sacci elliptical in polar view, with length 36–47 µm – about 80% of the corpus – and width10–25 µm; saccus overlap (attachment area) 6–11 µm, constituting ~30% of corpus breadth; sacci regularly reticulate to alveolate, with muri 1–1.5 µm wide and lumina 2–5 µm wide; reticulation is coarse and decreases towards the sacci margins.

Diagnosis: The reticulum is widely reticulate and sacci are elliptical (Haskell, 1968). Differentiated from *Podocarpidites* sp. (from this study) by elliptical sacci that are

hapxylonoid (outline of sacci is continuous with the corpus or almost the same length as the corpus) (Song *et al*., 2012).

Stratigraphic range: Palaeogene–Miocene (Stuchlik *et al*., 2002). Jurassic-Cretaceous, western Australia (Balme, 1957); Upper Cretaceous–early Palaeogene, Northern Iran (Rabbani *et al*., 2020); early Eocene, Patagonia, Argentina (Barreda *et al*., 2020); lower Oligocene-middle Miocene, Poland (Stuchlik *et al*., 2002).

Botanical affinity: Podocarpaceae (Stuchlik *et al*., 2002). Pollen grains are similar to pollen of modern *Podocarpus* L'Herit. Ex Pers. (Stuchlik *et al*., 2002) and *Afrocarpus*.

Geographic occurrence of extant taxa: *Podocarpus* is distributed throughout the subtropical-tropical montanes of the Southern Hemisphere (rainforests of South America; eastern Australasia) and to the north in Mexico, West Indies, southern China, southern Japan and Himalayas (Dettmann and Jarzen, 1990; Page, 1990; Stuchlik *et al*., 2002).

Distribution of fossil taxon in southern Africa: *Podocarpidites* from Upper Cretaceous sediments from the Orange Basin (Sandersen *et al*., 2011) and Oligocene–early Miocene sediments, Noordhoek (Sciscio, 2011); *Podocarpidites* spp. described from Eocene sediments of southern Namibian coast (Scott *et al*., 2006); Tertiary sediments from Koingnaas, Namaqualand (de Villiers and Cadman, 1997; de Villiers and Cadman, 2001). *Podocarpidites* spp. from late Oligocene–early Miocene, Saldanha Bay (Roberts *et al*., 2017) and early to late Miocene, Rondeberg (Sciscio, 2011; Roberts *et al*., 2013); Previous studies from LBW (Coetzee and Rogers, 1982; Sciscio *et al*., 2013).

Podocarpidites sp. Scholtz, 1985 (Plate 1, Fig. A)

Compare: *Alisporites grandis* (Cookson) Dettmann 1963

Preceding description: Circular corpus in polar view; large, semi-circular sacci; reticulum of sacci coarse, discontinuous towards margins; grain often collapsed, resulting in a narrow tenuitas; length of grain 88–119 µm; corpus diameter 60–63 µm; sacci length 68–75 µm; sacci width 25–32 µm; distance between attachment zones 25–33 µm; exine 4–8 µm (Scholtz, 1985).

Morphological description: Bisaccate; overall diameter of the grain 70–118 µm; large circular corpus 30–58 µm long and 31–47 µm wide in polar view; sacci large and semi-

circular, 32–50 µm wide and 40–67 µm long; sacci with coarse reticulum, becoming less prominent towards sacci margins; muri 1–2 µm and lumina 3–7 µm; attachment zone 20–23 µm in equatorial view.

Diagnosis: Laterally attached sacci that are diploxylonoid and semi-circular, appearing to be discontinuous with the corpus (Song *et al*., 2012). Sacci are much larger and almost 2x wider than those of *Podocarpidites ellipticus* (own observation). Scholtz (1985) compared *Podocarpidites* sp. to *Alisporites grandis*, according to the description of Haskell (1968, p. 217).

Stratigraphic range: Cretaceous (Raine *et al*., 2011). Upper Jurassic, western Australia Lower Cretaceous, Canada (Haskell, 1968); Lower Cretaceous, Antarctica (Riding *et al*., 1998); Cretaceous, Argentina (Archangelsky and Gamerro, 1967); Neogene, central Africa (Sah, 1967).

Botanical affinity: Podocarpaceae (Scholtz, 1985). Modern analogues of *Alisporites grandis* are *Podocarpus latifolius*, *Podocarpus elongatus* and *Podocarpus henkelii* (Martin, 1959; Pocknall, 1981; Scholtz, 1985). These three species, including *Podocarpus falcatus*, constitute the southern African species of *Podocarpus* (*Afrocarpus*) (Barker *et al*., 2004).

Geographic occurrence of extant taxa: Podocarpaceae are distributed in subtropical-tropical montane regions in the Southern Hemisphere (Page, 1990) in regions such as South America, Australia, Mexico, West Indies countries, southern China and Japan and the Himalayas (Dettmann and Jarzen, 1990; Stuchlik *et al*., 2002). The three species, including *Podocarpus falcatus*, constitute the southern African species of *Podocarpus* (*Afrocarpus*) and grow in warm-temperate to subtropical regions including the Cape region (Barker *et al*., 2004).

Distribution of fossil taxon in southern Africa: Upper Cretaceous–middle Palaeocene sediments, Arnot Pipe (Scholtz, 1985); *Alisporites* sp. from Tertiary sediments, Koingnaas, Namaqualand (de Villiers and Cadman, 2001).

3.1.3 Angiosperms

3.1.3.1 Monocolpate pollen

Genus: *Arecipites* Wodehouse emend. Anderson 1960

Type: *Arecipites punctatus* (Wodehouse 1933) Potonié 1958

Arecipites otagoensis (Couper 1960) Mildenhall & Pocknall 1989 (Plate 1, Fig. E)

Preceding description Monosulcate pollen grains; broad and long colpus; surface smooth to scabrate; exine 2 µm, thins around colpus; length: 30–40 µm; breadth 17–25 µm; depth: 17–22 µm (*Monosulcites otagoensis*, Couper 1960, p. 70**)**.

Morphological description: Pollen grains monocolpate, semitectate; polar axis 50–60 µm, equatorial diameter 23–45 µm; shape subprolate to prolate (P/E: 1.22–2.12); length of colpus 40–56 µm; colpus reaches equator and open with margo (2–3 µm); exine 2.5–4 µm thick; surface scabrate to microreticulate; lumina 0.2–0.55 µm and muri ~0.95–1 µm.

Diagnosis: *Arecipites otagoensis* from this study is morphologically similar to *Monosulcites otagoensis*, despite specimens from this study being ca. 10% larger. *Arecipites otagoensis* is characterised by a relatively smooth exine (Conran *et al*., 2015). This feature differentiates the taxon from *Arecipites plectilimuratus* (not identified in this study), which has a distinct reticulum with duplibaculate muri (Scholtz, 1985).

Stratigraphic range: Palaeogene–Neogene, New Zealand (Raine *et al*., 2011; Conran *et al*., 2015). Late Cretaceous–Cenozoic, across New Zealand (Conran *et al*., 2015); Eocene–Oligocene, New Zealand (Pocknall, 1991); Miocene, southern South America (Barreda and Palazzesi, 2014); *Monosulcites otagoensis* from Pliocene, New Zealand (Mildenhall, 2003).

Botanical affinity: Arecaceae (Stuchlik *et al*., 2014; Conran *et al*., 2015). Seven genera of palms are distributed in southern Africa and only six palm species, including *Jubaeopsis caffra*, *Raphia australis*, *Borassus aethiopum*, *Hyphaene coriacea*, *Hyphaene petersiana* and *Phoenix reclinata*, are indigenous to South Africa (Siebert *et al*., 2010; Siebert and Struwig, 2019).

Geographic occurrence of extant taxa: Arecaceae are distributed in warm temperate to tropical zones (Stuchlik *et al*., 2014; Conran *et al*., 2015).

Distribution of fossil taxon in southern Africa: *Arecipites otagoensis* from late Oligocene–early Miocene sediments, Saldanha Bay (Roberts *et al*., 2017); several types of Palmae described from other sites, including: Tertiary sediments of Saldanha region (Coetzee, 1980; 1983), Koingnaas, Namaqualand (de Villiers and Cadman, 2001), previous studies from LBW (Coetzee and Rogers, 1982; Sciscio *et al*., 2013), middle Miocene Makhulu Quarry sediments, Knysna (Carr *et al*., 2010; Goble, 2015), Miocene sediments from Rondeberg

(Roberts *et al*., 2013) and early to middle Miocene, Noordhoek (Coetzee, 1978; Sciscio *et al*., 2016).

3.1.3.2 Monoporate pollen

Genus: *Cyperaceaepollis* Krutzsch 1970

Type: *Cyperaceaepollis neogenicus* Krutzsch 1970

Cyperaceaepollis piriformis Thiele-Pfeiffer 1980 (Plate 2, Fig. B)

Preceding descriptions: Monoporate, heteropolar pollen grains; pore on the distal pole; lateral lacunae beyond ends of the poles; pear-shaped, with round distal pole and narrow proximal pole; equatorial diameter 32–56 µm and polar axis 74–82 µm; pore 10–12 µm wide, pieces of ectexine inside; three lacunae with a length of 5.0 µm in the middle section of the grain; exine ~1 µm thick; surface finely scabrate, scabrae 1 µm (Stuchlik *et al*., 2009).

Morphological description: Monoporate pollen grains; polar axis 42–64 µm; equatorial diameter 28–60 µm; Grains are prolate-spheroidal to prolate (P/E ratio: 1.05–1.52); narrow proximal pole and a broad distal pole, forming pear-shaped grains; exine 1–2 µm; surface of grains scabrate to granulate; lacunae on the sides of grains, not strongly visible.

Diagnosis: Specimens from this study are ca. 15% smaller than those described by Stuchlik *et al*. (2009), possibly due to different mounting mediums. *Cyperaceaepollis piriformis* has a distinctively constricted distal pole, resulting in a pear-shape which differs from other species of *Cyperaceaepollis* (Stuchlik *et al*., 2009).

Stratigraphic range: upper Eocene–Miocene (Stuchlik *et al*., 2009). upper Oligocene, western Germany (Poschmann *et al*., 2010); lower and middle Miocene in central and northern Poland (Stuchlik *et al*., 2009; Worobiec, 2009; Worobiec and Szulc, 2016); Pliocene–Pleistocene, Greece (Mulder *et al*., 2000).

Botanical affinity: Cyperaceae (Stuchlik *et al*., 2009). Pollen grains similar to extant species of *Cladium mariscus* (L.) Pohl. (Stuchlik *et al*., 2009).

Geographic occurrence of extant taxa: *Cladium* occurs in tropical and subtropical regions and is common in Europe (Stuchlik *et al*., 2009).

Distribution of fossil taxon in southern Africa: Rare in the Neogene record; late Oligocene–early Miocene sediments, Saldanha Bay (Roberts *et al*., 2017). *Cladium mariscus*

from archaeological records includes: 8000-year-old sediments from Groenvlei Lake, Knysna (Martin, 1968) and Middle Stone Age (77 to 38 ka), Sibudu Cave on the eastern coast of South Africa (Wadley *et al*., 2011; Sievers, 2015).

Genus: *Graminidites* Cookson 1947

Type: *Graminidites media* Cookson 1947

Graminidites cf. *crassiglobosus* (Trevisan 1967) Krutzsch 1970 (Plate 1, Fig. Y)

Preceding description: Monoporate, spheroidal pollen grains; equatorial diameter 23–26 μm; circular pore on distal side, 1.5–2.0 μm wide; annulus 1–2 μm wide and 2.5 μm thick; exine ~1 μm; surface finely granulate (Stuchlik *et al*., 2009).

Morphological description: Pollen monoporate; equatorial diameter 20–27 × 21–28 μm; pollen shape oblate to prolate spheroidal (P/E: 0.89–1.10); exine 1-1.5 μm thick; surface psilate to scabrate; pore small, with diameter 2–3 μm; annulus diameter 5–9 μm and with a thickness of 1.5–2.5 μm.

Diagnosis: The annulus of measured specimens from this study is ca. 10% wider than the specimens described in Stuchlik *et al*. (2009). *Graminidites* cf. *crassiglobosus* is differentiated from *Graminidites* cf. *neogenicus* by the smaller size (ca. 10% smaller), a thin exine that is usually folded and the psilate surface (own observation).

Stratigraphic range upper Oligocene–Pliocene (Stuchlik *et al*., 2009). Miocene–Pliocene, central and western Poland (Stuchlik *et al*., 2009; Worobiec, 2009; Ziembińska-Tworzydło, 1974); *Graminidites* undiff. (*G. crassiglobosus*, *G. gramineoide*s, *G. laevigatus*, *G. neogenicus*, *G. punctatus*, *G. subtiliglobosus*), Pliocene-Pleistocene, Greece (Mulder *et al*., 2000).

Botanical affinity: Poaceae (Stuchlik *et al*., 2009).

Geographic occurrence of extant taxa: Poaceae is cosmopolitan (occurs in all climatic zones (Stuchlik *et al*., 2009), including crop land, temperate grasslands and tropical savannas (Willis, 1966; Gibson, 2009).

Distribution of fossil taxon in southern Africa: late Oligocene–early Miocene, Saldanha Bay (Roberts *et al*., 2017); Sciscio *et al*. (2013) identified two species, Poaceae <25 μm and

Poaceae >25 *µm*, of which the former can be compared to *Graminidites* cf. *crassiglobosus*; *Graminidites* abundant in iddle Miocene deposits of Noordhoek and Saldanha region (Coetzee and Rogers, 1982; Coetzee, 1983), although rare in Knysna (Carr *et al*., 2010); *Graminidites* sp. from middle Miocene–lower Pliocene, Cape Basin, South Africa (Udeze and Oboh-Ikuenobe, 2005).

Graminidites cf. *neogenicus* Krutzsch 1970 (Plate 1, Fig. Z-AA)

Preceding description: Monoporate, heteropolar pollen grains; outline oval in in equatorial view; dimensions: 28–30 × 35–37 µm; circular to oval pore on distal side, with a diameter of ~2.5 µm; annulus 2.0–2.5 µm broad; exine 1.5–2.0 µm; surface finely granulate (Stuchlik *et al*., 2009).

Morphological description: Pollen monoporate; medium-sized; diameter 40–47 × 35–39 µm and the shape is prolate spheroidal to sub-prolate (P/E: 1.03–1.22); exine 1.5–2 µm thick; scabrate to finely granulate surface; pore 3–4 µm; annulus 10–15 µm in diameter and 3–4 µm thick.

Diagnosis: This species differs from *Graminidites* cf. *crassiglobosus* by its size and the granulate surface texture (own observation). It can be compared to the species with a diameter ≥ 25 *µm*, described by Sciscio *et al*. (2013).

Stratigraphic range: Miocene–Pliocene (Stuchlik *et al*., 2009). Neogene, Egypt (Kedves, 1981); middle Miocene, central and southwestern Poland (Stuchlik *et al*., 2009).

Botanical affinity: Poaceae (Stuchlik *et al*., 2009).

Geographic occurrence of extant taxa: Cosmopolitan (Stuchlik *et al*., 2009).

Distribution of fossil taxon in southern Africa: Can possibly be compared to "Poaceae > 25 µm", described by Sciscio *et al*. (2013).

Distribution of fossil taxon in southern Africa: Can possibly be compared to "Poaceae > 25 µm", described by Sciscio *et al*. (2013).

Genus: *Milfordia* Erdtman 1960 emend. Krutzsch 1970

Type: *Milfordia incerta* (Thomson & Pflug, 1963) Krutzsch, 1961

Milfordia hypolaenoides Erdtman, 1960 (Plate 2, Fig C)

Preceding description: Pollen grains monoporate, semitectate, tectum perforate; amb semi-circular; equatorial diameter 35–45 μm; large, circular to oval centrolepidoid pore, annulus absent; ragged margin around pore, slightly thickened pieces of ectexine; ectopore 6–13 × 18–22 μm; exine 1.5 μm thick; surface punctate with circular and regularly spaced puncta; puncta penetrate into ectexine with diameter less than 1 μm; surface between puncta granulate (Stuchlik *et al*., 2009).

Morphological description: Pollen grains monoporate; dimensions 22–30 μm × 24–32 μm; shape sub-oblate to prolate spheroidal (P/E: 0.78–1.08); centrolepidoid pore on distal face, pore diameter 4–7 μm; narrow annulus with diameter 7–11 μm and thickness 1–2 μm; margin ragged and loose pieces of ectexine inside pore; exine with thickness 1.5–2 μm; surface composed of fine punctae or scrobiculi, ranging from 0.5–1 μm; surface between puncta smooth to scabrate.

Diagnosis: *Milfordia hypolaenoides* from this study is only ca. 2% smaller than that described by Stuchlik *et al*. (2009), however, other features are similar. *Milfordia hypolaenoides* has a centrolepidoid pore, regularly spaced puncta and is smaller than *Milfordia homeopunctatus* (Scholtz, 1985; Stuchlik *et al*., 2009). Australian species of *Hypolaena* tend to be centrolepidoid, whereas the majority of southern African species are graminoid (Chanda, 1966).

Stratigraphic range: Palaeocene–middle Miocene (Stuchlik *et al*., 2009). Establishment of Restionaceae, Upper Cretaceous or Palaeogene (Scholtz, 1985); Upper Cretaceous, North America (Jarzen, 1978); lower Palaeocene–Miocene, Europe (Muller, 1981); Eocene–Oligocene, Australia (Stover and Partridge, 1973; Dettmann and Clifford, 2000; Macphail and Hill, 2018); Neogene–Pleistocene, New Zealand (Raine *et al*., 2011; Conran *et al*., 2015).

Botanical affinity: Restionaceae (Scholtz, 1985; Stuchlik *et al*., 2009). It can be compared to the modern-day species of *Hypolaena* R. Br. *Lepyrodia* R. Br. Centrolepidaceae (Stuchlik *et al*., 2009), which are typical for Australian species of Restionaceae (Chanda, 1966; Scholtz, 1985).

Geographic occurrence of extant taxa: Distributed in southern South Africa, Australia, New Zealand, Madagascar, southeastern China and Vietnam (Stuchlik *et al*., 2009)

Distribution of fossil taxon in southern Africa: Upper Cretaceous–middle Palaeocene, Arnot Pipe (Scholtz, 1985); Neogene, Knysna lignites (Thiergart *et al*., 1963; Carr *et al*., 2010); Restionaceae from late Oligocene–early Miocene, Saldanha Bay (Roberts *et al*., 2017), early–middle Miocene, Noordhoek (Sciscio, 2016; Sciscio *et al*., 2016); early to late Miocene, Rondeberg (Roberts *et al*., 2013; Sciscio, 2016) and a previous age of middle Miocene at LBW(Coetzee and Rogers, 1982; Sciscio *et al*., 2013).

Milfordia homeopunctatus (*Restioniidites homeopunctatus* Hekel 1972; *Restioniidites pascuali* Archangelsky 1973; *Milfordia homeopunctata* (McIntyre 1965) Stover and Partridge 1973 (Plate 2, Fig. D)

Compare: *Milfordia* sp. (Scholtz, 1985)

Preceding description: Large, monoporate pollen grains; small and circular pore, with defined margin; exine medium thick; surface finely scrobiculate; outline of grain smooth; dimensions 53 × 39 μm, pore 8 μm wide, exine 2 μm (Scholtz, 1985).

Morphological description: Pollen grains monoporate; diameter 50–79 × 51–77 μm, grains suboblate to sub-prolate (P/E: 0.87–1.15); large graminoid pore, with diameter 4–11 μm; diameter of margin 7–25 μm and thickness 1–8 μm; exine 1.5–3.0 μmthick, with a punctate or scrobiculate surface consisting of 0.5–1 μm punctae or scrobiculi.

Diagnosis: Specimens described from this study are ca. 10% larger than those described in Scholtz (1985). The graminoid aperture, smoother exine and spherical outline distinguish *Milfordia homeopunctatus* from *Milfordia hypolaenoides* (Scholtz, 1985). Additionally, punctae or scrobiculi are more pronounced and closer to each other (own observation).

Stratigraphic range: Upper Cretaceous–Miocene (Scholtz, 1985). Eocene–Oligocene, Australia (Dettmann and Clifford, 2000; Macphail and Hill, 2018); Palaeocene of America and Europe (Muller, 1981); described as *Milfordia homeopunctatus* from Eocene-Miocene sediments, Australia (Stover and Partridge, 1973; Martin, 1990) and Palaeogene-Neogene sediments, New Zealand (Raine *et al*., 2011).

Botanical affinity: Restionaceae (Scholtz, 1985). This species resembles the pollen of modern-day *Restio subverticillatus* (Scholtz, 1985).

Geographic occurrence of extant taxa: Restionaceae occurs in the Southern Hemisphere, predominantly in South Africa and Australia and additionally in New Zealand, Madagascar, Chile, Patagonia and southeastern Asia (Ladd, 1977). Graminoid *Restio subverticillatus*-type is mainly distributed in South Africa and some parts of Australia (Martin, 1990).

Distribution of fossil taxon in southern Africa: *Restio-subverticillatus*-type described from Upper Cretaceous–middle Palaeocene, Arnot Pipe (Scholtz, 1985)

Genus: *Sparganiaceaepollenites* Thiergart 1937

Type: *Sparganiaceaepollenites convexus* Thiergart, 1937

Sparganiaceaepollenites barungensis Harris 1972 (Plate 2, Fig. E-F)

Preceding description: Monoporate; pore 5–7 μm, with irregular edges; outline oval with rounded ends; exine reticulate, with simplibaculate muri; lumina ~2 μm and uniform in size; length: 28–40 μm (Scafati *et al*., 2009).

Morphological description: Monoporate pollen grains; dimension 23–40 μm × 25–34 μm; suboblate to subprolate shape (0.89–1.24); Circular porus, diameter 2–4 μm; raised margin around pore with diameter 7–11 μm and thickness 3–5 μm; exine 1–2 μm thick; surface reticulate, with a regular heterobrochate reticulum comprised of angular lumina; lumina 0.5–2.0 μm broad and muri simplibaculate and 0.2–0.8 μm thick; luminae decrease and become finer towards pore.

Diagnosis: *Sparganiaceapollenites barungensis* is differentiated from *Sparganiaceaepollenites sphericus* (not described in this study) by the heterobrochate reticulum with brochi that are uniform in size and simplibaculate muri (Mildenhall and Crosbie, 1979). *Sparganiaceaepollenites sphericus* is characterised by a duplibaculate muri and a coarser reticulum (Mildenhall and Crosbie, 1979).

Stratigraphic range: late Eocene–late Miocene (Harris, 1972); Palaeogene–early Neogene, Argentina (Palazzesi and Barreda, 2007; Scafati *et al*., 2009); Eocene–Miocene (Martin, 1990; Dettmann and Clifford, 2000); Palaeogene–Neogene, New Zealand (Mildenhall and

Crosbie, 1979; Raine *et al*., 2011); *Sparganiaceaepollenites* recorded from the Palaeogene of North America (Farley and Traverse, 1990).

Botanical affinity: Sparganiaceae (Mildenhall and Crosbie, 1979). Mildenhall and Crosbie (1979) proposed that the Australian *Aglaoreidia qualumis* and *Sparganiaceaepollenites barungensis* are fossil members, and that they are possibly one species. Pollen grains of *Sparganiaceaepollenites* are similar to modern species of *Sparganium* L. (Sparganiacee) and *Typha* L. (Typhaceae) (Stuchlik *et al*., 2009). However, modern *Sparganium* and *Typha* do not have a protruding pore (Punt, 1975).

Geographic occurrence of extant taxa: *Sparganiaceaepollenites barungensis* was distributed in wetland environments around freshwater lakes (Mildenhall and Crosbie, 1979; Coetzee and Muller, 1984). *Sparganium* and *Typha* are cosmopolitan species that are dominantly distributed in temperate regions of the Northern Hemisphere (Stuchlik *et al*., 2009).

Distribution of fossil taxon in southern Africa: *A. qualumis,* Palaeocene sediments at Koingnaas, South Africa (de Villiers and Cadman, 2001); late Oligocene–early Miocene, Saldanha Bay (Roberts *et al*., 2017); early Miocene, Noordhoek (Coetzee and Muller, 1984; Coetzee, 1993; Sciscio *et al*., 2011); middle Miocene (?)LBW, (Coetzee and Rogers, 1982; Sciscio *et al*., 2013); Noordhoek); late Neogene lignites, Knysna (Goble, 2015).

3.1.3.3 Tricolpate pollen

Genus: *Peregrinipollis* Clarke 1966

Type: *Peregrinipollis nigericus* Clarke 1966

Peregrinipollis nigericus Clarke 1966 (Plate 1, Fig. P)

Preceding description: Tricolpate; subspherical to prolate; colpi indistinct, delineated by sub-parallel muri; rope-like muri forming a reticulum, 2-5 µmwide; lumina 4–5 µm; endexine (?) attached to reticulum by short rods 1–2 µm broad and 1–2 µm high; apocolpia thin, covered with verrucae 0.5–1.5 µm broad and 1 µm high; mesocolpia reticulate; rope-like muri merge with the granulate-verrucose surface where the apocolpia and mesocolpia meet; equatorial diameter 32–50 µm, polar dimension 36–52 µm (Clarke, 1966).

Morphological description: Tricolpate pollen grains; polar axis 53–62 µm, equatorial axis is 26–35 µm in equatorial view; grains prolate to perprolate (P/E: 1.77–2.04); colpi long and

faint, with length up to 54 µm and breadth 2–4 µm; exine very thin; surface coarsely reticulate; reticulum heterobrochate, with lumina 2–11 µm and muri 0.5–1 µm; luminae smaller towards pole.

Diagnosis: Mesocolpia and apocolpia of grains not preserved in the two recorded specimens. Distinctly reticulate mesocolpia and verrucose apocolpia differentiates the taxon from any other palynomorphs (Clarke, 1966)**.**

Stratigraphic range: upper Tertiary, Niger Delta, Nigeria (Clarke, 1966). Upper Cretaceous–Tertiary, Cameroon (Salard-Cheboldaeff, 1981); West Africa (Niger Delta, Nigeria) in late Eocene–Pleistocene sediments (Oboh and Salami, 1989; Olayiwola *et al*., 2017; Okeke *et al*., 2021); Oligocene–Miocene, Ethiopia (Wolela, 2014); late Miocene–Pliocene, southeast Sudan (Eisawi and Schrank, 2008).

Botanical affinity: *Brachystegia* (Roberts *et al*., 2017). The pollen grains of extant *Brachystegia eurycoma* and *Brachystegia nigerica* are similar to that of the fossil *P. nigericus* (Sowunmi, 1973).

Geographic occurrence of extant taxa: *Brachystegia* is one of the dominant genera in the miombo woodland, which is situated in sub-humid tropical regions of south-central Africa (Frost, 1996; Pienaar *et al*., 2015). The South African miombo woodland, or relict thereof, is situated in the north-eastern Soutpansberg region of the Limpopo Province, where it is dominated by a single species known as *Brachystegia spiciformis* Benth. (Botha, 2002; Saidi and Tshipala-Ramatshimbila, 2006; Pienaar *et al*., 2015).

Distribution of fossil taxon in southern Africa: Rare; early Miocene, Saldanha Bay (Roberts *et al*., 2017).

3.1.3.4 Tricolporate pollen

Genus: *Cupuliferoipollenites* Potonié 1951

Type: *Cupuliferoipollenites pusillus* Potonié 1934 ex Potonié 1960

Cupuliferoipollenites oviformis (Potonié 1934) Potonié 1951 ex Potonié 1960 (Plate 1, Fig. H)

Preceding description: Tricolporate, tectate pollen grains; polar axis 10–18 µm, equatorial diameter 6–12 µm; shape of pollen grains prolate (P/E ~2); narrow or rounded apocolpia;

colpi with thickened costa colpi not reaching poles; circular pores 0.5–1 µm; two-layered exine 1 µm thick; smooth to scabrate surface, covered by flat rodlets under SEM (Stuchlik *et al*., 2014).

Morphological description: Pollen grains tricolporate; polar axis 15–23 µm, equatorial diameter 9–17 µm in equatorial view; shape prolate (P/E: 1.36–1.69); colpi, with costa colpi, 1–3 µm deep and 12–14 µm long, not reaching poles; apocolpia narrow, with a diameter 2–3 µm; pores circular, with equatorial diameter 2 µm and meridional diameter 1-3 µm; exine, 1–2 µm; surface psilate.

Diagnosis: *Cupuliferoipollenites oviformis* differs from *Cupuliferoipollenites pusillus* (polar axis 19–25 µm; equatorial diameter 10–17 µm) – not identified from this study – only by its smaller size (Stuchlik *et al*., 2014).

Stratigraphic range: Palaeocene–Miocene (Ziembińska-Tworzydło *et al*., 1994). Upper Cretaceous–Eocene, Tibet (Jianguo *et al*., 2008); early Eocene, Argentina (Barreda *et al*., 2020). middle Miocene, central Poland (Worobiec *et al*., 2021); late Neogene deposits, southeastern U.S.A. (Worobiec *et al*., 2013).

Botanical affinity: Fagaceae (Stuchlik *et al*., 2014). *Cupuliferoipollenites oviformis* displays morphological similarities to the extant subfamily, Castaneoideae, particularly pollen grains of *Castanea*, *Castanopsis*, *Lithocarpus*, *Passania* (Muller, 1981; Ziembińska-Tworzydło *et al*., 1994; Stuchlik *et al*., 2014).

Geographic occurrence of extant taxa: Tropical, subtropical and warm-temperate regions in the Northern Hemisphere, such as Asia, Europe and North America (Ziembińska-Tworzydło *et al*., 1994; Stuchlik *et al*., 2014).

Distribution of fossil taxon in southern Africa: Small Fagaceae pollen from Neogene lignites, Knysna (Thiergart *et al*., 1963; Goble, 2015); late Oligocene–early Miocene sediments, Saldanha Bay; previously dated middle Miocene Elandsfontein Formation sediments,LBW (Sciscio *et al*., 2013).

Genus: *Oleoidearumpollenites* Nagy 1969

Type: *Oleoidearumpollenites reticulatus* Nagy 1969

Oleoidearumpollenites reticulatus (Plate 1, Fig. K)

Preceding description: Tricolporate, reticulate pollen grains; polar axis 16–29 µm, equatorial diameter 15–23 µm, prolate spheroidal to subprolate (P/E 1.06–1.26); colpi narrow, 1–2 µm thick, almost reaching the poles; circular pores 1–2 µm wide; exine 4 µm thick; polygonal lumina 2–5 µm forming reticulum; muri simplocolumellate, up to 5 µm under SEM and lumina breadth equal to muri breadth (Stuchlik *et al*., 2015).

Morphological description: Pollen grains tricolporate; polar axis 21–36 µm, equatorial diameter 23–33 µm in equatorial view; shape of pollen grains oblate-spheroidal to prolate-spheroidal (P/E: 0.91–1.09); colpi 2 µm deep and 8–18 µm long, not reaching poles; pores circular, with meridional diameter 0.5–1 µm ; exine 2.5–4 µm thick and surface with heterobrochate reticulum; simplicolumellate muri 0.5-1 µm broad, with columellae 0.5–3 µm long; lumina polygonal.

Diagnosis: Specimens from this study are ca. 5%bigger than those described by Stuchlik *et al*. (2014). Distinguishable from *Oleadearumpollenites microreticulatus* (not described in this study) by larger polygonal lumina and a bigger size (Stuchlik *et al*., 2014).

Stratigraphic range: *Oleoidearumpollenites*, Oligocene–Pliocene (Muller, 1981; Ziembińska-Tworzydło *et al*., 1994). *Retitricolporites oleoides*, Oligocene sediments, Belgium (Roche and Schuler, 1976); Miocene, France (Naud and Suc, 1975); Miocene, Spain (van Campo, 1976); *Olea europaea* complex, Miocene, Mediterranean floristic region (Vargas *et al*., 2018).

Botanical affinity: Oleaceae (Stuchlik *et al*., 2014). Pollen grains can be compared to those of *Olea* L. (Stuchlik *et al*., 2014).

Geographic occurrence of extant taxa: *Olea* is distributed in tropical and warm-temperate zones of Asia, Australia and southwestern Europe (Ziembińska-Tworzydło *et al*., 1994; Stuchlik *et al*., 2014). *Olea* is distributed in South Africa, China, Macaronesia and the Mediterranean basin (Besnard *et al*., 2009).

Distribution of fossil taxon in southern Africa: Neogene, northeast of Knysna (Thiergart *et al*., 1963; Goble, 2015); early to late Miocene Noordhoek, Rondeberg (Sciscio, 2011; Roberts *et al*., 2013; Sciscio *et al*., 2013) and LBW (Coetzee and Rogers, 1982; Sciscio, 2011; Sciscio

et al., 2013); *Olea europaea* subsp. *africana*, Pliocene–Pleistocene, Tanzania (Domínguez-Rodrigo *et al*., 2001).

Genus: *Parthenopollenites* Traverse 1994

Type: *Parthenopollenites neshobensis* (Traverse 1955) Traverse 1994

Parthenopollenites marcodurensis (Pflug & Thomson in Thomson & Pflug 1953) Traverse 1994 (Plate 1, Fig. I)

Preceding description: Tricolporate, semitectate, reticulate pollen grains; polar axis 31–65 µm, equatorial diameter 13–33 µm, prolate to perprolate shape (P/E 1.9-2.3); apocolpia small and narrow; colpi long and narrow, with costa colpi; circular pores 2–4 µm; exine 4 µm; surface reticulate; lumina 1–1.5 wide, muri 2 µm high (Stuchlik *et al*., 2014).

Morphological description: Pollen grains tricolporate; polar axis 21–52 µm and equatorial diameter 14–24 µm in polar view, shape prolate to perprolate (P/E: 1.4–2.17); apocolpia narrow, with diameter 1–3 µm; colpi 18–49 µm long, almost reaching the poles and 2–3 µm deep, with slightly curved costa colpi; circular pores equatorial diameter 3–8 µm and meridional diameter of 2–6 µm; exine semitectate and 1.5-2 µm thick; surface reticulate; lumina 1–1.5 µm and muri 0.5–1 µm.

Diagnosis: The dimensions (polar axis and equatorial diameter) of specimens from this study are ca. 10% smaller than those described in Stuchlik *et al*. (2014). This species differs from *P. neshobensis* by an elongated outline and coarser reticulation (Stuchlik *et al*., 2014).

Stratigraphic range: *Tricolporopollenites marcodurensis*, Tertiary of Europe (Muller, 1981); Oligocene sediments, France (Gruas-Cavagnetto, 1978); middle Oligocene–upper Miocene deposits from Poland (Ziembińska-Tworzydło, 1974; Worobiec *et al*., 2019); late Neogene deposits from Tennessee, USA (Worobiec *et al*., 2013); Miocene records and younger abundant (Muller, 1981).

Botanical affinity: Vitaceae (Stuchlik *et al*., 2014). Similar extant species include, *Ampelopsis, Cayratia, Cissus, Cyphostemma* and *Parthenocissus* (Stuchlik *et al*., 2014).

Geographic occurrence of extant taxa: Extant species belonging to *Parthenocissus* occur in tropical to warm-temperate regions in Asia, North America, Europe and Africa (Trias-Blasi, 2012; Stuchlik *et al*., 2014).

Distribution of fossil taxon in southern Africa: Rare; late Oligocene–early Miocene sediments, Saldanha Bay (Roberts *et al*., 2017).

Parthenopollenites neshobensis (Traverse 1955) Traverse 1994 (Plate 1, Fig. J)

Preceding description: Tricolporate, semitectate, reticulate pollen grains; polar axis 42–48 µm; equatorial diameter 33–40 µm, pollen grain shape subprolate (P/E 1.2–1.26 µm); rounded apocolpia; narrow, long colpi with costa colpi, almost reaching poles; colpi borders 2 µm thick; microreticulum formed by small polygonal to circular luminae, 1 µm wide; muri up to 1 µm wide (Stuchlik *et al*., 2014).

Morphological description: Pollen grains tricolporate; polar axis 37–48 µm, equatorial diameter 31–47 µm in equatorial view; shape oblate-spheroidal to prolate (P/E: 0.94–1.55); rounded apocolpia, diameter of 3–24 µm thick; colpi 25–40 µm long, nearly reaching the poles and broad at the equator, with depth of 3–4 µm; costa colpi around well-defined circular pores with an equatorial diameter of 4–5 µm and a meridional diameter of 2–5 µm; exine 2–3 µm thick; surface microreticulate; lumina 0.5–1. µm and simplicolumellate muri up to 1 µm broad; columellae up to 0.5–1. µm.

Diagnosis: *Parthenopollenites neshobensis* has a finer reticulation and a rounder outline than *P. marcodurensis* (Stuchlik *et al*., 2014).

Stratigraphic range: middle early Miocene deposits of the Brandon Lignite of Vermont, U.S.A. (Traverse, 1994); Neogene, Poland (Stuchlik *et al*., 2014).

Botanical affinity: Vitaceae (Stuchlik *et al*., 2014). Pollen grains are morphologically similar to members of the extant genus, *Parthenocissus* (Traverse, 1994; Stuchlik *et al*., 2014), such as *Ampelopsis, Cayratia, Cissus, Cyphostemma* and *Parthenocissus* (Stuchlik *et al*., 2014). Six pollen grains were measured.

Geographic occurrence of extant taxa: Modern Vitaceae species are distributed in pantropical regions, including Africa, Asia, Australia, Europe, the Neotropics and North America (Trias-Blasi, 2012; Stuchlik *et al*., 2014).

Distribution of fossil taxon in southern Africa: Rare; late Oligocene–early Miocene sediments, Saldanha Bay (Roberts *et al*., 2017).

Genus: *Psilatricolporites* Van der Hammen 1956

Type: *Psilatricolporites operculatus* Van der Hammen and Wijmstra 1964

Psilatricolporites quenua Barreda and Palazessi 2009 (Plate 1, Fig. U)

Preceding description: Tricolpate, isopolar pollen grains; shape oblate to suboblate, circular in polar view; colpi short – do not reach equator; operculum protruding above indistinct endoaperture; exine 1.1–1.5 µmthick, nexine thinner than sexine; surface finely regulate with microspines; equatorial diameter 19–21.5 µm (Barreda *et al*., 2009).

Morphological description: Pollen grains tricolporate; Polar axis 33–42 µm and equatorial diameter 30–38 µm; grains are oblate spheroidal to sub-prolate (P/E: 0.92–1.23), with wide apocolpia; colpi very short, constituting about 30–50% of length of grain; operculae, with height 4–10 µm protrude from the colpi, forming a fusiform pattern; exine 2–3 µm thick; surface of exine covered with rugulae and/or microverrucae with a height of 0.5–11 μm, resembling fine striations.

Diagnosis: Measured specimens from this study are ca. 10% larger than the specimens described in Barreda *et al*. (2009). Pollen grains are characterised by a protruding operculum above the endoaperture and a microrugulate surface, by which it differs from *Psilatricolporites operculatus* (Barreda *et al*., 2009).

Stratigraphic range: Rosaceae, Eocene (DeVore and Pigg, 2007); Oligocene, South America (Barreda *et al*., 2009); *Polylepsis*/*Acaena* from Pliocene–Pleistocene, New Zealand (Mildenhall, 2001).

Botanical affinity: Rosaceae (Barreda *et al*., 2009). This species is compared to the South American *Acaena*/*Polylepis* of Rosaceae (Barreda *et al*., 2009; Barreda and Palazessi, 2014) and South African *Cliffortia* (also Rosaceae) (Scott, 1982; Roberts *et al*., 2017).

Geographic occurrence of extant: Today, the trees, shrubs and herbaceous plants of Rosaceae are globally found in all climatic zones (Stuchlik *et al*., 2014). In South Africa, *Cliffortia* is endemic to the CFR and the Drakensberg region, northern Kwa-Zulu Natal (Whitehouse, 2004).

Distribution of fossil taxon in southern Africa: *Cliffortia*-type, Palaeogene sediments Koingnaas, Namaqualand (de Villiers and Cadman, 2001); late Oligocene–early Miocene Noordhoek (Coetzee, 1983); Miocene Makhulu lignites (Carr *et al*., 2010; Goble, 2015); late Oligocene–early Miocene Saldanha Bay (Coetzee, 1983; Roberts *et al*., 2017); Miocene (?)LBW (Sciscio *et al*., 2013).

Genus: *Rhoipites* Wodehouse 1933

Type: *Rhoipites bradleyi* 1933

Rhoipites couperi Pocknall 1985 (Plate 1, Fig. L)

Synonymy: *Tricolpites pilatus* Couper 1960; *Rhoipites pilatus* (Couper 1960) Pocknall & Crosbie 1982 (Pocknall, 1985).

Preceding description (*Rhoipites pilatus*): Pollen grains tricolporate, sub-triangular and prolate to sub-prolate; colpi long, almost reaching poles; exine 1 µm at equatorial area and thicker at the poles, with nexine 1–1.5 µm and sexine 3–6 µm thick; exine reticulate, with circular or polygonal lumina that are 2.5–4.5 µm thick at poles and 1–1.5 µm towards colpi; polar diameter 30–44 µm, equatorial diameter 27.5–38.5 µm (Pocknall and Crosbie, 1982).

Morphological description: Tricolporate pollen grains; polar axis of 25–38 µm, equatorial axis 20–30 µm; pollen grains oblate spheroidal to sub-prolate (P/E: 0.93–1.30); costa colpi 17-21 µm long and 2–5 *µm* deep, with a slight curvature at the equator; pores with 2–3 µm equatorial diameter and 2–5 µm meridional diameter, with slightly rounded apocolpia 3–9 µm; exine 2–5 µm, appearing thicker at the poles than at the equator, with columellae 1–3 µm; surface reticulate, with lumina 0.5–1.5 µm and simplicolumellate muri up to 0.1–0.8 µm; reticulation increases towards the poles and decreases closer to the colpi.

Diagnosis: *Rhoipites couperi* differs from *R. sphaerica* - described by Pocknall and Crosbie (1982) - by its thicker exine, longer columellae and a coarser reticulum (Pocknall and Crosbie, 1982).

Stratigraphic range: Palaeogene–Neogene, New Zealand (Pocknall and Crosbie, 1982; Raine *et al*., 2011). *Rhoipites* was described from: late Eocene, East Antarctica (Truswell and Macphail, 2009); late Oligocene–early Miocene, Tibet (Sun *et al*., 2014).

Botanical affinity: Araliaceae (Roberts *et al*., 2017).

Geographic occurrence of extant taxa: Araliaceae grows worldwide, in tropical and temperate areas (Stuchlik *et al*., 2014).

Distribution of fossil taxon in southern Africa: late Oligocene–early Miocene, Saldanha Bay (Roberts *et al*., 2017), late Cenozoic, Noordhoek (Coetzee, 1978); *Rhoipites* from Eocene sediments, Shearwater Bay, southwestern Africa (Zavada and de Villiers, 2000); Previously dated middle Miocene sediments, LBW (Sciscio *et al*., 2013); Tertiary sediments, Namaqualand, South Africa (de Villiers and Cadman, 2001).

Genus: *Tubulifloridites* Cookson 1947 ex Potonié 1960

Type: *Tubulifloridites antipodica* Cookson 1947

Tubulifloridites antipodica Cookson 1947 ex Potonié 1960 (Plate 1, Fig. V)

Preceding description: Pollen grains tricolporate, spherical to sub-prolate shape, oval in equatorial view; colpi long, almost reaching three-quarters of the polar diameter; pores circular to lalongate; exine consists of ektexine and endexine; thick tectum is comprised of interconnected rods; exine surface echinate, with evenly distributed spines; spines are high with a length of 1–2.5 µm and become narrow towards the top; columellae are thick and stout and are resting on a homogeneous footlayer (Zavada and de Villiers, 2000). Polar diameter with spines 18–25.5 µm, equatorial diameter with spines 18–23.5 µm (Barreda, 1993).

Morphological description: Pollen grains are tricolporate, sub-prolate to spherical; polar diameter (with spines) ca. 24–30 µm and equatorial diameter (with spines) ca. 20–30 µm; colpi long, almost reaching the poles with a length of ca. 15 µm; pores circular, with an equatorial diameter of ca. 1.5 µm; exine ca. 1–3 µm thick, with echinate surface; spines are

ca. 1–3 μm high, with a wide base and tapered end; space between the spines is even, with a width of ca. 2–7 μm; columellae are ca. 0.5 μm thick.

Diagnosis: *Tubulifloridites antipodica* is larger and has higher spines than *T. viteauensis* (Barreda, 1993; Zavada and de Villiers, 2000). *Tubulifloridites antipodica* from this study has spines that are ca. 10% higher than those of *Mutisiapollis viteauensis*.

Stratigraphic range: Palaeogene to modern, New Zealand (Raine *et al*., 2011); late Oligocene (?) to Miocene, southeastern Argentina (Barreda, 1993); Upper Cretaceous–Pliocene (Zavada and de Villiers, 2000); Upper Cretaceous and Miocene, Australia (Martin, 1973; Stover and Partridge, 1973).

Botanical affinity: Asteraceae (Barreda, 1993; Zavada and de Villiers, 2000; Zavada and Lowrey, 2010).

Geographic occurrence of extant taxa: Asteraceae grows in all habitats across the globe, except Antarctica (Schuler and Hemp, 2016).

Distribution of fossil taxon in southern Africa: Palaeocene–Eocene, Koingnaas, South Africa (Zavada and de Villiers, 2000); Tertiary, Namaqualand, South Africa (de Villiers and Cadman, 2001); Eocene, Knysna Lignite in South Africa (Zavada and Lowrey, 2010); late Oligocene–early Miocene, Saldanha Bay (Roberts *et al*., 2017).

Mutisiapollis viteauensis (sub *Tubulifloridites viteauensis*) Barreda 1993 (Plate 1, Fig. W)

Preceding description: Pollen grains tricolporate, with a subprolate to spheroidal shape and oval amb in equatorial view; colpi long and almost reach the poles; pores large and circular; exine echinate, with widely spaced spines less than 1 μm high; pollen wall consists of endexine and ektexine; tectum comprised of interconnected rods forming a thick, homogeneous layer above columellae; digitate columellae rest on a thin footlayer (Zavada and de Villiers, 2000); polar diameter 23–43 μm; equatorial diameter 25–36.5 μm (Barreda, 1993).

Morphological description: Pollen grains tricolporate, and spheroidal to sub-prolate; polar diameter (with spines) ca. 30–40 μm and equatorial diameter (with spines) ca. 27–40 μm; colpi long, reaching a length of ca. 25–27 μm; pores circular, with an equatorial diameter of ca. 3–8 μm; exine echinate, with a thickness of ca. 4.5–6 μm; spines short, only reaching a

length of 0.2–0.5 µm; space between spines unevenly distributed, with a width of ca. 0.5–4.5 µm; columellae thick and stout, with a length of ca. 1.5–5 µm.

Diagnosis: *Tubulifloridites viteauensis* (*Mutisiapollis viteauensis*) can be differed from *T. antipodica* by its larger size, shorter spines and a thicker tectum and columellae (Barreda, 1993). *Mutisiapollis viteauensis* from this study is ca. 5% larger than *Tubulifloridites antipodica*.

Stratigraphic range: late Oligocene? to Miocene, southeastern Argentina (Barreda, 1993) and Patagonia, southern South America (Barreda *et al*., 2010); Eocene, southern Namibia (Zavada and de Villiers, 2000; Scott *et al*., 2006); Oligocene, Ninety East Ridge (Muller, 1981).

Botanical affinity: Asteraceae (Barreda, 1993; Zavada and de Villiers, 2000; Zavada and Lowrey, 2010). This species can be compared to pollen grains of the genus *Mutisia* (Barreda, 1993) and specifically, the *Dicoma* type of the Mutisieae (Scott *et al*., 2006) or the woody species *Tarchananthus* (Zavada and Lowrey, 2010).

Geographic occurrence of extant taxa: Asteraceae is cosmopolitan, apart from Antarctica (Schuler and Hemp, 2016). *Dicoma* is know from South and tropical Africa (Barreda *et al*., 2010) and *Tarchananthus* is known across southern Africa (Zavada and Lowrey, 2010).

Distribution of fossil taxon in southern Africa: Eocene, Shearwater Bay, southern Namibia (Zavada and de Villiers, 2000; Scott *et al*., 2006); Tertiary, Namaqualand, South Africa (De Villiers and Cadman, 2001); Eocene, Knysna Lignite, South Africa (Zavada and Lowrey, 2010); late Oligocene–early Miocene, Saldanha Bay (Roberts *et al*., 2017); Mutisiapollis from previously dated middle Miocene sediments, LBW (Sciscio *et al*., 2013).

Genus: *Zonocostites* Germeraad *et al*. 1968

Type: *Zonocostites ramonae* Germeraad *et al*. 1968

Zonocostites ramonae Germeraad *et al*. 1968 (Plate 1, Fig. M)

Preceding description: Tricolporate, elliptical, isopolar, radially symmetric pollen grains in equatorial view; zonorate, 1.8 µm wide, costate colpi, costae 1.5 µm thick; surface sculpture

reticulate; muri 0.8 µm, lumina 1 µm, exine 1.8 µm; polar axis 28 µm and equatorial diameter 25 µm (Aguilera *et al*., 2013).

Morphological description: Tricolporate pollen grains; polar axis 19–32 µm, equatorial diameter 18.5–24 µm in equatorial view; shape oblate spheroidal to prolate (P/E: 0.96–1.35); colpi 14–27 µm long, not reaching the poles and 2–4 µm deep; costa colpi prominent and thickened at equator; zonorate pores with equatorial diameter 3–13 µm and meridional diameter 2–3 µm; apocolpia 4–10 µm wide; exine 1–3 µm thick, surface scabrate to finely reticulate; muri 0.5–1 µm.

Diagnosis: *Zonocostites ramonae* is bigger than *Zonocostites minor* (not detected in this study) which is also microfoveolate (Aguilera *et al*., 2013).

Stratigraphic range: Upper Cretaceous to Oligo-Miocene, Brazil (Regali *et al*., 1974); lower-upper Eocene to Recent, North America (Germeraad *et al*., 1968; Lorente, 1986; Graham, 2006); upper Eocene, Caribbean (Germeraad *et al*., 1968); late Eocene to Recent, northern South America (Germeraad *et al*., 1968); late Oligocene–early Pliocene, Nigerian deposits (Adebayo *et al*., 2012; Bankole *et al*., 2014; Oloyede and Omoregbe, 2020); Miocene–Pliocene, Australia (Hekel, 1972).

Botanical affinity: Rhizophoraceae (Roberts *et al*., 2017). *Zonocostites ramonae* displays close links to *Rhizophora mangle* L. (Germeraad *et al*., 1968; Aguilera *et al*., 2013).

Geographic occurrence of extant taxa: Mangroves grow in tropical and warm temperate regions of Asia, Africa, North America, South America, Australia, New Zealand, Papua New Guinea and the Pacific Islands (Sandilyan and Kathiresan, 2012).

Distribution of fossil taxon in southern Africa: Rare; late Oligocene–early Miocene sediments at Saldanha Bay (Roberts *et al*., 2017).

3.1.3.5 Triporate pollen

Genus: *Proteacidites* (Cookson ex Couper 1953) Martin & Harris 1974

Type: *Proteacidites adenanthoides* Cookson 1950 ex Couper 1953

Proteacidites sp. A (Plate 1, Fig. R)

Compare: *Proteacidites* sp. de Villiers and Cadman 1997

Preceding description: Pollen grains triporate; triangular amb; circular to oval pores, 2–5 µm; exine 1–3 µm thick; surface psilate to granulate; equatorial diameter: 10–47 µm (de Villiers and Cadman, 1997).

Morphological description: Triporate pollen grains; sub-triangular amb with convex sides; equatorial diameter 21–28 µm; pores circular, with a thickening around the margin, 3–5 µm wide; exine 1–2 µm thick; surface scabrate to finely granulate.

Diagnosis: *Proteacidites* sp. A differs from *Proteacidites* sp. B by a scabrate to finely granulate surface and simple circular pores (own observation).

Stratigraphic range: Tertiary (de Villiers and Cadman, 1997). *Proteacidites*: UpperCretaceous-Tertiary (Martin and Harris, 1974), Upper Cretaceous, western North America (Nichols, 1994), Upper Cretaceous–early Palaeocene, Antarctica (Askin, 1990), Palaeocene–Eocene, eastern New Zealand (Crouch and Brinkhuis, 2005), early Eocene–early Oligocene, Argentina (Barreda and Palazzesi, 2007; Barreda *et al*., 2020); late Eocene–early Miocene, Cameroon (Moise *et al*., 2017); late Miocene–early Pliocene, southwestern Australia (Bint, 1981; Macphail, 1997).

Botanical affinity: Proteaceae (de Villiers and Cadman, 1997).

Geographic occurrence of extant taxa: Proteaceae are distributed in Australia, Melanesian islands, New Zealand, Madagascar, Asia, southern Africa and tropical Africa, South America and Central America (Weston, 2007).

Distribution of fossil taxon in southern Africa: Tertiary sediments, Koingnaas, Namaqualand (de Villiers and Cadman, 1997; 2001). *Proteacidites* has been recorded from: Cretaceous offshore sediments, southwestern Cape (McLachlan and Pieterse, 1978); Palaeocene-Eocene, Shearwater Bay, southwestern South Africa (Zavada and de Villiers, 2000); Early Miocene, Rondeberg (Roberts *et al*., 2013); early to middle Miocene, Noordhoek (Sciscio *et al*., 2016); Previously dated middle Miocene, LBW (Coetzee and Rogers, 1982; Sciscio *et al*., 2013); late Neogene, Knysna (Thiergart *et al*., 1963; Goble, 2015).

<u>*Proteacidites* sp. B (Plate 1, Fig. S)</u>

Compare: *Proteacidites tuberculatus* Cookson 1950

Preceding description (*P. tuberculatus*): Large, triporate pollen grains; triangular amb with convex sides; equatorial diameter 60–96 µm; exine 5.5 µm thick, clearly differentiated into nexine and sexine; surface baculate, with spherical tubercles 3–4 µm high, arranged in a reticuloid pattern (Cookson, 1950).

Morphological description: Triporate pollen grains; sub-triangular to triangular amb, with straight convex sides; pollen diameter 36–67 µm; pores angulaperturate, 3–6 µm wide; exine 2 µm; surface with by bacula up to 1–3 µm high, bacula absent on the margins of the pores; surface between bacula psilate.

Diagnosis: *Proteacidites* sp. 2 differs from *Proteacidites* sp. 1 by its larger size (ca. 30%) and baculate surface (own observation).

Stratigraphic range (*P. tuberculatus*): Palaeogene, New Zealand (Raine *et al*., 2011). early Oligocene–middle Oligocene, Australia (Macphail and Hill, 1994); early Oligocene–early Miocene, Australia **(**Stover and Partridge, 1973; Macphail, 1999; Partridge, 2006; Tarran *et al*., 2017).

Botanical affinity: Proteaceae (Raine *et al*., 2011).

Geographic occurrence of extant taxa: *Proteacidites tuberculatus* is not associated with any extant species of Proteaceae (Cookson, 1950).

Distribution of fossil taxon in southern Africa: This taxon has not been recorded from southern Africa.

3.1.4 Dinoflagellates

Genus: *Apteodinium* Eisenack 1958

Type: *Apteodinium granulatum* Eisenack 1958

Apteodinium spiridoides Benedek 1972 (Plate 2, Fig. U)

Preceding description (*Apteodinium* Eisenack 1958): Proximate, Gonyaulacacean cysts; spheroidal to ovoidal central body, with apical horn; wall acavate, weakly bicavate or conucavate; atabulate or weakly paratabulate surface; archaeopyle pericingular, formula $P_{3''}$ (Fensome *et al*., 2009).

Morphological description: Spheroidal to drop-shaped central bodies, 70.0–81.0 µm long and 60–79 µm wide; bicavate wall, 1.8–4 µm thick; apical horn 5–21 µm, apical pore 3–6 µm; thecae partially developed, weakly paratabulate surface; Surface granulate, with granules distributed in a non-tabular fashion; archaeopyle pericingular, 29–38 µm thick.

Diagnosis: Differentiated from other dinoflagellates by an apical horn, bicavate wall and pericingular archaeopyle (Fensome *et al*., 2009).

Stratigraphic range: late Eocene, North Atlantic (Costa and Downie, 1979); late Oligocene, Georgia, U.S.A. (Weems and Edwards, 2001); early Miocene, northern Belgium (Louwye and Laga, 1998); early Miocene (Burdigalian), Austria (Jiménez-Moreno *et al*., 2006); early Miocene, Egypt (Soliman and Ibrahim, 2012); middle Miocene (Early Serravallian), Canada (Fensome *et al*., 2009; 2016); *Apteodinium* spp., middle Miocene, Niger Delta (Durugbo *et al*., 2011).

Botanical affinity: Gonyaulacaceae. No motile affinity.

Distribution of fossil taxon in southern Africa: There are no known accounts of this species in southern Africa.

Genus: *Chiropteridium* Gocht 1960 emend. nov.

Type: *Chiropteridium lobospinosum* Gocht 1960

Chiropteridium lobospinosum Gocht 1960 (Plate 2, Fig. V)

Preceding description (*Chiropteridium* Gocht 1960 emend. nov.): Proximochorate to chorate Areoligeraceaen cysts; lenticular body, antapically asymmetrical; cavation restricted to ‘wings’ if wall cavate; if acavate, longitudinal crests form marginate wings; atabulate surface; apical archaeopyle, formula: $A_{(1\text{-}4')}$ (Fensome *et al*., 2009).

Morphological description: Proximate to proximochorate (process length/smallest diameter of cyst: 0.07–0.4) dinocysts; subspherical central body, 28-38 µm long and 31–36 µm wide; acavate wall, smooth and atabulate surface; processes 3–13 µm long, branching with bifurcate tips; processes nontabular and scarce in central areas of the body; archaeopyle is apical, 6–9 µm wide.

Diagnosis: Reduced processes in the mid-dorsal and mid-ventral areas of the central body (Carlsson, 2019). The genus *Chiropteridium* is differentiated from *Membranophoridium* (not described in this study) by the presence of lateral extensions or wings and processes (Fensome *et al*., 2009).

Stratigraphic range: *Chiropteridium* is a recognised Oligocene index fossil (Besems, 1992). late Eocene–late Oligocene, Australia (Martin, 1993); early Oligocene (Rupelian), north-eastern Morocco (Mahboub *et al*., 2019); late early Oligocene, Mediterranean region (Wilpshaar *et al*., 1996); late Oligocene, southeastern U.S.A. (Katuna *et al*., 1996); Oligocene, western Tethys, central Italy (Pross *et al*., 2010)

Botanical affinity: Areoligeraceae (Fensome *et al*., 2009; 2016). No motile affinity.

Distribution of fossil taxon in southern Africa: late Oligocene (Chattian), Angolan coast (Willumsen *et al*., 2014); late Oligocene–early Miocene, Saldanha Bay, (Roberts *et al*., 2017; Grímsson *et al*., 2018).

Genus: *Cordosphaeridium* Eisenack 1963

Type: *Hystrichosphaeridium inodes* Klummp 1953

Cordosphaeridium minimum (Morgenroth 1966) Benedek 1972 (Plate 2, Fig. W)

Preceding description (*Cordosphaeridium* Eisenack 1963): Chorate Gonyaulacacean cysts; spheroidal body, wall absent (acavate); one processes per plate, hollow, open or closed and nearly same length; atabulate surface; pericingular archaeopyle, formula $P_{3''}$ (Fensome *et al*., 2009).

Morphological description: Dinocysts proximochorate to chorate (process length/smallest diameter of cyst: 0.2–0.6); spheroidal central bodies, 30–37 µm long and 25–33 µm wide; central body acavate, with smooth surface; cylindrical and/or branching processes 5–17 µm long with bifurcate and trifurcate tips; archaeopyle is pericingular.

Diagnosis: Processes are not abundant and only one is typically found per plate (Fensome *et al.,* 2016).

Stratigraphic range: early Eocene (Morgenroth, 1966). upper Eocene, northeastern Morocco (Mahboub *et al*., 2019); early Oligocene (Rupelian), eastern Anatolia, Turkey (Bati and

Sancay, 2007); middle Miocene, north-eastern U.S.A. (de Verteuil, 1996); middle Miocene (early Serravallian), central Europe (Jiménez-Moreno *et al*., 2006).

Botanical affinity: Gonyaulacaceae (Fensome *et al*., 2009). No motile affinity.

Distribution of fossil taxon in southern Africa: late Oligocene–early Miocene, Saldanha Bay (Roberts *et al*., 2017); upper middle Miocene–lower upper Pliocene, Cape Basin, South Africa (Udeze and Oboh-Ikuenobe, 2005).

Genus: *Operculodinium* Wall 1967

Type: *Hystrichosphaeridium centrocarpum* Deflandre & Cookson 1955

Operculodinium centrocarpum (Deflandre & Cookson 1 955) Wall 1967 (Plate 2, Fig. X)

Preceding description: Dinocysts chorate, central body spherical; processes between 20–40, length varied; endophragm with columellae-like rods, periphragm microgranulate; processes simple, with conical bases and capitate or furcating tips, distribution in girdle region or intratabular; pericingular archaeopyle; dimensions: cyst body 33–48 μm, process length 7–14 μm (Marret and Zonneveld, 2003).

Morphological description: Dinocysts proximochorate (process length/smallest diameter of cyst: 0.12–0.24); spherical to subspherical central bodies, 60–80 μm long and 50–68 μm wide; central body acavate, wall 0.2–2 μm thick; surface of body smooth to granulate and paratabulate; isolated, nontabular processes; processes with bulbose and/or bifurcating tips, 3–13 μm high; archaeopyle pericingular, 23–31 μm wide.

Diagnosis: The maximum cyst length of specimens described by Marret and Zonneveld (2003) is two-thirds the maximum cyst length of specimens from this study. Characterised by the loss of a single plate, resulting in a pericingular archaeopyle (Zonneveld and Pospelova, 2015). It is distinguished from other species by the acuminate tips, hollow processes and microgranulate surface (Zonneveld and Pospelova, 2015).

Stratigraphic range: Eocene–present day (Zonneveld and Pospelova, 2015). Eocene–lower Oligocene, Gulf Coast, U.S.A. (Jaramillo and Oboh-Ikuenobe, 1999); late Oligocene–early Miocene, central Taiwan (Mao *et al.*, 2002); early to middle Miocene, central Europe (Jiménez-Moreno *et al*., 2006); late Miocene, Argentina, South America (Barreda *et al*.,

2008); middle Miocene–Early Pleistocene, western Niger Delta, Nigeria (Durugbo *et al*., 2011); late Quaternary and Recent, southeastern Australia (McMinn, 1992).

Botanical affinity: Gonyaulacaceae (Fensome *et al*., 2009). Its motile affinity is *Protoceratium reticulatum* (Marret and Zonneveld, 2003).

Geographic occurrence of extant taxa: Occurs in all environments (cosmopolitan), including polar, equatorial and coastal to oceanic areas (Zonneveld and Pospelova, 2015).

Distribution of fossil taxon in southern Africa: middle Miocene–late Pliocene, Cape Basin, southwestern South Africa (Udeze and Oboh-Ikuenobe, 2005); late Miocene–Pliocene, Walvis Ridge, southwestern coast of South Africa (Hoetzel *et al*., 2017); Holocene, Namaqualand mudbelt, southwestern South Africa (Zhao, 2017); Recent sediments, Southwest Africa (Sylvia Hill and mouth of Orange River) (Davey and Rogers, 1975).

Operculodinium sp. (Plate 2, Fig. Y)

Compare*:* cf. *Operculodinium eirikianum* Head, Norris and Mudie 1989

Preceding description (cf. *Operculodinium eirikianum*): Skolochorate cysts; central body spherical; wall 0.2 µm thick; surface microreticulate with muri 0.5 µm wide and lumina 0.5 *µm* in diameter; processes solid, acuminate tips and a non-tabular distribution; archaeopyle pericingular; dimensions: central body 27–35 *µm* wide; wall 0.5–1.0 µm; process length 4–9.5 µm (Head, 1997).

Morphological description: Proximate to proximochorate (process length/smallest diameter of cyst: 0.08–0.35) cysts; spheroidal central body, 33–37 µm long and 20–31 µm wide; body wall acavate and atabulate; surface smooth to microgranulate; solid processes 2–7 µm long, with sharp or acuminate tips, distribution of processes non-tabular; archaeopyle pericingular, 11–13 µm wide.

Diagnosis: Differs from *Operculodinium centrocarpum* by the solid processes with sharp tips and a non-tabular distribution (own observation).

Botanical affinity: Gonyaulacacean(?).

Geographic occurrence of extant taxa (cf. *Operculodinium eirikianum*):
Palaeoenvironments characterised by cold temperatures in mid to high-latitude sediments of neritic and oceanic zones (Head, 1997).

Distribution of fossil taxon in southern Africa: upper middle Miocene–lower upper Pliocene, Cape Basin, southwestern Africa (Udeze and Oboh-Ikuenobe, 2004).

Genus: *Spiniferites* Mantell 1850

Type: *Xanthidium ramosum* Ehrenberg 1838, designated as lectotype of *Hystrichosphaera ramosa* by Davey & Williams 1966, p. 32.

Spiniferites mirabilis Rossignol 1963 (Sarjeant, 1970) (Plate 2, Fig. Z)

Preceding description: Proximochorate cyst, ovoidal to elongate central body; periphragm microgranulate; weak paratabulation; hollow, gonal and intergonal processes; archaeopyle pericingular; dimensions: cyst body, 44–48 μm wide, 58–60 μm long, processes 16–21 μm long (Marret and Zonneveld, 2003).

Morphological description: Proximochorate (process length/smallest diameter of cyst: 0.15–0.4) cysts; spheroidal to ovoidal central body 33–46 μm long and 35–45 μm wide; body with acavate wall; surface of the cyst body smooth to granulate, weakly paratabulate; processes 5–16 μm, branching shape and terminating in bifurcate and trifurcate tips; processes proximally connected by crests 3–9 μm high, with gonal and intergonal distribution; archaeopyle pericingular, 20–26 μm wide.

Diagnosis: *Spiniferites mirabilis* is differentiated from other species, particularly *S. hypercanthus* (not described in this study) by a crown-like feature formed by antapical processes (Zonneveld and Pospelova, 2015).

Stratigraphic range: lower Oligocene to recent (Zonneveld and Pospelova, 2015). early Palaeocene (Danian), Israel (Eshet *et al*., 1992); late Eocene deposits, Rockall Plateau, North Atlantic (Costa and Downie, 1979); late Oligocene–early Miocene, eastern Venezuela, South America (Helenes and Cabrera, 2003); middle Miocene–Pliocene, Borneo, southeast Asia (Besems, 1992); early Miocene, central Taiwan (Mao *et al*., 2002); Pleistocene, eastern

Mediterranean, Israel (Rossignol, 1962); late Quaternary and recent sediments, southeastern Australia (McMinn, 1992).

Botanical affinity: Gonyaulacaceae. The motile affinity of *S. mirabilis* is *Gonyaulax spinifera* (Marret and Zonneveld, 2003).

Geographic occurrence of extant taxa: The genus *Spiniferites* is extensively recognised, both stratigraphically and geographically (Londeix, 2018) and is common in temperate to tropical regions of the northern and Southern Hemisphere (Marret and Zonneveld, 2003).

Distribution of fossil taxon in southern Africa: late Oligocene–early Miocene, Saldanha Bay (Roberts *et al*., 2017); late middle Miocene age for a section of Core BH2 (Roberts, 2006; Sciscio *et al*., 2013); late Miocene–Pliocene sediments, Walvis Ridge, southwestern South Africa (Hoetzel *et al*., 2017); Early Holocene sediments, Namaqualand mudbelt, southwestern South Africa (Zhao, 2017); Surficial sediments, southeastern South Atlantic Ocean (Zonneveld *et al*., 2001).

Spiniferites spp. (Plate 2, Fig. AA

Compare: *Spiniferites bentorii* (Rossignol 1964) Wall et Dale 1970

Preceding description (*Spiniferites bentorii*): Proximochorate cysts; pear-shaped central bodies with an apical projection; microgranulate wall 1–2 μm thick; processes short and stunted with bifurcating tips and a gonal and intergonal distribution; archaeopyle pericingular; dimensions: cyst body 45–63 µm wide, 60–73 µm long; process length 15–25 µm (Zonneveld and Pospelova, 2015).

Morphological description: Proximate to proximochorate (process length/smallest diameter of cyst: 0.07–0.29) cysts; spheroidal central body, 40–51 µm long and 30–48 µm wide; central body is acavate; smooth to granulate surface; processes branching, 2–11 µm long, with bifurcate tips; gonal and intergonal distribution, proximally connected; archaeopyle pericingular.

Diagnosis: Processes are shorter than *S. mirabilis* and are connected by fewer and shorter sutural crests (own observation). *Spiniferites bentorii*, with which it is compared, is distinguished from other species by its pear-shaped central bod, an apical protuberance and short processes (Zonneveld and Pospelova, 2015).

Stratigraphic range (*Spiniferites bentorii*): upper Miocene to recent (Zonneveld and Pospelova, 2015). late Miocene, Austria, central Europe (Soliman and Riding, 2017); early Pliocene–Early Pleistocene, western Niger Delta, Nigeria (Durugbo *et al*., 2011); Pleistocene, northeastern U.S.A. (de Verteuil, 1996); Holocene, central Bulgarian Black Sea (Filipova-Marinova *et al*., 2013); recent sediments, South China Sea (Marret and Zonneveld, 2003).

Botanical affinity (*Spiniferites bentorii*): Gonyaulacaceae (Zonneveld and Pospelova, 2015). The motile affinity of *S. bentorii* is *Gonyaulax digitale* (Zonneveld and Pospelova, 2015).

Geographic occurrence of extant taxa (*Spiniferites bentorii*): *Spiniferites bentorii* is distributed in temperate to equatorial regions, where it is abundant in areas of the East China Sea and the Yellow Sea (Zonneveld and Pospelova, 2015).

Distribution of fossil taxon in southern Africa: Holocene, Namaqualand mudbelt sediments, southwestern South Africa (Zhao, 2017).

PLATE 1

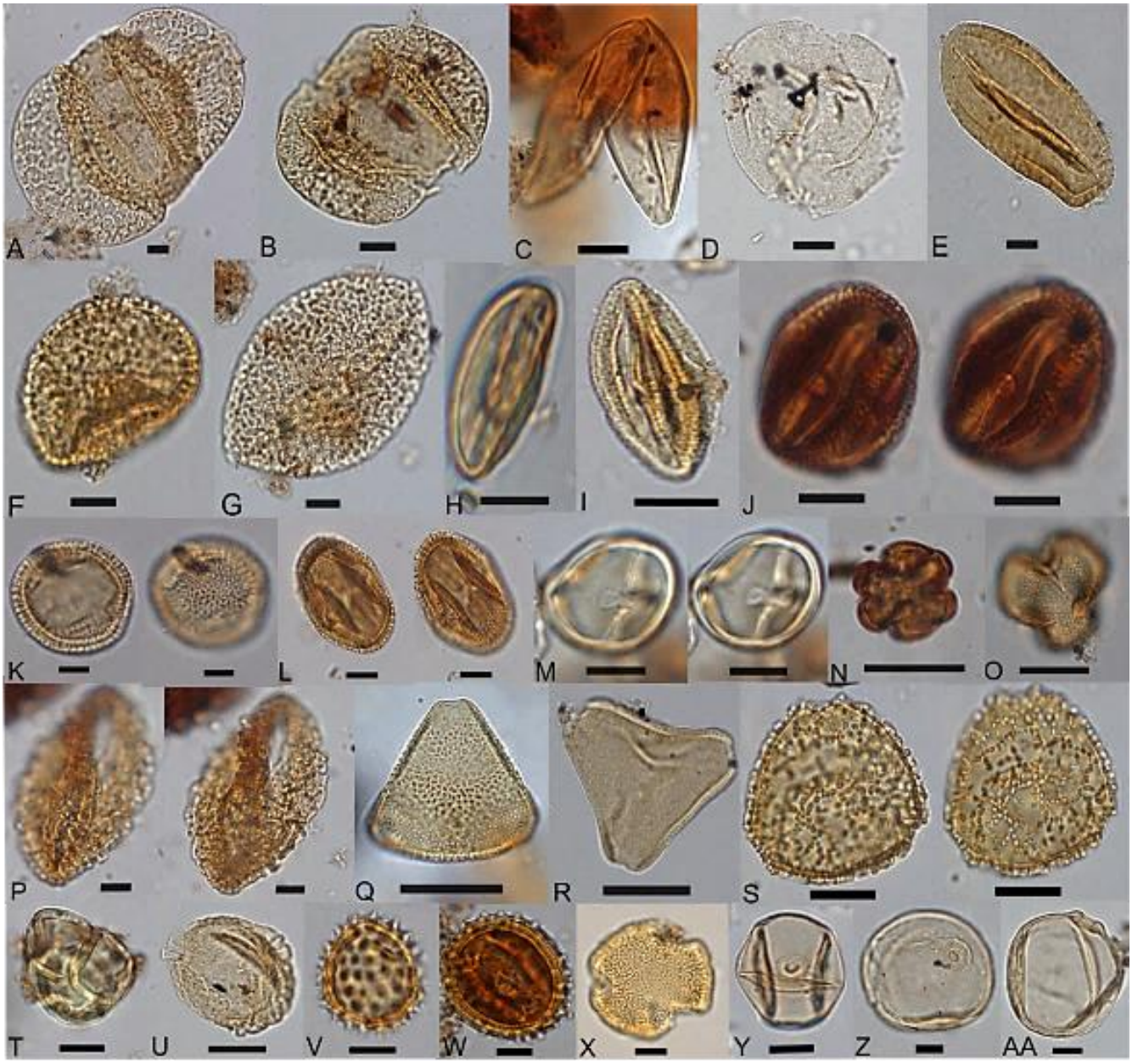

Plate 1. Photomicrographs of selected palynomorph types (pollen and spores) from LBW.

The scale bars represent 10 μm.

PLATE 1

A. *Podocarpidites* sp.

B. *Podocarpidites ellipticus*

C. *Cupressacites* sp.

D. cf. *Araucariacites australis*

E. *Arecipites otagoensis*

F. *Clavatipollenites* sp.

G. *Liliacidites* sp.

H. *Cupuliferoipollenites oviformis*

I. *Parthenopollenites marcodurensis*

J. *Parthenopollenites neshobensis*

K. *Oleoidearumpollenites reticulatus*

L. *Rhoipites couperi*

M. *Zonocostites ramonae*

N. Combretaceae

O. *Rhoipites alveolatus*

P. *Peregrinipollis nigericus*

Q. *Propylipollis meyeri*

R. *Proteacidites* sp. A

S. *Proteacidites* sp. B

T. *Ericipites callidus*

U. *Psilatricolporites quenua*

V. *Tubulifloridites antipodica*

W. *Mutisiapollis viteauensis*

X. *Rhoipites arnotiensis*

Y. *Graminidites* cf. *crassiglobosus*

Z-AA. *Graminidites* cf. *neogenicus*

PLATE 2

Plate 2. Photomicrographs of selected palynomorph types (pollen, spores, dinoflagellate cysts, microforaminiferal linings and fungal spores) from LBW. The scale bars represent 10 μm.

PLATE 2

A. *Cyperaceaepollenites* sp.

B. *Cyperaceaepollenites piriformis*

C. *Milfordia hypolaenoides*

D. *Milfordia homeopunctatus*

E-F. *Sparganiaceaepollenites barungensis*

G. *Baculatisporites* sp.

H. *Cyathidites australis*

I. *Gleicheniidites* spp.

J. *Laevigatosporites haardti*

K. *Leiotriletes maximus*

L. *Leiotriletes maxoides*

M. *Leiotriletes wolffii*

N. *Planctonites* cf. *stellarius*

O. *Botryococcus* sp.

P. *Debarya* sp.

Q. *Ovoidites vangeeli*

R. *Pediastrum*-type

S. *Stigmozygodites* sp.

T. Zygnemataceae

U. *Apteodinium spiridoides*

V. *Chiropteridium lobospinosum*

W. *Cordosphaeridium minimum*

X. *Operculodinium centrocarpum*

Y. *Operculodinium* sp.

Z. *Spiniferites mirabilis*

AA. *Spiniferites* spp.

AB. Microforaminiferal lining

AC-AD. Fungal spore

AE. Fungal fruit body

3.2 PALYNOLOGICAL FLUCTUATIONS – POLLEN ZONATION DIAGRAM

Core BH2 was divided into seven PAAZs (Palynomorph Zone 1–7) based on the diversity and trends of the analysed palynomorphs, using TILIA (CONISS). The hierarchical cluster analysis conducted by CONISS exclusively defined these assemblage groups. These trends reflect the changes in vegetation throughout the deposition of the Elandsfontyn Formation. A total of 76 slides were analysed and the majority yielded ≥ 300 palynomorphs. Palynomorphs showed a great level of preservation except for those from the *Leiotriletes maxoides* zone (defined below). Unidentifiable (crumpled or corroded palynomorphs referred to as "varia") amounted to 104. The PAAZs (Palynomorph Zones 1-7) are defined below from the oldest (PZ7) to the youngest (PZ1).

Palynomorph Zone 7 (33.03–28.26 m): *Podocarpidites* zone

Description: Dominated by arboreal forest and woodland elements, with some wetland taxa; herbs, and fynbos elements occurring in low percentages; cryptogams, fungi and algae very rare.

Podocarpidites sp. and *P. ellipticus* dominate this assemblage, both increasing towards the top of the zone and reaching a maximum of ca. 23% and ca. 22% respectively (Fig. 4). *Oleoidearumpollenites reticulatus* (ca. 20%) (Fig. 4) and *Milfordia homeopunctatu*s (ca. 15%) – both sub-dominant in this assemblage – decrease towards the top of the zone (Fig. 4 and 5). Several subtropical arboreal and herbal elements, such as *Psilatricolporites quenua* (9%), *Graminidites* cf. *neogenicus* (ca. 8%), *Rhoipites alveolatus* (ca. 8%), *Mutisiapollis viteauensis* (ca. 8%), *Arecipites otagoensis* (palmae) (7%), *Cupressacites* sp. (ca. 5%), *Graminidites* cf. *crassiglobosus* (ca. 4%), *Ilexpollenites margaritatus* (ca. 2%), *Ericipites callidus* (ca. 1.0%), *Tubulifloridites antipodica* (1.0%), *Zonocostites ramonae* (ca. 1.0%) and *Casuarinidites* sp. (0.5%), occur in low percentages (Fig. 4). All identified algae, cryptogams and fungi are very rare in this zone (Fig. 5).

Palynomorph Zone 6 (28.26–19.825 m): *Leiotriletes maxoides* zone

Description: Cryptogams and arboreal dicotyledons dominate this assemblage, followed by wetland taxa and open land herbs and shrubs; fungi and algae occur in the lowest percentages.

Leiotriletes maxoides (ca. 33%), *Cyathidites australis* (ca. 29%), *Milfordia homeopunctatus* (25%) and *Cupuliferoipollenites oviformis* (ca. 21%) are predominant at the bottom and all decrease towards the top of the assemblage (Fig. 4 and 5; Appendix B). *Podocarpidites ellipticus* (ca. 20%), *Sparganiaceaepollenites barungensis* (18%), *Rhoipites couperi* (14%), *Clavatipollenites* sp. (14%) are sub-dominant and decrease towards the top of the zone (Fig. 4 and 5; Appendix B). Other sub-dominant taxa include *Oleoidearumpollenites reticulatus*, *Arecipites otagoensis*, *Liliacidites* sp. and *Rhoipites arnotiensis*, however, they proportionally increase towards the top of the zone, reaching maximum percentages of ca. 14%, 23%, ca. 12% and 7% at 19.85 m (Fig. 4; Appendix B). cf. *Araucariacites australis* (0.6%) is low throughout the core but is highest in this zone (Fig. 4; Appendix B). *Zonocostites ramonae* (0.3%) occurs in low percentages but is more frequently occurring than in Pollen Zone 7 (Fig. 4; Appendix B).

Palynomorph Zone 5 (19.825–18.96 m): *Sparganiaceaepollenites barungensis* zone

Description: Assemblage is dominated by wetland taxa, followed by cryptogams and palms; forest and woodland elements have decreased from previous zones; herbs and algae have the lowest percentages in the zone.

The dominant taxa, including *Sparganiaceaepollenites barungensis* and *Milfordia homeopunctatus* both increase from the bottom contact towards the middle of the zone, where they reach a maximum of ca. 62% and ca. 36% respectively, followed by sporadic a decrease towards the top (Fig. 5; Appendix B). The sub-dominant taxa, including *Laevigatosporites haardti* (23%), *Parthenopollenites marcodurensis* (ca. 19%) and *Graminidites* cf. *neogenicus* (ca. 21%) follow the same trend, increasing from the bottom to the middle and decreasing from the middle to the top of the zone between 19.20 m and 18.96 m (Fig. 4 and 5; Appendix B). However, palmae (ca. 27%) are most abundant at the bottom and decrease towards the top of the zone (Fig. 4; Appendix B). Gymnosperms, subtropical and woodland trees such as *Podocarpidites* sp. (ca. 3%), *Dacrydiumites* sp. (0.2%), *Microcachrydites* sp. (0.1%), *Rhoipites couperi* (ca. 7%), *Oleoidearumpollenites reticulatus* (ca. 3%), *Zonocostites ramonae* (0.1%), fynbos elements and algae (dominated by *Ovoidites grandis*, *Botryococcus* sp. and *Planctonites cf. stellarius*) are low throughout the zone (Fig. 4 and 5; Appendix B).

Palynomorph Zone 4 (18.96–18.24 m): *Apteodinium spiridoides* zone

Description: Dinoflagellates, wetland taxa and cryptogams dominate the assemblage; algal elements gradually established; herbs and trees very low in abundance.

This zone is dominated by the dinoflagellate taxon *Apteodinium spiridoides*, which is initially low in abundance at the bottom contact, reaching a maximum of ca. 91% at the middle and finally decreasing to ca. 61% at the top of the zone (Fig. 5; Appendix B). The sub-dominant taxa – all wetland taxa - *Sparganiaceaepollenites barungensis* (ca. 27%), *Milfordia hypolaenoide*s (ca. 16%) and *Milfordia homeopunctatus* (ca. 22%) all follow the same trend as *Apteodinium spiridoides* throughout the zone (Fig. 5; Appendix B). Other dinoflagellates, spores, herbs and trees are low in this zone (Fig. 4 and 5; Appendix B). The diversity of gymnosperms (*Podocarpidites* sp., *Cupressacites* sp. and *Microcachrydites* sp.) has increased, but they occur in low percentages alongside palms (4%), *Rhuspollenites* (0.2%), *Proteacidites* sp. B (1%) and *Ericipites callidus* (0.3%) (Fig. 4; Appendix B). Algal cysts including *Debarya*, *Ovoidites grandis* and *Stigmozygodites* sp. are also low in abundance but appear regularly (Fig. 5; Appendix B). Dinoflagellate cysts belonging to *Spiniferites mirabilis* (ca. 9%) decrease towards the top whereas *Cordosphaeridium minimum* (ca. 4%) and *Operculodinium centrocarpum* (ca. 7%) increase towards the top of this zone (Fig. 5; Appendix B). *Gleicheniidites* spp. (ca. 10%) becomes strongly established in this zone and *Margocolporites rauvolfii* and *Cyperaceaepollenites piriformis* – both extremely rare – appear only in this zone (Fig. 4 and 5; Appendix B). Microforaminiferal linings are first recorded in this zone, where they reach a maximum of 0.6% (Fig. 5; Appendix B).

Palynomorph Zone 3 (18.24–16.865 m): *Milfordia* zone

Description: Dominantly wetland taxa, cryptogams and algae; trees, shrubs, herbs and microforamineral linings occur in the lowest percentages; subtropical trees and gymnosperms declining rapidly.

Milfordia homeopunctatus (ca. 42%), *Milfordia hypolaenoides* (42%) and *Sparganiaceaepollenites barungensis* (34%) account for the most abundant taxa, occurring in high percentages at the bottom contact and decreasing towards the top of the zone (Fig. 5; Appendix B). *Botryococcus* sp. (ca. 20%) and *Gleicheniidites* spp. (ca. 25%) are sub-dominant in this zone, starting with low occurrences and increasing towards the top of the zone (Fig. 5; Appendix B). Algae, dinoflagellates (all less than 5%), herbs and trees occur in the lowest percentages (Fig. 6; Appendix B). Although microforaminiferal linings are also low in abundance, they are most abundant in this zone at ca. 5% (Fig. 5; Appendix B). Trees

and herbs such as *Podocarpidites* sp. (5.1%), *Cupressacites* sp (ca. 4%), *Microcachryidites* sp. (0.3%), *Myricipites harisii* (1.2%) and *Tetracolporopollenites sapotoides* (0.5%), Combretaceae (0.2%), *Psilatricolporites operculatus* (0.9%), monocotyledons, *Tubulifloridites antipodica*, Poaceae, *Proteacidites* sp. A and *Propylipollis meyeri* are very low and *Psilatricoporites quenua* is substantially higher at 8% (Fig. 4; Appendix B). *Peregrinipollis nigericus* (0.3%), a very rare element, occurs only in this zone (Fig. 4; Appendix B). Microforaminiferal linings increase again in this zone, reaching ca. 4% (Fig. 5; Appendix B). *Cordosphaeridium minimum*, *Operculodinium* sp., *S. mirabilis*, *Pediastrum*-type, *Ovoidites grandis*, *Ovoidites vangeeli* and Zygnemataceae occur frequently, albeit in low percentages (Fig. 5; Appendix B).

Palynomorph Zone 2 (16.865–13.4 m): *Operculodinium centrocarpum* zone

Description: Dinoflagellates are the most abundant palynomorph, followed by freshwater algae, trees and shrubs, wetland taxa and herbs; trees, shrubs and herbs continue to be gradually phased out; all palynomorphs are generally low in abundance.

This zone is dominated by dinoflagellates, such as *Operculodinium centrocarpum*, *Spiniferites mirabilis*, *Apteodinium spiridoides* and *Cordosphaeridium minimum* (Fig. 5 and 6; Appendix B). *Operculodinium centrocarpum* (ca. 45%) and *Spiniferites mirabilis* (ca. 56%) follow opposing trends, with the former increasing from the bottom to top and the latter decreasing from the bottom to the top of the zone (Fig. 5; Appendix B). *Apteodinium spiridoides* (ca. 38%) and *Cordosphaeridium minimum* (ca. 31%) are both low in abundance at the bottom, reach a maximum in the middle and decrease to the top of the zone (Fig. 5; Appendix B). Most of the taxa occur sporadically, including *Podocarpidites ellipticus* (1%), *Psilatricolporites quenua* (1%), *Tubuliflorites antipodica* (ca. 3%), *Cyperaceaepollenites* sp. (ca. 3%), *Operculodinium* sp. (ca. 3%) and *Chiropeteridium lobospinosum* (ca. 5%) (Fig. 4 and 5; Appendix B). Cryptogams and algae are only represented by very low percentages of *Gleicheniidites* spp., *Leiotriletes wolffii*, *Polypodiaceoisporites* sp., *Botryococcus* sp., *Ovoidites vangeeli* and *Planctonites cf. stellarius* (Fig. 5; Appendix B).

Palynomorph Zone 1 (13.4–1.61 m): *Botryococcus* zone

Description: All palynomorphs are significantly reduced in this zone; freshwater algae are dominant, followed by wetland taxa (*Milfordia hypolaenoides*) and dinoflagellates

(*Apteodinium spiridoides*); trees and herbs are only represented by two and three taxa respectively; fungal spores are extremely abundant.

Botryococcus sp. is dominant and the only algae taxon in this assemblage, occurring at ca. 36% at the bottom and increasing to 100% at the top of the zone (Fig. 5; Appendix B). *Milfordia hypolaenoides* (ca. 47%) and *Apteodinium spiridoides* (ca. 21%) are both sub-dominant, but only *Milfordia hypolaenoides* occurs at both the bottom and upper contacts of this zone (Fig. 5; Appendix B). Palmae (ca. 12%), *Psilatricolpories quenua* (ca. 12%), *Cupaniedites* sp. (7%), *Tubulifloridites antipodica* (ca. 6%) and *Graminidites* cf. *crassiglobosus* (ca. 6%) are the only other present taxa throughout the zone (Fig. 4; Appendix B). Fungal spores are extremely abundant in this zone, reaching a maximum of 4200% (calculated in relation to the terrestrial pollen sum) (Fig. 5; Appendix B).

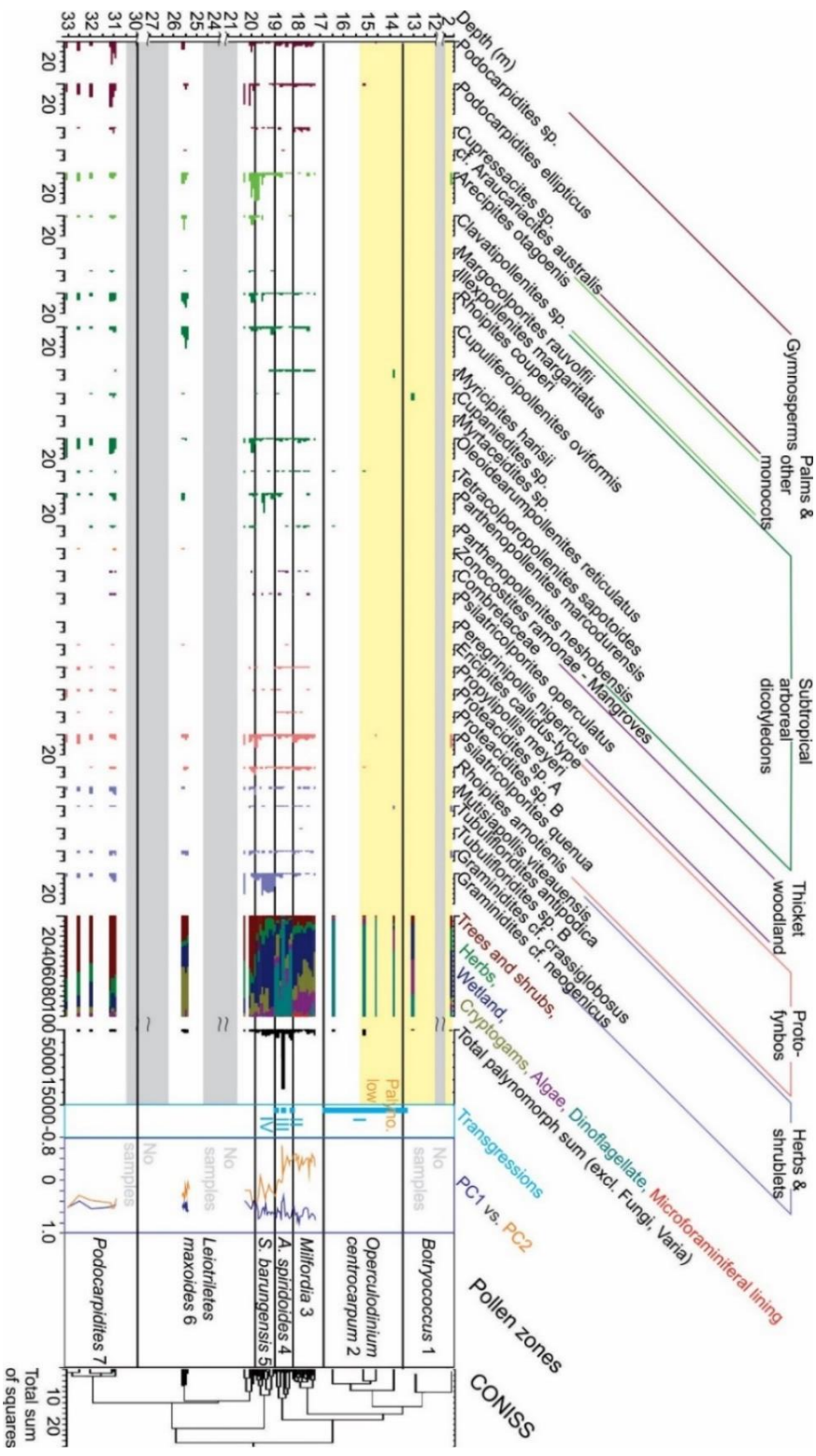

Figure 4. Histogram of palynomorphs (trees, shrubs and herbs) extracted from Core BH2 (depth interval of 33.03 m) sediments from the Elandsfontyn Formation, LBW. Seven PAAZs (Palynomorph Zones 1-7) were partitioned using cluster analysis (CONISS). Four marine transgressions (I-IV) are recorded at LBW in this study, with IV being the oldest and I being the youngest and longest. PC = Principal Components.

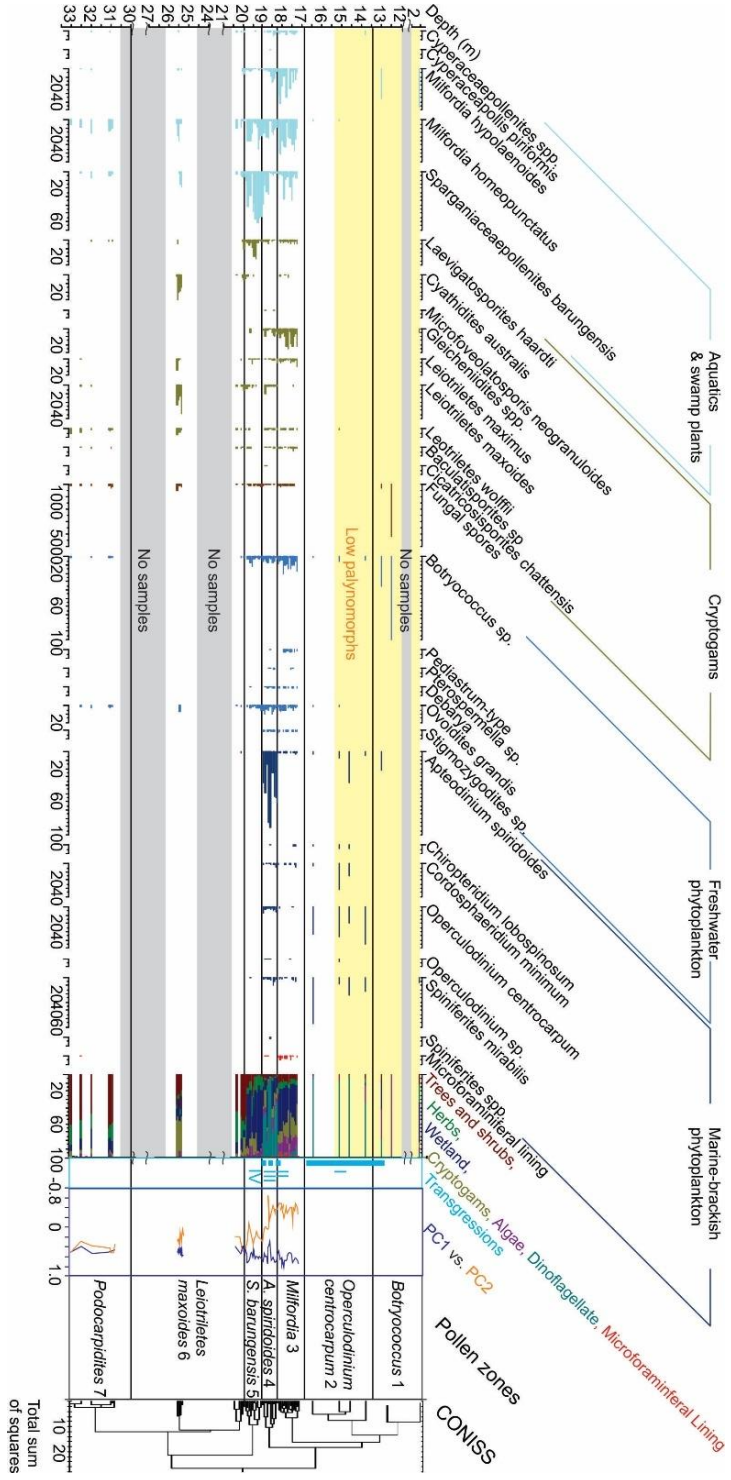

Figure 5. Histogram of palynomorphs (wetland taxa, cryptogams, algae and dinoflagellates) extracted from Core BH2 with a depth interval of 33.03 m, from the Elandsfontyn Formation, LBW. Seven PAAZs (Palynomorph Zones 1-7) were partitioned using cluster analysis (CONISS). Four marine transgressions (I-IV) are recorded in this study, with IV being the oldest and I being the youngest and longest. PC = Principal Components.

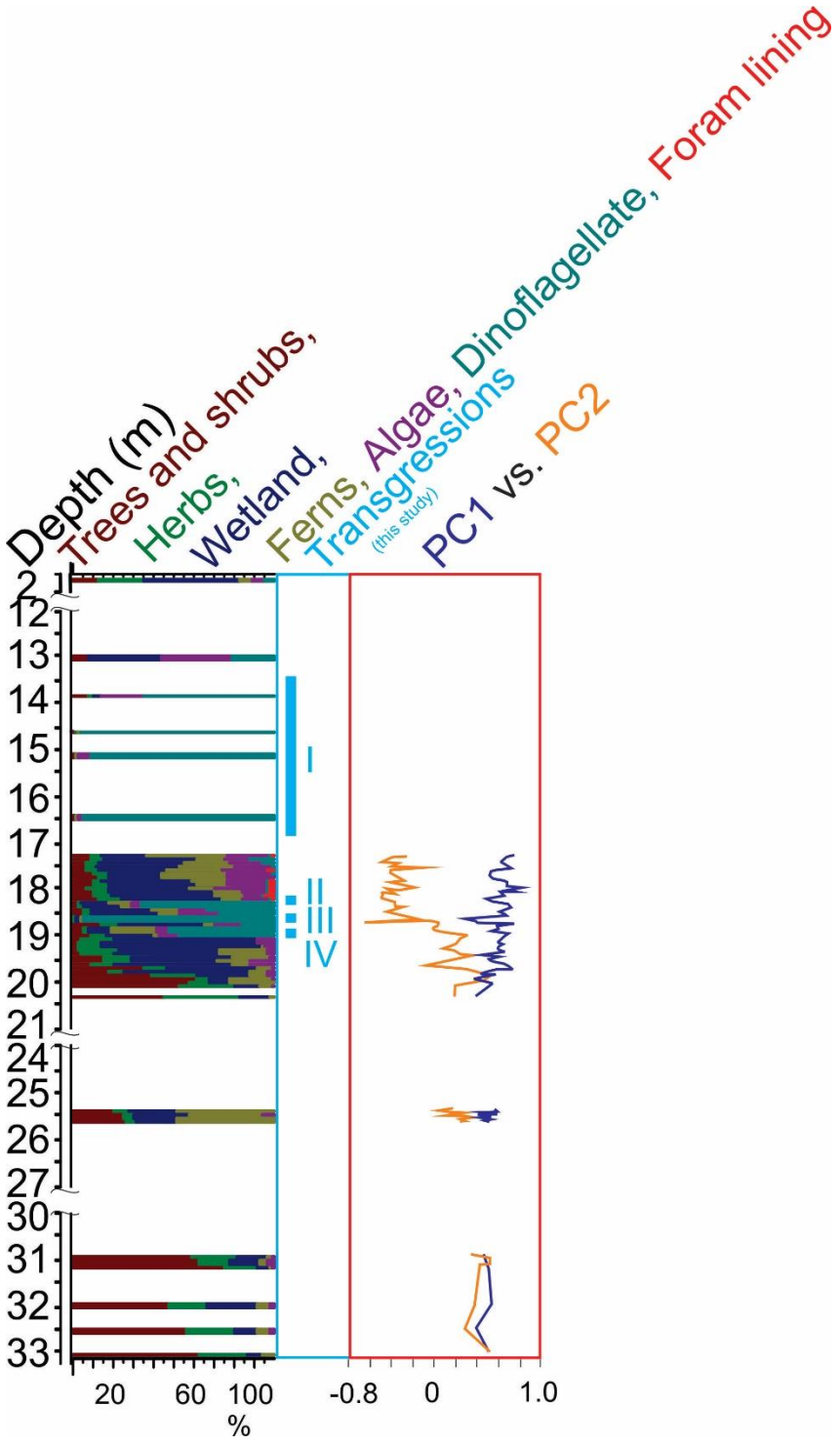

Figure 6. Summary histogram of palynomorphs found at Elandsfontyn Formation, LBW. Four marine transgressions (I – IV) obtained from this study are indicated by high percentages of dinoflagellates in palynomorph zones 4 and 2) are shown in light blue. The oldest transgression is represented by transgression IV and the youngest by I. Principal components (PC1 and PC2) scores represent stratigraphic variation of the PCs, with the dominant taxa removed.

3.3 Principal Components Analysis (PCA)

The PCA was conducted on 48 taxa that are representative of recognised plant ecological groups (forest; subtropical; mangrove; woodland thicket; proto-fynbos; herbs and shrublets; wetland taxa; cryptogams), which were selected as per the selection process in chapter two (Materials and Methods). Two analyses were conducted, with the core depths and ecological groups treated as variables in each analysis This was done to investigate prominent taxa across the core depths (17.28–33.03 m).

The results of the exploratory PCA between core depth is presented in figure 8 and Table 1. A total of 42.3% variance in the dataset is explained by the first five principal components, of which the first five (PC1 to PC5) capture the most significant information (Table 1; Fig. 7). PC1 and PC2 account for 15.3% and 10.1% of the variation, respectively. Therefore, PC1 retains 15.3% of the total variance, with the higher loadings on this axis corresponding to the principal species representing characteristics per depth interval. PC1 distinguished three different groups corresponding to the depth intervals (stratigraphic levels). The first group between 15–25 m – dominated by Cyperaceae and Gentianiaceae – is differentiated from the lowermost samples between 25–32.5 m with dominant species of Podocarpaceae, Arecaceae, Araliaceae and Oleaceae. PC2 separated 22.5–25 m – dominated by Gleicheniaceae and Lygodiaceae – from 15–20 m and 27.5–32.5 m, leading to a slight overlap between these groups. These groups, denoted by a colour gradation scheme (Fig. 8), can be identified as the wetland taxa group (15–20 m), the cryptogam taxa group (22.5–25 m) and subtropical and forest taxa (27.5–32.5 m) by the constellation of dominant species within groups that are separated by PC1 and PC2.

Table 1: Summary table of the highest eigenvalues and variances (%) of the first principal components (PC 1–5) of the PCA conducted on the core depths.

Number	Eigenvalue	Percent	20 40 60 80
1	7,3627	15,339	
2	4,8643	10,134	
3	3,5007	7,293	
4	2,3803	4,959	
5	2,2012	4,586	

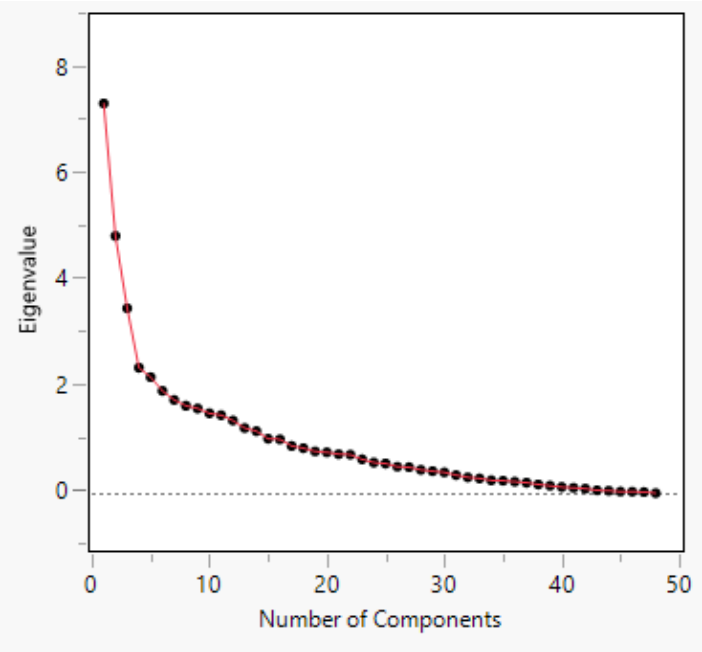

Figure 7. Scree plot (eigenvalues explained against corresponding principal component number) for the PCA on core depths. The first five components (PC 1–5) capture the highest variance in the data. The variance decreases with an increasing number of principal components.

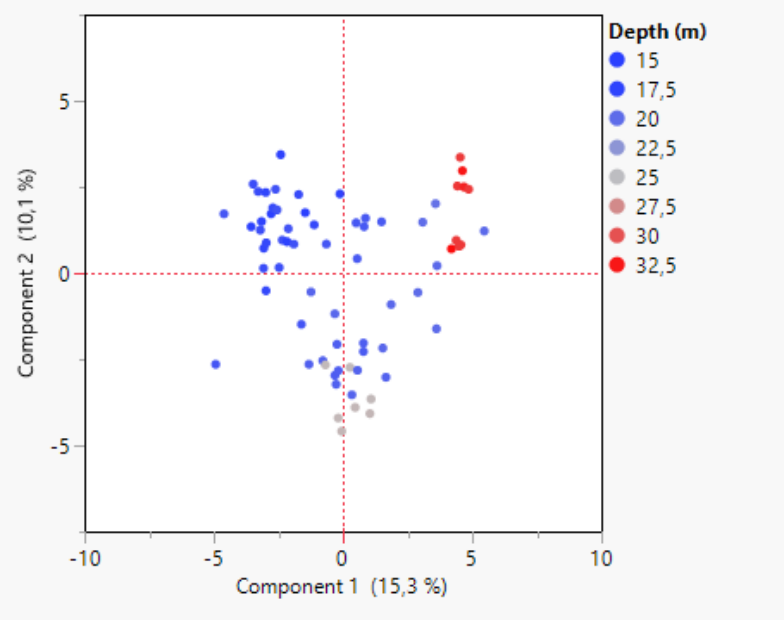

Figure 8. PCA loadings (PC1 and PC2) of variable ordinations according to depth levels of Core BH2.

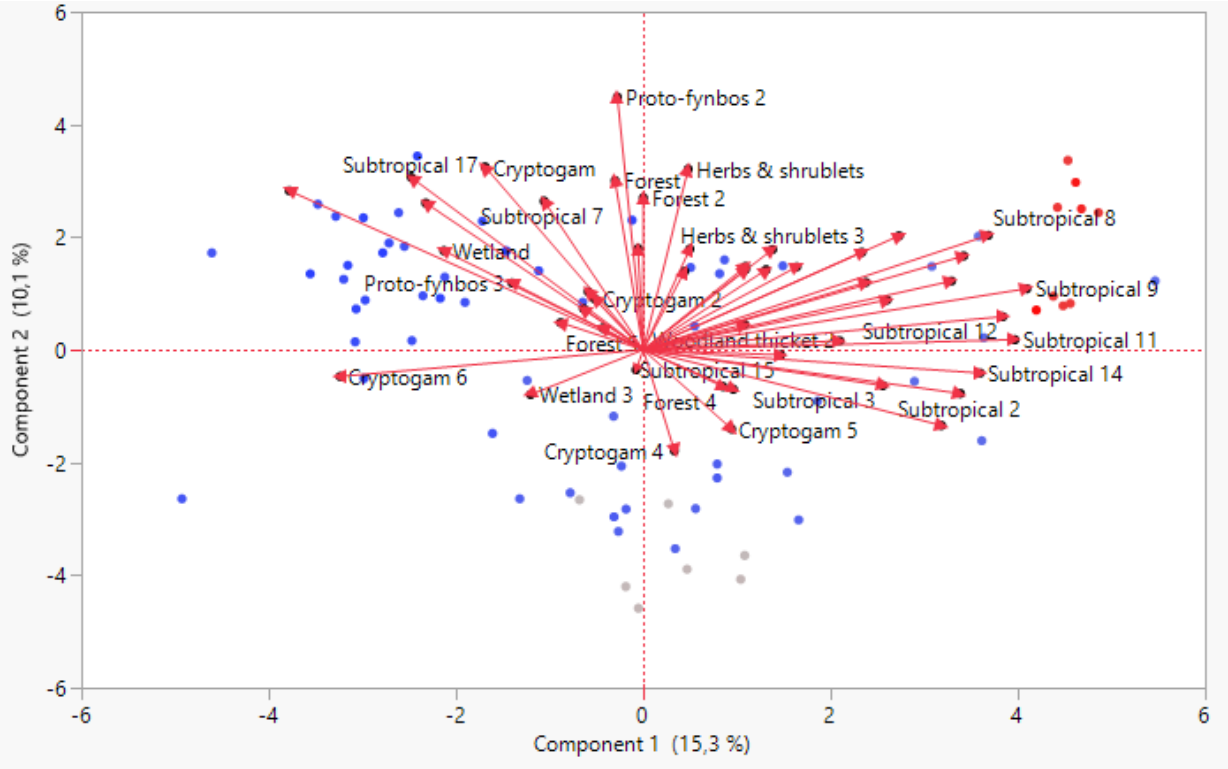

Figure 9. Biplot analysis graph showing PC1 and PC2 scores and loadings (vectors) of variables (palynomorphs from LBW). The vectors (red arrows) represent how strongly each taxa participates to create the given principal components and how they correlate to one another.

The biplot (Fig. 9) denotes how each taxon vectors representing the variables influences the principal components. The plot presents a clear visual of cluster drivers and correlated components of the LBW palaeoenvironment. The majority of vectors of forest taxa are almost parallel to and long in the direction of PC2, therefore, more variation of the taxa is shown by PC2 (Fig. 9). Forest taxa are positively correlated with subtropical, cryptogams, proto-fynbos and herbs and shrublet taxa and are negatively correlated with wetland, woodland thicket and mangrove taxa (Fig. 9). Subtropical elements are almost parallel to and longer in the direction of PC1 (more variability explained by PC1) (Fig. 9). They are positively correlated with mangroves, forest, cryptogams and wetland taxa, and are negatively correlated with herbs and shrublets, proto-fynbos and woodland thicket taxa (Fig. 9). Mangroves are almost parallel to PC1 and longer in its direction, thereby having more influence on PC1. They are positively correlated with subtropical elements, woodland thicket elements and herbs and shrublets, and are negatively correlated with forest, wetland, cryptogam and proto-fynbos taxa (Fig. 9).

Woodland thicket elements are almost parallel to both PC1 and PC2 but are longest in the direction of PC1 (Fig. 9). They are positively correlated with subtropical elements, herbs and shrublets, forest taxa, proto-fynbos taxa and mangroves, and are negatively correlated with cryptogams and wetland taxa (Fig. 9).

Proto-fynbos elements show an almost parallel orientation in relation to PC1, and vectors are longer in its direction (Fig. 9). They are positively correlated with forest, subtropical, wetland taxa and herbs and shrublets, and are negatively correlated with cryptogam, woodland thicket taxa and mangroves (Fig. 9). Herbs and shrublets are almost parallel to PC2, but one component is almost parallel to PC1 (Fig. 9). They are longer in the direction of PC1, and thus have more influence on it (Fig. 9). Subtropical, forest and proto-fynbos taxa show a positive correlation to herbs and shrublets, whereas wetland taxa and cryptogams indicate a negative correlation (Fig. 9). Wetland taxa are almost parallel to PC1 and longer in its direction (Fig. 9). They are positively correlated with cryptogam, proto-fynbos, subtropical and forest taxa, and are negatively correlated with woodland thicket taxa, herbs and shrublets and mangroves (Fig. 9). Cryptogams are almost parallel to both PC1 and PC1 but are longer in the direction of PC1 (Fig. 9). They are positively correlated with subtropical, wetland and forest taxa, and are negatively correlated with fynbos and woodland thicket taxa (Fig. 9).

According to the biplot analysis (Fig. 9), the strongest contributors to the data are subtropical, proto-fynbos and cryptogam elements. Additionally, these elements show a positive correlation to each other and to PC1 (Fig. 9). Based on this, we can assume that PC1 shows the most variance and can be used as a measure of the palaeoecological trend observed at LBW.

The following observations are based on the PCA conducted with ecological groups as variables (Fig. 11): The first five principal components hold the most variance of 63.48%, but only the first two are considered for the interpretation of the palaeoecological environment (Table 2; Fig. 10). Cryptogams are positively and negatively loaded (slightly more positively) on PC1 and largely negatively loaded on PC2. Forest taxa are positively and negatively loaded on PC1 and have a dominant negative loading on PC2, with a single positive loading indicated by *Podocarpidites ellipticus*. Herbs and shrublets have a predominant positive loading on both PC1 and PC2 although some taxa are negatively loaded. Mangroves are negatively loaded on PC1 and positively loaded on PC2. Proto-fynbos elements have an even distribution on PC1 and are predominantly negatively loaded on PC2. Subtropical plants

depict an even distribution on PC1 and a dominantly positive loading on PC2. Wetland elements are evenly distributed on PC1 and PC2. Savanna woodland trees are negatively loaded on both PC1 and PC2.

Table 2: Summary table of the highest eigenvalues and variances for the PCA conducted on ecological groups.

Number	Eigenvalue	Percent	20 40 60 80
1	25,3711	36,244	
2	8,5625	12,232	
3	4,5253	6,465	
4	3,5833	5,119	
5	2,3940	3,420	

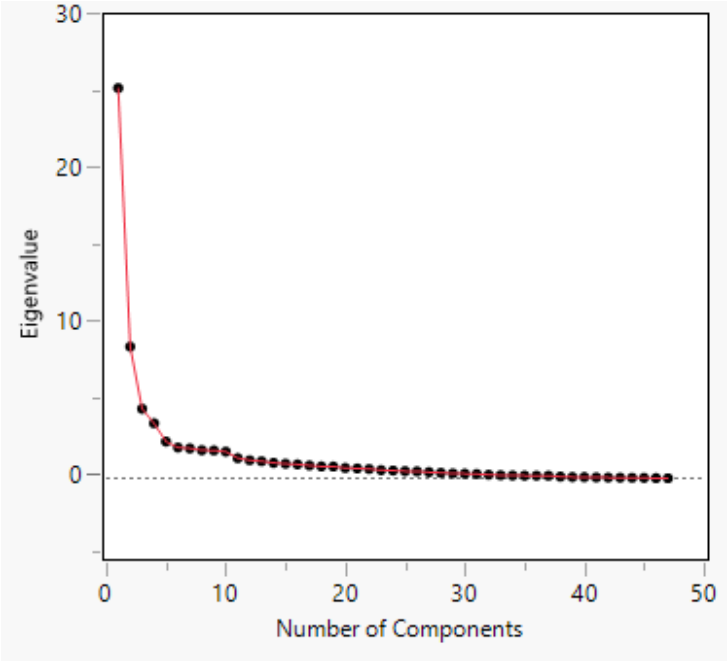

Figure 10. Scree plot (eigenvalues explained against corresponding principal component number) displaying the distribution of variance for the PCA on ecological groups. The first five components (PC 1–5) hold the highest variance in the data. The variance decreases with an increasing number of principal components.

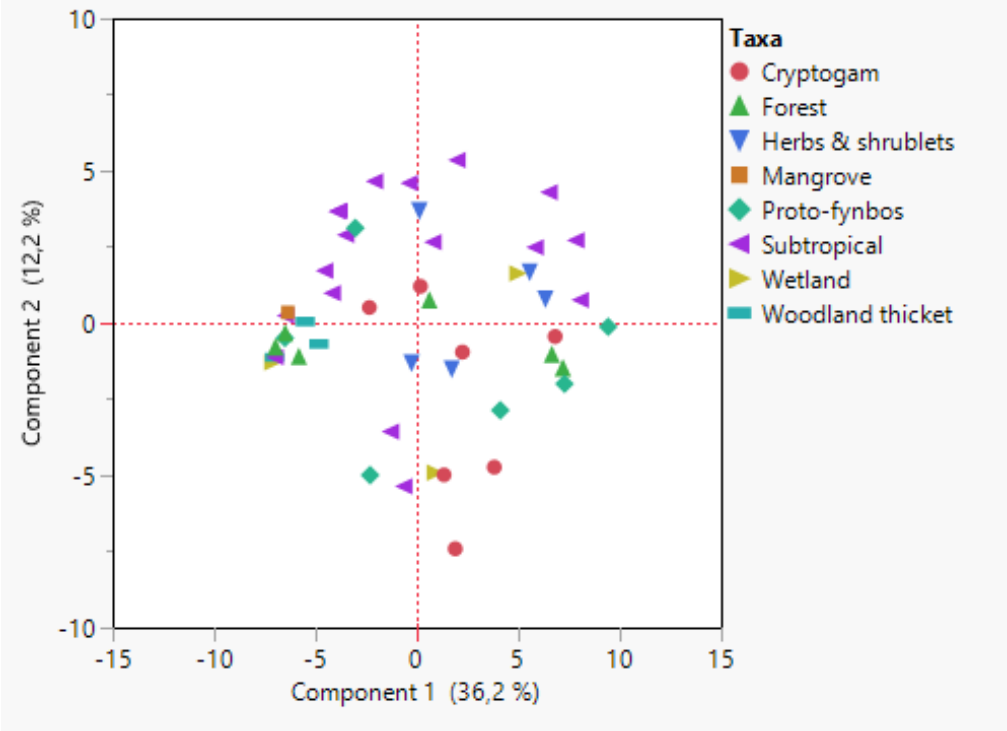

Figure 11. PCA loadings (PC1 and PC2) of plant ecological groups from the Elandsfontyn Formation, LBW, with dominant taxa (dinoflagellates, Restionaceae, Sparganiaceae and fungi) from aquatic habitats removed due to their observed influence on species constellation observed in the stratigraphic levels.

CHAPTER 4: DISCUSSION AND SYNTHESIS

4.1 VEGETATION HISTORY OF LANGEBAANWEG

4.1.1 Vegetation history based on pollen diagrams

Palynomorph Zone 7 (*Podocarpidites* zone) is dominated by evergreen trees with an understorey comprised of herbs, grasses and sparse proto-fynbos elements. Low percentages of possible Araucariaceae (cf. *Araucariacites australis*) can be attributed to low dispersal rates of the relatively heavy pollen grains of Araucariaceae (Heusser *et al*.,1988), alluding to the idea that they were deposited at a distance from the site. Cf. *Araucariacites australis* is a relict plant of Gondwana and is recorded from the Cretaceous (McLachlan and Pieterse, 1978; Adekola *et al*., 2014) and Tertiary (Scholtz, 1985; de Villiers and Cadman, 1997; Roberts *et al*., 2017) of the southwestern coast of South Africa. Araucariaceae is presently extinct from the southwestern Cape (Coetzee, 1983; Coetzee and Muller, 1984; Sciscio *et al*., 2013). However, a verification of the botanical affinity of the pollen grains on the base of SEM investigations is outstanding and can be attempted for future studies. Forest elements are abundant at the top of the zone, as subtropical forests spread throughout the environment. Possible summer rainfall only slightly raised the water table, positively influencing the growth of palms (*Arecipites otagoensis*), *Cliffortia* (*Psilatricolporites quenua*), Restionaceae (*Milfordia homeopunctatus*) and mangrove elements of Rhizophoraceae (*Zonocostites ramonae)*. However, their low percentages suggest that they were also not growing adjacent to the site, there were insufficient pollen producers, or they were produced in small quantities. This assemblage may indicate a warm, tropical to subtropical forest (Coetzee and Rogers, 1982; Sciscio *et al*., 2013) which was growing in depressions on the granite hills and along the meandering palaeo-Berg River. Marine indicators were not recorded from this zone.

Palynomorph Zone 6 (*Leiotriletes maxoides* zone) assemblage is marked by an increased level of cryptogams, especially ferns such as Lygodiaceae (*Leiotriletes maxoides*) and Cyatheaceae (*Cyathidites australis*), associated with humid conditions. This humid climate is postulated by the presence of moisture-loving *Cupuliferoipollenites oviformis* (Roberts *et al*., 2017), that might have been produced by several taxa including *Castanea*, *Castanopsis* and *Lithocarpus* (Stuchlik *et al*., 2014). Palms, Liliaceae (*Liliacidites* sp.) and *Ascarina* (*Clavatipollenites* sp.) represent coastal plants typically found in tropical to subtropical regions, however, they are all absent from the southwestern Cape today (Coetzee, 1981; Coetzee, 1983; Coetzee and Muller, 1984). Palms still occur on the southeastern coast with

its subtropical and humid climate and to the north of South Africa (Coetzee, 1981). The warm and humid climate provided favourable conditions for the growth of palms, at the expense of forest elements such Podocarpaceae and subtropical trees (Oleaceae, Aquifoliaceae, Araliaceae and Casuarinaceae). An attempt has been made to distinguish Casuarinaceae from Myricaceae, however, this cannot be confirmed without the use of SEM and further research on modern pollen. Mangroves (*Zonocostites ramonae*) increased at the top of the section, possibly due to their ability to withstand highly saline environments (Boizard and Mitchell, 2011). Moderate percentages (between 18% and 25%) of wetland perennials, including Sparganiaceae (*Sparganiaceaepollenites barungensis*) and Restionaceae at the bottom of the zone are probably linked to available groundwater. Proto-fynbos elements were generally low, however, *Psilatricolporites quenua* (possible botanical affinity: *Cliffortia)* increased as groundwater became more abundant. Some species of *Cliffortia* are known to occur along marshes and streams (Scott, 1982; Coates-Palgraves, 2002). Grasses (*Graminidites* cf. *crassiglobosus* and *Graminidites* cf. *neogenicus*) and *Pentzia*-type (Asteraceae) were becoming established in this zone as the forest canopy trees were probably subsiding due to saturated soils and brackish conditions. The palynomorphs from this assemblage possibly indicate a humid subtropical-tropical woodland growing along a floodplain with some taxa growing in adjacent granite hills.

Palynomorph Zone 5 (*Sparganiaceaepollenites barungensis* zone) is dominated by wetland elements, Sparganiaceae and Restionaceae, which commonly fluctuate together (Coetzee and Muller, 1984; Bonnefille *et al*., 1990). Sparganiaceae is found in swamps and marshes surrounding lakes (Coetzee and Muller, 1984; Martin, 1990), however, it does not occur at the Cape today (Coetzee and Muller, 1984). Extant species of Restionaceae can occur in a range of environments, from wet marshes to dry habitats (Linder, 2000). However, its co-occurrence with Sparganiaceae confirms that Restionaceae identified in this study are associated with a high water table in freshwater environments (Coetzee and Rogers, 1982; Martin, 1990). Palms may have reached a maximum in this zone due to humid conditions and excess water availability. Vitaceae (*Parthenopollenites marcodurensis*) grow in the form of vines or climbers and were also abundant due to the expansion of wetlands, where their nearest living relatives are commonly found (Schüler and Hemp, 2016). Furthermore, the moderate percentages (>20%) of Poaceae (*Graminidites* cf. *neogenicus*) and *Psilatricolporites quenua* (<13%) are an indication of a saturated water table. Grasses are generally rare at LBW, indicating that they probably formed a forest or woodland understorey

as opposed to open grasslands or savanna-like environments. However, their spread could have facilitated the transition from woodland to grasslands at a later point in the evolution of the palaeoenvironment at LBW. The high occurrence of *Laevigatosporites haardti* (botanical affinity: Aspleniaceae, Blechnaceae, Davalliaceae, Dryopteridaceae, Elaphoglossaceae, Hypolepidaceae, Lindsaeaceae, Lomariopsidaceae, Oleandraceae, Polypodiaceae, Pteridaceae, Thelypteridaceae and Vittariaceae) was probably linked to the occurrence of wetter conditions and/or the spread of aquatic environments. An input of seasonal fresh- or brackish water potentially favoured algae such *Botryococcus* sp., *Ovoidites grandis* and *Planctonites* cf. *stellarius.* This assemblage suggests a shift from a subtropical-tropical forest to a forested wetland that was inundated due to flooding of the palaeo-Berg River. Akin to Saldanha Bay, the prominent taxa (Sparganiaceae, Restionaceae and Poaceae) may have formed a reed belt along the wetland (Roberts *et al*., 2017). Some forest elements such as Podocarpaceae would have been growing farther away from the swamp site, as indicated by their low numbers.

Palynomorph Zone 4 (*Apteodinium spiridoides* zone) is characterised by an acme of the dinoflagellate *Apteodinium spiridoides* (>91%). This is an early Miocene (Burdigalian) index fossil (Louwye and Laga, 1998; Jiménez-Moreno, 2006; Soliman and Ibrahim, 2012), which is extinct today. It co-occurs with other dinoflagellate cysts (*Spiniferites mirabilis* and *Operculodinium centrocarpum*), algae and inner linings of benthic foraminifera, all indicating open (shallow) marine conditions. The fluctuations of these organisms are significant for the investigation of the sea level change in Palynomorph Zone 4. The presence of these organisms suggests that Palynomorph Zone 4 likely represents fluvial/estuarine transitioning to open shelf environments that are associated with a freshwater input and low salinity. This assumption is also supported by the preserved fine sands and silts sediments, alternating with carbonaceous peats of the Elandsfontyn Fm, as recorded by Sciscio *et al*. (2013). The depositional environment associated with Palynomorph Zone 4 is discussed below.

Apteodinium spiridoides is ca. 37% at the bottom contact of Palynomorph Zone 4 and reaches ca. 49% at the bottom layers (ca. 18.96–18.7 m) of Palynomorph Zone 4. It decreases from ca. 49% at 18.88 m to ca. 6% at 18.7 m. Algae (*Ovoidites grandis*, *Botryococcus* sp. and *Zygnema*) associated with freshwater and brackish water conditions are also common at the bottom of Palynomorph Zone 4. Tropical vine-like ferns, Gleicheniaceae (*Gleicheniidites* spp.) are gradually increasing as wet and humid conditions prevail. Wetland plants including

Restionaceae, *Sparganiaceaepollenites barungensis* and *Cyperaceaepollenites* sp. were widespread as the water table increased and woodlands retreated. Grasses, proto-fynbos elements (*Psilatricolporites quenua* and Proteaceae) and forest elements such as Podocarpaceae, palms, *Oleoidearumpollenites reticulatus* and Euphorbiaceae (*Rhoipites alveolatus*) occur at low percentages possibly due to increasing saline conditions and flooding caused by a sea level rise.

This sea level rise at the bottom of Palynomorph Zone 4 represents the onset of a marine transgression (marked IV in Fig. 6) – characterised by copious amounts of dinoflagellate cysts and foraminiferal test linings. The transgression possibly marks the beginning of a transgressive systems tract (TST) sequence, characterised by a sedimentation rate is slower than the rise in sea level. TSTs are typically associated with estuaries, and the decrease in *Apteodinium spiridoides* from 18.88 m to 18.7 m could be caused by a flood (tidal) current associated with estuaries.

The composition of the middle layers (ca. 18.68–18.43 m) of the zone is similar to that of the lower layers of this zone, however, *Apteodinium spiridoides* reaches its acme (ca. 91%), indicating the peak of the transgression (III in Fig. 6). This high abundance of *A. spiridoides* may point to the maximum flooding surface (MFS), at which the sea reached its most landward position within the estuary. The position of the MFS may point to even lower depositional rates in these levels. Percentages are lower for *Spiniferites mirabilis* and *Operculodinium centrocarpum*, possibly due to a lack of nutrients or a low number of cyst producers. *Cyperaceaepollenites piriformis* (botanical affinity: *Cladium mariscus*) occurs only in this section where aquatic environments acquired a maximum water incursion level due to the transgression. Algae, cryptogams, other swamp vegetation, and forest and subtropical trees like Podocarpacae, palms, Araliaceae (*Rhoipites couperi*), Fagaceae (*Cupuliferoipollenites oviformis)*, proto-fynbos elements and grasses have also possibly declined due to increasingly saline levels and flooding of the local environment. The sea level begins to fall again – as indicated by *Apteodinium spiridoides* from ca. 18.58 m (ca. 68%) to ca. 6% at 18.48 m.

In the uppermost layers of Palynomorph Zone 4 (18.38–18.28 m), *Apteodinium spiridoides* increases from ca. 54% at 18.38 m to ca. 61% at 18.28 m. Although *Spiniferites mirabilis*, *Operculodinium centrocarpum* and *Cordosphaeridium minimum* increase, there is a gradual decrease in the sea level from the middle layers. At this point, sedimentation rates may have

gradually increased again, and the position of the shoreline moved seaward. These sediments may have been derived from river aggradation and erosion of the hinterland. Podocarpaceae, palms, Sapotaceae (*Tetracolporopollenites sapotoides*), Myricaceae (*Myricipites harisii*) possibly occur more frequently as the sea level was being lowered. *Rauvolfia* (*Margocolporites rauvolfii*), a tree that commonly grows where there is sufficient groundwater in the summer rainfall region of eastern South Africa (Coates-Palgrave, 2002) is restricted to Palynomorph Zone 4. Proto-fynbos elements Ericaceae (*Ericipites callidus*) and *Psilatricolporites quenua* are decreasing as the substrate they were growing on was inundated with water.

Palynomorph Zone 4 possibly represents a fluviatile/estuarine and marine environment under the influence of a sea level rise and fall cycle. Transgressions are often marked by a stepwise progression of the landwards movement of the coastline, therefore, the short-term "regressions" that are recorded in Palynomorph Zone 4 may be a function of higher sedimentation rates than the production of accommodation space. Furthermore, the BH2 core site may have been more proximal to the terrestrial palynomorph source during these regressions but evidence of this may be concealed by reworking and erosion of sediment from the estuary.

A marine transgression was postulated to have induced the deposition of the Elandsfontyn Formation in the Oligo-Miocene (Coetzee and Rogers, 1982; Roberts *et al*., 2011; Sciscio *et*
A marine transgression was postulated to have induced the deposition of the Elandsfontyn Formation in the Oligo-Miocene (Coetzee and Rogers, 1982; Roberts *et al*., 2011; Sciscio *et* *al*., 2013; Roberts *et al*., 2017), and this transgression could possibly be correlated with the transgression cycle recorded from Palynomorph Zone 4. Additionally, mangroves are not recorded from this zone and the following zones, which may have been a result of the drowning of the coastline and lowered sea surface temperatures during the marine transgression (Tyson, 1995).

Palynomorph Zone 3 (*Milfordia* zone) suggests that the floodplain was locally flooded, or the water table was elevated by the third sea level rise (II in Fig. 6) that occurred in Palynomorph Zone 4), developing a wetland in which Restionaceae, Cyperaceae (*Cypeaceaepollis* sp.) and reeds *Sparganiaceaepollenites barungensis* grew. Algae (*Botryoccocus* sp., *Pediastrum*-type, *Ovoidites grandis* and Zygnemataceae) were abundant, underlining local moisture. Dinoflagellate cysts (all identified taxa <5%) and linings of benthic foraminifera – although

most abundant in this zone (ca. 5%) – were all low, indicating that the overall marine productivity or influence was reduced. Dinoflagellatecysts increased towards the top of the section, alluding to a gradual increase in marine influence and by extension, in the sea level. Gleicheniaceae (*Gleicheniidites* spp.) reaches a maximum (ca. 25%) in this zone, pointing to local moisture at LBW and possibly surrounding areas. Podocarpaceae, including *Microcachrydites* sp. and Cupressaceae (*Cupressacites* sp.) are low (all less than 10%), but increased in abundance from Palynomorph Zone 4, suggesting the lowered influence of brackish marine water. Subtropical trees including palms, Araliaceae (*Rhoipites couperi*), Myricaceae (*Myricipites harisii*) and Oleaceae (*Oleoidearumpollenites reticulatus*) are also low (all less than 5%) but increased from the previous zone for the same reason as the gymnosperms. The woodland trees such as Euphorbiaceae (*Rhoipites alveolatus*), Combretaceae, *Peregrinipollis nigericus* (*Brachystegia*) are occurring more frequently, suggesting the formation of a savanna woodland characterised by a smaller cover of trees and a herbaceous cover. *Brachystegia* and Combretaceae are important modern indicators of open canopy woodlands, known as miombo woodlands, a relict thereof occurring only in the northern region of South Africa today, Mozambique, Malawi, Zambia, Angola, Democratic Republic of Congo, Tanzania and Zimbabwe (Schüler and Hemp, 2016; Roberts *et al*., 2017). Arid conditions associated with subtropical thicket environments dominated by these elements were probably caused by higher seasonality and a strengthening summer rainfall (Roberts *et al*., 2017). Grasses and proto-fynbos plants such as Proteaceae, *Psilatricolporites quenua* (*Cliffortia*) and Rosaceae (*Rhoipites arnotiensis*) were increasing and co-occurring with the savanna woodland trees, suggesting the possible change from a subtropical forest to a subtropical and semi-arid savanna woodland with stronger seasonality including the likelihood of higher summer rainfalls. This assemblage possibly indicates that as sea levels and the water table dropped, the vegetation shifted from a subtropical woodland to a savanna woodland growing adjacent to a river/tidal environment, with some vegetation types growing further away on the Cape granite hills.

Palynomorph Zone 2 (*Operculodinium centrocarpum* zone) is characterised by abundant dinoflagellate cysts, particularly *Operculodinium centrocarpum* and *Spiniferites mirabilis*, indicating estuarine and shallow marine conditions. *Operculodinium centrocarpum* is found in a wide range of environments, whereas *Spiniferites mirabilis* occurs only in tropical and temperate regions (Marret and Zonneveld, 2003; Zonneveld and Pospelova, 2015). High levels of *Operculodinium centrocarpum* are documented in the region of the Benguela

Upwelling System in the present day (Marret and Zonneveld, 2003). *Apteodinium spiridoides*, *Cordosphaeridium minimum* and *Chiropteridium lobospinosum* are abundant in this zone and are all extinct taxa. A final rise in sea level (I in Fig. 6) is inferred by the high levels of dinoflagellates. A gradual increase in the sea level may have occurred when the rate of sedimentation was lowered. It is possible that transgressions I–IV are part of one transgressional cycle. Alternatively, these transgressions can be explained by eustatic sea level rise and fall oscillations that are related to the deglaciation of Antarctica during the same time period, leading to brief, rapid transgression cycles (Miller *et al*., 1991; 2021).

Botryococcus sp. and *Ovoidites vangeeli* are quite low in abundance, potentially pointing to a lowered input of fresh water from the palaeo-Berg River or unsatisfactory growth conditions in the water bodies. Deficient percentages of Myricaceae (*Myricipites harisii*) and Sapotaceae (*Tetracolporopollenites sapotoides*), grasses and *Psilatricolporites quenua* (*Cliffortia*) are possibly due to low pollen production and the retreat of the savanna woodland. Other trees, shrubs, herbs and shrublets are not recorded. An interpretation of the palaeoecological setting is hampered by the extremely low number of pollen grains in Palynomorph Zone 2. This assemblage suggests that terrestrial palynomorphs (from the savanna woodland) were transported by selected pollinators to an estuary influenced by a marine transgression or terrestrial vegetation was significantly reduced with the encroachment of brackish water during a marine transgression. However, changes in sedimentation rates or a low pollen preservation due to taphonomic factors are possible reasons for the low recovery of pollen in this zone.

Palynomorph Zone 1 (*Botryococcus* zone) is dominated by algae (*Botryococcus* sp.) and the dinoflagellate taxon *Apteodinium spiridoides*, probably due to persisting brackish conditions from the last recorded rise in sea level. The lower percentages and diversity of dinoflagellates reflect falling sea levels and decreased marine productivity. Swamp plants (*Milfordia hypolaenoides*), palms, Myrtaceae/Sapindaceae (*Cupaniedites* sp.), *Psilatricolporites quenua* and *Tubulifloridites antipodica* are the only recorded pollen grains suggesting that the terrestrial landscape was submerged or completely retreated. This assemblage suggests that palynomorphs from the savanna woodland were reworked and mixed with marine palynomorphs in a lagoon along the shoreline. Pollen recovery was also extremely low in this zone, possibly due to taphonomic processes, thus reducing the reliability of the palaeoecological interpretation.

The effects of taphonomic processes were not considered for this study, however, their effects may have contributed to poor pollen and low preservation of pollen (and other palynomorphs) that is observed in some of the palynomorph zones. The identified types of pollen damage include fracturing or breaking of grains; corrosion and thinning of the exine; compaction and thermal alteration by diagenetic processes within the depositional environment; and damage during the lab analysis. Pollen production may have also been influenced by the pollen productivity and the dispersal rates of the species. A thorough analysis of taphonomic effects should be considered to improve the designation of palynomorph zones of Core BH2 and associated palaeoenvironmental conditions that persisted at LBW. Additionally, these effects may influence PC scores (discussed below), which can support the investigation of palaeoenvironmental conditions that prevailed during the deposition of the Elandsfontyn Formation.

4.1.2 Principal Components Analysis (PCA): Association of palaeoecological trends

Palynomorph Zone 7 (33.03–30.92 m) depicts positive loadings on both PC1 and PC2, with PC1 recording probabilities with a minimum of ±0.4 and a maximum of ±0.58 for this interval (Appendix D; Fig. 4; 5). PC2 shows a minimum probability of 0.31 and a maximum probability of 0.56 (Appendix D; Fig. 4; 5). These positive loadings of PC1 can possibly be attributed to high percentages or occurrence of forest elements (Podocarpaceae), subtropical trees (palms, *Ilexpollenites margaritatus*, *Rhoipites couperi*, *Oleoidearumpollenites reticulatus*, *Cupuliferoipollenites oviformis*), herbs and shrublets (*Mutisiapollis viteauensis* and Poaceae) and proto-fynbos elements (*Psilatricolporites quenua* and *Rhoipites arnotiensis*). The taxa show a strong correlation supporting the existence of a subtropical-tropical forest and therefore, this layer can be correlated with group 27.5–32.5 m from the PCA conducted with depths as variables (Fig. 8).

In Palynomorph Zone 6 (25.6–19.85 m) both components (PC1 and PC2) only weakly fluctuate and range between probabilities of ±0.36–0.63 and ±0.04–0. 56, respectively (Appendix D; Fig. 4; 5;6). PC1 is higher than PC2, implying a positive correlation to the occurrence of cryptogams and associated humid conditions. PC2 is lower, which can be explained by decreasing forest and subtropical elements, mangroves, woodland trees and increasing wetland taxa (Sparganiaceae and Restionaceae) – although not all reflected – and

cryptogams. This zone can be compared with group 2 (22.5–25 m) (Fig. 8), which is dominated by cryptogams, possibly pointing to local moisture.

Palynomorph Zone 5 (19.8–18.96 m) shows strong fluctuations for both PC1 and PC2. PC1 has a range of 0.43–0.75 whereas PC2 records a range of –0.11–±0.39 (Appendix D; Fig. 4; 5; 6). Forest, subtropical, proto-fynbos and herbs and shrublets decrease along PC2. Grasses and wetland taxa (without the influence of Sparganiaceae and Restionaceae) increase on PC1, indicating a positive correlation with wetland taxa. This section can be correlated with group 1 (15–20 m) (Fig. 8), which possibly indicates the occurrence of a reed belt along a wetland.

Strong fluctuations also characterise Palynomorph Zone 4 (18.9–18.28 m) with PC1 recording a minimum probability of 0.29 and a maximum probability of 0.76 whereas PC2 show a minimum loading of –0.67 and a maximum loading of 0.06 (Appendix D; Fig. 4; 5; 6). Although marine taxa and some wetland taxa (Restionaceae and Sparganiaceae) were removed, the positive probabilities on PC1 can be attributed to an increasing marine influence which resulted in marine transgressions and negative probabilities on PC2 can possibly be linked to the low percentages of plant groups. This zone can also possibly be correlated with group 1 (15–20 m) (Fig. 8).

In Palynomorph Zone 3 (18.2–17.28 m) PC1 increases and reaches a maximum probability of ±0.83 and a minimum probability of 0.49, whereas PC2 reaches a maximum probability of –0.09 and a minimum probability of –0.54 (Appendix D; Fig. 4; 5; 6). Forest and subtropical elements are attributed to negative loadings on PC1, and proto-fynbos, wetland taxa and cryptogams are associated with positive loadings on PC1. PC2 depicts the decrease of other plant ecological groups, pointing to the onset of local arid climatic conditions. Palynomorph Zone 3 records palynological fluctuations that can also be correlated with group 1 (15–20 m) (Fig. 8). The highest loadings are associated with PC1 from Palynomorph Zone 7 to Palynomorph Zone 3, possibly implying more variation and a stronger influence on the dataset as opposed to PC2.

4.2 Tentative age determination based on dinoflagellate and pollen stratigraphy

The inferred biostratigraphic age of the Elandsfontyn Formation is based on important pollen and dinoflagellate indicators within each assemblage (Fig.12). The dating cannot be confirmed with a high degree of certainty as Core BH2 is not continuous throughout the

sequence. Palynomorphs do not occur continuously throughout the core, and this may reflect sedimentation rates that were not constant through time. Furthermore, sedimentological and taphonomic factors may have attributed to the possible time-averaging of palynomorphs, leading to the assumption that palynomorphs found in the same deposit but representing different time periods are synchronous.

Figure 12. Tentative age of the Elandsfontyn Formation at LBW based on pollen and dinoflagellate cyst stratigraphy (adapted from Roberts *et al*., 2017). The red arrow indicates that the taxon extends to the present day. Black star = Palynomorph Zone 7 (*Podocarpidites* zone at 33.03–28.6 m); Red star = Palynomorph Zone 6 (*Leiotriletes maxoides* zone at 28.6–19.825 m); Green star = Palynomorph Zone 5 (*Sparganiaceaepollenites barungensis* zone at 19.825–18.96 m); Light blue star = Palynomorph Zone 4 (*Apteodinium spiridoides* zone at 18.96–18.24 m); Dark blue star = Palynomorph Zone 3 (*Milfordia zone* at 18.24–16.865 m); Yellow star = Palynomorph Zone 2 (*Operculodinium centrocarpum zone*) at 16.865–13.4 m; Purple star = Palynomorph Zone 1 (*Botryococcus* zone at 13.4–1.61 m). Morgenroth (1966)[(3)]; Costa and Downie (1979)[(1)]; Barreda (1993)[(6;7)]; Martin (1993)[(2)]; Katuna *et al*. (1996)[(2)]; Louwye and Laga (1998)[(1)]; Weems and Edwards (2001)[(1)]; Jiménez-Moreno *et al*. (2006)[(3)]; Bati and Sancay (2007)[(3)]; Fensome *et al*. (2009)[(1)]; Zonneveld and Pospelova (2015)[(4;5)]; Mahboub *et al*. (2019)[(2)].

A suggested age of early late Oligocene (early Chattian) (Fig. 12) is given for Palynomorph Zone 7, which is marked by the presence of *Mutisiapollis viteauensis*, a late Oligocene marker in the Southern Hemisphere (Guerstein *et al*., 2004; Barreda *et al*., 2010). Asteraceae, including *Tubulifloridites antipodica*, is known to have evolved during the Oligocene (Muller, 1981; Coetzee and Rogers, 1982; Barreda, 1993). *Tubulifloridites* first appears in the Oligocene (Muller, 1981; Barreda *et al*., 2010) but becomes dominant in the Miocene (Barreda *et al*., 2010). Asteraceae has been reported from the Palaeocene–Eocene of Southern Africa (Zavada and de Villiers, 2000). African species of Mutisieae (*Mutisiapollis viteauensis*) were assigned a Palaeocene–Eocene age from the study by Zavada and de Villiers (2000). Scott *et al*. (2006) referred to the African species as *Dicoma* type during a reassessment of the same core material and assigned them a Middle Eocene age. According to Zavada and de Villiers (2002) and Scott *et al*. (2006), the African species of Mutisieae are similar to the South American species studied by Barreda (1993). The presence of *Oleoidearumpollenites reticulatus*, which first appeared in the Oligocene (Stuchlik *et al*., 2014), further supports a late Oligocene (early Chattian?) age for this assemblage. Palaeoenvironments in the late Oligocene were dominated by palynoflora comprising Araucariaceae, Nothofagaceae, Podocarpaceae, Casuarinaceae, Arecaceae, Proteaceae, Poaceae and ferns of Lygodiaceae and Cyatheaceae (Barreda and Palazzesi, 2007; Barreda *et al*., 2009; Kumar *et al*., 2012; Conran *et al*., 2014). The components of these palaeoenvironments are similar to those of Palynomorph Zone 6 and Palynomorph Zone 5, implying that they may also be of late Oligocene (early and middle Chattian) age (Fig. 12).

The appearance of *Apteodinium spiridoides* – an index fossil of the Burdigalian (Louwye and Laga, 1998; Jiménez-Moreno *et al*., 2006; Soliman and Ibrahim, 2012) – and *Chiropteridium lobospinosum*, a known Oligocene marker (Besems, 1992; Katuna *et al*., 1996; Willumsen *et al*., 2014), are important biostratigraphic age indicators for determining the age of Pollen Zone 4. However, *Apteodinium spiridoides* has been recorded in older late Eocene, (North Atlantic; Costa and Downie, 1979) and late Oligocene (U.S.A.; Weems and Edwards, 2001) sediments.

Previous studies (Tankard and Rogers, 1978; Siesser and Dingle, 1981; Hendey, 1982; Roberts and Brink, 2002) along the southwestern Cape reflect the effect of changes in the relative sea level on Cenozoic palaeoenvironments. Several of these studies postulate that the initial deposition of the Elandsfontyn Formation started during a sea level rise, causing

transgressions (initially – 36 m and finally ~ 13 m asl at LBW) at the Oligo-Miocene boundary (Rogers, 1980; Coetzee and Rogers, 1982; Roberts and Brink, 2002; Roberts *et al*., 2011; 2017). Diester-Haass (1988) studied carbonate dissolution rates of benthos/plankton foraminifera at Eastern Walvis Ridge, southwest Africa and found good preservation of the foraminifera in the late Oligocene–early Miocene. The low dissolution rates were linked to high sea levels. Stable $\delta^{18}O$ and $\delta^{13}C$ isotopes of benthic foraminifera are linked to changes in global ice volume (thus glacio-eustatic changes), ocean circulations and carbon cycling (Holbourn *et al*., 2018; Lisiecki and Raymo, 2005; Miller *et al*., 2020). Oxygen isotopes of benthic foraminifera indicate a global sea level rise in the late Oligocene (Miller *et al*., 1991; 1996; Rasmussen, 2004). This global sea level might be correlated with the first increase of oxygen isotopes of benthic foraminifera (event Mi1) (Miller *et al*., 1996) and the first sea level rise of cycle TB 1.4 (Haq *et al*., 1987; Miller *et al*., 1996) (Fig. 13). Therefore, the marine transgressions recorded in Palynomorph Zone 4 can be assumed to be shorter, second-order transgressions that are linked to this global late Oligocene sea level rise. A correlation of local and global sea level changes and the occurrence of index dinoflagellate fossil, typically of the early Miocene, assumes a late Chattian (late Oligocene) age for Palynomorph Zone 4 (Fig. 12).

The *Milfordia* zone (Palynomorph Zone 3) represents the renewed establishment of a wetland environment (dominated by Restionaceae) that prevailed during a gradual sea level fall. A similar late Oligocene–early Miocene Restionaceae dominated swamp environment from Australia was documented by Martin (1990), which occurred with other wetland elements (Sparganiaceae and Cyperaceae), grasses, Podocarpaceae, Casuarinaceae, Myrtaceae, Gleicheniaceae, *Pediastrum* and *Botryococcus*. Archangelsky and Zamaloa (2003) described early early Miocene (Aquitanian) Patagonian swamp environments dominated by Sparganiaceae, often occurring with Restionaceae, *Mutisiapollis viteauensis* and Poaceae (Barreda and Palazessi, 2007). Although the proliferation of savannas and grasslands in southern Africa occurred during the Miocene (Bredenkamp, *et al*., 2002; Linder and Rudall, 2005), the recorded Poaceae percentages from this study are not high enough to constitute those of a grassland or savanna. They can be considered as part of the reed belt associated with the wetlands or possibly signal the onset of an expansion of savannas. Low pollen percentages of forest trees, which coincided with these early early Miocene swamps, were thought to have been the result of increasing aridity (Barreda and Palazzesi, 2007). Southern African records of this assemblage, particularly from the Cape region, are reported from early

to middle Miocene (Coetzee and Rogers, 1982; Coetzee and Muller, 1984; Sciscio *et al*., 2016).

The Oligo-Miocene Boundary transition is characterised by Antarctic ice expansion (due to global cooling) and a resultant sea level fall (Miller *et al*., 1991; Rasmussen, 2004; Miller *et al.*, 2020). According to Miller *et al*. (1991), this transitional period defines the base of the oxygen isotope zone or event "Mi-1" that takes place in the Oligocene through to the early Miocene. The low percentages of dinoflagellates and linings of benthic foraminifera at the bottom of Palynomorph Zone 3 (following the previous marine transgression in Pollen Zone 4) can possibly be attributed to falling sea levels comparable to cycle 1.4 of Haq *et al*. (1987) or the onset of decreased levels of oxygen isotopes of benthic foraminifera associated with event Mi1 of Miller *et al*. (1996) (Fig. 13). Therefore, an Oligocene/Miocene (late Chattian to early Aquitanian) age can be suggested for Palynomorph Zone 3 (Fig. 12).

Operculodonium centrocarpum is the dominant fossil of Palynomorph Zone 2, however, it has a long history spanning from the Eocene to present day. Palynomorph Zone 2 experienced the longest and final transgression event of the entire sequence (I in Fig. 6). *Cordosphaeridium minimum*, now extinct, might be suitable for determining the age, as its oldest record is in the early Eocene (Morgenroth, 1966) but has also been recorded from middle Miocene deposits (de Verteuil, 1996; Jiménez-Moreno, 2006). Global sea level changes ~ 30–40 m asl (Miller *et al*., 2020) corroborate the occurrence of two Oligo-Miocene transgression analogous to Mi1 (Miller *et al*., 1996) due to the deglaciation of the East Antarctica Ice Sheet (EAIS) (Haq *et al*., 1987; Kominz *et al*., 1998; Miller *et al*., 1996; Miller *et al*., 2011; Miller *et al*., 2020). Although the EAIS was not fully developed, sea levels consistently remained below the ice levels (Miller *et al*., 2020). Therefore, Palynomorph Zone 2, may be compared to the recorded increase of oxygen isotopes of benthic foraminifera of event Mi1a (Miller *et al*., 1996) or the first transgression of cycle 1.5 (Haq *et al*., 1987; Miller *et al*., 1996) (Fig. 13), thus assigning it a possible middle to late Aquitanian age (Fig. 12).

Palynomorph Zone 1 (*Botryococcus* zone) experiences a final regression event, indicated by declining dinoflagellates and encroaching freshwater organisms. This regression can possibly be correlated with the initial glaciation event and the first decrease of oxygen isotopes of benthic foraminifera of event Mi1a (Miller *et al*., 1996) or the first regression of cycle TB 1.5 (Haq *et al*., 1987; Miller *et al*., 1996) (Fig. 13), suggesting an early Miocene (early

Burdigalian?) age for the sequence (Fig. 12). Sciscio *et al*. (2013) proposed a middle Miocene age for Core BH2, however, a re-analysis of the core material with records of significant biostratigraphic markers, points to a late Oligocene–early Miocene age, confirming the initial age suggestion of Coetzee and Rogers (1982). Therefore, LBW is assumed to have formed at around the same time as Saldanha Bay palaeoenvironments with which it shares many palynological similarities (Roberts *et al*., 2017).

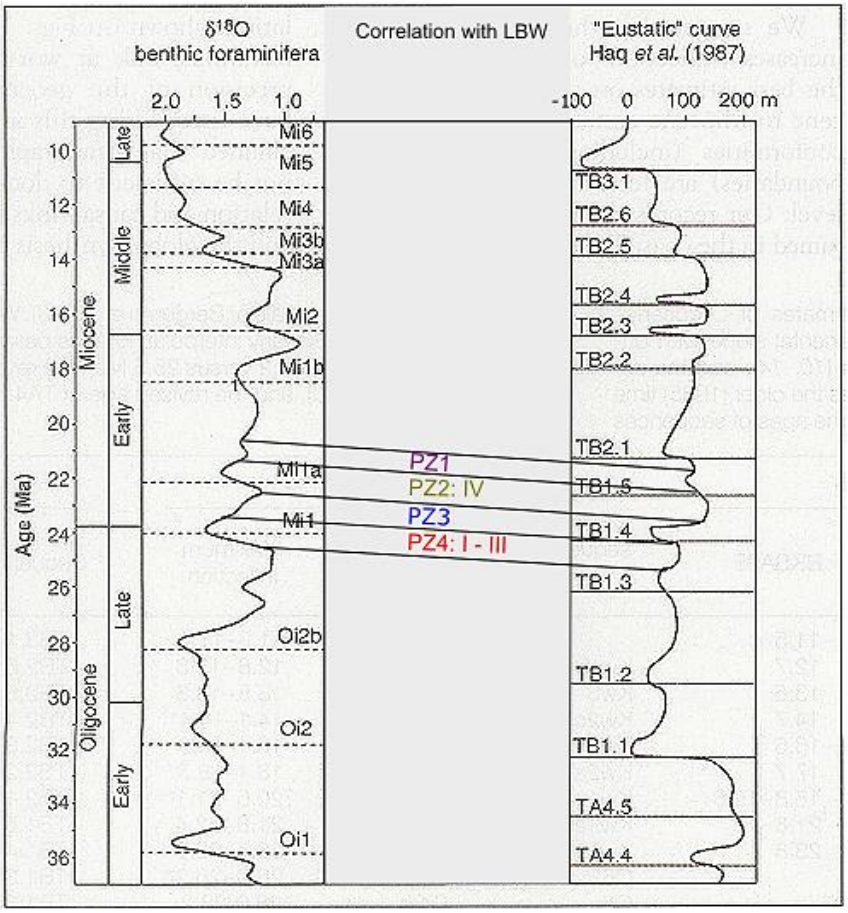

Figure 13. Correlation of palynomorph zones from LBW with global oxygen isotopes of benthic foraminifera and eustatic sea level changes (adapted from Haq *et al*., 1987 and Miller *et al*., 1996). PZ = Palynomorph Zone (from LBW).

4.3 REGIONAL COMPARISON

This section is a comparison of palaeoenvironments along the southwestern Cape (Fig. 2) which are relatively similar and in proximity to that described from LBW in this study. Table

3 provides a suggestion of the stratigraphic correlation between LBW (this study), the previously dated middle Miocene LBW (Sciscio *et al*., 2013) and late Oligocene–early Miocene Saldanha Bay (~24 km from LBW; ~147 km north of Cape Town) (Roberts *et al*., 2017). Other regional sites including the early Miocene, Rondeberg (~ 60 km from Cape Town; ~102 km to LBW) (Roberts *et al*., 2013), early to middle Miocene Noordhoek (~34 km south of Cape Town; ~160 km from LBW) (Sciscio *et al*., 2016), and the Miocene Knysna (~ 490 km southeast of Cape Town; ~ 552 km from LBW) (Carr *et al*., 2010; Goble, 2015) are discussed below.

These studies report the existence of an initial tropical to subtropical forest, dominated by Podocarpaceae, palms, Cupressaceae, Araucariaceae, Oleaceae, Casuarinaceae and Myrtaceae/Sapindaceae (*Cupaniedites*). The forest proceeds to a wetland (marsh) environment with abundant Sparganiaceae (*Sparganiaceaepollenites barungensis*), Restionaceae, Cyperaceae and Poaceae. Taxathat are extinct from southwestern Cape today but are recorded in the present study or similar studies at the Cape include *Microcachryidites* sp. (Podocarpaceae), Casuarinaceae, Oleaceae, *Cupaniedites* (Mytaceae/Sapindaceae) and *Sparganiaceaepollenites barungensis* (Sparganiaceae).

Fynbos elements (macchia) are already established at these sites but occur only sparsely. Ericaceae seems to be the least abundant in all the sites apart from Rondeberg (Roberts *et al*., 2013). They only propagate at a later stage, signalling the initiation of drier conditions throughout the region. Although the vegetation composition of these sites is similar, an accurate correlation cannot be achieved due to discrepancies in the dating between this study and previous studies.

4.3.1 Elandsfontyn Formation, Langebaanweg (this study) and Elandsfontyn Formation, Langebaanweg (Fig.14) (Sciscio *et al*., 2013)

This study is a re-analysis of the previous studies on the Elandsfontyn Formation at LBW and has produced a better resolution of the palaeoecology of LBW at this site. The limited samples and the sampling interval for the pilot study by Sciscio *et al*. (2013) is possibly the cause of the disparity identified in both studies and hampers the correlation between both studies which were performed on the same sediments. Sciscio *et al*. (2013), like this study, inferred the existence of a subtropical-tropical forest, alternating with marsh/swamp environments.

Subsection III (30.915–33.025 m) (Sciscio *et al*., 2013) (Fig. 14) represents a Podocarpaceae-dominated forest comprising *Podocarpidites* (Podocarpaceae) and *Microcachrydites* (Podocarpaceae), alongside subtropical arboreal trees such palms, *Tricolporopollenites reticulatus* (Oleaceae), *Celtispollenites* (Ulmaceae) and Casuarinaceae. The forest is gradually replaced by wetland taxa such as Restionaceae, *Sparganiaceaepollenites* sp. (Sparganiaceae) and Poaceae. This subsection is equivalent to the *Podocarpidites* zone in the current LBW study, however, *Microcachyrdites* is not recorded in Palynomorph Zone 7 from the current study. Araucariaceae (cf. *Araucariacites australis*) is not recorded (possibly due to the low occurrence of the taxon) in the pilot study (Sciscio *et al.*, 2013) and in Noordhoek (Sciscio *et al*., 2016), which were previously thought to be of the same age. Both assemblage zones confirm an initial subtropical-tropical forest environment with summer rainfall. Mean annual temperatures (MATs) were higher in the sections that possibly experienced higher rainfall indicated by acidic or lower pH soils (Sciscio *et al*., 2013). An equivalent of Palynomorph Zone 6 (*Leiotriletes maxoides* zone) was not recorded in the pilot study by Sciscio *et al*. (2013).

Subsection II (16.47–20.32 m) (Sciscio *et al*., 2013) (Fig. 14) reflects a wetter subtropical environment, initially dominated by *Podocarpidites* and *Rhoipites pilatus* (Araliaceae). Increasing palms, Apocynaceae (*Margocolporites rauvolfii*), Restionaceae, Sparganiaceae, Poaceae, cryptogams and algae signal wetter conditions and a higher water table due to increased rainfall. Dinoflagellates (only *Spiniferites* was recorded) become more abundant due to encroaching marine waters. Gymnosperms are reduced due to brackish and wetter conditions. The *Sparganiaceaepollenites barungensis* to *Milfordia* zones (Palynomorph Zone 5 – 3) in the present study assimilates Subsection II in the pilot study (Sciscio *et al*., 2013), but dinoflagellates – which are important for determining the stratigraphy – are only superficially described and assigned to a single genus (*Spiniferites*) in Sciscio *et al*. (2013). Additionally, only a single regression was proposed (Sciscio *et al*., 2013), posing difficulty in correlating the transgression events with global sea level changes. The present study indicates that three second-order marine transgressions occurred at this depth range, which can be explained by the much higher resolution provided in the current study.

In subsection I (7.20–7.61 m) (Sciscio *et al*., 2013) (Fig. 14), Restionaceae are abundant, alongside forest elements (podocarps and *Cupressacites*) and subtropical trees such as palms and Euphorbiaceae. Fynbos elements (better suited to arid conditions and winter rainfall) are

still moderately diverse but occur in low percentages, indicating that conditions were still warm, and that rainfall was inter-annual (Sciscio *et al*., 2013). The *Operculodinium centrocarpum* to *Botryoccocus* zones (this study) are comparable to subsection I in Sciscio *et al*. (2013). However, Sparganiaceae, ferns and algae are abundant in subsection I in the Sciscio *et al*. (2013) study. In this study, these levels have the lowest pollen and spore preservation. The longest marine transgression (I in Fig. 6) as evidenced by *Operculodinium centrocarpum* (this study) is not recorded in Sciscio *et al*. (2013), possibly due to a much lower sample resolution. The re-analysis of this pilot study improved the palynological record, with a much higher diversity, including the discovery of cf. *Araucariacites australis*, mangroves, Vitaceae, *Peregrinipollis nigericus* (*Brachystegia*) and ferns. An enhanced biostratigraphy was also possible through the identification of dinoflagellates such as *Apteodinium spiridoides*, *Cordosphaeridium minimum* and *Chiropteridium lobospinosum*), thus assigning the Elandsfontyn Formation at LBW a late Oligocene to early Miocene age. However, this time period is only tentative and requires confirmation by other regional studies.

4.3.2 Elandsfontyn Formation, Langebaanweg and Elandsfontyn Formation, Saldanha Bay (Fig. 15) (Roberts *et al*., 2017)

Two subzones and one zone (Zone 1a, 1b and 2) were identified at Saldanha Bay (Roberts *et al*., 2017), which reflect significant similarities to the assemblage zones identified at the current study of LBW.

Zone 1 (1a and 1b) covering 27.75–22.90 m at Saldanha Bay (Roberts *et al*., 2017) (Fig. 15) represents a forest dominated by Podocarpaceae, with other forest canopy trees such as Araucariaceae, *Dacrydiumites* sp. – also identified from in this study, in Knysna (Carr *et al*., 2010) and within Arnot Pipe sediments (Scholtz, 1985) – Fagaceae (*Cupuliferoipollenites oviformis*) and Sapotaceae. *Pseudowinterapollis couperi* (Winteraceae), an extinct taxon that was not recorded at LBW was also identified in a previous study of Saldanha Bay by Coetzee (1983). Mangroves are more abundant and continuous at Saldanha Bay, possibly indicating that they were producing sufficient pollen close to the coastline (Roberts *et al*., 2017). LBW is presently located ~ 24 km from Saldanha Bay and this distance from the coastline may have hindered the transportation of mangrove pollen at LBW, as seen by the low percentages from this study. Savanna woodland elements are more common at Saldanha Bay (Roberts *et*

al., 2017), including *Brachystegia* (*Peregrinipollis nigericus*), which is rare at LBW (this study). Fynbos elements are recorded, and Ericaceae in particular, is found to have occurred

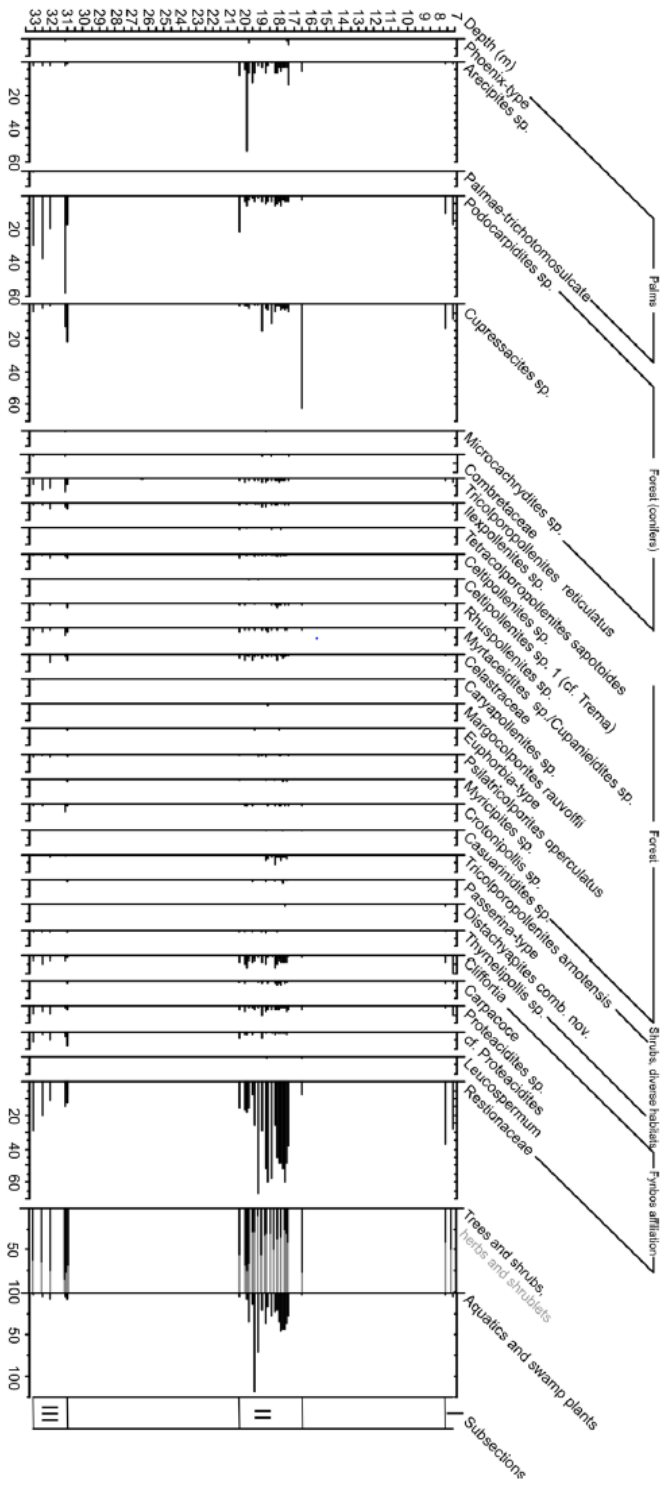

Figure 14. Pollen diagram of selected palynomorphs from LBW (taken from Sciscio *et al*., 2013)

at both sites, although in very low percentages at LBW. Wetland taxa (Restionaceae, Sparganiaceae and Cyperaceae) are common in this zone, forming a reed belt (with Poaceae), which could also have been the case at LBW. Lygodiaceae and Gleicheniaceae spores are abundant, indicating humid conditions. Freshwater algae, dinoflagellates and microforaminiferal linings are recorded, signalling a marine influence at Saldanha Bay. Zone 1 (a and b) at Saldanha Bay might possibly be compared to Palynomorph Zone 7 – Palynomorph Zone 6 at LBW.

Zone 2 at 22.75–18.70 m (Roberts *et al*., 2017) (Fig. 15) transitions from a forest to a swamp environment, dominated by Cyperaceae and Sparganiaceae. Gymnosperms, except Cupressaceae have decreased. Mangroves have also decreased, possibly due to submersion of the coastline. Fynbos elements have reportedly experienced little change. Dinoflagellates and microforaminiferal linings are evidence of a transgression. Saldanha Bay shows a single transgression only in this zone (Roberts *et al*., 2017) and may represent a shorter time period than the time period suggested for LBW in this study. This may also mean that only one transgression is recorded there, or in the case of more than one transgression, are either not preserved or are cannibalised during base level regression. Only *Spiniferites*, *Cordoshpaeridium minimum*, *Operculodinium centrocarpum* and *Chiropteridium lobospinisum* occur at both sites. LBW is ca. 14 km inland from Saldanha Bay (Roberts *et al*., 2017), which may account for the lower diversity of recorded dinoflagellate cysts. Zone 2 can be compared to Palynomorph Zone 5 – Palynomorph Zone 2, both representing early Miocene deposits.

4.3.3 Elandsfontyn Formation, Langebaanweg and Elandsfontyn Formation (clay pits), Rondeberg (Roberts *et al*., 2013)

The Elandsfontyn Formation at Rondeberg (~ 102 km from LBW) is preserved as clay pits deposited by a meandering river in fluvio-lacustrine environments. Palynomorph preservation is generally poor at Rondeberg and a biostratigraphic correlation of the two sites is especially difficult or even impossible. The lowest level (1.1 m) at Rondeberg is dominated by subtropical arboreal trees (*Ilex*-type, Oleaceae, Rhamnaceae) and fynbos elements and ferns. Ericaceae is far more abundant at Rondeberg than at LBW and Saldanha Bay (Roberts *et al*., 2013). Ericaceae forms a major component of the modern fynbos vegetation, therefore it is probably more abundant at Rondeberg as the deposits are slightly younger than at LBW and Saldanha Bay (Roberts *et al*., 2013).

Podocarpaceae (also preserved as wood), is indicative of forest environments and only appears in the middle section (1.79–1.96 m) at Rondeberg alongside increasing palms, Liliaceae, Euphorbiaceae, *Pellaea*-type and Proteaceae and Restionaceae (Roberts *et al*., 2013). The oldest assemblage at LBW is dominated by Podocarpaceae, however, gymnosperms are also common in the *Milfordia* assemblage zone at LBW. Although the palynomorphs in this zone (except *Pellaea*-type) occur at LBW this assemblage does not seem to correspond with any zone at LBW.

The uppermost section (3.2? – 4? m) at Rondeberg comprises abundant reticulate tricolporites pollen types with podocarps, palms, Oleaceae, Proteaceae, and ferns (Polypodiaceae) being common (Roberts *et al*., 2013). This assemblage is slightly similar to the *Milfordia* assemblage zone at LBW, although, Restionaceae is absent from this zone. Therefore, it can also not be compared to any of the assemblage zones at LBW. Although marine indicators are not recorded from Rondeberg, Roberts *et al*. (2013) notes the influence of glacio-eustatic sea level change on the deposition of the Rondeberg clays and assumes that the deposits are younger, as they would have experienced higher marine transgressions than Noordhoek and LBW. In addition to its younger age (Roberts *et al*., 2013), the distance from LBW may have also played a role in these sites not being successfully correlated.

4.3.4 Elandsfontyn Formation, Langebaanweg and Elandsfontyn Formation, Noordhoek (Sciscio *et al*., 2016)

Noordhoek is situated ~34 km from Cape Town and ~160 km from LBWElandsfontyn Formation deposits at Noordhoek show palynological similarities to the succession at LBW in this study. The age of the deposits is given as early to middle Miocene (Sciscio *et al*., 2016).

The lowermost section (35.5–39.5 m) from Core NH1 records abundant Podocarpaceae with palms, Oleaceae and Asteraceae, establishing a forested environment (Sciscio *et al*., 2016). Although Araucariaceae are very rare elements at Saldanha Bay (Roberts *et al*., 2017) and LBW they are not recorded at Noordhoek, possibly implying that this section is younger than the lowermost zone Palynomorph Zone 7) at LBW.

This zone is followed by a palm dominated tropical-subtropical environment (29.1–31.3 m) characterised by decreasing podocarps and Oleaceae (Sciscio *et al*., 2016). Fynbos elements are still low, and the presence of palms indicates that this zone is influenced by summer

rainfall. Palms have the highest abundances in the *Leiotriletes maxoides* zone (Pollen Zone 6), but ferns are not recorded from this zone at Noordhoek (Sciscio *et al*., 2016).

Restionaceae become widespread at Noordhoek from 25.8–27.1 m, whereas palms decrease, and podocarps disappear. Marine indicators were not identified at Noordhoek (Sciscio *et al*., 2016) and the age of this level (and the overall deposits) cannot be verified. Restionaceae percentages are almost equal (31%, Noordhoek and 36%, LBW), and a single taxon abundant only in a particular zone is not enough to construct a correlation between the two deposits. Palms slightly increase in the next zone (22.5–24 m) and podocarps re-appear with low abundances. Liliaceae, Celastraceae, Myricaceae and Proteaceae are common.

In the next level (18–22.5 m), Restionaceae reaches a maximum (40%), podocarps decrease, and palms become extinct. At LBW, Restionaceae is the most abundant (42%) in the *Milfordia* zone (Palynomorph Zone 3), following a transgression which may have inundated the depositional environment. This level at Noordhoek could possibly be compared to the *Milfordia* zone at LBW but the overall palynomorph assemblages are not consistent at both sites e.g *Sparganiaceaepollenites barungensis*, which typically fluctuates with *Milfordia*, is not recorded at Noordhoek (Scicio *et al*., 2016).

The *Apteodinium zone* (Palynomorph zone 4) cannot be correlated with due to the lack of marine indicators including dinoflagellates and benthic foraminifera at Noordhoek (Scicio *et al*., 2016). The uppermost level (1–2.5 m) is characterised by decreasing Restionaceae and increasing fynbos elements (due to increasing aridity), which include Ericaeae and Proteaceae. However, Ericaceae is very scarce at LBW and at Saldanha Bay (Roberts *et al*., 2017).

Similar to Rondeberg (Roberts *et al*., 2013), younger deposits and distance from LBW may have resulted in a correlation between the sites being unsuccessful. It appears that sites outside the palaeo-Berg River system (Rondeberg and Noordhoek) are difficult to correlate with LBW possibly due to unique factors such as sea level changes, sedimentological settings, local climatic conditions and time periods at these sites.

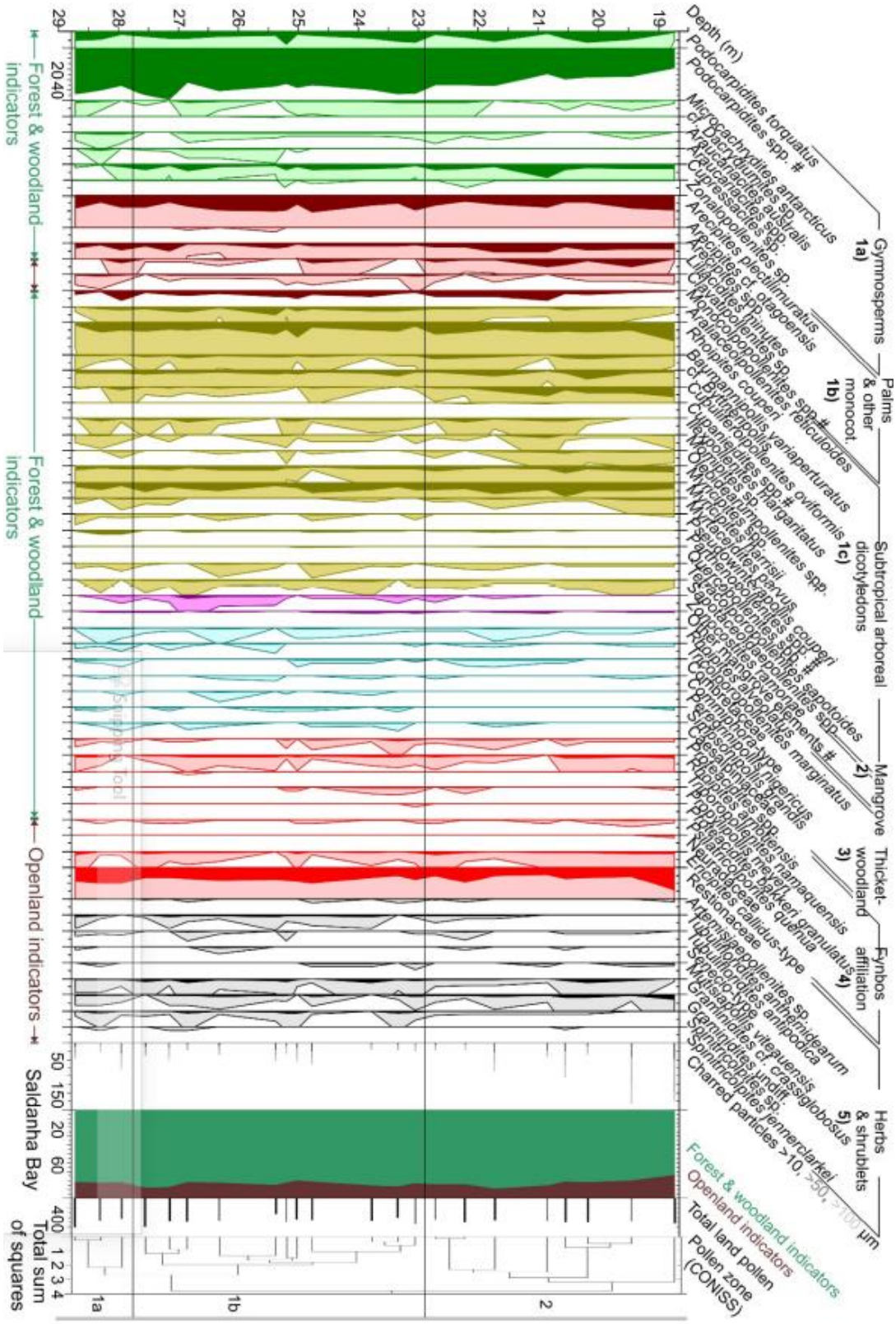

Figure 15. Pollen diagram of selected palynomorphs from the Elandsfontyn Formation, Saldanha Bay (taken from Roberts *et al*., 2017).

4.3.5 Elandsfontyn Formation, Langebaanweg and Knysna Formation, Knysna (Carr *et al*., 2010; Goble, 2015)

The Knysna Formation comprises rare lignite deposits, which bear striking similarities to the Elandsfontyn Formation at LBW, Noordhoek and Rondeberg (Carr *et al*., 2010; Sciscio *et al*., 2016; Roberts *et al*., 2017). Afromontane forests, dominated by forest trees such as Podocarpaceae, Oleaceae and Lauraceae were documented in Knysna lignite deposits (Carr *et al*., 2010). However, the Knysna deposits were dominated by palms, which are now locally extinct (Carr *et al*., 2010). *Podocarpus* (which is present in Knysna today), subtropical-tropical vegetation (Anacardiaceae, Sapotaceae, Malvaceae, Oleaceae) as well as wetland plants such as Cyperaceae and *Sparganiaceaepollenites barungensis* (Carr *et al*., 2010). Grasses and fynbos vegetation (Proteaceae, Ericaceae *Cliffortia*-type, *Anthospermum*-type) associated with dry conditions) were also common (Carr *et al*., 2010).

Both studies reflected the poor palynomorph preservation and discontinuous nature of Knysna lignite succession, impeding a concise comparison with other sites. With that said, the vegetation history (from what was successfully analysed) follows that of many southwestern Cape sites and is in particular very similar to the Elandsfontyn Formation at LBW (Carr *et al*., 2010; Sciscio *et al*., 2013). The palaeoenvironment represents a subtropical environment with podocarps, palms, and other arboreal plants with surrounding wetlands/swamps. The Knysna deposits are assumed to have a Miocene age (Carr *et al*., 2010). The age of the Knysna Formation deposits may not be comparable to the Elandsfontyn Formation due to its distance away from the southwestern coast localities. More studies need to be conducted to ascertain the correlation (or lack thereof) with the LBW deposits.

4.3.6 Elandsfontyn Formation, Langebaanweg and other Southern Hemisphere sites

The floral elements from the southwestern Cape fossil sites are not unique to South Africa and have been recorded in other modern-day Southern Hemisphere regions including Australia, New Zealand, South America and Antarctica. These locations were once part of the supercontinent Gondwana, which began breaking up during the Jurassic (McLoughlin, 2001; Jordan *et al*., 2017). The breakup of Gondwana fostered the diversification of previously isolated taxa, which were dominated by gymnosperms and ferns (McLoughlin, 2001). Late Oligocene to early Miocene assemblages from Antarctica (Kulhanek *et al*., 2019), Australia

(Martin, 1990), New Zealand (Pocknall, 1989) and South America (Barreda *et al*., 2009) show significant similarities to the LBW palaeoenvironment.

Gondwanan lineages such as Podocarpaceae, Araucariaceae, Proteaceae are common, and they occur with Nothofagaceae, Casuarinaceae, Myrtaceae and Euphorbiaceae. However, Nothofagaceae has not been recorded thus far in southern Africa. These taxa provided canopies in temperate rainforests surrounding peat swamps that were dominated by *Sparganiaceaepollenites barungensis*, Restionaceae and Cyperaceae. Ferns (Cyatheaceae, Gleicheniaceae and Polypodiaceae) and algae (*Botryococcus* and *Pediastrum*) were recorded from Australia, New Zealand and South America. Grasses were relatively scarce during this time period, possibly indicating the expansion of grasslands in the middle Miocene to Pliocene (Hoetzel *et al*., 2013; Strömberg, 2011). *Sparganiaceaepollenites barungensis*, *Microcachrydites*, Araucariaceae and Casuarinaceae are all extinct in South Africa, but their occurrence in other Southern Hemisphere continents can provide evidence for the shared origins of primitive gymnosperms and angiosperms in Gondwana. However, some studies (Linder, 2005 and references therein) have shown that long-distance dispersal of pollen could have contributed to the growth of similar vegetations across continents. While modern ecological assemblages can possibly be attributed to divergence of the old taxa (de Villiers and Cadman, 1997; McLoughlin, 2001), the evolutionary histories of plants need to be explored further to ascertain a biogeographic influence. The effects of local relative and glacio-eustatic sea levels in conjunction with tectonic activity are likely to have also been a major influence on the establishments of these palaeoenvironments.

Table 3: Regional comparison of Neogene sites along the southwest Cape coast

Elandsfontyn Formation, Langebaanweg (this study) **Age:** Late Oligocene to Late Miocene	**Elandsfontyn Formation, Langebaanweg (Sciscio *et al.*, 2013)** **Age:** Middle Miocene	**Elandsfontyn Formation, Saldanha Bay (Roberts *et al.*, 2017)** **Age:** Late Oligocene to Early Miocene	**Elandsfontyn Formation, Noordhoek (Sciscio *et al.*, 2016)** **Age:** Early to Middle Miocene
PAAZ 1: *Botryococcus* zone (13.4-1.61 m) **Age**: Late Miocene (Early Burdigalian)	**Subsection I (7.20-7.61 m):** • Restionaceae • *Cupressacites* • *Podocarpidites* • *Psilatricolporites operculatus* (*Alchornea*)	Correlation unsuccessful	Correlation unsuccessful
PAAZ 2: *Operculodinium centrocarpum* zone (16.865-13.4 m) **Age**: Early Miocene (Middle Aquitanian to Late Aquitanian)	**Subsection II (16.47-20.32 m)**: • Podocarpaceae • *Arecipites* (Arecaceae) • *Clavatipollentites* (Chloranthaceae) • Araliaceae (*Rhoipites Pilatus*) • Oleaceae (*Tricolporopollenites microreticulatus*/*T. oleoides*) • Apocynaceae (*Margocolporites rauvolfii*) • Restionaceae • Sparganiaceae • Poaceae • Cryptogams • Algae • *Spiniferites* sp. (dinoflagellate cyst)	**Zone 2 (22.75-18.70 m):** • Cyperaceae • Sparganiaceae • Restionaceae • *Spiniferites* • *Cordosphaeridium minimum* (dinoflagellate cyst) • *Operculodinium centrocarpum* (dinoflagellate cyst dominating the uppermost level at Saldanha Bay) • *Chiropteridium lobospinosum* (dinoflagellate cyst) • reduced gymnosperms (except *Cupressacites*), mangroves and palms • Only recorded marine transgression	Correlation unsuccessful
PAAZ 3: *Milfordia* zone (18.24-16.865 m) **Age**: Oligocene/Miocene (Late Chattian to Early Aquitanian)			**1-2.5 m:** • Low Restionaceae • Increasing Ericaceae and Proteaceae **18-22.5 m**: • Restionaceae reaches maximum (40%) • Podocarps low • Palms extinct
PAAZ 4: *Apteodinium spiridoides* zone (18.96-18.24 m) **Age**: Late Oligocene (Late Chattian)			Correlation unsuccessful
PAAZ 5: *Sparganiaceaepollenites barungensis* zone (19.825-18.96 m) **Age**: Late Oligocene (Middle Chattian)			**22.5-24 m:** • Palms • Podocarpaceae • Liliaceae • Celastraceae • Myricaceae • Proteaceae **25.8-27.1 m**: • Palms decrease • Podocarps disappear • Restionaceae almost equal to Langebaaweg
PAAZ 6: *Leiotriletes maxoides* zone (28.26-19.825 m) **Age**: Late Oligocene (Early Chattian)		**Zone 1 (a & b), 27.75-22.90 m):** • Podocarpaceae • Araucariaceae • *Cupuliferoipollenites oviformis* (Fagaceae) • Sapotaceae • Mangroves (*Zonocostites ramonae*) • Restionaceae • Sparganiaceae • Cyperaceae • Poaceae • Gleicheniaceae • Lygodiaceae	**29.1-31.3 m**: • Palms • Decreasing podocarps and Oleaceae • Fynbos elements low
PAAZ 7: *Podocarpidites* zone (33.03-28.6 m) **Age**: Late Oligocene (Early Chattian)	**Subsection III (30.915-33.025 m)**: • Podocarpaceae • Oleaceae • *Celtispollenites* • Casuarinaceae • Restionaceae • Sparganiaceae		**35.5-39.5 m**: • Podocarpaceae • Palms • Oleaceae • Asteraceae

CHAPTER 5: CONCLUSIONS AND OUTLOOK

The re-analysis of Core BH2 in this study provides new insight into the palaeoenvironment and chronology of the Elandsfontyn Formation deposits at LBW, in comparison with the pilot study by Sciscio *et al*. (2013). This was achieved by a higher sample resolution (76 slides) and improved sediment processing. A late Oligocene (Chattian) to early Miocene (early Burdigalian) age was determined based on the presence of pollen and dinoflagellate index fossils. The results of this dissertation indicate that:

- Late Oligocene (early Chattian) environments, preserved by Palynomorph Zone 7, were dominated by Podocarpaceae-dominated forests along with subtropical arboreal trees growing in depressions or on the granite hills and floodplains surrounding the palaeo-Berg River. Gondwanan lineages were common and occurred with other angiosperms including Oleaceae, Arecaceae, Araliaceae, Aquifoliaceae, Fagaceae, Rhizophoraceae, Proteaceae and Asteraceae. Proto-fynbos elements, cryptogams and algae were not abundant. This finding is supported by positive loadings of forest elements on PCA curves and correlates with subsection III of the pilot study by Sciscio *et al*. (2013) and other Neogene sites including Saldanha Bay (Roberts *et al*., 2017).

- Abundant fern spores, palms, some forest and wetland taxa dominated wetlands (Palynomorph Zone 6) growing on the floodplain and adjacent granite hills in the early Chattian (late Oligocene). These taxa are indicative of local moisture (humid conditions) and available groundwater in this environment. PCA plots show that cryptogams are more widespread than forest and subtropical trees in these environments. A similar environment was described in the previous study by Sciscio *et al*. (2013) and in Zone 1 at Saldanha Bay (Roberts *et al*., 2017).

- Forests surrounding wetlands (Palynomorph Zone 5) with abundant fern spores, sedges, rushes and grasses and arboreal elements such podocarps, palms and subtropical trees became widespread during the early Oligocene (middle Chattian). High rainfall resulted in flooding of the river and the development of wetlands, also shown by positive loadings of wetland taxa on PC1. Sciscio *et al*. (2013) documented low mean annual temperatures for samples below 19.50 m, postulating that samples in

subsection II are also associated with high rainfall. Zone 2 of Saldanha Bay (Roberts of Saldanha Bay (Roberts *et al*., 2017) also recorded similar wetland environments dominated by Sparganiaceae, Restionaceae, Cyperaceae and Poaceae.

- Sea level change, possibly due to deglaciation events in Antarctica and Milankovitch cycles in the late Chattian (late Oligocene) resulted in the landward movement of the sea in Palynomorph Zone 4. The tidal currents, caused by earth's orbital activity (Milankovitch cycles), influenced the strength of marine transgressions and regressions during sea level changes (Boggs, 2010) observed at LBW. Three second-order marine transgressions (IV–II on Fig 6**.**) periodically covered the forest and wetland environments and arboreal elements retreated due to high salinity levels in the brackish water associated with these transgressions. Shallow marine indicators including dinoflagellate cysts (dominated by *Apteodinium spiridoides*, *Operculodinium centrocarpum* and *Spiniferites mirabilis*) were brought to the coastal and estuarine interface. These marine incursions are based on the percentages of *Apteodinium spiridoides*, with 49% at bottom, 91% in the middle and 61% at the top of the Pollen Zone 4 (18.96–18.24 m). These transgressions are linked to a global late Oligocene sea level rise, as indicated by oxygen isotopes of benthic foraminifera (Miller *et al*., 1991; Rasmussen, 2004) which first appear in this zone. Since marine indicators were removed from the PCA, their influence cannot be justified with the results obtained from the PCA. This section corresponds with subsection II from the pilot study due to the presence of abundant *Spiniferites* (Sciscio *et al*., 2013). However, dinoflagellate cysts were not fully identified and described in the previous study. Other Neogene sites along the southwest coast (Carr *et al*., 2010; Rondeberg *et al*., 2013; Sciscio *et al*., 2016) did not record the influence of sea level changes (based on marine indicators) in their studies.

- Oligocene/Miocene (late Chattian to early Aquitanian) assemblages in Palynomorph Zone 3 were dominated by *Milfordia* (Restionaceae) and fern spores growing along coastal plains. Subtropical and forest arboreal elements were on the decline, however, the diversity of savanna woodland elements increased, with *Peregrinipollis nigericus* (*Brachystegia*) making an appearance. PCA showed negative loadings of woodland

elements, indicating that they are weakly correlated with some moisture-retaining elements including subtropical trees and cryptogams.

- These savanna woodland taxa are indicative of ensuing drier conditions which were probably strengthening due to higher seasonality and a stronger summer rainfall (Roberts *et al*., 2017). This (a similar record and climatic conditions) can also be seen in subsection I of LBW (Sciscio *et al*., 2013) and Zone 2 at Saldanha Bay (Roberts *et al*., 2017).

- The final and most pronounced transgression (I in Fig. 6) occurred during the early Miocene (middle to late Aquitanian) in Palynomorph Zone 2 and is associated with the increase of dinoflagellate taxa (*Operculodinium spiridoides*, *Spiniferites* and *Cordosphaeridium minimum*) in an estuary. Plant taxa were significantly reduced due to an incursion of brackish water. This transgression can possibly be linked to a global transgression caused by the deglaciation of Antarctica during the Mi1a event (Miller *et al*., 1996). PCA was not conducted on the samples from this depth. A similar environment with abundant *Operculodinium centrocarpum* was reported in Zone 2 of the Elandsfontyn Formation at Saldanha Bay (Roberts *et al*., 2017).

- By the early Miocene (early Burdigalian), sea levels had fallen again, and marine productivity dropped. *Botryococcus*, *Milfordia* (Restionaceae) and *Apteodinium spiridoides* possibly dominated a lagoon. Low pollen production hinders an accurate reconstruction of Palynomorph Zone 1. Brackish conditions were persistent, and plants were scarce, and some were probably reworked or destroyed by taphonomic processes. This final regression could be linked to the global regression at the base of the glacial event of Mi1a (Miller *et al*., 1996). No other southwestern coast sites, e.g. Saldanha Bay (Roberts *et al*., 2017), have reported a similar zone.

- This study affirms the existence of a subtropical-tropical environment co-fluctuating with fynbos vegetation providing an understorey, albeit in low abundances, during the deposition of the Elandsfontyn Formation at LBW. Therefore, a transition to a fynbos ecotone cannot be determined from this study. Additionally, marine fluctuations at LBW and other southwestern Neogene sites should be further explored to determine

their influence on the configuration of depositional environments and to improve their chronology.

- A thorough palynofacies reconstruction, with an investigation of taphonomic processes is suggested to improve the overall palaeoenvironmental reconstruction at LBW. Additionally, SEM analysis can be used for a future study at LBW to allow a much higher resolution of the ultrastructure and to obtain additional morphological information to improve pollen identification, for example of Araucariaceae. Grimsson *et al*. (2017), studying an early Miocene core at Saldanha Bay from LBW, showed that the pollen morphology of extant Winteraceae taxa can be determined in the systematic-phylogenetic framework by using high resolution scanning electron microscopy in comparison to light microscope photographs of the same pollen grains.

REFERENCES

Adebayo, O.F., Orijemie, A.E. and Aturumu, A.O. 2012. Palynology of Bog-1 Well, southeastern Niger Delta Basin, Nigeria. *International Journal of Science and Technology*, 2: 214 – 222.

Adekola, S.A., Akinlua, A., Fadiya, S.L., Fajemila, O.T., Ugwu, G.C. 2014. Palynological and paleoenvironmental analyses of selected shale samples from Orange Basin, South Africa. *Ife Journal of Science* 16: 45-55.

Aguilera, O., Guimarães, J.T.F. and Moraes-Santos, H. 2013. Neogene Eastern Amazon carbonate platform and the palaeoenvironmetal interpretation. *Swiss Journal of Palaeontology*, 132: 99-118.

Akkiraz, M.S., Akgün, F., Örçen, S., Bruch, A.A. and Mosbrugger, V. 2006. Stratigraphic and palaeoenvironmental significance of Bartonian-Priabonian (Middle-Late Eocene) microfossils from the Başçeşme Formation, Denizli Province, Western Anatolia. *Turkish Journal of Earth Sciences* 15: 155-180.

Archangelsky, S. and Gamerro, J.C. 1967. Spore and pollen types of the Lower Cretaceous in Patagonia (Argentina). *Review of Palaeobotany and Palynology* 1: 211-217.

Archangelsky, A. and Zamaloa, M.C. 2003. Primeros resultados palinológicos del Paleógeno del sector oriental de la Sierra La Colonia, provincial del Chubut, Argentina. *Revista del Museo Argentino de Ciencias Naturales* N. S. 5: 119–124.

Askin, R.A. 1990. Cryptogam spores from the upper Campanian and Maastrichtian of Seymour Island, Antarctica. *Micropalaeontology* 36: 141-156.

Balme, B.E. 1957. Spores and pollen grains from the Mesozoic of Western Australia. *Coal Research C.S.I.R.O* 25: 1-48.

Bankole, S.I., Schrank, E. and Osterloff, P.L. 2014. Palynostratigraphy, palaeoclimates and palaeodepositional environments of the Miocene aged Agbada Formation in the Niger Delta, Nigeria. *Journal of African Earth Sciences*, 95: 41-62.

Barker, N.P., Muller, E.M. and Mill, R.R. 2004. A yellowwood by any other name: molecular systematics and the taxonomy of Podocarpus and the Podocarpaceaen southern Africa. *South African Journal of Science* 100: 630-632.

Barreda, V.D. 1993. Late Oligocene?–Miocene pollen of the families Compositae, Malvaceae and Polygonaceae from the Chenque Formation, Golfo San Jorge Basin, southeastern Argentina. *Palynology* 17: 169-186.

Barreda, V. and Palazzesi, L. 2007. Patagonian vegetation turnovers during the Paleogene-Early Neogene: origin of arid-adapted floras. *The Botanical Review* 73: 31-50.

Barreda, V., Guler, V. and Palazzesi, L. 2008. Late Miocene continental and marine palynological assemblages from Patagonia. *Developments in Quaternary Sciences* 11: 343-350.

Barreda, V., Palazzesi, L. and Marenssi, S. 2009. Palynological record of the Palaeogene Río Leona Formation (southernmost South America): stratigraphical and paleoenvironmental implications. *Review of Palaeobotany and Palynology* 154: 22-33.

Barreda, V., Palazzesi, L., Tellería, M.C., Katinas, L. and Crisci, J.V. 2010. Fossil pollen indicates an explosive radiation of basal Asteracean lineages and allied families during Oligocene and Miocene times in the Southern Hemisphere. *Review of Palaeobotany and Palynology* 160: 102-110.

Barreda, V. and Palazzesi, L. 2014. Response of plant diversity to Miocene forcing events: the case of Patagonia. In: Stevens, W.D., Montiel, O.M. and Raven, P.H. (eds.). *Paleobotany and Biogeography*: *A festschrift for Alan Graham in his 80th year*: 1-25.

Barreda, V.D., Zamaloa, M.C., Gandolfo, M.A., Jaramillo, C. and Wilf, P. 2020. Early Eocene spore and pollen assemblages from the Laguna del Hunco fossil lake beds, Patagonia, Argentina. *International Journal of Plant Sciences* 181: 594-615.

Bati, Z. and Sancay, R.H. 2007. Palynostratigraphy of Rupelian sediments in the Mus Basin, Eastern Anatolia, Turkey. *Micropalaeontology* 53: 249-283.

Besems, R.E. 1992. Dinoflagellate cyst biostratigraphy of Tertiary and Quatenary deposits of Offshore NW Borneo. *Geological Society of Malaysia* 33: 65-93.

Besnard, G., de Casas, R.R., Christin, P-A. and Vargas, P. 2009. Phylogenetics of *Olea* (Oleaceae) based on plastid and nuclear ribosomal DNA sequences: Tertiary climatic shifts and lineage differentiation times. *Annals of Botany* 104: 143-160.

Bint, A.N. 1981. An Early Pliocene pollen assemblage from Lake Tay, south-western Australia, and its phytogeographic implications. *Australian Journal of Botany* 29: 277-291.

Birkenmajer, K., Gedl, P. and Worobiec, E. 2010. Dinoflagellate cyst and spore-pollen spectra from the Lower Oligocene Krabbedalen Formation at Kap Brewster, East Greenland. *Polish Polar Research* 31: 103-140.

Boggs, S. 2010. Principles of sedimentology and stratigraphy (4th edition). New Jersey, Pearson Education, Inc.: 343-411.

Boizard, S.D. and Mitchell, S.J. 2011. Resistance of red mangrove (*Rhizophora mangle* L.) seedlings to deflection and extraction. *Trees – Structure and Function* 25: 371-381.

Bolchovitina, N.A. 1966. The fossil spores of the family Gleicheniaceae (morphology and taxonomy). *Review of Palaeobotany and Palynology* 3: 59-64.

Bonnefille, R., Hamilton., A.C., Linder, H.P., Riollet, G. 1990. 30 000-year-old fossil Restionaceae pollen from Central Equatorial Africa and its biogeographical significance. *Journal of Biogeography* 17: 307-314.

Born, J., Linder, H., Desmer, P. 2007. The greater cape floristic region. *Journal of Biogeography* 34: 147-162.

Botha, M. 2002. Our own miombo. *Veld and Flora* 18: 16-17.

Bredenkamp, G.J., Spada, F. and Kazmierczak, E. 2002. On the origin of northern and Southern Hemisphere grasslands. *Plant Ecology* 163: 209-229.

Burger, J.M., Moloney, C.L., Walker, D.R., Parrot, R.G., Fawcett, S.E. 2020. Drivers of short-term variability in phytoplankton production in an embayment of the southern Benguela upwelling system. *Journal of Marine Systems* 208: 1-16.

Carr, A.S., Boom, A., Dunajko, A., Bateman, M.D., Holmes, P.J., Berrio, J.C. 2010. New evidence for the age and palaeoecology of the Knynsa Formation, South Africa. *South African Journal of Geology* 113.3: 241-256.

Chanda, S. 1966. On the pollen morphology of the Centrolepidaceae, Restionaceae and Flagellariaceae, with special reference to taxonomy. *Grana* 6: 355-391.

Clarke, R.T. 1966. *Peregrinipollis nigericus*, A new palynomorph from the Upper Tertiary of Nigeria. *Grana Palynologica* 6: 544-546.

Coates-Palgraves, M. 2002. Trees of Southern Africa (3rd edition). Cape Town, Struik Publishers.

Coetzee, J.A. 1978. Late Cainozoic palaeoenvironments of southern Africa. In: Van Zinderen Bakker, E.M. (Ed.), Antarctic Glacial History and World Palaeoenvironments. A.A. Balkema, Rotterdam, 115–127 pp.

Coetzee, J.A. 1980. Tertiary environmental changes along the south-western African coast. *s*

Coetzee, J.A. 1981. A palynological record of very primitive angiosperms in Tertiary Deposits of the south-western Cape province, South Africa. *South African Journal of Science* 77: 341-343.

Coetzee, J.A. and Rogers, J. 1982. Palynological and lithological evidence for the Miocene palaeoenvironment in the Saldanha region (South Africa). *Palaeogeography, Palaeoclimatology, Palaeoecology* 39: 71-85.

Coetzee, J.A. 1983. Intimations on the Tertiary vegetation of southern Africa. *Bothalia* 14: 345-354.

Coetzee, J.A. and Muller, J. 1984. The phytogeographic significance of some extinct Gondwana pollen types from the Tertiary of the southwestern Cape (South Africa). *Annals of the Missouri Botanical Garden* 71: 1088-1099.

Coetzee, J.A. and Praglowski, J. 1984. Pollen evidence for the occurrence of *Casuarina* and *Myrica* in the Tertiary of South Africa. Grana 23: 23-41.

Conran, J.G., Mildenhall, D.C., Lee, D.E., Lindqvist, J.K., Shepherd, C., Beu, A.G., Bannister, J.M. and Stein, J.K. 2014. Subtropical rainforest vegetation from Cosy Dell,

Southland: plant fossil evidence for Late Oligocene terrestrial ecosystems. *New Zealand Journal of Geology and Geophysics* 57: 236-252.

Cookson, I.C. 1947. Plant microfossils from the lignite of Kerguelen Archipelago. British, Australian, New Zealand Antarctic Research Expedition 1929-1931, Reports A 2: 127-142.

Cookson, I.C. 1950. Fossil pollen grains of proteaceous type from tertiary deposits, Australia. Botany School, University of Melbourne.

Costa, L.I. and Downie, C. 1979. Dinoflagellates. In: Montadert L *et al*. (eds) Sites 405 and 406. Deep Sea Drilling Project, Initial Reports 48: Washington: U.S. Government Printing Office: 228-232.

Couper, R.A. 1953. Upper Mesozoic and Cainozoic spores and pollen grains from New Zealand. *New Zealand Geological Survey Palaeontological Bulletin* 22: 1-97.

Couper, R.A. 1960. New Zealand Mesozoic and Cainozoic plant microfossils. *New Zealand Geological Survey Palaeontological Bulletin* 32: 1-87.

Crouch, E.M. and Brinkhuis, H. 2005. Environmental change across the Palaeocene-Eocene transition from eastern New Zealand: A marine palynological approach. *Marine Micropalaeontology* 56: 138-160.

Davey, R.J. and Rogers, J. 1975. Palynomorph distribution in Recent offshore sediments along two traverses off South West Africa. *Marine Geology* 18: 213-225.

Dettmann, M.E. and Jarzen, D.M. 1990. The Antarctic/Australian rift valley: Late Cretaceous of northeastern Australasian relicts? *Review of Palaeobotany and Palynology* 65: 131-144.

Dettmann, M.E. and Clifford, H.T. 2000. Monocotyledon fruits and seeds, and an associated palynoflora from Eocene-Oligocene sediments of coastal Queensland, Australia. *Review of Palaeobotany and Palynology* 110: 141-173.

Dettmann, M.E. and Clifford, H.T. 2005. Biogeography of Araucariaceae. *Australian Forest History Society Inc* 2: 1-9.

de Verteuil, L. 1996. Data report: Upper Cenozoic dinoflagellate cysts from the continental slope and rise off New Jersey. *Proceedings of the Ocean Drilling Program, Scientific Results* 150: 439-454.

de Villiers, S.E. and Cadman, A. 1997. The palynology of Tertiary sediments from a palaeochannel in Namaqualand, South Africa. *Palaeontologia Africana* 34: 69-99.

de Villiers, S.E. and Cadman, A. 2001. An analysis of the palynomorphs obtained from Tertiary sediments at Koingnaas, Namaqualand, South Africa. *Journal of African Earth Sciences* 33: 17-47.

DeVore, M.L. and Pigg, K.B.2007. A brief review of the fossil history of the family Rosaceae with a focus on the Eocene Okanogan Highlands of eastern Washington State, USA, and British Columbia, Canada. *Plant Systematics and Evolution* 266: 45-57.

Diester-Haass, L. 1988. Sea level changes, carbonate dissolution and history of the Benguela Current in the Oligocene-Miocene off southwest Africa (DSDp site 362, Leg 40). *Marine Geology* 79: 213-242.

Domínguez-Rodrigo, M., Lopez-Saez, J.A., Vincens, A., Alcala, L., Luque, L. and Serrallonga, J. 2001. Fossil pollen from the Upper Humbu Formation of Peninj (Tanzania): hominid adaptation to a dry open Plio-Pleistocene savanna environment. *Journal of Human Evolution* 40: 151-157.

Dörhöfer, G. and Norris, G. 1977. Discrimination and correlation of Highest Jurassic and Lowest Cretaceous terrestrial palynofloras in North-West Europe. *Palynology* 1: 79-93.

Dupont, L.M., Linder, H.P., Rommerskirchen, F. and Schefuß, E. 2011. Climate-driven rampant speciation of the Cape flora. *Journal of Biogeography* 38. 1059-1068.

Durak, S.D., Akkiraz, M.S. and Nazik, A. 2020. Early Miocene micropalaeontological record of the Aspiras (Kastamonu), north-west Anatolia, Turkey. *Geological Journal* 56: 704-728.

Durugbo, E.U., Ogundipe, O.T. and Ulu, O.K. 2011. Preliminary reports on Middle Miocene – Early Pleistocene dinoflagellate cysts from the western Niger Delta, Nigeria. *Ozean Journal of Applied Sciences* 4: 373 -394.

Eisawi, A. and Schrank, E. 2008. Upper Cretaceous to Neogene palynology of the Melut Basin, Southeast Sudan. *Palynology* 32: 101-129.

Eshet, Y., Moshkovitz, S., Habib, D., Benjamini, C. and Magaritz, M. 1992. Calcareous nannofossil and dinoflagellate stratigraphy across the Cretaceous/Tertiary boundary at Hor Hahar, Israel. *Marine Micropalaeontology* 18: 199-228.

Eze, P.N. and Meadows, M.E. 2013. Geochemistry and palaeoclimatic reconstruction of a palaeosol sequence at Langebaanweg, South Africa. *Quaternary International*, http://dx.doi.org/10.1016/j.quaint.2013.09.048: 1-9 pp.

Farley, M.B. and Traverse, A. 1990. Usefulness of palynomorph concentrations in distinguishing Paleogene depositional environments in Wyoming, (U.S.A.). *Review of Palaeobotany and Palynology* 64: 325-329.

Fawcett, A., Pitcher, G.C., Bernard, S., Cembella, A.D. and Kudela, R.M. 2007. Contrasting wind patterns and toxigenic phytoplankton in the southern Benguela upwelling system. *Marine Ecology Progress Series* 348: 19-31.

Fensome, R.A., Williams, G.L. and McRae, A. 2009. Late Cretaceous and Cenozoic fossil dinoflagellates and other palynomorphs from the scotian margin, offshore eastern Canada. *Journal of Systematic Palaeontology* 7: 1-79.

Fensome, R.A., Nøhr-Hansen, H. and Williams, G.L. 2016. Cretaceous and Cenozoic dinoflagellate cysts and other palynomorphs from the western and eastern margins of the Labrador-Baffin Seaway. *Geological survey of Denmark and Greenland Bulletin* 36: 1-144.

Filipova-Marinova, M., Pavlov, D., Coolen, M. and Giosan, L. 2013. First high-resolution marinopalynological stratigraphy of Late Quaternary sediments from the central part of the Bulgarian Black Sea area. *Quaternary International* 293: 170-183.

Frost, P. 1996. The ecology of miombo woodlands. In: B. Campbell (ed.) *The Miombo in Transition: Woodlands and Welfare in Africa*, 11-57. Centre for International Forestry Research, Bogor, Indonesia.

Germeraad, J.H., Hopping, C.A. and Muller, J. 1968. Palynology of Tertiary sediments from tropical areas. *Review of Palaeobotany and Palynology* 6: 189-348.

Gibson, D.J. 2009. Grasses and Grassland Ecology. York: Oxford University Press. 305 pp.

Goble, E. 2015. Palynological analysis of the Knysna lignites at Makhuku Quarry, South Africa. University of Leicester, Leicester, United Kingdom. BSc Honours (Unpublished).

Goldblatt, P. 1997. Floristic diversity in the Cape flora of South Africa. *Biodiversity and Conservation* 6: 359-377.

Google Earth. Langebaanweg, South Africa. SIO, NOAA, U.S. Navy, NGA, GEBCO. [May 25, 2021].

Graham, A. 2006. Paleobotanical evidence and molecular data in reconstructing the historical phytogeography of Rhizophoraceae. *Annals of the Missouri Botanical Garden*, 93: 325-334.

Grímsson, F., Xafis, A., Neumann, F.H. and Zetter, R. 2017. Pollen morphology of extant Winteraceae: a study allowing SEM-based affiliation of its fossil representatives. *Acta Palaeobotanica* 57: 339-396.

Grímsson, F., Xafis, A., Neumann, F.H., Scott, L., Bamford, M.K. and Zetter, R. 2018. The first Loranthaceae fossils from Africa. *Grana* 57: 249-259.

Grímsson, F., Graham, S.A., Coiro, M., Jacobs, B.F., Xafis, A., Neumann, F.H., Scott., Sakala, J., Currano, E.D. and Zetter, R. 2019. Origin and divergence of Afro-Indian Picrodendraceae: linking pollen morphology, dispersal modes, fossil records, molecular dating and paleogeography. *Grana* 58: 227-275.

Gruas-Cavagnetto, C. 1978. Etude palynologique de l'Eocene du Bassin Anglo-Parisien. *Mémoires de la Société géologique de France* 131: 1-64.

Guerstein, G.R., Guler, M.V. and Casadío, S. 2004. Palynostratigraphy and palaeoenvironments across the Oligocene-Miocene boundary within the Centinela Formation, southwestern Argentina. *The Geological Society of London, Special Publications* 230: 325-343.

Hammer, Ø, Harper, D.A.T., Ryan, P.D. 2001. PAST: Paleontological Statistics Software Package for Education and Data Analysis. *Palaeontologia Electronica* 4: 1-9.

Hammer, Ø, Harper, D.A.T. 2006. Palaeontological Data Analysis. Blackwell Publishing, Oxford, 83.

Haq, B.U., Hardenbol, J. and Vail, P.R. 1987. Chronology of fluctuating sea levels since the Triassic (250 million years ago to present). *Science* 235: 1156-1167.

Harris, W.K. 1972. New form species of pollen from southern Australian Early Tertiary sediments. *Transactions of the Royal Society of South Australia* 96: 53-65.

Haskell, T.R. 1968. Saccate Pollen Grains from the Lower Cretaceous of the Great Artesian Basin, Australia. *University of Queensland Papers* 6: 211-243.

Head, M.J. 1997. Thermophilic dinoflagellate assemblages from the Mid Pliocene of Eastern England. *Journal of Paleontology* 71: 165-193.

Head, M.J. 1998. Pollen and dinoflagellates from the Red Crag at Walton-on-the-Naze, Essex: evidence for a mild climatic phase during the early Late Pliocene of eastern England. *Geological Magazine* 135: 803-817.

Heinrich, S., Zonneveld, K.A.F., Bickert, T. and Willems, H. 2011. The Benguela upwelling related to the Miocene cooling events and the development of the Antarctic Circumpolar Current: Evidence from calcareous dinoflagellate cysts. *Palaeoceanography* 26: 1-11.

Hekel, H. 1972. Pollen and spore assemblages from Queensland Tertiary sediments. *Palaeontological Papers* 30: 1-33.

Helenes, J. and Cabrera, D. 2003. Oligocene-Miocene palynomorph assemblages from eastern Venezuela. *Palynology* 27: 5-25.

Hendey, Q.B. 1982. Langebaanweg: A record of Past Life. Cape Town, The Rustica Press.

Henrot, A.J., François, Favre, E., Butzin, M., Oberdous, M. and Munhoven, G. 2010. Effects of CO_2, continental distribution, topography and vegetation changes on the climate at the Middle Miocene: a model study. *Climate of the Past* 6: 67-694.

Heusser, C.J., Rabassa, J., Brandant, A. and Stuckenrath, R. 1988. Late-Holocene vegetation of the Andean Araucaria region, Province Nequen, Argentina. *Mountain Research and Development* 8: 53-63.

Hoetzel, S., Dupont, L., Schefuß, E., Rommerskirchen, F. and Wefer, G. 2013. The role of fire in Miocene to Pliocene C_4 grassland and ecosystem evolution. *Nature Geoscience* 6: 1027-1030.

Hoetzel, S., Dupont, L.M., Marret, F., Jung, G. and Wefer, G. 2017. Steps in the intensification of Benguela upwelling over the Walvis Ridge during the Miocene and Pliocene. *International Journal of Earth Sciences (Geologische Rundschau)* 106: 171-183.

Holbourn, A.E., Kuhnt, W., Clemens, S.C., Kochhann, K.G.D., Jöhnck., Lübbers, J. and Andersen, N. 2018. Late Miocene climate cooling and intensification of southeast Asian winter monsoon. *Nature Communications* 9: 1-13.

Jaramillo, C.A. and Oboh-Ikuenobe, F.E. 1999. Sequence stratigraphic interpretations from palynofacies, dinocyst and lithological data of Upper Eocene-Lower Oligocene strata in southern Mississippi and Alabama, U.S, Gulf Coast. *Palaeogeography, Palaeoclimatology, Palaeoecology* 145: 259-302.

Jarzen, D.M. 1978. The terrestrial palynoflora from the Cretaceous-Tertiary transition, Alabama, U.S.A. *Pollen Spores* 20: 535-553.

Jha, N., Prakash, N. and Joshi, H. 2017. Integrated palaeobotanical and palynological analysis of subsurface Gondwana sedimentary succession (Jurassic-Cretaceous) in Jangareddygudem area, Chintalapudi sub-basin, South India: stratigraphical and phytogeographical implications. *Palaeoworld* 26: 173-193.

Jianguo, L., Batten, D.J. and Yiyong, X. 2008. Palynological indications of environmental changes during the Late Cretaceous-Eocene on the southern continental margin of Laurasia, Xizang (Tibet). *Palaeogeography, Palaeoclimatology, Palaeoecology* 265: 78-86.

Jiménez-Moreno, G., Head, M.J. and Harzhauser, M. 2006. Early and Middle Miocene dinoflagellate cysts stratigraphy of the Central Paratethys, Central Europe. *Journal of Micropalaeontology* 25: 113-139.

Jolley, D.W. and Morton, A.C. 1992. Palynological and petrological characterization of a North Sea Palaeocene volcaniclastic sequence. *Proceedings of the Geologists' Association* 103: 119-127.

Jordan, T.A., Ferraccioli, F. and Leat, P.T. 2017. A new model for microplate movement, magmatism, and distributed extension in the Weddell Sea Rift System of West Antarctica. *Gondwana Research* 42: 29-48.

Katuna, M.P., Geisler, J.H., Colquhoun, D.J. 1996. Stratigraphic correlation of Oligocene marginal marine and fluvial deposits across the middle and lower coastal plain, South Carolina. *Sedimentary Geology* 108: 181-194.

Kedves, M. 1981. Études palynologiques sur les sediments préquaternaires de l'Egypte. Néogène I. *Grana* 20: 119-130.

Knobloch, E. and Konzalová, M. 1998. Comparison of the Eocene plant assemblages of Bohemia (Czech Republic) and Saxony (Germany). *Review of Palaeobotany and Palynology* 101: 29-41.

Kominz, M.A., Miller, K.G. and Browning, J.V. 1998. Long-term and short-term global Cenozoic sea-level estimates. *Geology* 26: 311-314.

Kulhanek, D.K., Levy, R.H., Clowes, C.D., Prebble, J.G., Rodelli, D., Jovane, L., Morgans, H.E.G., Kraus, C., Zwingmann, H., Griffith, E.M., Scher, H.D., McKay, R.M. and Naish, T.R. 2019. Revised chronostratigraphy of DSDP Site 270 and late Oligocene to early Miocene palaeoecology of the Ross Sea sector of Antarctica. *Global and Planetary Change* 178: 46-64.

Kumar, M., Srivastava, G., Spicer, R.A., Spicer, T.E.V., Mehrotra, R.C., Mehrotra, N.C. 2012. Sedimentology, palynostratigraphy and palynofacies of the late Oligocene Makum Coalfield, Assam, India: A window on lowland tropical vegetation during the most recent episode of significant global warmth. *Palaeogeography, Palaeoclimatology, Palaeoecology* 342-343: 143-162.

Ladd, P.G. 1977. Pollen morphology of some members of the Restionaceae and related families, with notes on the fossil record. *Grana* 16: 1-14.

Lehnert, M. 2009. Three new species of scaly tree-ferns (Cyathea-Cyatheaceae) from the northern Andes. *Phytotaxa* 1: 43-56.

Linder, H.P. 2000. Vicariance, climate change, anatomy and phylogeny of Restionaceae. *Botanical Journal of the Linnean Society* 134: 159-177.

Linder, H.P. 2003. The radiation of the Cape flora, southern Africa. *Biological Reviews* 78: 597-638.

Linder, H.P. and Hardy, C.R. 2004. Evolution of the species-rich Cape flora. *Philosophical Transactions of the Royal Society London B* 359: 1623-1632.

Linder, H.P. and Rudall, P.J. 2005. Evolutionary history of Poales. *Annual Review of Ecology, Evolution, and Systematics* 36: 107-124.

Linder, H.P. 2005. Evolution of diversity: the Cape Flora. *Trends in Plant Science* 10: 536-541.

Lisiecki, L.E. and Raymo, M.E. 2005. A Pliocene-Pleistocene stack of 57 globally distributed benthic δ^{18}O records. *Paleoceanography* 20: 1-17.

Londeix, L. 2018. Quantitative biostratigraphical ranges of some late Cenozoic species of the dinoflagellate genus *Spiniferites* and taxonomic considerations. *Palynology* 42: 203-220.

Lorente, M. A. 1986. Palynology and palynofacies of the upper Tertiary in Venezuela. *Dissertationes Botanicae* 99: 222. Berlin-Stuttgart: Lubrecht & Cramer Ltd.

Louwye, S. and Laga, P. 1998. Dinoflagellate cysts of the shallow marine Neogene succession in the Kalmhout well, northern Belgium. *Bulletin of the Geological Society of Denmark* 45: 73-86.

Macphail, M.K. and Hill, R.S. 1994. K-Ar dated palynofloras in Tasmania 1: Early Oligocene, *Proteacidites tuberculatus* Zone sediments, Wilmot Dam, northwestern Tasmania. *Papers and Proceedings of the Royal Society of Tasmania* 128: 1-15.

Macphail, M.K. 1997. Late Neogene climates in Australia: Fossil Pollen- and spore-based estimates in retrospect and prospect. *Australian Journal of Botany* 45: 425-464.

Macphail, M.K. 1999. Palynostratigraphy of the Murray Basin, inland southeastern Australia. *Palynology* 23: 197-240.

Macphail, M.K. and Hill, R.S. 2018. What was the vegetation in northwest Australia during the Paleogene, 66-23 million years ago? *Australian Journal of Botany* 66: 556-574.

Mahboub, I., Slimani, H., Toufiq, A., Chekar, M., Djeya, K.L., Jbari, H. and Chakir, S. 2019. Middle Eocene to early Oligocene dinoflagellate cyst biostratigraphy and paleoenvironmental interpretations of the Ben Attaya section at Taza, eastern External Rif, Morocco. *Journal of African Earth Sciences 149*: 154-169.

Manning, J. and Goldblatt, P. 2012. Plants of the Greater Cape Floristic Region 1: the Core Cape flora, *Strelitzia* 29. South African National Biodiversity Institute, Pretoria.

Mao, S., Huang, C. and Lei, Z. 2002. Late Oligocene to early Miocene dinoflagellate cysts from the Kuohsing area, central Taiwan. *Review of Palaeobotany and Palynology* 122: 77-98.

Marret, F. and Zonneveld, K.A.F. 2003. Atlas of modern organic-walled dinoflagellate cyst distribution. *Review of Palaeobotany and Palynology* 125: 1-200.

Martin, A.R.H. 1959. South African palynological studies. 1. Statistical and morphological variations in the South African species of *Podocarpus*. *Grana* 2: 40-53.

Martin, A.R.H. 1968. Pollen analysis of Groenvlei Lake sediments, Knysna (South Africa). *Review of Palaeobotany and Palynology* 7: 107-144.

Martin, A.R.H. and Harris, W.K. 1974. Reappraisal of some palynomorphs of supposed proteaceous affinity. *Grana* 14: 108-113.

Martin, H.A. 1973. Upper Tertiary palynology in southern New South Wales. In: Glover, J.E., Playford, G. (Eds.), Mesozoic and Cainozoic Palynology: Essays in Honour of Isabel Cookson: *Geological Society of Australia Special Publication* 4: 35–54.

Martin, H.A. 1990. The palynology of the Namba Formation in the Wooltana-1 bore, Callabonna Basin (Lake Frome), South Australia, and its relevance to Miocene grasslands in central Australia. *Alcheringa* 14: 247.

Martin, H.A. 1993. Middle Tertiary dinoflagellate and spore/pollen biostratigraphy and palaeoecology of the Mallee Cliffs bore, central Murray Basin. *Alcheringa* 17: 91-124.

McLachlan, I.R. and Pieterse, E. 1978. Preliminary palynological results: Site 362, Leg 40, Deep Sea Drilling Project. *Initial Report Deep Sea Drilling Project* 4: 857–881.

McLoughlin, S. 2001. The breakup history of Gondwana and its impact on pre-Cenozoic floristic provincialism. *Australian Journal of Botany* 49: 271-300.

McMinn, A. 1992. Recent and Late Quaternary dinoflagellate cyst distribution on the continental shelf and slope of southeastern Australia. *Palynology* 16: 13-24.

Mildenhall, D.C. and Crosbie, Y.M. 1979. Some porate pollen from the upper Tertiary of New Zealand. *New Zealand Journal of Geology and Geophysics* 22: 499-508.

Mildenhall, D.C. 2001. Pollen analysis of Pliocene-Pleistocene spores and pollen from Central Otago, South Island, New Zealand. New Zealand Geological Survey. *Paleontological Bulletin* 59: 1-128.

Mildenhall, D.C. 2003. Deep-sea record of Pliocene and Pleistocene terrestrial palynomorphs from offshore eastern New Zealand (ODP Site 1123, Leg 181). *New Zealand Journal of Geology & Geophysics* 46: 343-361.

Miller, K.G., Wright, J.D. and Fairbanks, R.G. 1991. Unlocking the Ice House: Oligocene-Miocene oxygen isotopes, eustasy, and margin erosion. *Journal of Geophysical Research* 96: 6829-6848.

Miller, K.G. and Mountain, G.S. 1996. Drilling and dating New Jersey Oligocene-Miocene sequences: Ice volume, global sea level and Exxon records. Science 271: 1092-1095.

Miller, K.G., Mountain, G.S., Wright, J.D. and Browning, J.V. 2011. A 180-million-year record of sea level and ice volume variations from continental margin and deep-sea isotopic records. *Oceanography* 24: 40-53.

Miller, K.G., Browning, J.V., Schmelz, W.J., Kopp, R.E., Mountain, G.S. and Wright, J.D. 2020. Cenozoic sea-level and cryospheric evolution from deep-sea geochemical and continental margin records. *Science Advances* 6: 1-15.

Moise, B., Victor, H.J., Burkhardt, S.F., Samankassou, E., Bennami, M., Désiré, N.J., Olive, M.C., Adatte, T., Martini, R. and Brunet, M. 2017. First palynostratigraphical evidence for a Late Eocene to Early Miocene age of the volcano-sedimentary series of Dschang, western part of Cameroon and its implications for the interpretation of palaeoenvironment. *Palaeogeography, Palaeoclimatology, Palaeoecology* 485: 517-530.

Moll, E.J., Campbell, B.M., Cowling, R.M., Bossi, L., Jarman, M.L., Boucher, C. 1984. A description of major vegetation categories in and adjacent to the Fynbos biome. *South African National Scientific Programmes* 83: 1-29.

Morgenroth, P. 1966. Mikrofossilien und Konkretionen des nordwest-europäischen Untereozäns. *Palaeontographica, Abteilung B* 119: 1-53.

Mucina, L. and Rutherford, M.C. 2006. The vegetation of South Africa, Lesotho and Swaziland. South African National Biodiversity Institute, Pretoria, South Africa.

Mulder, C., Sakorafa, V., Burragato, F. and Visscher, H. 2000. Ecohydrological perspective of phytogenic organic and inorganic components in Greek lignites: a quantitative reinterpretation. *Earth and Planetary Science Letters* 1: 167-181.

Muller, J. 1981. Fossil pollen records of extant angiosperms. *The Botanical Review* 47: 1-142.

Naud, G. and Suc, J-P. 1975. Contribution à l'étude paléofloristique des Coirons (Ardèche): premières analyses polliniques dans les alluvions sous-basaltiques et interbasaltiques de Mirabel (Miocène supérieur). *Bulletin de la Société géologique de France* 17: 820-827.

Neumann, F.H. and Bamford, M.K. 2015. Shaping of modern southern African biomes: Neogene vegetation and climate changes. *Transactions of the Royal Society of South Africa* 70: 195-212.

Nichols, D.J. 1994. A revised palynostratigraphic zonation of the nonmarine Upper Cretaceous, Rocky Mountain Region, United States. *Mesozoic Systems of the Rocky Mountain Range, USA* 1994: 503-522.

Oboh, F.E. and Salami, M.B. 1989. Lithostratigraphical and palynostratigraphical studies of Igbomotoru-1 Well, Niger Delta. *Journal of African Earth Sciences (and the Middle East)* 9: 531-540.

Okeke, K.K., Osterloff, P. and Ukeri, P. 2021. Sequence stratigraphical interpretation of the Paleocene to Miocene (Selandian-Aquitanian) palynofacies framework of the Niger delta basin, southeastern Nigeria. *Journal of African Earth Sciences* 178: 1-15.

Olayiwola, M.A., Bamford, M.K. and Durugbo, E.U. 2017. Graphic correlation: A powerful tool for biostratigraphic correlation of petroleum exploration and production in the Cenozoic deep offshore Niger Delta, Nigeria. *Journal of African Earth Sciences* 131: 156-165.

Oloyede, D.A. and Omoregbe, O.A. 2020. Palynology and paleoenvironmental study of Well LW, Niger Delta Basin, Nigeria. *International Journal of Scientific and Research Publications*, 10: 586 – 598.

Page, C.N. 1990. Podocarpaceae. In: Kramer, K., Green, P. (Eds.), Pteridophytes and Gymnosperms, The Families and Genera of Vascular Plants, vol. 1. Springer, Heidelberg, Berlin, pp. 332-346.

Palazzesi, L. and Barreda, V. 2007. Major vegetation trends in the Tertiary of Patagonia (Argentina): A qualitative paleoclimatic approach based on palynological evidence. *Flora – Morphology, Distribution, Functional Ecology of Plants* 202: 328-337.

Partridge, A.D. 2006. Palynological analysis of core sample at 270.5 metres in Banjo-1A, onshore Gippsland Basin. *Biostrata Report* 2006/04A: 1-4.

Paterson, N.W. and Mangerud, G. 2015. Late Triassic (Carnian-Rhaetian) palynology of Hopen, Svalbard. *Review of Palaeobotany and Palynology* 220: 98-119.

Peng, Y., Yu, J., Gao, Y. and Yang, F. 2006. Palynological assemblages of non-marine rocks at the Permian-Triassic boundary, western Guizhou and eastern Yunnan, South China. *Journal of Asian Earth Sciences* 28: 291-305.

Pienaar, B., Thompson D.I., Erasmus, B.F.N., Hill, T.R. and Witkowski, ETF. 2015. Evidence for climate-induced range shift in *Brachystegia* (miombo) woodland. *South African Journal of Science* 111: 1-9.

Pitcher, G.C. and Joyce, L.B. 2009. Dinoflagellate cyst production on the southern Namaqua shelf of the Benguela upwelling system. *Journal of Plankton Research* 31: 865-875.

Pitcher, G.C. and Louw, D.C. 2021. Harmful algal blooms of the Benguela eastern boundary upwelling system. Harmful Algae 102: 1-12.

Pocknall, D.T. 1981. Pollen morphology of the New Zealand species of *Dacrydium* Solander, *Podocarpus* L'Heritier and *Dacrycarpus* Endlicher (Podocarpaceae). *New Zealand Journal of Botany* 19: 67-95.

Pocknall, D.T and Crosbie, Y.M. 1982. Taxonomic revision of some Tertiary tricolporate and tricolpate pollen grains from New Zealand. *New Zealand Journal of Botany* 20: 7-15.

Pocknall, D.T. 1989. Late Eocene to Early Miocene vegetation and climate history of New Zealand. *Journal of the Royal Society of New Zealand* 19: 1-18.

Pocknall, D.T. 1991. Palynostratigraphy of the Te Kuiti Group (late Eocene-Oligocene), Waikato Basin, New Zealand. *New Zealand Journal of Geology and Geophysics* 34: 407-417.

Poschmann, M., Schindler, T. and Uhl, D. 2010. Fossil-Lagerstätte Enspel – a short review of current knowledge, the fossil association, and a bibliography. *Palaeobiodiversity and Palaeoenvironments* 90: 3-20.

Pound, M.J., Haywood, A.M., Salzmann, U. and Riding, J.B. 2012. Global vegetation dynamics and latitudinal temperature gradients during the Mid to Late Miocene (15.97-5.33 Ma). *Earth-Science Reviews* 112: 1-22.

Pross, J., Houben, A.J.P., van Simaeys, S., Williams, G.L., Kotthoff, U., Coccioni, R., Wilpshaar, M. and Brinkhuis, H. 2010. Umbria-Marche revisted: A refined magnetostratigraphic calibration of dinoflagellate cyst events for the Oligocene of the Western Tethys. *Review of Palaeobotany and Palynology* 158: 213-235.

Punt, W. 1975. Sparganiaceae and Typhaceae. *Review of Palaeobotany and Palynology* 19: 75-88.

Rabbani, J., Emamgholi, R., Abbassi, N. and Shariatzadeh, M.S. 2020. Late Cretaceous to Early Paleogene global sea fluctuations and the sedimentary environment in central Alborz (Northern Iran). *Arabian Journal of Geosciences* 13: 1-12.

Raine, J.I., Mildenhall, D.C. and Kennedy, E.M. 2011. New Zealand Fossil Spores and Pollen: an Illustrated Catalogue. 4th Edition. *GNS Science Miscellaneous Series* no.4.

Rasmussen, E.S. 2004. The interplay between true eustatic sea-level changes, tectonics, and climatic changes: what is the dominating factor in sequence formation of the Upper Oligocene–Miocene succession in the eastern North Sea Basin, Denmark? *Global and Planetary Change* 41: 15-30.

Rebelo, A.G., Boucher, C., Helme, N., Mucina, L. and Rutherford, M.C. 2006. Fynbos Biome. *Strelitzia* 19: 53 - 219.

Regali, M. S. P., Uesugui, N., & Santos, A. S. 1974. Palinologia dos sedimentos meso-cenozóicos do Brasil (I). *Boletim Técnico da Petrobrás* 13: 177–191.

Riding, J.B., Crame, J.A., Dettmann, M.E. and Cantrill, D.J. 1998. The age of the base of the Gustav Group in the James Ross Basin, Antarctica. *Cretaceous Research* 19: 87-105.

Roberts, D.I. and Brink, J.S. 2002. Dating and correlation of Neogene coastal deposits in the Western Cape (South Africa): Implications for Neotectonism. *South African Journal of Geology* 105: 337-352.

Roberts, D.I. 2006. Lithostratigraphy of the Varswater Formation (Sandveld Group). *South African Committee for Stratigraphy, Lithostratigraphic Series* 9: 17-20.

Roberts, D.I., Mathhews, T., Herries, A.I.R., Boulter, C., Scott, L., Dondo, C., Mtembi, P., Browning, C., Smith, R.M.H., Haarhoff, P and Bateman, M.D. 2011. Regional and global context of the Late Cenozoic Langebaanweg (LBW) palaeontological site: West Coast of South Africa. *Earth-Science Reviews* 106: 191-214.

Roberts, D.I., Sciscio, L., Herries, A.I.R., Scott, L., Bamford, M.K., Musekiwa, C. and Tsikos, H. 2013. Miocene fluvial systems and palynofloras at the southwestern tip of Africa: Implications for regional and global fluctuations in climate and ecosystems. *Earth-Science Reviews* 124: 184-201.

Roberts, D.I., Neumann, F.H., Cawthra, H.C., Carr, A.S., Scott, L., Durugbo, E.U., Humphries, M.S., Cowling, R.M., Bamford, M.K., Musekiwa, C. and MacHutchon, M. 2017. Palaeoenvironments during a terminal Oigocene or early Miocene transgression in a fluvial system at the southwestern tip of Africa. *Global and Planetary Change* 150: 1-23.

Roche, E. and Schuler, M. 1976. Analyse palynologique (pollen et spores) de divers gisements du Tongrien de Belgique. Interprétation palaeoécologique et stratigraphique. *Service Géologique de Belgique* 11: 1-57.

Rogers, J. 1980. First report on the Cenozoic sediments between Cape Town and Eland's Bay. *Geological Survey of South Africa*, Report No. 1980-136: 136 pp.

Rommerskirchen, F., Condon, T., Mollenhauer, G., Dupont, L. and Schefuss, E. 2011. Miocene to Pliocene development of surface and subsurface temperatures in the Benguela Current System. *Paleoceanography* 26: 1-15.

Rossignol, M. 1962. Analyse pollinique de sediments marins quaternaires en Israël. II. Sédiments Pleistocènes. *Pollen Spores* 4: 121-149.

Rossouw, L., Stynder, D.D. and Haarhof, P. 2009. Evidence for opal phytolith preservation in the Langebaanweg, 'E' Quarry Varswater Formation and its potential for palaeohabitat reconstruction. *South African Journal of Science* 105: 223-227.

Ruddiman W.F., Sarnthein, M., Backman, J., Baldauf, J.G., Curry, W., Dupont, L.M., Janecek, T., Pokras, E.M., Raymo, M.E., Stabell, B., Stein, R. and Tiedemann, R. 1989. Proceedings of the Ocean Drilling Program. *Scientific Results* 108: 463-483.

Rundel, P.W., Arroyo, M.T.K., Cowling, R.M., Keeley, J.E., Lamont, B.B., Pausas, J.G. and Vargas, P. 2018. Fire and Plant Diversification in Mediterranean-Climate Regions. *Frontiers in Plant Science* 9: 1-13.

Rundel, P.W. 2019. A Neogene Heritage: Conifer Distributions and Endemism in Mediterranean-Climate Ecosystems. *Fronteirs in Ecology and Evolution* 7: 1-19.

Sah, S.C.D. 1967. Palynology of an upper Neogene profile from Rusizi Valley (Burundi). *Annales du Musée Royal de l'Afrique Centrale Série in Octavo* (Sci. géol.) 57: 1-173.

Saidi, T.A. and Tshipala-Ramatshimbila, T.V. 2006. Ecology and management of a remnant *Brachystegia spiciformis* (miombo) woodland in north eastern Soutpansberg, Limpopo Province. *South African Geographical Journal* 88: 205-212.

Salard-Cheboldaeff, M. 1981. Palynologie Maestrichtienne et Tertiaire du Cameroun. Resultats botaniques. *Review of Palaeobotany and Palynology* 32: 401-439.

Sandersen, A., Scott, L., McLachlan, I.R. and Hancox, P.J. 2011. Cretaceous biozonation based on terrestrial palynomorphs from two wells in the offshore Orange Basin of South Africa. *Palaeontologia africana* 46: 21-41.

Sandilyan, S. and Kathiresan, K. 2012. Mangrove conservation: a global perspective. *Biodiversity and Conservation* 21: 3523-3542.

Scafati, L., Melendi, D.L. and Volkheimer, W. 2009. A Danian subtropical lacustrine palynobiota from South America (Bororó Formation, San Jorge Basin, Patagonia – Argentina). *Geologica Acta* 7: 35-61.

Scholtz, A. and Deacon, H.J. 1982. *Report on the fossil pollens from sediments associated with a group of kimberlite pipes in Botswana*. Internal Report, Department of Archaeology, University of Stellenbosch, to a diamond mining company.

Scholtz, A. 1985. The palynology of the upper lacustrine sediments of the Arnot Pipe, Banke, Namaqualand. *Annals of the South Africa Museum* 95: 1-109.

Schüler, S. and Hemp, A. 2016. Atlas of pollen and spores and their parent taxa of Mt Kilimanjaro and tropical East Africa. *Quaternary International* 425: 301-306.

Sciscio, L. 2011. Neogene deposits along the southwest coast of South Africa: understanding the palaeoclimate through proxies. Rhodes University, Grahamstown, South Africa. MSc Thesis (Unpublished).

Sciscio, L., Neumann, F.H., Roberts, D., Tsikos, H., Scott, L. and Bamford, M. 2013. Fluctuations in Miocene climate and sea levels along the southwestern South African coast: inferences from biogeochemistry, palynology and sedimentology. *Palaeontologia Africana* 48: 2-18.

Sciscio, L. Tsikos, H., Roberts, D.L., Scott, L., van Breugel, Y., Sinninghe Damste, J.S., Schouten, S. and Grocke, D.R. 2016. Miocene climate and vegetation changes in the Cape Peninsula, South Africa: Evidence from biogeochemistry and palynology. *Palaeogeography, Palaeoclimatology, Palaeoecology* 445: 124-137.

Scott, L. 1976. Palynology of Lower Cretaceous deposits from the Algoa basin (Republic of South Africa). *Pollen Spores* 18: 563–609.

Scott, L. 1982. Late Quaternary fossil pollen grains from the Transvaal, South Africa. *Review of Palaeobotany and Palynology* 36: 241-278.

Scott, L., Cadman, A. and McMillan, I. 2006. Early history of Cainozoic Asteraceae along the Southern African west coast. *Review of Palaeobotany and Palynology* 142: 47-52.

Siebert, S.J., Zobolo, A.M. and Dowe, J.L. 2010. Arecaceae: Livistonia Chinensis, a first record of a naturalized palm in South Africa. *Bothalia* 40: 55-102.

Siebert, S.J. and Struwig, M. 2019. Borassus aethiopum Mart. (Arecaceae) in Limpopo province with a key to South African palms. *Bothalia* 49: 1-6.

Siesser, W.G. and Dingle, R.V. 1981. Tertiary sea-level movements around Southern Africa. *The Journal of Geology* 89: 83-96.

Sievers, C. 2015. Nuts for dinner? *Cladium mariscus* in the Middle Stone Age at Sibudu, South Africa. *Transactions of the Royal Society of South Africa* 70: 213-218.

Soliman, A. and Ibrahim, M. 2012. Dinoflagellate cyst stratigraphy and paleoenvironment of the Lower and Middle Miocene, Gulf of Suez, Egypt. *Egyptian Journal of Paleontology* 12: 97-122.

Soliman, A. and Riding, J.B. 2017. Late Miocene (Tortonian) gonyaulacacean dinoflagellate cysts from the Vienna Basin, Austria. *Review of Palaeobotany and Palynology* 244: 325-346.

Song, U., Park, J. and Song, M. 2012. Pollen morphology of Pinus (Pinaceae) in northeast China. *Forest Science and Technology* 8: 179-186.

Sowunmi, M.A. 1973. Pollen grains of Nigerian plants. *Grana* 13: 145-186.

Srivastava, S.K. 1966. Jurassic microflora from Rajasthan, India. *Micropalaeontology* 12: 87-103.

Steinthorsdottir, M., Coxall, H.K., de Boer, A.M., Huber, M., Barbolini, N., Bradshaw, C.D., Burls, N.J., Feakins, S.J., Gasson, E., Henderiks, J., Holbourn, A.E., Kiel, S., Kohn, M.J., Knorr, G., Kürschner, W.M., Lear, C.H., Liebrand, D., Lunt, D.J., Mörs, T., Pearson, P.N., Pund, M.J., Stoll, H. and Strömberg, C.A.E. 2021. The Miocene: The future of the past. *Paleoceanography and Paleoclimatology* 36: 1-72.

Stover, L.E. and Partridge, A.D. 1973. Tertiary and Late Cretaceous spores and pollen from the Gippsland Basin, southeastern Australia. *Proceedings of the Royal Society of Victoria* 85: 237-286.

Strömberg, C.A.E. 2011. Evolution of grasses and grassland ecosystems. *The Annual Review of Earth and Planetary Sciences* 39: 517-544.

Stuchlik, L., Ziembińska-Tworzydło, M., Kohlman-Adamska, A., Grabowska, Ważyńska, H., Słodkowska, E. and Sadowska, A. 2001. Atlas of pollen and spores of the Polish Neogene. *Spores* Vol. 1. Polish Academy of Sciences, W. Szafer Institute of Botany, Kraków.

Stuchlik, L., Ziembińska-Tworzydło, M., Kohlman-Adamska, A., Grabowska, Ważyńska, H. and Sadowska, A. 2002. Atlas of pollen and spores of the Polish Neogene. *Gymnosperms* Vol. 2. Polish Academy of Sciences, W. Szafer Institute of Botany, Kraków.

Stuchlik, L., Ziembińska-Tworzydło, M., Kohlman-Adamska, A., Grabowska, I., Słodkowska, Ważyńska, H. 2009. Atlas of pollen and spores of the Polish Neogene. *Angiosperms* (1) Vol. 3. Polish Academy of Sciences, W. Szafer Institute of Botany, Kraków.

Stuchlik, L., Ziembińska-Tworzydło, M., Kohlman-Adamska, A., Grabowska, I., Słodkowska, E., Worobiec, E. and Durska, E., 2014. Atlas of pollen and spores of the Polish Neogene. *Angiosperms* (2) Vol. 4. Polish Academy of Sciences, W. Szafer Institute of Botany, Kraków.

Sun, J., Xu, Q., Liu, W., Zhang, Z., Xue, L. and Zhao, P. 2014. Palynological evidence for the latest Oligocene-early Miocene palaeoelevation estimate in the Lunpola Basin, central Tibet. *Palaeogeography, Palaeoclimatology, Palaeoecology* 399: 21-30.

Takahashi, M. 1997. Fossil spores and pollen grains of Cretaceous (Upper Campanian) from Sakhalin, Russia. *Journal of Plant Research* 110: 283-298.

Takhtajan A. 1986. Floristic regions of the world. Berkeley, CA: University of California Press.

Tankard, A.J. and Rogers, J. 1978. Late Cenozoic palaeoenvironments on the west coast of Southern Africa. *Journal of Biogeography* 5: 319-337.

Tarran, M., Wilson, P.G., Macphail, M.K., Jordan, G.J. and Hill, R.S. 2017. Two fossil species of Metrosideros (Myrtaceae) from the Oligo-Miocene Golden Fleece locality in Tasmania, Australia. *American Journal of Botany* 104: 891-904.

Thiergart, F., Frantz, U. and Raukopf, K. 1963. Palynologische untersuchungen von Tertiärkohlen und einer oberflächen-probe nahe Knysna, Südafrika. *Advancing Frontiers of Plant Sciences* 4: 151-178.

Traverse, A. 1994. Palyofloral geochronology of the Brandon Lignite of Vermont, USA. *Review of Palaeobotany and Palynology* 82: 265-297.

Trias-Blasi, A., Parnell, J.A.N. and Hodkinson, T.R. 2012. Multi-gene region phylogenetic analysis of the grape family (Vitaceae). *Systematic Botany* 37: 941-950.

Truswell, E.M. and Macphail, M.K. 2009. Polar forests on the edge of extinction: what does the fossil spore and pollen evidence from East Antarctica say? *Australian Systematic Botany* 22: 57-106.

Tyson, R.V. 1995. Sedimentary Organic Matter - Organic Facies and Palynofacies. Chapman & Hall, London: 615 pp.

Udeze, C.U. and Oboh-Ikuenobe, F.E. 2005. Neogene palaeoceanographic and palaeoclimatic events inferred from palynological data: Cape Basin off South Africa, ODP Leg 175. *Palaeogeography, Palaeoclimatology, Palaeoecology* 219: 199-223.

Vargas, P., Fernández-Mazuecos, M. and Heleno, R. 2018. Phylogenetic evidence for a Miocene origin of Mediterranean lineages: species diversity, reproductive traits and geographical isolation. *Plant Biology* 20: 157-165.

van Campo, E. 1976. La flore sporopollénique du gisement Miocene terminal de Venta del Moro (Espagne). Thesis. Montpellier.

van Santen, M. and Linder, H.P. 2020. The assembly of the Cape flora is consistent with an edaphic rather than climatic filter. *Molecular Phylogenetics and Evolution* 142: 1-11.

Wadley, L., Sievers, C., Bamford, M., Goldberg, P., Berna, F. and Miller, C. Middle Stone Age bedding construction and settlement patterns at Sibudu, South Africa. *Science* 334: 1388-1391.

Weems, R.E. and Edwards, L.E. 2001. Geology of Oligocene, Miocene and younger deposits in the coastal area of Georgia. *U.S. Geological Survey, Bulletin* 131: 1-124.

Weston, P.H. (2007) Proteaceae. In: Kubitzki K. (eds) Flowering Plants - Eudicots. The Families and Genera of Vascular Plants 9: 364 – 404. Springer, Berlin, Heidelberg.

Whitehouse, C.M. 2004. The genus *Cliffortia* (Rosaceae) in KwaZulu-Natal. *Bothalia* 34: 1-10.

Willis, J.C. 1966. *A dictionary of the flowering plants and ferns*. Seventh edition revised by Airy Shaw, HK. Cambridge: The University Press.

Willumsen, P.S., Dale, B., Jolley, D.W. and Laursen Vestergaard, G. 2014. Palynostratigraphy and palaeoenvironmental shifts in Oligocene and Miocene strata from offshore Angola, west-central Africa. *Palynology* 38: 259-279.

Wilpshaar, M., Santarelli, A., Brinkhuis, H. and Visccher, H. 1996. Dinoflagellate cysts and mid-Oligocene chronostratigraphy in the central Mediterranean region. *Journal of the Geological Society* 153: 553-561.

Wingate, F.H. 1983. Palynology and age of Elko Formation (Eocene) near Elko, Nevada. *Palynology* 7: 93-132.

Wolela, A. 2014. Volcanism, sedimentation, K/Ar and palynology studies, Yayu and Delbi-Moye Basins, Southwestern Plateau of Ethiopia. *Journal of African Earth Sciences* 93: 1-13.

Wood, G.D., Gabriel, A.M., and Lawson, J.C. 1996. Chapter 3. Palynological techniques – processing and microscopy. In: Jansonius, J., McGregor, D.C. (Eds). Palynology: Principles and Applications. American Association of Stratigraphic Palynologists Foundation, Dallas, pp. 29-50.

Worobiec, E. 2009. Middle Miocene palynoflora of the Legnica lignite deposit complex, Lower Silesia, Poland. *Acta Palaeobotanica* 49: 5-133.

Worobiec, E., Worobiec, G. and Gedl, P. 2009. Occurrence of fossil bamboo pollen and a fungal conidium of Tetraploa cf. aristate in Upper Miocene of Józefina (Poland). *Review of Palaeobotany and Palynology* 157: 211-17.

Worobiec, E and Worobiec, E. 2010. Late Miocene freshwater phytoplankton from Józefina (Poland). *Micropalaeontology* 56: 517-537.

Worobiec, E., Liu, Y-S. and Zavada, M.S. 2013. Palaeoenvironment of Late Neogene lacustrine sediments at the Gray Fossil Site, Tennessee, USA. *Annals Societatis Geologorum Poloniae* 83: 51-63.

Worobiec, E. and Szulc, J. 2016. Middle Miocene palynoflora from sinkhole deposits from Upper Silesia, Poland and its palaeoenvironmental context. *Review of Palaeobotany and Palynology* 163: 1-10.

Worobiec, E., Widera, M., Worobiec, G. and Kurdziel, B. 2019. Middle Miocene palynoflora from the Adamów lignite deposit, central Poland. *Palynology*, DOI: 10.1080/01916122.2019.1697388: 1-30.

Worobiec, E., Widera, M., Worobiec, G. and Kurdziel, B. 2021. Middle Miocene palynoflora from the Adamów lignite deposit, central Poland. *Palynology* 45: 59-71.

Zavada, M. and de Villiers, S. 2000. Pollen of the Asteraceae from the Palaeocene-Eocene of South Africa. *Grana* 39: 39-45.

Zavada, M. and Lowrey, T.K. 2010. Comparative pollen morphology of *Brachylena*, *Tarchananthus* and two species of *Tubulifloridites* (Asteraceae) from the Eocene, Knysna Lignite of South Africa.

Zhao, X. 2017. Palynological investigation of Holocene climatic and oceanic variability in South Africa and the southern Benguela upwelling system. University of Bremen, Bremen, Germany. Dissertation for the Doctoral Degree (PhD) in Natural Sciences.

Zhenghao, X. and Deng, M. 2017. Gleicheniaceae. *Identification and Control of Common* Weeds 2: 17-23.

Ziembińska-Tworzydło, M. 1974. Palynological characteristics of the Neogene of western Poland. *Acta Palaeontologica Polonica* 19: 309-432.

Ziembińska-Tworzydło, M., Grabowska, I., Kohlman-Adamska, A., Skawińska, K., Słodkowska, B., Stuchlik, L., Sadowska, A. and Ważyńska, H. 1994. Taxonomical revision of selected pollen and spores taxa from Neogene deposits. *Acta Palaeobotanica* (suppl.) 1: 5-30.

Zonneveld, K.A.F. and Pospelova, V. 2015. A determination key for modern dinoflagellate cysts. *Palynology* 39: 387- 407.

Zonneveld, K.A.F., Hoek, R.P., Brinkhuis, H. and Willems, H. 2001. Geographical distributions of organic-walled dinoflagellate cysts in surficial sediments of the Benguela upwelling region and their relationship to upper ocean conditions. *Progress in Oceanography* 48: 25-72.

APPENDICES

Appendix A. Nomenclature and botanical affinities of the most important palynomorphs from LBW, including taxa in photo plates and discussed in the text.

Name (form genus, form species)	Botanical affinity	Reference
Gymnosperms, subtropical trees and shrubs and fynbos elements		
Podocarpidites sp. (compare *Alisporites grandis* (Cookson) Dettmann 1963)	*Podocarpus (*Podocarpaceae)	Scholtz, 1985
Podocarpidites ellipticus Cookson 1947 ex Couper 1953	*Podocarpus* (Podocarpaceae)	Haskell, 1968
Microcachrydites sp. (*Microcachrydites* Cookson 1947)	*Microcachrys* (Podocarpaceae)	Cookson, 1947
Dacrydiumites sp. (Compare *Lygistepollenites florinii* Cookson and Pike 1954)	*Dacrydium* (Podocarpaceae)	Askin, 1990
Cupressacites sp. (*Cupressacites* Bolchovitina 1956 ex Krutzsch 1971)	Cupressaceae, Taxaceae	Stuchlik *et al*. 2002
cf. *Araucariacites australis* (*Araucariacites australis* Cookson ex Couper 1953)	Araucariaceae	Scholtz, 1985
Arecipites otagoensis (Couper 1960) Mildenhall & Pocknall 1989	Arecaceae	Raine *et al*., 2011
Clavatipollenites sp. (*Clavatipollenites* Couper 1958)	Chloranthaceae	Couper, 1958
Liliacidites sp. (*Liliacidites* Couper 1953)	Liliaceae, Araceae, Asparagaceae, Amarylladiaceae, Iridaceae	Stuchlik *et al*., 2014
Cupuliferoipollenites oviformis (Potonié 1934) Potonié 1951 ex Potonié 1960	Castanea, Castanopsis, Lithocarpus, Passania (Fagaceae)	Stuchlik *et al*., 2014
Parthenopollenites marcodurensis (Pflug & Thomson in Thomson & Pflug 1953)	*Ampelopsis*, *Cayratia*, *Cissus*, *Cyphostemma* and *Parthenocissus* (Vitaceae)	Stuchlik *et al*., 2014
Parthenopollenites neshobensis (Traverse 1955) Traverse 1994	*Ampelopsis*, *Cayratia, Cissus*, *Cyphostemma* and *Parthenocissus* (Vitaceae)	Stuchlik *et al*., 2014
Oleoidearumpollenites reticulatus Nagy 1969	*Olea L.* (Oleaceae)	Stuchlik *et al*., 2014
Rhoipites couperi Pocknall 1985	Araliaceae	Pocknall and Crosbie, 1982
Margocolporites rauvolfii Salard-Cheboldaeff 1978	*Rauvolfia*, Apocynaceae	Coetzee and Rogers, 1982
Myricipites harrisii (Couper 1953)	Myricaceae or Casuarinaceae	Raine *et al*., 2011
Casuarinidites sp. (*Casuarinidites* Cookson and Pike 1954)	Myricaceae or Casuarinaceae	Raine *et al*., 2011

Name (form genus, form species)	Botanical affinity	Reference
Tetracolporopollenites sapotoides Pflug & Thomson in Thomson & Pflug 1953	*Mimusops* (Sapotaceae)	Stuchlik *et al*., 2014
Zonocostites ramonae Germeraad *et al. 1968*	Rhizophoraceae	Germeraad *et al*., 1968
Rhoipites alveolatus (Couper 1953) Pocknall & Crosbie 1982	Euphorbiaceae	Raine *et al*. 2011
Ilexpollenites margaritatus (Potonié 193) Thiergart 1938	Aquifoliaceae	Stuchlik *et al*., 2014
Peregrinipollis nigericus Clarke 1966	*Brachystegia* (Caesalpiniaceae)	Clarke, 1966
Propylipollis meyeri Scholtz 1985	*Leucospermum, Lomatia (Grevilleoideae, Persoonioideae, Proteoideae)*	Scholtz, 1985
Proteacidites sp. A (*Proteacidites* sp. de Villiers and Cadman, 1997)	Proteaceae	de Villiers and Cadman, 1997
Proteacidites sp. B (Compare *Proteacidites tuberculatus* Cookson 1950)	Proteaceae	Cookson, 1950; Macphail and Hill, 1994; Raine *et al*., 2011
Ericipites callidus (Potonié 1931) Krutzsch 1970	Ericaceae	Stuchlik *et al*., 2014
Psilatricolporites quenua Barreda & Palazzesi 2009	*Acaena, Polylepis, Cliffortia* (Rosaceae)	Barreda *et al.,* 2009
Tubulifloridites antipodica Cookson 1947	*Tubuliflorae* (Asteraceae)	Zavada and Lowrey, 2010
Mutisiapollis viteauensis Barreda 1993	*Mutisieae*	Barreda, 1993; Compare Coetzee and Rogers, 1982
Rhoipites arnotiensis (Scholtz 1985) de Villiers 1999	*Anthospermum* (Rubiaceae)	Scholtz, 1985
Graminidites cf. *crassiglobosus* (Trevisan 1967) Krutzsch 1970	Poaceae	Stuchlik *et al*., 2009
Graminidites cf. *neogenicus* Krutzsch 1970	Poaceae	Stuchlik *et al*., 2009
Wetland taxa, algae & dinoflagellates		
Cyperaceaepollenites sp. (*Cyperaceaepollis* Krutzsch 1970)	Cyperaceae	Stuchlik *et al*., 2009
Cyperaceaepollenites piriformis Thiele-Pfeiffer 1980	Cyperaceae	Stuchlik *et al*. 2009
Milfordia hypolaenoides Erdtman 1960	Restionaceae	Stuchlik *et al*., 2009
Milfordia homeopunctatus (McIntyre 1965) Stover and Partridge 1973	Restionaceae	Stover and Partridge, 1973
Sparganiaceaepollenites barungensis Harris 1972	*Sparganium* L. (Sparganiaceae), *Typha* L. (Typhaceae)	Harris, 1972; Mildenhall and Crosbie, 1979
Baculatisporites sp. *(Baculatisporites* Pflug & Thomson in Thomson and Pflug 1953	*(Osmunda)* Osmundaceae	Stuchlik *et al*., 2001
Cyathidites australis Couper 1953	*Cyathea* (Cyatheaceae)*;*	Scholtz, 1985; Raine *et*

Name (form genus, form species)	Botanical affinity	Reference
	Lygodium (Shizaeaceae)	*al*., 2011
Gleicheniidites spp. (*Gleicheniidites* Ross 1949 emend. Skarby 1964)	Gleicheniaceae	Stuchlik *et al*., 2001; Raine *et al*., 2011
Laevigatosporites haardti (Potonié & Venitz 1934) Thomson & Pflug 1953	Polypodiaceae; Pteridaceae	Stuchlik *et al*., 2001
Leiotriletes maximus (Pflug in Thomson and Pflug 1953) Krutzsch 1959	*Lygodium* (Lygodiaceae)	Stuchlik *et al*., 2001
Leiotriletes maxoides Krutzsch 1952	*Lygodium* (Lygodiaceae)	Stuchlik *et al*., 2001
Leiotriletes wolffii Krutzsch 1962	*Lygodium* (Lygodiaceae)	Stuchlik *et al*., 2001
Planctonites stellarius (Potonié 1934) Gruas-Cavagnetto 1968	*Closterium colosporum, Penium*, *Pleurotaenium* (Zygospores)	Worobiec, 2014
Botryococcus sp. *(Botryococcus* Kützing 1849)	*Botryococcus* (Dictyosphaeriaceae), (Botryococcaceae)	Worobiec and Worobiec, 2010
Debarya-type *(*Compare *Lecaniella forma* 4 Head 1992)	*Debarya*	Worobiec, 2014
Ovoidites grandis (Pocock 1962) Zippi 1998	Zygnemataceae	Worobiec and Worobiec, 2010
Ovoidites vangeeli (Worobiec 2014)	*Spirogyra* (Zygnemataceae)	Worobiec, 2014
Pediastrum-type (*Pediastrum* Meyen 1829)	Hydrodictyaceae	Worobiec, 2014
Stigmozygodites sp. (*Stigmozygodites* Krutzsch & Pacltová 1990)	Zygnemataceae	Worobiec, 2014
Apteodinium spiridiodes Benedek 1972	Gonyaulacaceae	Fensome *et al*., 2009; Fensome *et al*., 2016;
Chiropteridium lobospinosum Gocht 1960	Areoligeraceae	Fensome *et al*., 2009; Fensome *et al*., 2016
Cordosphaeridium minimum (Morgenroth 1966) Benedek 1972	Gonyaulacaceae	Fensome *et al*., 2009
Operculodinium centrocarpum (Deflandre & Cookson 1 955) Wall 1967	Gonyaulacaceae	Marret and Zonneveld, 2003
Operculodinium sp. (compare cf. *Operculodinium eirikianum* Head, Norris and Mudie 1989)	Gonyaulacaceae	Head, 1997
Spiniferites mirabilis Rossignol 1963 (Sarjeant, 1970)	Gonyaulacaceae	Marret and Zonneveld, 2003
Spiniferites spp. (compare *Spiniferites bentorii* (Rossignol 1964) Wall and Dale 1970)	Gonyaulacaceae	Zonneveld and Pospelova, 2015

Appendix B: Percentages of the LBW palynomorphs to determine palynomorph fluctuations across Core BH2

Samples (m)	*Podocarpidites* sp.	*Podocarpidites ellipticus*	*Microcachrydites* sp.	*Dacrydiumites* sp.
1,61	0	0	0	0
12,49	0	0	0	0
12,99	0	0	0	0
13,81	0	0	0	0
14,63	1	0	0	0
15,13	0	0,4	0	0
16,45	0	0	0	0
17,28	0,8	0,5	0	0
17,32	2,9	0,9	0,2	0
17,4	1,5	1,2	0	0
17,44	3,5	0,4	0	0
17,48	2,1	0,4	0	0
17,53	1,4	0,1	0	0
17,57	1,1	0,5	0,1	0
17,62	2,4	0,3	0	0
17,7	1,2	0,3	0	0
17,8	1,9	0,3	0	0
17,86	1,7	0,6	0	0
17,92	2,3	0,2	0	0
17,97	1,5	0,6	0	0
18,02	2,5	0,7	0,1	0
18,07	1,2	0,8	0	0
18,11	2,9	0,4	0	0
18,15	2,9	1,2	0	0
18,2	2,5	1,4	0	0
18,28	0,7	0,1	0	0
18,33	1	0,3	0	0
18,38	1,2	0,1	0	0
18,43	1,8	0,5	0	0
18,48	3,6	0,1	0	0
18,53	0,8	0,7	0	0
18,58	1,2	0,4	0	0
18,63	0,3	0	0	0
18,68	0,4	0,1	0	0
18,7	2,1	1,4	0	0
18,75	1,4	0,8	0	0

Samples (m)	*Podocarpidites* sp.	*Podocarpidites ellipticus*	*Microcachrydites* sp.	*Dacrydiumites* sp.
18,8	3	0	0	0
18,88	0,8	0,1	0	0
18,9	2,4	0	0,2	0
18,96	2,6	0,1	0	0
19	0	0,4	0	0
19,06	0	0,3	0	0
19,1	0	0,1	0	0
19,18	0	0,1	0	0
19,2	0,5	0,1	0	0
19,25	0,6	0	0	0
19,33	0,2	0	0,1	0
19,38	0,6	0	0	0
19,43	0	0	0	0
19,48	0,2	0	0	0
19,52	1,2	0	0	0
19,63	0,5	0	0	0
19,7	0,7	0,4	0	0,1
19,75	0,2	0,2	0	0
19,8	1	0,5	0	0
19,85	0,7	0,7	0	0
19,93	0,5	3,8	0	0
19,95	2,6	0	0	0
20	7,1	0,8	0	0
20,08	2,1	12,1	0	0
20,33	0,2	13,4	0	0
25,4	0	0,4	0	0
25,45	0	0,3	0	0
25,48	0	2	0	0
25,52	0	0,3	0	0
25,55	0	0,9	0	0
25,58	0,6	0	0	0
25,6	0,9	0	0	0
30,92	5,8	2,1	0	0
30,97	3,2	1,2	0	0
31,01	1,4	0,8	0	0
31,05	3,1	5,3	0	0
31,09	11,5	5,1	0	0
31,13	3,1	13,3	0	0
32	1,9	7,2	0	0

Samples (m)	*Podocarpidites* sp.	*Podocarpidites ellipticus*	*Microcachrydites* sp.	*Dacrydiumites* sp.
32,53	5,5	6,4	0	0
33,03	2,6	3,2	0,1	0

Samples	*Cupressacites* sp.	cf. *Araucariacites australis*	*Distachyapites*-type	*Arecipites otagoenis*
1,61	0	0	0	8,7
12,49	0	0	0	0
12,99	0	0	0	0
13,81	0	0	0	0
14,63	0	0	0	0
15,13	0	0	0	0
16,45	0	0	0	0
17,28	0	0	0	1,2
17,32	0	0	0	0
17,4	0	0	0	0
17,44	0	0	0	0
17,48	0,2	0	0	0,1
17,53	2,2	0	0	1,4
17,57	0,8	0	0	0,1
17,62	0	0	0	0
17,7	1,2	0	0	0
17,8	2,2	0	0	0
17,86	1,5	0	0	0
17,92	1	0	0	0,3
17,97	0,2	0	0	0,1
18,02	0,6	0	0	0
18,07	0	0	0	0
18,11	2,9	0	0	0,4
18,15	0,2	0	0	0
18,2	0	0	0	0
18,28	0	0	0	0,1
18,33	0	0	0	0,4
18,38	0	0	0	0,1
18,43	0	0	0	0,2
18,48	0	0	0	0,1
18,53	0,2	0	0	0,3
18,58	0	0	0	0,1
18,63	0	0	0	0
18,68	0	0	0	0

Samples	*Cupressacites* sp.	cf. *Araucariacites australis*	*Distachyapites*-type	*Arecipites otagoenis*
18,7	0	0	0	3,3
18,75	0,5	0	0	3,1
18,8	1,1	0	0	1,7
18,88	0	0	0	0,6
18,9	0	0	0	1,5
18,96	0,2	0	0	0,8
19	0	0	0	1,4
19,06	0,1	0	0	0,4
19,1	0,3	0	0	0,8
19,18	0	0	0	0,3
19,2	0	0	0	0,6
19,25	0,1	0	0	0,6
19,33	0	0	0	1,2
19,38	0	0	0	1,2
19,43	0	0	0	2,4
19,48	0,1	0	0	2,5
19,52	0	0,3	0	8,5
19,63	0	0	0	1,3
19,7	0,2	0	0	15,8
19,75	0	0	0	5,9
19,8	1,3	0	0	17,7
19,85	0,7	0	0	16
19,93	0,5	0	0	10,8
19,95	0,2	0	0	4,9
20	0	0	0	16,8
20,08	0	0,4	0	4,7
20,33	0	0,4	0	6,2
25,4	0	0	0	0,3
25,45	0,2	0	0	1,2
25,48	0	0	0	2,9
25,52	0	0,1	0	0,9
25,55	0	0	0	0,7
25,58	0	0	0	0,3
25,6	0	0	0	1,3
30,92	0,4	0	0	0,9
30,97	0,2	0	0	0,8
31,01	1,2	0	0	1
31,05	0,2	0	0,2	2,1
31,09	0	0	0	1,1

Samples	*Cupressacites* sp.	cf. *Araucariacites australis*	*Distachyapites*-type	*Arecipites otagoenis*
31,13	1,1	0	0	2,1
32	0	0	0	2,8
32,53	0,2	0	0	4,5
33,03	0,4	0	0	2,6

Samples	*Clavatipollenites* sp.	*Liliacidites* sp.	*Rhoipites couperi*	*Cupuliferoipollenites oviformis*
1,61	0	0	0	0
12,49	0	0	0	0
12,99	0	0	0	0
13,81	0	0	0	0
14,63	0	0	0	0
15,13	0	0	0	0
16,45	0	0	0	0
17,28	0,2	0	0,9	0,1
17,32	0,1	0	0,5	0,1
17,4	0,1	0	0,2	0
17,44	0	0	0,1	0,1
17,48	0	0	0,2	0,2
17,53	0	0	0,3	2,3
17,57	0	0	0	0
17,62	0	0	0	0
17,7	0	0	0	0,9
17,8	0	0	0	0,6
17,86	0	0	0,1	0,3
17,92	0	0	0,3	0,3
17,97	0	0	0,2	0,1
18,02	0	0	0,7	0,1
18,07	0	0,2	0	0,3
18,11	0	0	0	0
18,15	0	0	0,6	0,2
18,2	0	0	0,6	1,1
18,28	0	0	0,1	0
18,33	0,1	0	0,2	0,1
18,38	0	0	0,2	0
18,43	0	0	0,1	0,2
18,48	0	0	0,2	0
18,53	0	0	0,6	0

Samples	*Clavatipollenites* sp.	*Liliacidites* sp.	*Rhoipites couperi*	*Cupuliferoipollenites oviformis*
18,58	0	0	0,1	0
18,63	0	0	0	0
18,68	0	0	0	0
18,7	0	0,1	1,1	0,3
18,75	0	0	0,4	1
18,8	0	0,3	0,7	0,5
18,88	0	0,1	0,3	0,5
18,9	0	0,1	0,2	0
18,96	0	0,1	0,1	0,3
19	0	0	0,2	1,8
19,06	0	0	0,1	0,1
19,1	0	0	0,1	3,4
19,18	0	0	0,1	0,4
19,2	0,1	0	0,4	0
19,25	0	0	0,1	0
19,33	0	0	0,1	0,6
19,38	0	0	0,4	0,1
19,43	0	0,1	0,2	0
19,48	0	0	1,2	0,5
19,52	2,7	0,3	5,7	0,2
19,63	0	0	0,5	1,4
19,7	0,4	0	0,1	0,7
19,75	0,1	0,1	1,1	2,6
19,8	0,8	0,5	1	0
19,85	2,7	0	4,6	1,3
19,93	3	4,7	5,8	1,5
19,95	6,2	9,5	7,5	2,6
20	4,4	0,2	3,5	1,2
20,08	1,4	0,2	1,8	0,4
20,33	0,8	0	0,8	0,8
25,4	0,1	0	1,8	4,4
25,45	0,4	0	5,2	7,9
25,48	1,4	0	6,3	7,2
25,52	1,4	0	5,5	5,1
25,55	11,5	0	7,9	1,5
25,58	0,4	0	1,1	1
25,6	0,2	0	1,1	0,4
30,92	0,1	0	0,8	1,5
30,97	0,2	0	1,9	1,5
31,01	0,3	0	1,7	0,8

Samples	*Clavatipollenites* sp.	*Liliacidites* sp.	*Rhoipites couperi*	*Cupuliferoipollenites oviformis*
31,05	0,8	0	2,1	1,2
31,09	0,4	0	3,5	0
31,13	0,9	0	4,6	1,1
32	0,6	0	1,3	0,7
32,53	0,9	0	4,2	1,3
33,03	0,5	0	3,1	0,5

Samples	*Cupaniedites* sp.	*Myrtaceidites* sp.	*Oleoidearumpollenites reticulatus*	*Tetracolporopollenites sapotoides*
1,61	0	0	0	0
12,49	0	0	0	0
12,99	1,7	0	0	0
13,81	0	0	0	0
14,63	0	0	0	0
15,13	0	0	0	0,3
16,45	0	0	0	0,4
17,28	0	0	1,7	0,1
17,32	0	0	0,5	0,1
17,4	0	0	0,6	0,2
17,44	0,1	0	0,8	0,3
17,48	0	0	0	0,2
17,53	0	0	1,5	0,1
17,57	0	0	0,2	0
17,62	0	0	1	0
17,7	0	0	1,8	0,3
17,8	0	0	0,3	0
17,86	0	0	0,8	0
17,92	0	0	3,1	0,2
17,97	0	0	0,5	0
18,02	0	0	0,4	0,3
18,07	0	0	0,4	0,2
18,11	0	0	0,4	0
18,15	0	0	0,6	0,2
18,2	0	0	0	0,3
18,28	0,1	0	0,3	0,1
18,33	0	0	0,1	0,1
18,38	0	0	0,3	0

Samples	*Cupaniedites* sp.	*Myrtaceidites* sp.	*Oleoidearumpollenites reticulatus*	*Tetracolporopollenites sapotoides*
18,43	0	0	0,5	0,1
18,48	0	0	1,2	0
18,53	0	0	0,6	0
18,58	0	0	0,2	0
18,63	0	0	0	0
18,68	0	0	0,2	0,1
18,7	0	0	2,4	0
18,75	0	0	1,9	0
18,8	0	0	1,2	0
18,88	0,1	0	1,1	0,2
18,9	0	0	1,3	0
18,96	0	0	0,8	0
19	0	0	0,4	0
19,06	0	0	0,2	0
19,1	0	0	0,3	0
19,18	0	0	0,2	0
19,2	0	0	0,1	0
19,25	0	0	0,1	0,1
19,33	0	0	0,1	0
19,38	0	0	0	0
19,43	0	0	0,3	0
19,48	0	0	0,3	0
19,52	0	0	1,3	0
19,63	0	0	1,9	0,2
19,7	0	0	1	0
19,75	0	0	0,7	0
19,8	0,3	0	0,8	0
19,85	0	0	3,3	0
19,93	0,2	0	8,8	0
19,95	0	0	10,8	0,2
20	0	0,2	1,7	0
20,08	0	0	2,5	0
20,33	0,2	0,2	2,7	0,6
25,4	0	0	0	0
25,45	0	0	0,7	0
25,48	0,1	0	0,7	0
25,52	0	0	0	0
25,55	0	0	0,6	0
25,58	0	0	0,1	0

Samples	*Cupaniedites* sp.	*Myrtaceidites* sp.	*Oleoidearumpollenites reticulatus*	*Tetracolporopollenites sapotoides*
25,6	0	0	0	0
30,92	0	0	3,8	0,5
30,97	0,7	0	3,3	0
31,01	0,9	0	2,8	0,1
31,05	0	0	6	0
31,09	0,2	0	4,1	0
31,13	0,9	0	8,9	0
32	0,2	0	3,5	0,2
32,53	0	0	6,2	0,9
33,03	0,5	0	8,7	0

Samples	*Celtispollenites* sp.	*Rhuspollenites* sp.	*Maytenus*-type	*Rhoipites alveolatus*	*Crotonipollis* sp.
1,61	0	0	0	0	0
12,49	0	0	0	0	0
12,99	0	0	0	0	0
13,81	0	0	0	0	0
14,63	0	0	0	0	0
15,13	0	0	0	0	0
16,45	0	0	0	0	0
17,28	0	0	0	0,3	0
17,32	0	0	0	0	0
17,4	0	0	0	0	0
17,44	0	0	0	0	0
17,48	0	0,1	0	0,1	0
17,53	0	0	0	0,1	0
17,57	0	0	0	0,1	0
17,62	0,1	0	0	0,1	0
17,7	0	0	0	0,6	0
17,8	0	0	0	0,3	0
17,86	0	0	0	0	0
17,92	0	0	0	0	0
17,97	0	0	0	0,4	0
18,02	0	0	0	0,3	0
18,07	0	0	0	0,2	0
18,11	0	0	0	0	0
18,15	0	0,1	0	0	0

Samples	*Celtispollenites* sp.	*Rhuspollenites* sp.	*Maytenus*-type	*Rhoipites alveolatus*	*Crotonipollis* sp.
18,2	0	0,3	0	0	0
18,28	0	0	0	0	0
18,33	0	0,1	0	0	0
18,38	0	0	0	0	0
18,43	0	0	0	0	0
18,48	0	0,1	0	0	0
18,53	0	0,1	0	0	0
18,58	0	0,1	0	0	0,2
18,63	0	0	0	0	0
18,68	0	0	0	0	0
18,7	0	0	0	0	0
18,75	0	0,1	0	0,4	0,5
18,8	0	0	0	0,7	0
18,88	0,1	0,1	0	0	0
18,9	0,1	0	0	0,3	0,2
18,96	0	0,2	0,1	0,3	0,2
19	0	0,2	0	0,2	0
19,06	0	0	0	0	0
19,1	0	0	0	0,1	0
19,18	0	0	0	0	0
19,2	0	0	0	0	0
19,25	0	0,2	0	0	0
19,33	0	0	0	0	0,1
19,38	0	0	0	0,1	0
19,43	0	0	0	0,1	0,1
19,48	0	0	0	0	0
19,52	0	0	0	0,2	0
19,63	0,2	0	0	0	0
19,7	0	0	0	0	0
19,75	0	0	0,1	0	0,1
19,8	0,3	0	0	0,3	0
19,85	0,5	0	0,2	0,4	0
19,93	0,7	0	0,3	0,5	0,2
19,95	0	0,4	0,2	0,2	0,2
20	0	0	0,4	2,3	0,2
20,08	0,5	0,9	0,5	0,9	0,4
20,33	0,6	0,2	0	1,7	0,2
25,4	0	0	0	0	0,1
25,45	0	0	0	0	0

Samples	*Celtispollenites* sp.	*Rhuspollenites* sp.	*Maytenus*-type	*Rhoipites alveolatus*	*Crotonipollis* sp.
25,48	0	0	0,1	0	0
25,52	0	0	0	0	0
25,55	0	0	0	0	0,2
25,58	0	0	0	0	0,1
25,6	0	0	0	0	0
30,92	0,6	0	0,5	2,1	0,3
30,97	0,7	0	0,3	1,7	0,2
31,01	1,6	0,1	0,1	1	0,1
31,05	1,7	0	1,2	0,8	0,2
31,09	1,3	0,2	0,6	2	1,9
31,13	1,2	0	0,9	3,2	1,4
32	0,7	0,2	0,6	4,4	0,9
32,53	0,6	0,2	0,6	1,3	0,6
33,03	0,6	0	0	1	0,1

Samples	*Ilexpollenites margaritatus*	*Casuarinidites* sp.	*Parthenopollenites marcodurensis*	*Parthenopollenites neshobensis*
1,61	0	0	0	0
12,49	0	0	0	0
12,99	0	0	0	0
13,81	0	0	0	0
14,63	0	0	0	0
15,13	0	0	0	0
16,45	0	0	0	0,4
17,28	0	0	0	0,1
17,32	0	0	0	0,1
17,4	0	0	0	0
17,44	0	0	0	0
17,48	0	0	0	0,2
17,53	0	0	0,6	0,3
17,57	0	0	0	0
17,62	0	0	0	0,1
17,7	0	0	0	0,3
17,8	0	0	0	0
17,86	0	0	0	0
17,92	0	0	0	0,2
17,97	0	0	0,1	0,5

Samples	*Ilexpollenites margaritatus*	*Casuarinidites* sp.	*Parthenopollenites marcodurensis*	*Parthenopollenites neshobensis*
18,02	0	0	0	0,1
18,07	0	0	0	0
18,11	0	0	0	0
18,15	0	0	0	0
18,2	0	0	0	0,3
18,28	0	0	0	0
18,33	0	0	0	0
18,38	0	0	0,3	0
18,43	0	0	0,1	0
18,48	0	0	0	0,1
18,53	0	0	0,1	0
18,58	0	0	0	0
18,63	0	0	0	0
18,68	0	0	0	0
18,7	0	0	0,5	0
18,75	0	0	1,3	0
18,8	0	0	1,9	0
18,88	0	0	0,1	0
18,9	0,1	0	0,6	0
18,96	0	0	0,6	0,1
19	0	0	2,2	0
19,06	0	0	0	0
19,1	0,2	0	2,2	0
19,18	0	0	0,2	0
19,2	0	0	0	0
19,25	0	0	0,2	0
19,33	0	0	0,8	0
19,38	0	0	0,3	0
19,43	0,2	0	12,9	0
19,48	0	0	6,9	0
19,52	0	0	0	0
19,63	0	0	0	0
19,7	0	0	0	0
19,75	0	0	0,1	0
19,8	0	0	1	0
19,85	0,2	0	2,6	0,4
19,93	0,5	0	1,5	0,2
19,95	0,2	0	1,1	0,4
20	0,4	0	0,6	0,2

Samples	*Ilexpollenites margaritatus*	*Casuarinidites* sp.	*Parthenopollenites marcodurensis*	*Parthenopollenites neshobensis*
20,08	0,9	0	0,9	0,4
20,33	0,4	0	0	1
25,4	0	0	0	0
25,45	0	0	0	0
25,48	0	0	0,2	0
25,52	0,1	0	0	0
25,55	0	0	1,5	0
25,58	0	0	0,1	0
25,6	0	0	0,8	0
30,92	0,3	0,1	0,4	0,1
30,97	0	0	1,7	0,1
31,01	0,1	0	1,2	0,1
31,05	0,2	0,2	1	0,4
31,09	1,1	0	0,2	0
31,13	0,2	0	0,9	0,2
32	0,4	0,2	0,7	0,6
32,53	0	0,2	0,9	0
33,03	0,4	0	1,6	0

Samples	*Baumanipollis variaperturatus*	*Gothanipollis* sp.	*Canthium*-type	Rhamnaceae	Thymelaceae
1,61	0	0	0	0	0
12,49	0	0	0	0	0
12,99	0	0	0	0	0
13,81	0	0	0	0	0
14,63	0	0	0	0	0
15,13	0,2	0	0	0	0
16,45	0	0	0	0	0
17,28	0,1	0	0,1	0	0
17,32	0	0	0,1	0	0
17,4	0,1	0	0,5	0	0
17,44	0	0	0,3	0	0
17,48	0	0	0,1	0	0
17,53	0	0	0,1	0	0
17,57	0	0	0,1	0	0
17,62	0	0	0,4	0	0
17,7	0	0	0	0	0

Samples	*Baumanipollis variaperturatus*	*Gothanipollis* sp.	*Canthium*-type	Rhamnaceae	Thymelaceae
17,8	0	0	0	0	0
17,86	0	0	0	0	0
17,92	0	0	0,5	0	0
17,97	0	0	0,1	0	0
18,02	0	0	0,7	0	0
18,07	0,2	0	0,4	0	0
18,11	0	0	0	0	0
18,15	0	0	0,3	0	0
18,2	0	0	0,3	0	0
18,28	0	0	0,1	0	0
18,33	0	0	0	0	0
18,38	0	0	0	0	0
18,43	0,1	0	0	0	0
18,48	0	0	0	0	0
18,53	0	0	0	0	0
18,58	0,1	0	0	0	0
18,63	0	0	0	0	0
18,68	0	0	0	0	0
18,7	0	0	0	0	0
18,75	0	0	0,1	0	0
18,8	0,1	0	0	0,1	0
18,88	0	0	0	0	0
18,9	0,1	0	0	0	0
18,96	0	0,1	0,1	0	0
19	0	0	0	0	0
19,06	0,1	0	0	0	0
19,1	0	0,1	0	0	0
19,18	0	0	0	0	0
19,2	0	0	0	0	0
19,25	0	0	0	0	0
19,33	0	0	0	0	0
19,38	0	0	0	0	0
19,43	0	0	0	0	0
19,48	0,1	0	0	0	0
19,52	0	0	0	0	0
19,63	0,2	0	0	0	0
19,7	0,2	0	0	0	0
19,75	0	0	0	0	0
19,8	0	0	0	0	0

Samples	*Baumanipollis variaperturatus*	*Gothanipollis* sp.	*Canthium*-type	Rhamnaceae	Thymelaceae
19,85	0	0	0	0	0
19,93	0	0	0	0	0
19,95	0	0	0	0	0
20	0	0	0	0	0
20,08	0	0	0	0	0
20,33	0	0	0	0	0
25,4	0	0	0	0	0
25,45	0	0	0	0	0
25,48	0	0	0,1	0	0
25,52	0	0	0	0	0
25,55	0	0	0	0	0
25,58	0	0	0	0	0
25,6	0	0	0	0	0
30,92	0	0,1	0,3	0	0
30,97	0	0,1	0,1	0	0
31,01	0	0	0,1	0	0
31,05	0	0	0	0	0
31,09	0	0	0	0	0
31,13	0	0	0	0	0,2
32	0	0	0	0,2	0,2
32,53	0	0	0	0	0
33,03	0	0,5	0	0	0

Samples	*Tricolporopollenites* sp. (Fabaceae)	*Zonocostites ramonae*	Combretaceae	*Diospyros*-type	*Euclea*-type
1,61	0	0	0	0	0
12,49	0	0	0	0	0
12,99	0	0	0	0	0
13,81	0	0	0	0	0
14,63	0	0	0	0	0
15,13	0	0	0	0	0
16,45	0	0	0	0	0
17,28	0	0	0	0	0
17,32	0	0	0	0	0
17,4	0	0	0	0	0
17,44	0	0	0	0	0
17,48	0	0	0	0	0

Samples	*Tricolporopollenites* sp. (Fabaceae)	*Zonocostites ramonae*	Combretaceae	*Diospyros*-type	*Euclea*-type
17,53	0	0	0	0	0
17,57	0	0	0	0	0
17,62	0	0	0,1	0	0
17,7	0	0	0	0	0
17,8	0	0	0	0	0
17,86	0	0	0	0	0
17,92	0	0	0,2	0	0
17,97	0	0	0	0	0
18,02	0	0	0	0	0
18,07	0	0	0	0	0
18,11	0	0	0	0	0
18,15	0	0	0	0	0
18,2	0	0	0	0	0
18,28	0	0	0	0	0
18,33	0	0	0	0	0
18,38	0	0	0	0	0
18,43	0	0	0	0	0
18,48	0	0	0,4	0	0
18,53	0	0	0,1	0	0
18,58	0	0	0	0	0
18,63	0	0	0	0	0
18,68	0	0	0,1	0	0
18,7	0	0	0	0	0
18,75	0	0	0	0	0
18,8	0	0	0,1	0	0
18,88	0	0	0	0	0
18,9	0	0	0	0	0,1
18,96	0	0	0	0	0
19	0	0	0,1	0	0
19,06	0	0	0	0	0
19,1	0	0	0	0	0
19,18	0	0	0	0	0
19,2	0	0	0	0	0
19,25	0	0	0	0	0
19,33	0	0	0	0	0
19,38	0	0	0	0	0
19,43	0	0	0	0	0
19,48	0	0	0	0	0
19,52	0,7	0	0	0	0

Samples	*Tricolporopollenites* sp. (Fabaceae)	*Zonocostites ramonae*	Combretaceae	*Diospyros*-type	*Euclea*-type
19,63	0	0	0	0	0
19,7	1,2	0	0	0	0
19,75	0,1	0	0	0	0
19,8	0	0	0	0	0
19,85	0	0	0	0	0
19,93	0	0,2	0,2	0	0
19,95	0	0	0	0	0
20	0	0	0,2	0	0
20,08	0	0,2	0	0	0
20,33	0	0,2	0	0	0
25,4	0	0	0	0	0
25,45	0	0	0	0	0
25,48	0	0	0	0	0,1
25,52	0	0	0	0	0
25,55	0	0	0	0	0
25,58	0	0	0	0	0
25,6	0	0	0	0	0
30,92	0	0	0,2	0,1	0,4
30,97	0	0,3	0	0	0,1
31,01	0	0	0	0	0,1
31,05	0	0	0	0	0,2
31,09	0	0	0	0	0
31,13	0	0	0,4	0	0,2
32	0	0	0	0	0,4
32,53	0	0,2	0	0	0,6
33,03	0	0	0	0	0,5

Samples	*Margocolporites vanwijhei*	*Spirostachys*-type	*Psilatricolporites operculatus*	*Margocolporites rauvolfii*
1,61	0	0	0	0
12,49	0	0	0	0
12,99	0	0	0	0
13,81	0	0	0	0
14,63	0	0	0	0
15,13	0	0	0	0
16,45	0	0	0	0
17,28	0	0	0	0

Samples	*Margocolporites vanwijhei*	*Spirostachys*-type	*Psilatricolporites operculatus*	*Margocolporites rauvolfii*
17,32	0	0	0	0
17,4	0	0	0	0
17,44	0	0	0	0
17,48	0	0,1	0	0
17,53	0	0	0,1	0
17,57	0	0	0	0
17,62	0	0	0	0
17,7	0	0	0	0
17,8	0	0	0	0
17,86	0	0	0	0
17,92	0	0	0	0
17,97	0	0	0	0
18,02	0	0,1	0	0
18,07	0	0	0	0
18,11	0	0	0	0
18,15	0	0	0	0
18,2	0	0,3	0,6	0
18,28	0	0	0	0
18,33	0	0	0	0
18,38	0	0,1	0	0
18,43	0	0	0	0,1
18,48	0	0	0	0
18,53	0	0	0	0
18,58	0	0	0	0
18,63	0	0	0	0
18,68	0	0	0	0
18,7	0	0,3	0	0
18,75	0	0,2	0	0
18,8	0	0,3	0,1	0
18,88	0	0,2	0	0
18,9	0	0	0	0
18,96	0	0,2	0	0
19	0	0	0	0
19,06	0	0	0	0
19,1	0	0	0	0
19,18	0	0	0,1	0
19,2	0	0	0	0
19,25	0	0	0	0
19,33	0	0	0	0

Samples	*Margocolporites vanwijhei*	*Spirostachys*-type	*Psilatricolporites operculatus*	*Margocolporites rauvolfii*
19,38	0	0	0	0
19,43	0	0,1	0	0
19,48	0	0	0	0
19,52	0	0	0,2	0
19,63	0	0	0	0
19,7	0	0	0	0
19,75	0	0,2	0	0
19,8	0	0	0	0
19,85	0	0,4	0	0
19,93	0	0,2	0,2	0
19,95	0	0,4	0	0
20	0	0	0	0
20,08	0	0	0	0
20,33	0	0,2	0	0
25,4	0	0	0	0
25,45	0	0	0	0
25,48	0	0	0	0
25,52	0	0	0	0
25,55	0	0	0	0
25,58	0	0	0	0
25,6	0	0	0	0
30,92	0	0,6	0	0
30,97	0,2	0,3	0,1	0
31,01	0	0,1	0	0
31,05	0,2	0,2	0	0
31,09	0	0,6	0	0
31,13	0,2	0	0,2	0
32	0	0	0	0
32,53	0	0,4	0	0
33,03	0	0,3	0	0

Samples	*Peregrinnipollis nigericus*	*Proteacidites* sp. A	*Proteacidites* sp. B	*Propylipollis meyeri*	*Rhoipites arnotienis*
1,61	0	0	0	0	0
12,49	0	0	0	0	0
12,99	0	0	0	0	0
13,81	0	0	0	0	0

Samples	*Peregrinnipollis nigericus*	*Proteacidites* sp. A	*Proteacidites* sp. B	*Propylipollis meyeri*	*Rhoipites arnotienis*
14,63	0	0	0	0	0
15,13	0	0	0	0	0,1
16,45	0	0	0	0	0
17,28	0	0	0	0,6	0,3
17,32	0	0	0	0,2	0,1
17,4	0	0	0,2	0,4	0,2
17,44	0	0	0	0	0,6
17,48	0,2	0,1	0,1	0,2	0,4
17,53	0	0,5	0	0,3	1,2
17,57	0	0	0,2	0,1	0,5
17,62	0	0	0	0,1	0,7
17,7	0	0	0	0,3	0,3
17,8	0	0	0	0,3	0,6
17,86	0	0	0,3	0,3	0,6
17,92	0	0	0	0,5	1,6
17,97	0	0	0,2	0,2	0,4
18,02	0	0	0	0,3	1,3
18,07	0	0	0,3	0,4	0,5
18,11	0	0	0,4	0,4	1,5
18,15	0	0	0,3	0,2	0,6
18,2	0	0	0,3	0,8	1,4
18,28	0	0	0,1	0,3	0,2
18,33	0	0	0,1	0,2	0,3
18,38	0	0	0,4	0,1	0,6
18,43	0	0	0,8	0,5	0,7
18,48	0	0	0,5	0,7	0,1
18,53	0	0	0,4	0,2	0,7
18,58	0	0	0	0	0,3
18,63	0	0	0	0	0,1
18,68	0	0	0,1	0,1	0,1
18,7	0	0	0,5	0,6	1
18,75	0	0,1	0	1	0,4
18,8	0	0,1	0	1,1	0,8
18,88	0	0,4	0,1	0,6	0
18,9	0	0	0	0,5	1,3
18,96	0	0	0	0,8	0,8
19	0	0	0	0	0,3
19,06	0	0	0	0	0
19,1	0	0,1	0	0	0,1

Samples	*Peregrinnipollis nigericus*	*Proteacidites* sp. A	*Proteacidites* sp. B	*Propylipollis meyeri*	*Rhoipites arnotienis*
19,18	0	0	0	0	0,1
19,2	0	0	0	0	0
19,25	0	0	0	0	0,1
19,33	0	0	0	0	0,1
19,38	0	0	0	0	0,3
19,43	0	0,2	0	0	0
19,48	0	0,2	0	0	0
19,52	0	0	0	0	0,3
19,63	0	0	0	0,3	0,5
19,7	0	0	0	0,1	0,1
19,75	0	0	0	0	0,4
19,8	0	0	0	0,3	0,5
19,85	0	0,4	0	0,2	4,7
19,93	0	1,3	0	0,3	3,2
19,95	0	0	0	0	0,7
20	0	0	0	0,2	2,1
20,08	0	0	0	1,2	0,7
20,33	0	0	0	0,6	0,8
25,4	0	0	0	0	0,5
25,45	0	0	0	0,1	0,1
25,48	0	0	0	0	0,4
25,52	0	0	0	0	0,9
25,55	0	0	0	0	0,4
25,58	0	0	0	0	0
25,6	0	0	0	0	0
30,92	0	0,1	0	0,1	0
30,97	0	0,5	0	0	0,2
31,01	0	0,3	0	0,3	0,1
31,05	0	0	0	0,2	0,2
31,09	0	0,4	0	0,2	0,2
31,13	0	0,4	0,2	0,2	0,5
32	0	0,7	0	0,2	0,2
32,53	0	0,9	0,2	1,5	0
33,03	0	3,6	0	0,8	0

Samples	*Psilatricolporites quenua*	*Ericipites callidus*	*Perfortricolpites digitatus*	Picrodendraceae

Samples	*Psilatricolporites quenua*	*Ericipites callidus*	*Perfortricolpites digitatus*	Picrodendraceae
1,61	8,7	0	0	0
12,49	0	0	0	0
12,99	0	0	0	0
13,81	0	0	0	0
14,63	1	0	0	0
15,13	0	0	0	0
16,45	0	0	0	0
17,28	2,2	0	0	0
17,32	2,9	0	0	0
17,4	2,2	0	0	0
17,44	2,3	0	0	0
17,48	2,1	0	0	0
17,53	0,9	0	0	0
17,57	1,4	0	0	0
17,62	2,5	0	0	0
17,7	1,8	0	0	0
17,8	1,4	0	0	0
17,86	2	0	0	0
17,92	2,9	0	0	0
17,97	4	0	0	0
18,02	3,1	0	0	0
18,07	2,8	0	0	0,1
18,11	1,8	0	0	0
18,15	4,4	0	0	0
18,2	3,4	0	0	0
18,28	0,4	0	0	0
18,33	0,7	0	0	0
18,38	0,7	0	0	0
18,43	0,5	0	0	0
18,48	2,1	0,2	0	0
18,53	0,7	0	0	0
18,58	0,9	0	0	0
18,63	0,1	0	0	0
18,68	0,3	0	0	0
18,7	1,4	0	0	0
18,75	3,2	0	0	0
18,8	3	0	0	0
18,88	0,2	0	0	0
18,9	1,3	0	0	0
18,96	1,3	0	0	0

Samples	*Psilatricolporites quenua*	*Ericipites callidus*	*Perfortricolpites digitatus*	Picrodendraceae
19	1	0	0	0
19,06	0,3	0	0	0
19,1	0,3	0	0	0
19,18	0,8	0	0	0
19,2	0,5	0	0	0
19,25	0,4	0	0	0
19,33	0,9	0	0	0
19,38	0,7	0	0	0
19,43	0,1	0	0	0
19,48	0,6	0	0	0
19,52	1,3	0	0	0
19,63	3,5	0	0	0
19,7	2,3	0	0	0
19,75	1,2	0	0	0
19,8	8,5	0	0	0
19,85	3,8	0	0	0
19,93	2	0	0	0
19,95	0	0	0	0
20	4,1	0	0	0
20,08	4,4	0	0	0
20,33	6,6	0,4	0	0
25,4	0,7	0	0	0
25,45	1	0	0	0
25,48	2,6	0	0	0
25,52	1,4	0	0	0
25,55	1,3	0	0	0
25,58	0,4	0	0	0
25,6	0,2	0	0	0
30,92	1,7	0	0	0,2
30,97	1	0	0	0
31,01	0,6	0	0	0
31,05	1,2	0,4	0	0
31,09	2	0	0	0
31,13	1,2	0	0	0
32	3,1	0	0,2	0
32,53	5,8	0,4	0	0,6
33,03	3,2	0	0	0,4

Samples	*Tubulifloridites antipodica*	*Tubulifloridites* sp.	*Mutisiapollis viteauensis*	*Artemisiaepollenites* sp.
1,61	4,3	0	0	0
12,49	0	0	0	0
12,99	0	0	0	0
13,81	3,4	0	0	0
14,63	0	0	0	0
15,13	0	0	0	0
16,45	0	0	0	0
17,28	0	0	0,3	0
17,32	0,2	0	0	0
17,4	0	0	0	0
17,44	0,4	0,1	0	0
17,48	0,1	0	0	0
17,53	0,4	0	0,1	0
17,57	0,1	0	0	0
17,62	0	0	0	0
17,7	0	0	0,3	0
17,8	0	0	0	0
17,86	0,3	0,1	0	0
17,92	0,3	0	0,2	0
17,97	0,1	0,2	0	0
18,02	0	0	0	0
18,07	0,2	0	0	0
18,11	0,7	0	0	0
18,15	0,4	0	0	0
18,2	0,3	0	0	0
18,28	0	0	0,1	0
18,33	0	0	0	0
18,38	0,1	0,1	0,1	0,1
18,43	0,3	0	0	0
18,48	0,8	0	0	0
18,53	0,4	0	0	0,1
18,58	0	0	0	0
18,63	0	0	0	0
18,68	0,1	0	0	0
18,7	0,3	0	0,1	0
18,75	0,5	0	0	0
18,8	0,5	0	0,1	0,1

Samples	*Tubulifloridites antipodica*	*Tubulifloridites* sp.	*Mutisiapollis viteauensis*	*Artemisiaepollenites* sp.
18,88	0,2	0	0,1	0
18,9	0	0	0,2	0
18,96	0,2	0	0,3	0
19	0	0	0,1	0
19,06	0	0	0	0
19,1	0	0	0	0
19,18	0	0	0,2	0
19,2	0	0	0,1	0
19,25	0	0	0	0
19,33	0	0	0	0
19,38	0	0	0	0
19,43	0	0	0	0
19,48	0,1	0	0	0
19,52	0	0	0	0
19,63	0	0	0,2	0
19,7	0,2	0	0	0
19,75	0,2	0	0	0
19,8	0	0	0	0
19,85	0	0	4,6	0
19,93	0	0	0,2	0
19,95	0,2	0	0,2	0
20	0	0	0,4	0
20,08	0,7	0	0,9	0
20,33	0,4	0	1	0
25,4	0,1	0	0	0
25,45	0	0	0	0
25,48	0	0	0	0
25,52	0	0	0	0
25,55	0	0	0,4	0
25,58	0	0	0,1	0
25,6	0	0	0	0
30,92	0,2	0,1	2,9	0,2
30,97	0,2	0	1,4	0,1
31,01	0	0	1,4	0,1
31,05	0,2	0	1,2	0,6
31,09	0,2	0	0,4	0,2
31,13	0,2	0	2,1	0,5
32	0,6	0	3,5	0
32,53	0,4	0	1,9	0

Samples	*Tubulifloridites antipodica*	*Tubulifloridites* sp.	*Mutisiapollis viteauensis*	*Artemisiaepollenites* sp.
33,03	0,1	0	1	0,1

Samples	*Polygala japonica*-type	Scrophulariaceae	*Graminidites* cf. *crassiglobosus*	*Graminidites* cf. *neogenicus*
1,61	0	0	4,3	0
12,49	0	0	0	0
12,99	0	0	0	0
13,81	0	0	0	0
14,63	0	0	0	0
15,13	0	0	0	0
16,45	0	0	0	0
17,28	0	0	0,6	0,6
17,32	0	0	0,9	0,2
17,4	0	0	0,8	0,4
17,44	0	0	0,4	0,1
17,48	0	0	0,3	0,1
17,53	0	0	0,2	0,5
17,57	0	0	0,2	0
17,62	0	0	0,4	0,3
17,7	0	0	0	0
17,8	0	0	0	0
17,86	0	0	0,3	0
17,92	0	0	0	0,7
17,97	0	0	1,5	0,6
18,02	0	0	0,1	0,1
18,07	0	0	0,2	0,9
18,11	0	0	1,1	0
18,15	0	0	1,2	0,3
18,2	0	0	0,6	0
18,28	0	0	0	0
18,33	0	0	0,2	0,3
18,38	0	0	0,1	0
18,43	0	0	0,3	0,1
18,48	0	0	0,2	0,5
18,53	0	0	0,1	0,2
18,58	0	0	0,2	0,2
18,63	0	0	0	0

Samples	*Polygala japonica*-type	Scrophulariaceae	*Graminidites* cf. *crassiglobosus*	*Graminidites* cf. *neogenicus*
18,68	0	0	0	0
18,7	0	0	0,3	3,3
18,75	0	0	0,7	0,6
18,8	0	0	0,3	1,7
18,88	0	0	0,3	0,3
18,9	0	0	0,8	2,3
18,96	0	0	0,5	1,8
19	0	0	1,2	7,5
19,06	0	0	0,1	6,4
19,1	0	0	0	8,1
19,18	0	0	0,7	6,5
19,2	0	0	0	9,8
19,25	0	0	0	13
19,33	0	0	0	14,7
19,38	0	0	0,1	12,2
19,43	0	0	0,1	10,9
19,48	0	0	0,9	8,8
19,52	0	0	0	16,2
19,63	0	0	0	2,5
19,7	0	0	0,6	3,9
19,75	0	0	0	3,2
19,8	0	0	0,3	4,4
19,85	0	0	1,6	3,3
19,93	0	0	0,8	2,7
19,95	0	0	0,7	2
20	0	0	1,7	0
20,08	0	0	2,5	0
20,33	0	0	1,7	13,9
25,4	0	0	1,4	0,1
25,45	0	0	1,4	0
25,48	0	0	1,3	0
25,52	0	0	0,7	0
25,55	0	0	0	0
25,58	0	0	0,2	0
25,6	0	0	0,4	0
30,92	0	0,2	1,7	1,5
30,97	0	0	0,1	2,3
31,01	0	0	0,2	0,8
31,05	0	0	0,4	2,1

Samples	*Polygala japonica*-type	Scrophulariaceae	*Graminidites* cf. *crassiglobosus*	*Graminidites* cf. *neogenicus*
31,09	0,2	0	0,4	1,7
31,13	0	0	2,5	1,8
32	0	0	0,7	1,3
32,53	0	0	0,9	2,5
33,03	0	0	0,1	1,4

Samples	*Polycolporopollenites* sp.	*Pentzia*-type	*Umbelliferoipollenites* sp.	Caryophyllaceae
1,61	0	0	0	0
12,49	0	0	0	0
12,99	0	0	0	0
13,81	0	0	0	0
14,63	0	0	0	0
15,13	0	0	0	0
16,45	0	0	0	0
17,28	0	0,1	0	0
17,32	0	0,2	0	0
17,4	0	0	0	0
17,44	0	0,3	0	0
17,48	0	0,1	0	0
17,53	0	0,1	0	0,1
17,57	0	0,3	0	0
17,62	0	0,1	0	0
17,7	0	0	0	0
17,8	0	0	0	0
17,86	0	0	0	0
17,92	0	0,2	0	0
17,97	0	0,2	0	0
18,02	0	0	0	0
18,07	0	0	0	0
18,11	0	0	0	0
18,15	0	0,1	0	0
18,2	0	0	0	0
18,28	0	0	0	0
18,33	0	0,1	0	0
18,38	0	0,1	0	0
18,43	0	0,1	0	0

Samples	*Polycolporopollenites* sp.	*Pentzia*-type	*Umbelliferoipollenites* sp.	Caryophyllaceae
18,48	0	0	0	0
18,53	0	0	0	0,2
18,58	0	0	0	0,1
18,63	0	0	0	0
18,68	0	0	0	0
18,7	0	0,5	0	0
18,75	0	0,1	0	0
18,8	0	0	0	0
18,88	0	0	0	0
18,9	0	0,6	0,2	0,1
18,96	0	0,3	0	0,1
19	0	0	0	0
19,06	0	0	0	0
19,1	0	0	0	0
19,18	0	0,1	0	0
19,2	0	0	0	0
19,25	0	0	0	0
19,33	0	0,1	0	0
19,38	0	0,1	0	0
19,43	0	0,1	0	0
19,48	0	0	0	0
19,52	0	0	0	0
19,63	0	0	0	0
19,7	0	0	0	0
19,75	0	0	0	0
19,8	0	0,3	0	0
19,85	0	0,4	0	0
19,93	0	0,2	0	0
19,95	0	0	0	0
20	0	7,3	0	0
20,08	0,2	5,8	0	0
20,33	0	0,8	0	0
25,4	0	0	0	0
25,45	0	0	0	0
25,48	0	0	0	0
25,52	0	0	0	0
25,55	0	0	0	0
25,58	0	0	0	0
25,6	0	0	0	0
30,92	0	0,1	0	0

Samples	*Polycolporopollenites* sp.	*Pentzia*-type	*Umbelliferoipollenites* sp.	Caryophyllaceae
30,97	0	0	0	0
31,01	0	0	0	0
31,05	0	0	0	0
31,09	0	0	0	0
31,13	0	0	0	0
32	0	0	0	0
32,53	0	0	0	0
33,03	0	0	0	0

Samples	*Persicaria*-type	Onagraceae	*Selago*-type	Gentianaceae	*Sparganiaceaepollenites barungensis*
1,61	0	0	0	0	0
12,49	0	0	0	0	0
12,99	0	0	0	0	0
13,81	0	0	0	0	0
14,63	0	0	0	0	0
15,13	0	0	0	0	0,1
16,45	0	0	0	0	0
17,28	0	0,1	0	0	6,2
17,32	0	0	0	0,1	6,2
17,4	0	0,1	0	0	2
17,44	0	0,1	0	0,1	3,8
17,48	0	0	0	0,1	3,9
17,53	0	0,1	0	0,5	23
17,57	0,1	0	0	0,1	3,5
17,62	0	0	0	0	8,5
17,7	0	0	0	0	3,1
17,8	0	0	0	0,3	3,3
17,86	0	0	0	0,3	4,3
17,92	0	0	0	0,3	24
17,97	0	0	0	0,2	3,2
18,02	0	0	0	0,1	3,2
18,07	0,2	0	0	0,1	1,3
18,11	0	0	0	0,7	0,7
18,15	0	0	0	0	1,8
18,2	0	0	0	0,6	4,2

Samples	*Persicaria*-type	Onagraceae	*Selago*-type	Gentianaceae	*Sparganiaceaepollenites barungensis*
18,28	0	0	0	0	1,4
18,33	0	0	0	0	1,7
18,38	0	0	0	0,1	1,6
18,43	0,2	0	0	0,2	1,4
18,48	0	0	0	0	3
18,53	0	0	0	0	2,5
18,58	0	0	0	0	1,3
18,63	0	0	0	0	0,2
18,68	0	0	0	0	0,5
18,7	0	0	0	0,5	22,1
18,75	0	0	0	0,8	17,5
18,8	0	0	0	1,7	18
18,88	0	0	0	0,2	2,4
18,9	0	0	0	1,6	12,8
18,96	0	0	0	1,4	6,8
19	0	0	0	0,2	23,9
19,06	0	0	0	0	22,2
19,1	0	0	0	0,1	20,1
19,18	0	0	0	0,1	40,3
19,2	0	0	0	0	35,2
19,25	0	0	0	0	42,5
19,33	0	0	0	0,1	36,9
19,38	0	0	0	0,1	45,1
19,43	0	0	0	0,2	25,3
19,48	0	0	0	0,5	37
19,52	0,3	0	0	0,5	1
19,63	0	0,3	0	0,2	18,8
19,7	0	0	0	0,2	17,6
19,75	0	0	0	0,1	28,6
19,8	0	0,3	0	0,3	9,7
19,85	0	0	0	0	6,7
19,93	0,2	0	0	0	4
19,95	1,1	0	0	1,8	0,7
20	0	0	0	3,9	4,1
20,08	0	0	0	0,4	2,8
20,33	0	0	0	0	2,5
25,4	0	0	0	0,3	6,5
25,45	0	0	0	0,3	5,6
25,48	0	0	0	0,9	0,5

Samples	*Persicaria*-type	Onagraceae	*Selago*-type	Gentianaceae	*Sparganiaceaepollenites barungensis*
25,52	0	0	0	1,2	0,1
25,55	0	0	0	14	0
25,58	0	0	0	1,6	0
25,6	0	0	0	1,3	0
30,92	0	0	0	0,7	1,1
30,97	0	0	0,1	0,3	0,5
31,01	0	0	0	0,4	0,8
31,05	0	0	0	0	0,2
31,09	0	0	0	0	2,2
31,13	0	0	0,2	0,4	0,4
32	0	0,2	0	0,2	4,1
32,53	0	0	0	0,8	1,3
33,03	0	0	0	0,6	0,1

Samples	*Milfordia homeopunctatus*	*Milfordia hypolaenoides*	*Cyperaceaepollenites* sp.	*Cyperaceapollis piriformis*
1,61	0	34,8	0	0
12,49	0	0	0	0
12,99	0	8,6	0	0
13,81	0	0	3,4	0
14,63	0	0	0	0
15,13	0,1	0	0	0
16,45	0,4	0	0	0
17,28	7,8	3,3	0,3	0
17,32	18,1	10	1,8	0
17,4	27,7	1,2	3,3	0
17,44	17,2	13,1	0	0
17,48	19,6	1,7	1,4	0
17,53	5,9	1,5	0	0
17,57	9	2,1	0,4	0
17,62	10,1	11,6	0,8	0
17,7	11,6	0	0	0
17,8	1,1	19,9	2,2	0
17,86	16,1	1,8	0,3	0
17,92	7,2	6,9	0	0
17,97	22,3	2,1	0,9	0
18,02	16,4	14	0,8	0

Samples	*Milfordia homeopunctatus*	*Milfordia hypolaenoides*	*Cyperaceaepollenites* sp.	*Cyperaceapollis piriformis*
18,07	16,7	1,4	0,3	0
18,11	4,4	28,9	0	0
18,15	21,5	2,5	1,1	0
18,2	5,3	19	1,1	0
18,28	7,3	2,9	1	0
18,33	7,5	5,2	1,7	0
18,38	8,7	4,1	1	0
18,43	9,8	10,4	2,9	0
18,48	13,8	12,3	4	0
18,53	11,4	12,9	0,2	0
18,58	1,2	8,6	0,9	0
18,63	0,1	1,8	0,3	0,1
18,68	0,2	3,5	0,4	0
18,7	18,3	0,4	0	0
18,75	15,9	1,3	0,5	0
18,8	14,6	0,7	0	0
18,88	5,9	1,4	0	0
18,9	13	0,2	0,2	0
18,96	10,5	0,4	0	0
19	9,7	0,4	0	0
19,06	7,5	0,1	0	0
19,1	6,4	0,3	0	0
19,18	16,4	1,7	0	0
19,2	27,8	0,1	0	0
19,25	6	0	0	0
19,33	2,2	0,1	0	0
19,38	3	0,1	0,1	0
19,43	0,6	0,2	0	0
19,48	1,9	0,6	0	0
19,52	12,5	1,5	0	0
19,63	16,1	2,5	0	0
19,7	8,4	1	0	0
19,75	16,9	0	0	0
19,8	6,4	1,5	0	0
19,85	0	1,5	0	0
19,93	0,2	2,8	0,2	0
19,95	0,2	4,9	0,4	0
20	0,4	2,5	0	0
20,08	4,7	0	0,2	0

Samples	*Milfordia homeopunctatus*	*Milfordia hypolaenoides*	*Cyperaceaepollenites* sp.	*Cyperaceapollis piriformis*
20,33	7,3	0	0,4	0
25,4	1,3	0,6	0	0
25,45	1,3	0	0,1	0
25,48	2,3	0	0	0
25,52	13,7	0	0,2	0
25,55	15,9	0,7	0,2	0
25,58	1,4	0	0	0
25,6	0,4	0	0	0
30,92	3,5	0,2	0	0
30,97	3,3	0,1	0	0
31,01	1	0	0	0
31,05	5,8	0	0,6	0
31,09	6,7	0	0	0
31,13	2,5	0	0	0
32	8,9	0,9	0,4	0
32,53	5,5	0,4	0	0
33,03	2,5	0	0	0

Samples	*Baculatisporites* sp.	*Camarozonosporites heskemensis*	*Laevigatosporites haardti*	*Cyathidites australis*
1,61	0	0	0	0
12,49	0	0	0	0
12,99	0	0	0	0
13,81	0	0	0	0
14,63	0	0	0	0
15,13	0	0	0	0
16,45	0	0	0	0
17,28	0,6	0	4,1	0
17,32	0,9	0	1,6	0
17,4	1,1	0	3,2	0
17,44	2,9	0	1,5	0
17,48	1	0	0,9	0
17,53	0,1	0	1,3	0
17,57	0,2	0	1,7	0
17,62	0,1	0	0,8	0
17,7	0,3	0	1,5	1,2
17,8	0	0	1,1	0

Samples	*Baculatisporites* sp.	*Camarozonosporites heskemensis*	*Laevigatosporites haardti*	*Cyathidites australis*
17,86	0,1	0	0,6	0,1
17,92	0	0	1,1	0
17,97	0,1	0	1,9	0
18,02	0,4	0	1,1	0
18,07	0,1	0	1	0,1
18,11	0,4	0	0,4	0,4
18,15	0,2	0	1,1	0
18,2	0,8	0	0	0
18,28	0,7	0	0,2	0,3
18,33	0,2	0	0	0,2
18,38	1,1	0	0,3	0
18,43	0,7	0	0,3	0
18,48	0,4	0	0,5	0,1
18,53	0	0	1	0
18,58	0	0	0,2	0
18,63	0,1	0	0	0
18,68	0,2	0	0	0
18,7	0	0	4,2	0
18,75	0	0	1,4	0
18,8	0,1	0	1,2	0
18,88	0,1	0	0,8	0
18,9	0	0	1,3	0
18,96	0	0	0,6	0
19	0	0	1,2	0
19,06	0	0	0,6	0
19,1	0	0	0,3	0
19,18	0	0	0,4	0
19,2	0	0	0,9	0
19,25	0	0	2,4	0
19,33	0	0	18,7	0
19,38	0	0	13,9	0
19,43	0	0	13	0
19,48	0	0	12,4	0,3
19,52	0	0	6,7	0
19,63	0,3	0,2	1,6	0
19,7	0	0	3,4	0
19,75	0,2	0	2	0,6
19,8	0	0	1,5	0,8
19,85	0	0	0,5	3,3

Samples	*Baculatisporites* sp.	*Camarozonosporites heskemensis*	*Laevigatosporites haardti*	*Cyathidites australis*
19,93	0	0	4,3	1,2
19,95	0	0	7,9	4,9
20	0,2	0	1	1,7
20,08	0,4	0	0,2	0
20,33	0,6	0	0	0,2
25,4	0,1	0	0,2	5,3
25,45	0	0	0	4,2
25,48	0	0	0	10,1
25,52	0	0	0	10,4
25,55	0	0	0	16,6
25,58	0	0	0,7	4,3
25,6	0	0	0	0,2
30,92	0,1	0	0,3	0
30,97	0,4	0	0	0
31,01	0	0	0	0
31,05	0	0	0,2	0
31,09	0	0	0	0
31,13	0,2	0	0,5	0
32	0,2	0,6	0,7	0
32,53	0,2	0	0	0
33,03	0	0	0,1	0

Samples	*Leotriletes wolffii*	*Leiotriletes maxoides*	*Leiotriletes maximus*	*Cryptogrammasporis* sp.	*Verrucatosporites* sp.
1,61	0	0	0	0	0
12,49	0	0	0	0	0
12,99	0	0	0	0	0
13,81	0	0	0	0	0
14,63	0	0	0	0	0
15,13	0,5	0	0	0	0
16,45	0	0	0	0	0
17,28	0,2	0	7,6	0	0,9
17,32	0	0	1,9	0	0,1
17,4	0	0	2,5	0	0,4
17,44	0,6	0,3	3,3	0	0,3
17,48	0,3	0	2	0	0
17,53	0	0	0,2	0	0

Samples	*Leotriletes wolffii*	*Leiotriletes maxoides*	*Leiotriletes maximus*	*Cryptogrammasporis* sp.	*Verrucatosporites* sp.
17,57	0	0	2,1	0	0,2
17,62	0,2	0	0,2	0	0,1
17,7	0	0	1,2	0	0,3
17,8	0	0	0,6	0	0
17,86	0,6	0	0,9	0	0,3
17,92	0,2	0	0	0	0,2
17,97	0,2	0	2,7	0	0,2
18,02	0,3	0	2,2	0	0,7
18,07	0,2	0	1,7	0	0,1
18,11	0	0	1,1	0	0
18,15	0	0	1,7	0	0,6
18,2	0	0	0	0	0,6
18,28	0,4	0,2	4,1	0	0,1
18,33	0,2	0,4	0,1	0	0,1
18,38	0,5	0,4	1,5	0	0,4
18,43	0,7	0,4	1,4	0	0,3
18,48	0,5	0,2	0,7	0	0,2
18,53	1,2	0,6	1,6	0	0,1
18,58	0,2	0,7	0,2	0	0,1
18,63	0,1	0	0,7	0	0
18,68	0,2	0,9	0,2	0	0
18,7	0	0	0	0	0,1
18,75	0,5	0,2	0	0	0
18,8	0	0	0	0,1	0,1
18,88	0,3	8,1	0,3	0	0,5
18,9	0	0	0,2	0	0,1
18,96	0,1	0	0	0,1	0,1
19	0	0	0	0	0
19,06	0	0	0	0	0
19,1	0	0	0	0	0
19,18	0	0	0,1	0	0
19,2	0	0	0	0	0
19,25	0	0	0,1	0	0
19,33	0	0,3	0,1	0	0,4
19,38	0	0	0,3	0	0,1
19,43	0	0	0,2	0	0,1
19,48	0	0,3	0,5	0	0
19,52	0	1,3	5	0	0
19,63	0	0	0,3	0	0

Samples	*Leotriletes wolffii*	*Leiotriletes maxoides*	*Leiotriletes maximus*	*Cryptogrammasporis* sp.	*Verrucatosporites* sp.
19,7	0,2	0,5	0,2	0	0
19,75	0	0,3	0	0	0,1
19,8	0	3,1	0	0	0
19,85	0,2	2,6	0	0	0,2
19,93	0	1	0	0	0
19,95	0	4,6	0	0	0
20	0	1	0	0	0,2
20,08	0,2	0,2	0,9	0	0,7
20,33	0,2	0,6	0	0	0,2
25,4	0,1	12,1	0	0	0,1
25,45	1,3	3,5	0,1	0	0
25,48	1,3	6,8	0,1	0	0
25,52	1,8	9,8	0,8	0	0
25,55	0,2	6,7	0,6	0	0
25,58	0	1,5	0,7	0	0
25,6	0,8	2,9	1,7	0	0
30,92	0,3	0	0	0	0,1
30,97	0,5	0	0,3	0	0,2
31,01	0,1	0	0	0	0
31,05	1,2	0	0	0	0,2
31,09	0,6	0	0	0	0
31,13	0,5	0	0	0	0
32	0,6	0,9	0	0	0,4
32,53	3	0,2	0,4	0	0
33,03	2,2	0	0	0,1	0,1

Samples	*Microfoveolatosporis neogranuloides*	*Gleicheniidites* spp.	*Cicatricosisporites chattensis*	*Polypodiaceoisporites* sp.	*Debarya*
1,61	0	4,3	0	0	0
12,49	0	0	0	0	0
12,99	0	0	0	0	0
13,81	0	0	0	0	0
14,63	0	1	0	0	0
15,13	0	0,1	0	0,2	0,1
16,45	0	0,7	0	0	0
17,28	0,2	17,6	0,1	0,5	0,4
17,32	0,1	5,2	0	0	0,1

Samples	*Microfoveolatosporis neogranuloides*	*Gleicheniidites* spp.	*Cicatricosisporites chattensis*	*Polypodiaceoisporites* sp.	*Debarya*
17,4	0	7,9	0,1	0	0,1
17,44	0	9,6	0	0	0,5
17,48	0	14	0	0	0,3
17,53	0	5,5	0	0	0,1
17,57	0	8,1	0	0	0,1
17,62	0	1,7	0	0	0
17,7	0	14,1	0	0	0,3
17,8	0	13	0	0	0
17,86	0	4,8	0	0	0,4
17,92	0	3,1	0	0	0,2
17,97	0	4,3	0	0	0,4
18,02	0	4,2	0,1	0	0,1
18,07	0	1,6	0	0	0
18,11	0	8,1	0	0	0
18,15	0	2,1	0	0	0,3
18,2	0	4,5	0	0	0,6
18,28	0	5,7	0	0,1	0,2
18,33	0	2,9	0	0,1	0,3
18,38	0,1	8,5	0,1	0	0,2
18,43	0,2	6,7	0	0,2	0,5
18,48	0	3,4	0	0	0,5
18,53	0	3,8	0	0	0,5
18,58	0,1	0,8	0	0	0,3
18,63	0	0,3	0	0	0
18,68	0	1,3	0	0	0,1
18,7	0	0,9	0	0	0,4
18,75	0	1,7	0	0	0,4
18,8	0	2,1	0,1	0	0,3
18,88	0,1	7,7	0,1	0,2	0,1
18,9	0	0,9	0	0	0,1
18,96	0	1,4	0	0	0
19	0	0	0	0	0
19,06	0	0	0	0	0
19,1	0	0,1	0	0	0
19,18	0	0	0	0	0
19,2	0	0	0	0	0
19,25	0	0	0	0	0
19,33	0	0	0	0	0
19,38	0	0	0	0	0

Samples	*Microfoveolatosporis neogranuloides*	*Gleicheniidites* spp.	*Cicatricosisporites chattensis*	*Polypodiaceoisporites* sp.	*Debarya*
19,43	0	0	0	0	0
19,48	0	0	0	0	0
19,52	0	0	0	0	0
19,63	0	3,7	0	0	0,2
19,7	0	0	0	0	0
19,75	0	0	0	0	0
19,8	0	0	0	0	0
19,85	0	0	0	0	0
19,93	0	0	0	0	0
19,95	0	0	0	0	0
20	0	0	0	0	0
20,08	0	0,7	0	0	0
20,33	0	0	0	0	0
25,4	0	0	0	0	0
25,45	0	0	0	0	0
25,48	0	0	0	0	0
25,52	0	0	0	0	0
25,55	0	0	0	0	0
25,58	0	0	0	0	0
25,6	0	0	0	0	0
30,92	0	0	0,1	0	0
30,97	0	0	0	0	0
31,01	0	0	0	0	0
31,05	0	0	0	0	0
31,09	0	0	0	0	0
31,13	0	0	0	0	0
32	0	0	0	0	0
32,53	0	0	0	0	0
33,03	0	0	0	0	0

Samples	*Botryococcus* sp.	*Ovoidites grandis*	*Ovoidites vangeeli*	*Planctanites stellanus*	*Sigmopollis* sp.	*Stigmozygodites* sp.
1,61	0	4,3	0	0	0	0
12,49	2,3	0	0	0	0	0
12,99	8,6	0	0	0	0	0
13,81	3,4	0	13,8	3,4	0	0
14,63	0	0	0	0	0	0

Samples	*Botryococcus* sp.	*Ovoidites grandis*	*Ovoidites vangeeli*	*Planctanites stellanus*	*Sigmopollis* sp.	*Stigmozygodites* sp.
15,13	5,5	0,5	0,1	0	0	0
16,45	1,5	0,7	0,7	0	0	0
17,28	13,3	0,7	0,1	0,3	0,1	0,6
17,32	4,6	1,9	1,3	0,2	0,3	0,4
17,4	7,2	0,8	1,3	0,1	0	0
17,44	4,5	5,1	2,3	0	0,1	0
17,48	6,5	0,9	1,6	0,1	0	0,4
17,53	6,1	2,3	0,7	0,7	1,5	0
17,57	6,2	0,9	1,1	0,2	0,4	0
17,62	0,7	0,7	0,1	0,4	0	0
17,7	8,6	1,2	0,9	0,3	0	0,6
17,8	4,7	0	0,3	0	0	0,6
17,86	4,9	2,8	0,3	0	0,1	0
17,92	4,6	4,4	0	2,6	0,2	0
17,97	14,7	2,3	0,2	0,4	0	0,7
18,02	2,8	4,2	0,7	0,3	0	0
18,07	1,2	3,1	0,2	0,1	0	0
18,11	2,9	3,7	0	0	0	0
18,15	3,1	2,4	0,2	0,1	0	0,2
18,2	5	1,1	0,3	0,3	0	1,1
18,28	1,9	1,5	0,2	0,1	0,1	0,1
18,33	1	2,4	0,2	0,1	0	0
18,38	1,1	2,4	0,4	0,1	0,2	0
18,43	4,9	3,7	0,2	0,1	0,4	0,5
18,48	5	5,8	0,2	0,4	0,2	0,9
18,53	4,9	8,4	0,5	0,2	0,6	0,1
18,58	2,3	1,2	0	0	0,4	0,2
18,63	0,6	0,3	0,2	0	0,1	0
18,68	0,6	0,5	0,2	0	0,1	0,1
18,7	3,3	4,9	0,1	0	0,6	0
18,75	6,2	2,6	0,2	0,4	0,5	0,7
18,8	4	3,4	0,1	1,1	0,1	0
18,88	2,3	3,1	0	0,2	0,1	0
18,9	1,6	8	0	1,5	0	0,1
18,96	2,9	3,7	0,2	0,7	0,8	0,2
19	3,5	3,3	0,2	0,5	0	0
19,06	0,5	1,9	0	0,1	0	0
19,1	0,7	2,5	0	1	0	0
19,18	1,6	1,6	0	0,4	0	0

Samples	*Botryococcus* sp.	*Ovoidites grandis*	*Ovoidites vangeeli*	*Planctanites stellanus*	*Sigmopollis* sp.	*Stigmozygodites* sp.
19,2	0,8	0,9	0	0,1	0	0
19,25	0,1	1,4	0	1	0	0
19,33	0,4	2,1	0	1,2	0	0
19,38	0,2	0,1	0	0,3	0	0
19,43	1,5	0,1	0	0	0	0
19,48	0,9	0,8	0	0,2	0	0
19,52	8,7	0,3	0	0,7	0,2	0
19,63	4,8	1,6	1	0,3	0,2	0
19,7	1,2	0	0	0	0	0
19,75	1,3	0	0	0,2	0	0
19,8	1,5	0,8	0	0,3	0,3	0
19,85	0	0	0	0	0	0
19,93	0,7	0	0	0,2	0	0
19,95	0,2	0	0	0	0	0
20	0	0	0	0	0	0
20,08	0,5	0,7	0	0	0	0
20,33	0	0,2	0	0	0	0
25,4	0	0	0	0	0	0
25,45	0	2,3	0	0	0	0
25,48	0	3,5	0	0	0	0
25,52	0	0	0	0	0	0
25,55	0	0	0	0	0	0
25,58	0	0	0	0	0	0
25,6	0	0	0	0	0	0
30,92	0,2	0,2	0	0	0	0
30,97	0	0,2	0	0	0	0
31,01	0,1	0,4	0	0	0	0
31,05	0,4	1,2	0	0	0	0
31,09	0,7	0,9	0	0	0	0
31,13	0,7	0,2	0	0	0	0
32	0,6	1,5	0	0	0	0
32,53	0	1,1	0	0	0	0
33,03	0,3	0	0	0	0	0

Samples	*Pediastrum*-type	*Pterospermella* sp.	*Zygnema* sp. A	*Zygnema* sp. B	*Apteodinium spiridoides*	*Chiropteridium lobospinosum*
1,61	0	0	0	0	0	0

Samples	*Pediastrum*-type	*Pterospermella* sp.	*Zygnema* sp. A	*Zygnema* sp. B	*Apteodinium spiridoides*	*Chiropteridium lobospinosum*
12,49	0	0	0	0	0	0
12,99	0	0	0	0	5,2	0
13,81	0	0	0	0	3,4	0
14,63	0	0	0	0	37,5	4,2
15,13	0	0	0	0	7,5	4,6
16,45	0	0	0	0	2,6	1,5
17,28	0,3	0	0,7	0,3	1,2	0
17,32	0,2	0	0,7	0	1,9	1,3
17,4	1,9	0	1,4	0,5	1,2	0,9
17,44	0	0	0,5	0,3	0,3	1,5
17,48	0	0,2	0,5	1,1	0	0
17,53	1,3	0	0	0,4	0	0,1
17,57	0,4	0,3	0	0,2	0,2	0
17,62	1	0	0	0	0	0
17,7	0,6	0	0	0,6	0	0
17,8	0,6	0	0,6	0	0,6	0
17,86	1,3	0	0,3	0	0,3	0
17,92	1,6	0	0	1,6	0	0
17,97	0,7	0	0	0,7	0,2	0
18,02	0	0	0,3	0,6	0	0
18,07	0	0	0,2	0,5	0,3	0
18,11	0	0	0	0	0	0
18,15	0	0	0	0	0,3	0
18,2	0	0	0	0	0,3	0
18,28	0	0,1	0,1	0	56	0
18,33	0	0,2	0	0	47,1	0
18,38	0	0,1	0,5	0	46,3	0
18,43	0	0,4	0,7	0	20,6	0
18,48	0	0	0	0	4,4	0
18,53	0	0	0	0	20,2	0
18,58	0	0,2	0	0	63,9	0
18,63	0	0	0	0	90,8	0,4
18,68	0	0,1	0	0	82,5	0
18,7	0	0	0	0	4,9	0
18,75	0	0	0	0,2	11,8	0
18,8	0	0	0	0	5,7	0
18,88	0	0	0	0	40,9	0
18,9	0	0	0	2,3	17	0
18,96	0	0,2	0	0	30,3	0

Samples	*Pediastrum*-type	*Pterospermella* sp.	*Zygnema* sp. A	*Zygnema* sp. B	*Apteodinium spiridoides*	*Chiropteridium lobospinosum*
19	0	0	0	0	0,8	0
19,06	0	0	0	0	0	0
19,1	0	0	0	0	0	0
19,18	0	0	0	0	0	0
19,2	0	0	0	0	0	0
19,25	0	0	0	0	0	0
19,33	0	0	0	0	0	0
19,38	0	0	0	0	0	0
19,43	0	0	0	0	0	0
19,48	0	0	0	0	0,2	0
19,52	0	0	0	0	0	0
19,63	0	0	0,3	0	0	0
19,7	0	0	0	0	0	0
19,75	0	0	0	0	0	0
19,8	0	0	0	0	0	0
19,85	0	0	0	0	0	0
19,93	0	0	0,2	0	0,2	0
19,95	0	0	0	0	0	0
20	0	0	0	0	0	0
20,08	0	0	0	0	0,2	0
20,33	0	0	0	0	0	0
25,4	0	0	0	0	0	0
25,45	0	0	0	0	0	0
25,48	0	0	0	0	0	0
25,52	0	0	0	0	0	0
25,55	0	0	0	0	0	0
25,58	0	0	0	0	0	0
25,6	0	0	0	0	0	0
30,92	0	0	0,1	0	0	0
30,97	0	0	0	0	0	0
31,01	0	0	0	0	0	0
31,05	0	0	0	0	0	0
31,09	0	0	0	0	0	0
31,13	0	0	0	0	0	0
32	0	0	0	0	0	0
32,53	0	0	0,6	0	0	0
33,03	0	0	0	0	0	0

Samples	*Cordosphaeridium minimum*	*Spiniferites mirabilis*	*Spiniferites* spp.	*Operculodinium centrocarpum*	*Operculodinium* sp.
1,61	0	4,3	0	0	0
12,49	0	0	0	0	0
12,99	0	0	0	0	0
13,81	0	17,2	0	44,8	0
14,63	14,6	21,9	0	18,8	0
15,13	31,2	8,7	0,2	36,5	2,7
16,45	3	54,3	0	31,5	0
17,28	0	0	0	0	0
17,32	3,1	3,5	0	0	0,4
17,4	0,9	0,7	0	0	0
17,44	0	2,5	0	0	0,3
17,48	0	0,9	0	0,2	0
17,53	0,1	0	0	0	0
17,57	0	0	0	0	0
17,62	0,8	0	0	0	0,1
17,7	0	0	0	0	0
17,8	0	0,3	0	0	0
17,86	0,3	0,5	0	0	0
17,92	0	0	0	0	0
17,97	0,2	0,2	0	0	0,7
18,02	0	0,8	0	0	0
18,07	0	0,4	0	0	0,2
18,11	0	0,7	0	0	0
18,15	0	0,7	0	0,4	0
18,2	0,6	0	0	0	0
18,28	0,8	0,9	0	2,3	0,1
18,33	3,2	2,2	0	4,6	0,3
18,38	0,4	1,1	0	0	0
18,43	1,6	3,8	0	2	0
18,48	1,2	7,1	0	2,8	0,2
18,53	0,2	0,8	0	1,4	0,1
18,58	0,6	3,7	0	2,4	0,2
18,63	0,5	1,1	1,1	0	0,1
18,68	0,3	1,8	0	1,4	0,1
18,7	0	1,8	0	0	0
18,75	0	1,4	0	0,7	0,4
18,8	0,1	0,3	0	0,8	0

Samples	*Cordosphaeridium minimum*	*Spiniferites mirabilis*	*Spiniferites* spp.	*Operculodinium centrocarpum*	*Operculodinium* sp.
18,88	0	0,1	0	2,5	0,2
18,9	0	1,4	0	1,1	0,2
18,96	0,9	1,4	0	5,4	0,7
19	0	0,1	0	0	0
19,06	0	0	0	0	0
19,1	0	0	0	0	0
19,18	0	0	0	0	0
19,2	0	0	0	0	0
19,25	0	0	0	0	0
19,33	0	0	0	0	0
19,38	0	0	0	0	0
19,43	0	0	0	0	0
19,48	0	0	0	0	0
19,52	0	0	0	0	0
19,63	0	0,3	0	0	0
19,7	0	0	0	0	0
19,75	0	0	0	0	0
19,8	0	0	0	0	0
19,85	0	0	0	0	0
19,93	0	0	0	0	0
19,95	0	0	0	0	0
20	0	0	0	0	0
20,08	0	0	0	0	0
20,33	0	0	0	0	0
25,4	0	0	0	0	0
25,45	0	0	0	0	0
25,48	0	0	0	0	0
25,52	0	0	0	0	0
25,55	0	0	0	0	0
25,58	0	0	0	0	0
25,6	0	0	0	0	0
30,92	0	0	0	0	0
30,97	0	0	0	0	0
31,01	0	0	0	0	0
31,05	0	0	0	0	0
31,09	0	0	0	0	0
31,13	0	0	0	0	0
32	0	0	0	0	0
32,53	0	0	0	0	0

Samples	*Cordosphaeridium minimum*	*Spiniferites mirabilis*	*Spiniferites* spp.	*Operculodinium centrocarpum*	*Operculodinium* sp.
33,03	0	0	0	0	0

Samples	Microforaminiferal lining	Fungal spore	Pollen Varia	Trilete Spore Varia	Monolete Spore Varia
1,61	0	17,4	8,7	0	0
12,49	0	97,7	0	0	0
12,99	0	75,9	0	0	0
13,81	0	0	0	0	0
14,63	0	0	0	0	0
15,13	0	0,4	0	0	0
16,45	0	0,7	1,1	0,4	0
17,28	1,1	19,1	1,4	0	0
17,32	0	21	2	0,1	0
17,4	0,2	23	1,6	0	0
17,44	0,5	13,5	3,4	2,1	0
17,48	0,1	32,1	2,7	0	0
17,53	0,6	27,9	4,4	0	0
17,57	1,9	50,8	4,5	0	0
17,62	0,2	51,3	1,6	0,1	0
17,7	0,3	40,1	3,1	0	0,3
17,8	1,9	40,1	1,4	0	0
17,86	1,5	44	4,5	0,4	0
17,92	0	21,6	5,2	0	0
17,97	0	26,5	1,5	0	0
18,02	1,7	29,2	3,1	0,3	0
18,07	0	57,5	2,6	0	0
18,11	3,7	26,4	4,4	0,4	0
18,15	0	43,2	2,2	0	0
18,2	1,4	34,4	3,6	0,8	0
18,28	0	5,5	1,9	0,6	0
18,33	0	11,9	1,2	0,6	0,1
18,38	0	11	1,7	1,6	0
18,43	0	14	2	1,5	0,1
18,48	0,1	17,8	1,8	0,8	0
18,53	0	16,9	2,2	0,7	0
18,58	0,1	3	1,6	1,3	0
18,63	0	0,4	0	0,2	0

Samples	Microforaminiferal lining	Fungal spore	Pollen Varia	Trilete Spore Varia	Monolete Spore Varia
18,68	0	2	0,6	0,7	0
18,7	0	15,3	2,6	0	0,1
18,75	0,2	9,1	6	0,6	0,2
18,8	0	21,4	3,8	0,3	0,1
18,88	0,5	11,6	2,2	2	0,1
18,9	0,1	17	3,2	0,3	0
18,96	0,1	15,3	2,7	0,4	0
19	0	38,1	1,2	0,2	0
19,06	0	55,5	3	0	0
19,1	0	48,2	4,4	0	0
19,18	0	22,9	4,6	0,1	0
19,2	0	17,1	3,8	0,8	0
19,25	0	28,6	1,4	1	0,1
19,33	0	14,7	3,2	0,6	0,1
19,38	0	13	5,3	1,6	0,7
19,43	0	24,2	6,9	0,3	0
19,48	0	16,2	4,6	0,9	0,4
19,52	0	3,3	12,2	6,7	0
19,63	0	20,4	12,6	1,3	0,2
19,7	0	26,8	10,3	1,2	0,4
19,75	0	13,8	17,7	0,8	0,6
19,8	0	16,2	14,1	3,8	0
19,85	0	14	13,7	3,5	0,4
19,93	0	11,7	13	5,5	0
19,95	0	8,8	4,2	8,6	0
20	0	11,8	10,6	6,4	0
20,08	0	16,3	20,6	3	0,2
20,33	0	1,9	25,9	2,5	0,2
25,4	0	61,2	0,3	2,2	0
25,45	0	40,7	3,4	18,7	0
25,48	0	16	8,1	25,1	0
25,52	0	9,3	14	21,8	0,3
25,55	0	17,7	0	0	0,6
25,58	0	58,9	4,4	22	0
25,6	0	64,1	8	14,3	0,8
30,92	0	58,9	3,1	0,3	0
30,97	0	65,7	4	0	0
31,01	0	74,4	2,3	0,5	0
31,05	0	46,6	9,2	0	0

Samples	Microforaminiferal lining	Fungal spore	Pollen Varia	Trilete Spore Varia	Monolete Spore Varia
31,09	0	39,6	9,7	0	0
31,13	0	32,2	7,6	0,2	0
32	0	33,9	6,7	1,1	0
32,53	0,2	27,7	7,7	0,2	0
33,03	0	47,4	7,8	0,4	0

Appendix C: Spreadsheet used for the PCA. Key: 1 = Presence in sample and 0 = Absence in sample of selected taxa from eight ecological groups includingsubtropical, forest, mangrove, savanna woodland, proto-fynbos, herbs & shrublets, wetlands and cryptogams. The ecological groups were created to reduce and standardise the number of taxa. Each successive page displays a table with the sample header showing depth of core in meters (over the interval 17.28–33.03 m).

Samples	17,28	17,32	17,4	17,44	17,48	17,53	17,57	17,62
Subtropical	1	0	0	0	1	1	1	0
Subtropical	1	1	1	0	0	0	0	0
Forest	1	1	1	1	1	1	1	1
Forest	1	1	1	1	1	1	1	1
Forest	0	0	0	0	1	1	1	0
Forest	0	0	0	0	0	0	0	0
Subtropical	1	1	1	1	1	1	0	0
Subtropical	1	1	0	1	1	1	0	0
Subtropical	0	0	0	1	0	0	0	0
Subtropical	1	1	1	1	0	1	1	1
Subtropical	1	1	1	1	1	1	0	0
Subtropical	0	0	0	0	0	0	0	1
Subtropical	0	0	0	0	0	0	0	0
Subtropical	1	0	0	0	1	1	1	1
Subtropical	0	0	0	0	0	0	0	0
Subtropical	0	0	0	0	0	0	0	0
Subtropical	0	0	0	0	0	0	0	0
Subtropical	0	0	0	0	0	1	0	0
Mangrove	0	0	0	0	0	0	0	0
Savanna woodland	0	0	0	0	0	0	0	1
Subtropical	0	0	0	0	0	0	0	0

Samples	17,28	17,32	17,4	17,44	17,48	17,53	17,57	17,62
Savanna woodland	0	0	0	0	0	1	0	0
Forest	0	1	0	0	0	0	1	0
Subtropical	0	0	0	0	0	0	0	0
Forest	0	0	0	0	0	0	0	0
Subtropical	1	1	1	1	1	1	0	1
Savanna woodland	0	0	0	0	1	0	0	0
Proto-fynbos	0	0	0	0	1	1	0	0
Proto-fynbos	1	1	1	0	1	1	1	1
Proto-fynbos	1	1	1	1	1	1	1	1
Proto-fynbos	1	1	1	1	1	1	1	1
Proto-fynbos	0	0	0	0	0	0	0	0
Herbs & shrublets	0	1	0	1	1	1	1	0
Herbs & shrublets	1	0	0	0	0	1	0	0
Herbs & shrublets	1	1	1	1	1	1	1	1
Herbs & shrublets	1	1	1	1	1	1	0	1
Herbs & shrublets	1	1	0	1	1	1	1	1
Proto-fynbos	0	0	1	0	1	0	1	0
Wetland	1	1	1	0	1	0	1	1
Wetland	0	1	0	1	1	1	1	0
Wetland	0	0	0	0	0	0	0	0
Cryptogam	1	1	1	1	1	1	1	1
Cryptogam	1	1	1	1	1	1	1	1
Cryptogam	1	0	0	1	1	0	0	1
Cryptogam	0	0	0	0	0	0	0	0
Cryptogam	0	0	0	1	0	0	0	0
Cryptogam	1	1	1	1	1	1	1	1
Cryptogam	1	1	1	1	1	1	1	1

Depth	17,7	17,8	17,86	17,92	17,97	18,02	18,07	18,11
Subtropical	0	0	0	1	1	0	0	1
Subtropical	0	0	0	0	0	0	0	0
Forest	1	1	1	1	1	1	1	1
Forest	1	1	1	1	1	1	1	1
Forest	1	1	1	1	1	1	0	1
Forest	0	0	0	0	0	0	0	0
Subtropical	0	0	1	1	1	1	0	0
Subtropical	1	1	1	1	1	1	1	0
Subtropical	0	0	0	0	0	0	0	0
Subtropical	1	1	1	1	1	1	1	1

Depth	17,7	17,8	17,86	17,92	17,97	18,02	18,07	18,11
Subtropical	1	0	0	1	0	1	1	0
Subtropical	0	0	0	0	0	0	0	0
Subtropical	0	0	0	0	0	0	0	0
Subtropical	1	1	0	0	1	1	1	0
Subtropical	0	0	0	0	0	0	0	0
Subtropical	0	0	0	0	0	0	0	0
Subtropical	0	0	0	0	0	0	0	0
Subtropical	0	0	0	0	1	0	0	0
Mangrove	0	0	0	0	0	0	0	0
Savanna woodland	0	0	0	1	0	0	0	0
Subtropical	0	0	0	0	0	0	1	0
Savanna woodland	0	0	0	0	0	0	0	0
Forest	0	0	0	0	0	1	0	0
Subtropical	0	0	0	0	0	0	0	0
Forest	0	0	0	0	0	0	0	0
Subtropical	1	0	0	1	1	1	1	0
Savanna woodland	0	0	0	0	0	0	0	0
Proto-fynbos	0	0	0	0	0	0	0	0
Proto-fynbos	1	1	1	1	1	1	1	1
Proto-fynbos	1	1	1	1	1	1	1	1
Proto-fynbos	1	1	1	1	1	1	1	1
Proto-fynbos	0	0	0	0	0	0	0	0
Herbs & shrublets	0	0	1	1	1	0	1	1
Herbs & shrublets	1	0	0	1	0	0	0	0
Herbs & shrublets	0	0	1	0	1	1	1	1
Herbs & shrublets	0	0	0	1	1	1	1	0
Herbs & shrublets	0	0	0	1	1	0	0	0
Proto-fynbos	0	0	1	0	1	0	1	1
Wetland	0	1	1	0	1	1	1	0
Wetland	0	1	1	1	1	1	1	1
Wetland	0	0	0	0	0	0	0	0
Cryptogam	1	0	1	0	1	1	1	1
Cryptogam	1	1	1	1	1	1	1	1
Cryptogam	0	0	1	1	1	1	1	0
Cryptogam	1	0	1	0	0	0	1	1
Cryptogam	0	0	0	0	0	0	0	0
Cryptogam	1	1	1	0	1	1	1	1
Cryptogam	1	1	1	1	1	1	1	1

Depth	18,15	18,2	18,28	18,33	18,38	18,43	18,48	18,53
Subtropical	0	0	1	1	1	1	1	1
Subtropical	0	0	0	1	0	0	0	0
Forest	1	1	1	1	1	1	1	1
Forest	1	1	1	1	1	1	1	1
Forest	1	0	0	0	0	0	0	1
Forest	0	0	0	0	0	0	0	0
Subtropical	1	1	1	1	1	1	1	1
Subtropical	1	1	0	1	0	1	0	0
Subtropical	0	0	1	0	0	0	0	0
Subtropical	1	0	1	1	1	1	1	1
Subtropical	1	1	1	1	0	1	0	0
Subtropical	0	0	0	0	0	0	0	0
Subtropical	0	0	0	0	0	0	0	0
Subtropical	0	0	0	0	0	0	0	0
Subtropical	0	0	0	0	0	0	0	0
Subtropical	0	0	0	0	0	0	0	0
Subtropical	0	0	0	0	0	0	0	0
Subtropical	0	0	0	0	1	1	0	1
Mangrove	0	0	0	0	0	0	0	0
Savanna woodland	0	0	0	0	0	0	1	1
Subtropical	0	0	0	0	0	0	0	0
Savanna woodland	0	1	0	0	0	0	0	0
Forest	0	0	0	0	0	0	0	0
Subtropical	0	0	0	0	0	1	0	0
Forest	0	0	0	0	0	0	0	0
Subtropical	1	1	0	1	0	1	1	1
Savanna woodland	0	0	0	0	0	0	0	0
Proto-fynbos	0	0	0	0	0	0	0	0
Proto-fynbos	1	1	1	1	1	1	1	1
Proto-fynbos	1	1	1	1	1	1	1	1
Proto-fynbos	1	1	1	1	1	1	1	1
Proto-fynbos	0	0	0	0	0	0	1	0
Herbs & shrublets	1	1	0	0	1	1	1	1
Herbs & shrublets	0	0	1	0	1	0	0	0
Herbs & shrublets	1	1	0	1	1	1	1	1
Herbs & shrublets	1	0	0	1	0	1	1	1
Herbs & shrublets	1	0	0	1	1	1	0	0
Proto-fynbos	1	1	1	1	1	1	1	1
Wetland	1	1	1	1	1	1	1	1

Depth	18,15	18,2	18,28	18,33	18,38	18,43	18,48	18,53
Wetland	0	1	0	0	1	1	0	0
Wetland	0	0	0	0	0	0	0	0
Cryptogam	1	1	1	1	1	1	1	0
Cryptogam	1	0	1	0	1	1	1	1
Cryptogam	0	0	1	1	1	1	1	1
Cryptogam	0	0	1	1	0	0	1	0
Cryptogam	0	0	1	1	1	1	1	1
Cryptogam	1	0	1	1	1	1	1	1
Cryptogam	1	1	1	1	1	1	1	1

Depth	18,58	18,63	18,68	18,7	18,75	18,8	18,88	18,9
Subtropical	1	0	0	1	1	1	1	1
Subtropical	0	0	0	0	0	0	0	0
Forest	1	1	1	1	1	1	1	1
Forest	1	0	1	1	1	0	1	0
Forest	0	0	0	0	1	1	0	0
Forest	0	0	0	0	0	0	0	0
Subtropical	1	0	0	1	1	1	1	1
Subtropical	0	0	0	1	1	1	1	0
Subtropical	0	0	0	0	0	0	1	0
Subtropical	1	0	1	1	1	1	1	1
Subtropical	0	0	1	0	0	0	1	0
Subtropical	0	0	0	0	0	0	1	1
Subtropical	0	0	0	0	0	0	0	0
Subtropical	0	0	0	0	1	1	0	1
Subtropical	1	0	0	0	1	0	0	1
Subtropical	0	0	0	0	0	0	0	1
Subtropical	0	0	0	0	0	0	0	0
Subtropical	0	0	0	1	1	1	1	1
Mangrove	0	0	0	0	0	0	0	0
Savanna woodland	0	0	1	0	0	1	0	0
Subtropical	0	0	0	1	0	1	1	1
Savanna woodland	0	0	0	0	0	1	0	0
Forest	0	0	0	0	0	0	0	1
Subtropical	0	0	0	0	0	0	0	0
Forest	0	0	0	0	0	0	0	0
Subtropical	0	0	1	1	1	1	0	1
Savanna woodland	0	0	0	0	0	0	0	0

Depth	18,58	18,63	18,68	18,7	18,75	18,8	18,88	18,9
Proto-fynbos	0	0	0	0	1	1	1	0
Proto-fynbos	0	0	1	1	1	1	1	1
Proto-fynbos	1	1	1	1	1	1	0	1
Proto-fynbos	1	1	1	1	1	1	1	1
Proto-fynbos	0	0	0	0	0	0	0	0
Herbs & shrublets	0	0	1	1	1	1	1	0
Herbs & shrublets	0	0	0	1	0	1	1	1
Herbs & shrublets	1	0	0	1	1	1	1	1
Herbs & shrublets	1	0	0	1	1	1	1	1
Herbs & shrublets	0	0	0	1	1	0	0	1
Proto-fynbos	0	0	1	1	0	0	1	0
Wetland	1	1	1	0	1	0	0	1
Wetland	0	0	0	1	1	1	1	1
Wetland	0	1	0	0	0	0	0	0
Cryptogam	0	1	1	0	0	1	1	0
Cryptogam	1	0	0	1	1	1	1	1
Cryptogam	1	1	1	0	1	0	1	0
Cryptogam	0	0	0	0	0	0	0	0
Cryptogam	1	0	1	0	1	0	1	0
Cryptogam	1	1	1	0	0	0	1	1
Cryptogam	1	1	1	1	1	1	1	1

Depth	18,96	19	19,06	19,1	19,18	19,2	19,25	19,33
Subtropical	1	1	1	1	1	1	1	1
Subtropical	0	0	0	0	0	1	0	0
Forest	1	0	0	0	0	1	1	1
Forest	1	1	1	1	1	1	0	0
Forest	1	0	1	1	0	0	1	0
Forest	0	0	0	0	0	0	0	0
Subtropical	1	1	1	1	1	1	1	1
Subtropical	1	1	1	1	1	0	0	1
Subtropical	0	0	0	0	0	0	0	0
Subtropical	1	1	1	1	1	1	1	1
Subtropical	0	0	0	0	0	0	1	0
Subtropical	0	0	0	0	0	0	0	0
Subtropical	1	0	0	0	0	0	0	0
Subtropical	1	1	0	1	0	0	0	0
Subtropical	1	0	0	0	0	0	0	1
Subtropical	0	0	0	1	0	0	0	0
Subtropical	0	0	0	0	0	0	0	0
Subtropical	1	1	0	1	1	0	1	1

Depth	18,96	19	19,06	19,1	19,18	19,2	19,25	19,33
Mangrove	0	0	0	0	0	0	0	0
Savanna woodland	0	1	0	0	0	0	0	0
Subtropical	1	0	0	0	0	0	0	0
Savanna woodland	0	0	0	0	1	0	0	0
Forest	0	0	0	0	0	0	0	1
Subtropical	0	0	0	0	0	0	0	0
Forest	0	0	0	0	0	0	0	0
Subtropical	1	0	0	0	1	0	0	0
Savanna woodland	0	0	0	0	0	0	0	0
Proto-fynbos	0	0	0	1	0	0	0	0
Proto-fynbos	1	0	0	0	0	0	0	0
Proto-fynbos	1	1	0	1	1	0	1	1
Proto-fynbos	1	1	1	1	1	1	1	1
Proto-fynbos	0	0	0	0	0	0	0	0
Herbs & shrublets	1	0	0	0	0	0	0	0
Herbs & shrublets	1	1	0	0	1	1	0	0
Herbs & shrublets	1	1	1	0	1	0	0	0
Herbs & shrublets	1	1	1	1	1	1	1	1
Herbs & shrublets	1	0	0	0	1	0	0	1
Proto-fynbos	0	0	0	0	0	0	0	0
Wetland	0	0	0	0	0	0	0	0
Wetland	1	1	0	1	1	0	0	1
Wetland	0	0	0	0	0	0	0	0
Cryptogam	0	0	0	0	0	0	0	0
Cryptogam	1	1	1	1	1	1	1	1
Cryptogam	1	0	0	0	0	0	0	0
Cryptogam	0	0	0	0	0	0	0	0
Cryptogam	0	0	0	0	0	0	0	1
Cryptogam	0	0	0	0	1	0	1	1
Cryptogam	1	0	0	1	0	0	0	0

Depth	19,38	19,43	19,48	19,52	19,63	19,7	19,75	19,8
Subtropical	1	1	1	1	1	1	1	1
Subtropical	0	0	0	1	0	1	1	1
Forest	1	0	1	1	1	1	1	1
Forest	0	0	0	0	0	1	1	1
Forest	0	0	1	0	0	1	0	1
Forest	0	0	0	1	0	0	0	0

Depth	19,38	19,43	19,48	19,52	19,63	19,7	19,75	19,8
Subtropical	1	1	1	1	1	1	1	1
Subtropical	1	0	1	1	1	1	1	0
Subtropical	0	0	0	0	0	0	0	1
Subtropical	0	1	1	1	1	1	1	1
Subtropical	0	0	0	0	1	0	0	0
Subtropical	0	0	0	0	1	0	0	1
Subtropical	0	0	0	0	0	0	1	0
Subtropical	1	1	0	1	0	0	0	1
Subtropical	0	1	0	0	0	0	1	0
Subtropical	0	1	0	0	0	0	0	0
Subtropical	0	0	0	0	0	0	0	0
Subtropical	1	1	1	0	0	0	1	1
Mangrove	0	0	0	0	0	0	0	0
Savanna woodland	0	0	0	0	0	0	0	0
Subtropical	0	1	0	1	0	0	1	1
Savanna woodland	0	0	0	1	0	0	0	0
Forest	0	0	0	0	0	0	0	0
Subtropical	0	0	0	0	0	0	0	0
Forest	0	0	0	0	0	1	0	0
Subtropical	0	0	0	0	0	0	0	0
Savanna woodland	0	0	0	0	0	0	0	0
Proto-fynbos	0	1	1	0	0	0	0	0
Proto-fynbos	0	0	0	0	1	1	0	1
Proto-fynbos	1	0	0	1	1	1	1	1
Proto-fynbos	1	1	1	1	1	1	1	1
Proto-fynbos	0	0	0	0	0	0	0	0
Herbs & shrublets	0	0	1	0	0	1	1	0
Herbs & shrublets	0	0	0	0	1	0	0	0
Herbs & shrublets	1	1	1	0	0	1	0	1
Herbs & shrublets	1	1	1	1	1	1	1	1
Herbs & shrublets	1	1	0	0	0	0	0	1
Proto-fynbos	0	0	0	0	0	0	0	0
Wetland	1	0	0	0	0	0	0	0
Wetland	1	1	1	1	1	1	1	1
Wetland	0	0	0	0	0	0	0	0
Cryptogam	0	0	0	0	1	0	1	0
Cryptogam	1	1	1	1	1	1	1	1
Cryptogam	0	0	0	0	0	1	0	0
Cryptogam	0	0	1	0	0	0	1	1

Depth	19,38	19,43	19,48	19,52	19,63	19,7	19,75	19,8
Cryptogam	0	0	1	1	0	1	1	1
Cryptogam	1	1	1	1	1	1	0	0
Cryptogam	0	0	0	0	1	0	0	0

Depth	19,85	19,93	19,95	20	20,08	20,33	25,4	25,45
Subtropical	1	1	1	1	1	1	1	1
Subtropical	1	1	1	1	1	1	1	1
Forest	1	1	1	1	1	1	0	0
Forest	1	1	0	1	1	1	1	1
Forest	1	1	1	0	0	0	0	1
Forest	0	0	0	0	1	1	0	0
Subtropical	1	1	1	1	1	1	1	1
Subtropical	1	1	1	1	1	1	1	1
Subtropical	0	1	0	0	0	1	0	0
Subtropical	1	1	1	1	1	1	0	1
Subtropical	0	0	1	0	0	1	0	0
Subtropical	1	1	0	0	1	1	0	0
Subtropical	1	1	1	1	1	0	0	0
Subtropical	1	1	1	1	1	1	0	0
Subtropical	0	1	1	1	1	1	1	0
Subtropical	1	1	1	1	1	1	0	0
Subtropical	0	0	0	0	0	0	0	0
Subtropical	1	1	1	1	1	0	0	0
Mangrove	0	1	0	0	1	1	0	0
Savanna woodland	0	1	0	1	0	0	0	0
Subtropical	0	1	1	1	1	0	0	0
Savanna woodland	0	1	0	0	0	0	0	0
Forest	0	0	0	0	0	0	0	0
Subtropical	0	0	0	0	0	0	0	0
Forest	0	0	0	0	0	0	0	0
Subtropical	0	0	0	0	0	0	0	0
Savanna woodland	0	0	0	0	0	0	0	0
Proto-fynbos	1	1	0	0	0	0	0	0
Proto-fynbos	1	1	0	1	1	1	0	1
Proto-fynbos	1	1	1	1	1	1	1	1
Proto-fynbos	1	1	0	1	1	1	1	1
Proto-fynbos	0	0	0	0	0	1	0	0
Herbs & shrublets	0	0	1	0	1	1	1	0

Depth	19,85	19,93	19,95	20	20,08	20,33	25,4	25,45
Herbs & shrublets	1	1	1	1	1	1	0	0
Herbs & shrublets	1	1	1	1	1	1	1	1
Herbs & shrublets	1	1	1	0	0	1	1	0
Herbs & shrublets	1	1	0	1	1	1	0	0
Proto-fynbos	0	0	0	0	0	0	0	0
Wetland	0	1	1	0	1	1	0	1
Wetland	0	0	1	1	1	0	1	1
Wetland	0	0	0	0	0	0	0	0
Cryptogam	0	0	0	1	1	1	1	0
Cryptogam	1	1	1	1	1	0	1	0
Cryptogam	1	0	0	0	1	1	1	1
Cryptogam	1	1	1	1	0	1	1	1
Cryptogam	1	1	1	1	1	1	1	1
Cryptogam	0	0	0	0	1	0	0	1
Cryptogam	0	0	0	0	1	0	0	0

Depth	25,48	25,52	25,55	25,58	25,6	30,92	30,97
Subtropical	1	1	1	1	1	1	1
Subtropical	1	1	1	1	1	1	1
Forest	0	0	0	1	1	1	1
Forest	1	1	1	0	0	1	1
Forest	0	0	0	0	0	1	1
Forest	0	1	0	0	0	0	0
Subtropical	1	1	1	1	1	1	1
Subtropical	1	1	1	1	1	1	1
Subtropical	1	0	0	0	0	0	1
Subtropical	1	0	1	1	0	1	1
Subtropical	0	0	0	0	0	1	0
Subtropical	0	0	0	0	0	1	1
Subtropical	1	0	0	0	0	1	1
Subtropical	0	0	0	0	0	1	1
Subtropical	0	0	1	1	0	1	1
Subtropical	0	1	0	0	0	1	0
Subtropical	0	0	0	0	0	1	0
Subtropical	1	0	1	1	1	1	1
Mangrove	0	0	0	0	0	0	1
Savanna woodland	0	0	0	0	0	1	0
Subtropical	0	0	0	0	0	0	0

Depth	25,48	25,52	25,55	25,58	25,6	30,92	30,97
Savanna woodland	0	0	0	0	0	0	1
Forest	0	0	0	0	0	0	0
Subtropical	0	0	0	0	0	0	0
Forest	0	0	0	0	0	0	0
Subtropical	0	0	0	0	0	1	0
Savanna woodland	0	0	0	0	0	0	0
Proto-fynbos	0	0	0	0	0	1	1
Proto-fynbos	0	0	0	0	0	1	0
Proto-fynbos	1	1	1	0	0	0	1
Proto-fynbos	1	1	1	1	1	1	1
Proto-fynbos	0	0	0	0	0	0	0
Herbs & shrublets	0	0	0	0	0	1	1
Herbs & shrublets	0	0	1	1	0	1	1
Herbs & shrublets	1	1	0	1	1	1	1
Herbs & shrublets	0	0	0	0	0	1	1
Herbs & shrublets	0	0	0	0	0	1	0
Proto-fynbos	0	0	0	0	0	0	0
Wetland	0	1	1	0	0	0	0
Wetland	1	1	1	1	1	1	1
Wetland	0	0	0	0	0	0	0
Cryptogam	0	0	0	0	0	1	1
Cryptogam	0	0	0	1	0	1	0
Cryptogam	1	1	1	0	1	1	1
Cryptogam	1	1	1	1	1	0	0
Cryptogam	1	1	1	1	1	0	0
Cryptogam	1	1	1	1	1	0	1
Cryptogam	0	0	0	0	0	0	0

Depth	31,01	31,05	31,09	31,13	32	32,53	33,03
Subtropical	1	1	1	1	1	1	1
Subtropical	1	1	1	1	1	1	1
Forest	1	1	1	1	1	1	1
Forest	1	1	1	1	1	1	1
Forest	1	1	0	1	0	1	1
Forest	0	0	0	0	0	0	0
Subtropical	1	1	1	1	1	1	1
Subtropical	1	1	1	1	1	1	1
Subtropical	1	0	1	1	1	0	1
Subtropical	1	1	1	1	1	1	1

Depth	31,01	31,05	31,09	31,13	32	32,53	33,03
Subtropical	1	0	0	0	1	1	0
Subtropical	1	1	1	1	1	1	1
Subtropical	1	1	1	1	1	1	0
Subtropical	1	1	1	1	1	1	1
Subtropical	1	1	1	1	1	1	1
Subtropical	1	1	1	1	1	0	1
Subtropical	0	1	0	0	1	1	0
Subtropical	1	1	1	1	1	1	1
Mangrove	0	0	0	0	0	1	0
Savanna woodland	0	0	0	1	0	0	0
Subtropical	0	0	0	0	0	0	0
Savanna woodland	0	0	0	1	0	0	0
Forest	0	0	0	0	0	0	1
Subtropical	0	0	0	0	0	0	0
Forest	0	0	0	0	0	0	0
Subtropical	0	0	0	0	0	0	0
Savanna woodland	0	0	0	0	0	0	0
Proto-fynbos	1	1	1	1	1	1	1
Proto-fynbos	1	1	1	1	1	1	1
Proto-fynbos	1	1	1	1	1	0	0
Proto-fynbos	1	1	1	1	1	1	1
Proto-fynbos	0	1	0	0	0	1	0
Herbs & shrublets	0	1	1	1	1	1	1
Herbs & shrublets	1	1	1	1	1	1	1
Herbs & shrublets	1	1	1	1	1	1	1
Herbs & shrublets	1	1	1	1	1	1	1
Herbs & shrublets	0	0	0	0	0	0	0
Proto-fynbos	0	0	0	1	0	1	0
Wetland	0	1	0	0	1	0	0
Wetland	1	0	0	1	1	1	1
Wetland	0	0	0	0	0	0	0
Cryptogam	0	0	0	1	1	1	0
Cryptogam	0	1	0	1	1	0	1
Cryptogam	1	1	1	1	1	1	1
Cryptogam	0	0	0	0	0	0	0
Cryptogam	0	0	0	0	1	1	0
Cryptogam	0	0	0	0	0	1	0
Cryptogam	0	0	0	0	0	0	0

Appendix D: Loading matrix of the first five principal components (Prin1–Prin5) for the PCA with ecological groups as variables. Only PC1 and PC2 were included in the study because they showed the most significant weighting (percentage) of the total variance.

Depth (m)	Prin1	Prin2	Prin3	Prin4	Prin5
17,28	0,75525	-0,25057	-0,06998	0,14299	0,32928
17,32	0,68292	-0,40539	-0,06647	-0,03702	0,06196
17,4	0,62737	-0,49470	-0,00351	0,11346	0,16550
17,44	0,67802	-0,31637	0,07488	-0,02282	-0,13274
17,48	0,64897	-0,41256	-0,22667	0,04607	-0,19118
17,53	0,74017	-0,09729	-0,42609	-0,13901	-0,15404
17,57	0,59400	-0,40784	-0,15475	-0,05542	0,04240
17,62	0,54038	-0,43302	-0,20707	0,14738	0,41633
17,7	0,52209	-0,34756	-0,17650	0,09029	0,11724
17,8	0,62888	-0,26418	-0,11592	-0,05950	0,13496
17,86	0,69865	-0,40467	0,15058	0,13164	-0,22217
17,92	0,67318	-0,15459	-0,29450	-0,00885	-0,11273
17,97	0,82639	-0,30092	-0,18026	-0,05255	-0,09178
18,02	0,70459	-0,39606	-0,15565	0,02915	0,03365
18,07	0,62120	-0,50071	-0,03594	0,09243	-0,02339
18,11	0,63008	-0,34271	0,03859	-0,00947	-0,23513
18,15	0,68194	-0,54316	-0,20322	0,03370	-0,04803
18,2	0,48749	-0,48888	-0,06713	0,18375	-0,20437
18,28	0,54217	-0,35814	0,33603	0,21693	0,15486
18,33	0,65294	-0,38294	0,34350	0,16511	0,11440
18,38	0,72855	-0,26300	0,16302	0,02724	0,02678
18,43	0,74877	-0,40094	0,08786	-0,06521	-0,11242
18,48	0,59643	-0,45983	0,22938	0,09328	-0,01456
18,53	0,68302	-0,30156	0,02947	-0,01773	-0,08863
18,58	0,69762	-0,10561	0,28338	-0,04496	0,22294
18,63	0,28858	-0,51350	0,23645	0,12884	0,23507
18,68	0,39993	-0,67094	0,14085	0,33021	0,01557
18,7	0,71633	-0,05857	-0,26377	-0,22794	-0,05307
18,75	0,76143	0,04027	-0,18146	-0,03401	-0,04366
18,8	0,58791	0,06028	-0,48225	-0,20227	-0,16543
18,88	0,61963	-0,00969	-0,01985	0,12181	-0,28169
18,9	0,53032	0,05983	-0,26324	-0,29665	0,52767
18,96	0,71146	0,16893	-0,35771	-0,05975	0,01482
19	0,66234	0,33897	-0,15057	-0,23798	0,01527
19,06	0,65583	0,21101	-0,09669	-0,17116	-0,19746
19,1	0,59823	0,27721	-0,27009	-0,23672	-0,08323
19,18	0,65437	0,12830	-0,07590	-0,42290	-0,00111
19,2	0,59569	0,26028	-0,01369	-0,03555	0,13214
19,25	0,61673	0,05393	-0,06807	-0,31298	0,00102
19,33	0,59754	0,20840	0,14820	-0,49921	0,09764
19,38	0,67693	0,10393	-0,01115	-0,40046	0,18220
19,43	0,43314	0,39380	-0,16701	-0,43667	0,15331

Depth (m)	Prin1	Prin2	Prin3	Prin4	Prin5
19,48	0,62527	0,25689	0,12473	-0,33835	-0,41332
19,52	0,50542	0,21062	0,20121	-0,41345	0,11316
19,63	0,66466	-0,11105	-0,10944	-0,06504	0,07916
19,7	0,74502	0,07368	0,20946	-0,01227	-0,26567
19,75	0,58161	0,33618	0,25068	-0,10721	-0,09500
19,8	0,58097	0,33745	0,02345	-0,13667	0,15305
19,85	0,58931	0,50033	-0,03791	0,19488	0,16725
19,93	0,36384	0,56950	-0,07910	0,07924	0,36046
19,95	0,45862	0,46480	0,05075	-0,07321	0,07124
20	0,53372	0,41550	0,10034	-0,01774	0,29251
20,08	0,56957	0,18701	0,14634	0,16248	0,35243
20,33	0,38164	0,19492	0,21785	0,49749	0,30226
25,4	0,59404	0,20467	0,38977	0,07414	-0,23224
25,45	0,63025	0,04764	0,52438	0,08498	-0,08638
25,48	0,52491	0,31503	0,58138	0,01560	-0,14020
25,52	0,43444	0,12019	0,68014	0,02825	0,04123
25,55	0,53412	0,27363	0,58449	0,00389	0,07298
25,58	0,57098	0,39643	0,39474	-0,25627	-0,02231
25,6	0,50500	0,26462	0,58604	-0,11832	-0,19364
30,92	0,50154	0,37838	-0,42768	0,30766	-0,09740
30,97	0,49819	0,45145	-0,06820	0,26172	-0,20667
31,01	0,52837	0,56462	-0,18597	0,38893	0,00711
31,05	0,50939	0,46887	-0,21985	0,39041	0,08244
31,09	0,50678	0,56016	-0,14693	0,47380	0,07532
31,13	0,53225	0,44909	-0,28649	0,36028	-0,17990
32	0,57854	0,41753	-0,03009	0,46416	0,05311
32,53	0,42845	0,31069	-0,00331	0,40404	-0,33911
33,03	0,53354	0,54796	-0,26540	0,22774	-0,12697

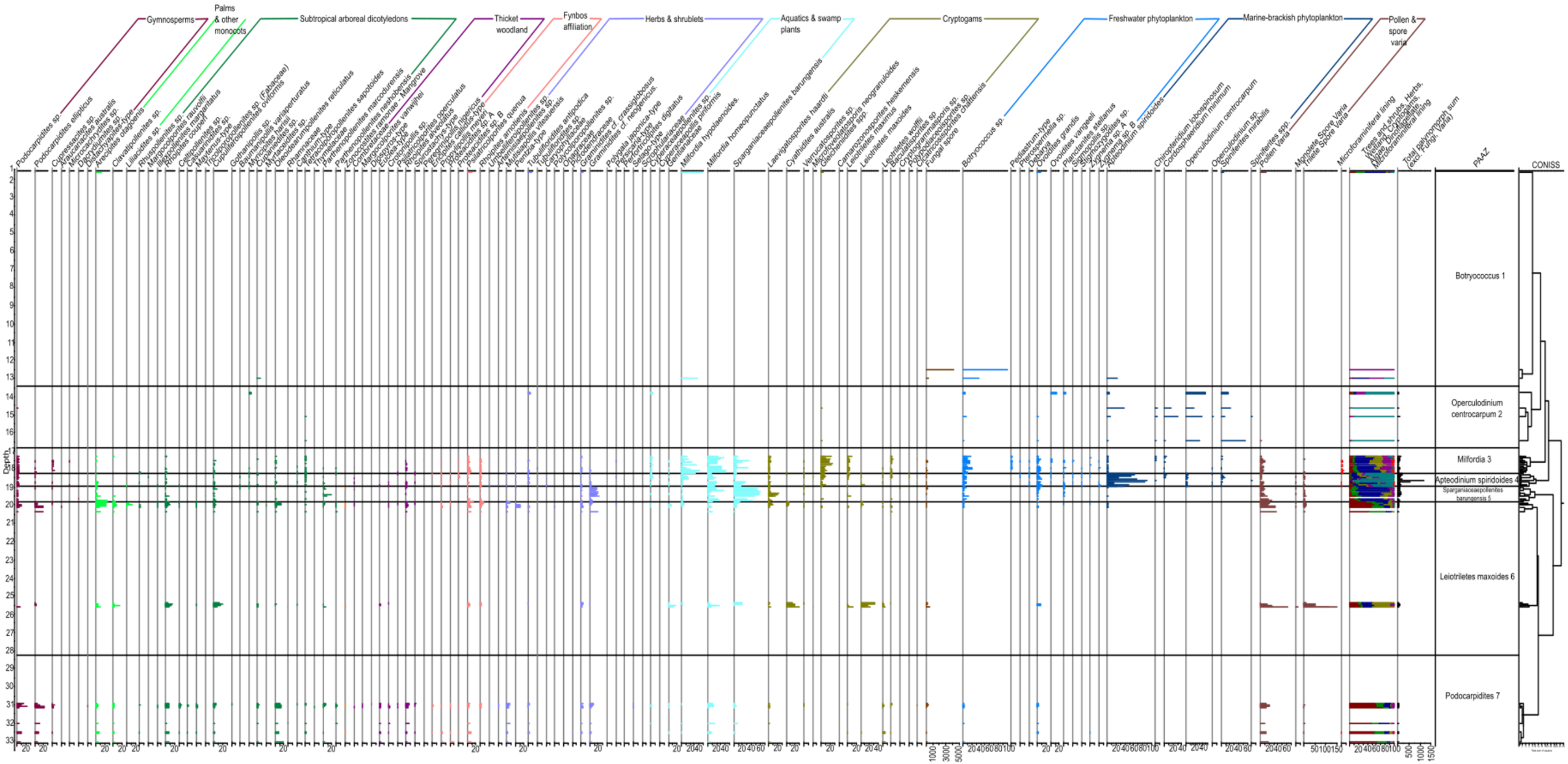

Appendix E: Comprehensive pollen diagram of palynomorphs from Elandsfontyn Formation, Langebaanweg